Exploring the Role for IPPK-1 and PAL-1 in the Genetic Landscape of *C. elegans* Ventral Nerve Cord Assembly

Nathaniel Noblett

Thesis submitted to the University of Ottawa

in partial Fulfillment of the requirements

for the Doctor of Philosophy in Neuroscience

Department of Cellular and Molecular Medicine, Neuroscience Program

Faculty of Medicine

University of Ottawa

Abstract

Formation of the neural tube, from which the central nervous system develops, depends on convergent extension (CE) movements that constrict and elongate neuroepithelial tissue. Genetic regulators of CE include components of inositol phosphate metabolism, the caudal CDX transcription factor family, and the non-canonical WNT/planar cell polarity (PCP) pathway. To better understand the genetic mechanisms underlying CE, we examined the assembly of the *C. elegans* ventral nerve cord (VNC), which undergoes CE during its formation. This process involves the coordination of multiple neuron subtypes and is regulated by the PCP pathway. However, the genetic regulation of VNC assembly and the morphogenetic processes involved remain poorly understood.

This dissertation explores the roles of two conserved regulators of embryonic nerve cord assembly in *C. elegans*: the inositol phosphate (IP) pathway and the transcription factor PAL-1/CDX. We found that disruption of the central IP kinase IPPK-1 caused defects in initial contacts between left and right VNC motor neurons and delayed the resolution of multicellular rosettes, which are critical for driving anterior-posterior junction extension. These defects impaired CE, leading to persistent cell contacts later in embryogenesis and resulting in the mispositioning of neurons. Additionally, we identified a region approximately 10 kb upstream of the *pal-1* start site that is required for its expression in DA and DD neurons. Loss of the nuclear hormone receptor SEX-1 produced a similar phenotype and exacerbated *pal-1* defects in compound mutants. Mutation of both *ippk-1* or *pal-1* and the PCP component *vang-1*/Van Gogh, similarly increased severity in neuron positioning defects. This work highlights the regulatory network underlying VNC assembly, which involves tissue-specific transcription factor cascades and coordinated cell movements. Moreover, it demonstrates that nematode VNC assembly shares genetic pathways, mechanisms, and defects with neurulation, suggesting that the VNC serves as a valuable model for further investigation.

Thesis Format and Scholarly Contributions

Based on the guidelines set by the University of Ottawa Department of Cellular and Molecular Medicine, this thesis is presented as a general introduction, multiple manuscripts and a combined discussion.

Manuscript #1:

Noblett, N., Roenspies, T., Kirezi, C. B., Stubbert, C., Flibotte, S., Shah, P. K., & Colavita, A. (2025). IPPK-1 and IP6 contribute to ventral nerve cord assembly in C. elegans. Developmental Biology, 526, 159–172. https://doi.org/10.1016/j.ydbio.2025.07.007.

Manuscript #2:

Noblett, N., Roenspies, T., Flibotte, S., & Colavita, A. (2025). Nuclear hormone receptor regulation of PAL-1/Caudal mediates ventral nerve cord assembly in C. elegans (p. 2025.03.02.641102). bioRxiv. https://doi.org/10.1101/2025.03.02.641102.

Acknowledgments

I would like to thank my supervisor Dr. Antonio Colavita for his support and for giving me the opportunity to work in his lab. His guidance during my graduate research and writing has been valuable to this project. Throughout both my Masters' and Ph.D thesis work, he has strived to make the lab a productive and open environment. I would also like to thank the members of my thesis advisory committee; Dr. John Copeland, Dr. David Lohnes and Dr. Stephen Gee for their support, advice and feedback throughout this work.

I would like to thank the past and current members of the Colavita lab for their help. Wesley Chan for his ideas and advice, Saber Saharkhiz for advice with coding, Tony Roenspies, who provided the training needed for some technical aspects of the project and Chloe Kirezi, who helped to score the *unc-59* and *unc-61* worms for the IPPK-1 publication. Science is rarely done in a vacuum and only through circulating knowledge is the process of scientific progress realized. In such an environment, I would also like to thank several others. This includes our collaborators, Dr. Pavak Shah, Clover Stubbert and Dr. Stephane Filbolette. Dr. Katherine Maniates for feedback on this thesis. Members of the University of Ottawa Cell Biology Imaging and Acquisition (CBIA) Core for the use of their equipment and training. Also, the University of Minesota Caenorhabditis Genetic Center (CGC), Dr. Shohei Mitani and Dr. Chris Li, who have shared resources with us.

Finally, I would like to thank my family who have supported my graduate education in numerous ways. Without them, these few years would not have been possible.

TABLE OF CONTENTS

List of Figures

List of Tables

List of Abbreviations

AF2 - Activated function-2

APC - Adenoma polyposis coli

ANR5 - Ankrin repeats domain protein 5

BMP – Bone morphogenic protein

CE – Convergent extension

CNS – Central nervous system

CK1 - Casein kinase 1

CBF1 - C Promoter binding factor

DAG - Diacylglycerol

DVL/DSH – Dishevelled

DSL - Delta/Serrate/Lag2

FZD – Frizzled

FMI – Flamingo

FGF - Fibroblast growth factor

GAG - Glycosaminoglycan

GPI - Glycosylphosphatidylinositol

GSK3 - Glycogen synthase kinase 3

HOX - Homeobox

LRP5/6 - LDL receptor-related proteins 5/6

LEF1 - Lymphoid enhancer factor 1

LTZ2 - Leucine zipper tumor suppressor 2

MINPP1 - Multiple inositol polyphosphate phosphatase

NHR – Nuclear hormone receptor

NTD – Neural tube defect

NFAT - Nuclear factor of activated T cells

PCP – Planar cell polarity

PAG - Pre-anal ganglion

PI - Phosphatidylinositol

PIP2 - Phosphatidylinositol 4,5-biphosphate

PIP3 – Phosphatidylinositol 3,4,5-triphosphate

PK/PRKL – Prickle

PLC – Phospholipase C

PKC - Protein kinase C

IP – Inositol phosphate

IP3 – Inositol triphosphate

IP4 – Inositol tetraphosphate

IP5 – Inositol pentakisphospahte

IP6 – Inositol hexaphosphate

IP7 – 1-Diphosphoinositol pentakisphosphate

IP8 – 1-5-Bis-diphosphoinositol tetrakisphosphate

IPMK - Inositol polyphosphate multikinase

ITPK1 - Inositol triphosphate 5,6- kinase

IPPK1/IP5K - Inositol pentakisphosphate kinase 1

RA – Retinoic acid

RAR – Retinoic acid receptor

RI – Radial intercalation

RVG - Retrovesticular ganglion

STAT - Signal transducer and activator of transcription

TCF - T-cell factor

VNC – Ventral nerve cord

Vang – Van Gogh

Chapter 1: General Introduction

1.1 Embryogenesis, Collective Cell Movements and Convergent Extension

1.1.1 The Importance of Collective Cell Movements to Early Neural Development

During early embryo development, aggregates of cells transition from relatively simple clusters into more complex morphologies, composed of increasingly distinct and diverse cellular populations. Collective movements are involved in facilitating this transition, which requires coordination between cell migration, proliferation and rearrangement (Ciruna et al., 2006; Keller et al., 2000). The resulting changes alter the shape of tissues during morphogenesis, thinning, elongating or narrowing cellular populations. Collective cell movements are important in the development of the nervous system at different stages and scales. During early development, movements coincide with specification of the body axis, where they help to maintain the patterning of tissue (Vroomans et al., 2015). This includes a prominent role for mechanisms that converge and elongate tissues during gastrulation, coordinate development of the neural plate and eventually shape the neural tube, which forms the underlying structure for the central nervous system (Ybot-Gonzalez et al., 2007; Williams et al., 2014; Araya et al., 2016; Bénazéraf, 2018). Additional movements are required later in development to facilitate morphogenesis of specific cells populations. This includes the sensory epithelium of the cochlea and regions of the mammalian forbrain, including the neocortex (Chacon-Heszele et al., 2012; Driver et al., 2017; Werner et al., 2021; Xie and Bankaitis, 2022). Failure of these movements, resulting from genetic or environmental factors can have severe consequences on development. Dysregulation of signaling mechanisms during morphogenesis of the neural tube for example, leads to embryonic lethality or developmental abnormalities (Verbsky et al., 2005; Ybot-Gonzalez et al., 2007; Lesko et al., 2021).

1.1.2 Classification of Collective Cell Movements

A diverse set of cell movements underlie the development of multiple tissues during embryogenesis (reviewed in Sutherland et al., 2020). Cell shape changes for example, can drive expansion of a tissue in combination with and without cell rearrangement during *Drosophila melanogaster* imaginal disk elongation or neurulation in chick embryos (Condic et al., 1991; Nishimura et al., 2012). In tissues where cells are actively dividing, polarized cell divisions can also drive growth (Fischer et al., 2006). Radial intercalation (RI) involves the intercalation of cells orthogonally to the extending axis (Szabó et al., 2016; Shook et al., 2022). This movement drives

tissue thinning and is widely involved during gastrulation, mammary duct development and epithelial to mesodermal transitions in the central lumen of the mouse embryo (Bensch et al., 2013; Neumann et al., 2018; Gredler and Zallen, 2023). Given that the direction of intercalation is orthogonal to the plane of extension, RI movements favor multilayered tissues (Szabó et al., 2016). It can drive both unbiased expansion of tissue, such as in the animal cap of *Xenopus laevis* or biased expansion along a single axis (Shih and Keller, 1992; Szabó et al., 2016). Convergent extension, in contrast to unbiased radial intercalation or convergent thickening, is the process by which a tissue narrows along one axis and elongates in a perpendicular direction (Shindo, 2018). It is critical for the development of various tissues, including notochord and neural tube development in *Xenopus*, zebrafish and mammals, in addition to germband extension in *Drosophila* (Irvine and Wieschaus, 1994; Wallingford and Harland, 2002; Kida et al., 2007; Ybot-Gonzalez et al., 2007).

While differences between movements are reflective of the diversity during developmental, mechanisms which facilitate and regulate tissue growth are largely shared. Mechanisms that establish and maintain polarity are important in many examples of collective cell movements (Ossipova et al., 2015; Shi, 2024). Similarly, both medial-lateral and radial intercalations are driven by common cellular mechanisms that form multicellular rosettes (Trichas et al., 2012; Williams et al., 2014; Gredler and Zallen, 2023). In certain tissues, including the developing neural tube, changes in tissue shape, cell rearrangement during convergent extension and polarized cell divisions are coupled to produce more elaborate morphologies (Davidson and Keller, 1999; Werner et al., 2021; Christodoulou and Skourides, 2022). The remainder of this review will focus primarily on convergent extension, as it is one of the most essential morphogenetic processes and is ubiquitous across many organisms and tissue types.

1.2 Convergent Extension

Work over the past 3 decades has provided multiple lines of evidence that highlight the importance of convergent extension. These studies have shown that gastrulation, notochord development and neurulation in chordates require convergent extension movements and have established them as essential models (Keller et al., 1985; reviewed in Tada and Heisenberg, 2012; Sutherland et al., 2020). Studies in zebrafish show that failed cell intercalation during convergent extension leads to a broad undeveloped neuroepithelium (Ciruna et al., 2006). Similar phenotypes

can be observed in mice and *Xenopus* with mutations affecting convergent extension (Greene et al., 1998; Wallingford and Harland, 2002; Goto and Keller, 2002). This work has also uncovered shared and divergent molecular mechanisms which are required during development.

Neural tube defects (NTDs) are a group of heterogenic developmental defects caused by improper closure of the neural tube (reviewed in Greene and Copp, 2014; Lee and Gleeson, 2020). In general, disruption in multiple mechanisms that occur during both primary neurulation, the initial bending and fusion of the neural plate, and secondary neurulation, in which mesenchymal cells undergo tubulogenesis in the caudal neural tube, are sufficient to induce NTDs. This includes disruption of bending of the neural plate at the medial or dorsal hinge regions, failure of neural fold fusion or apical constriction, cell proliferation imbalances and somite development (Copp et al., 1988; Pyrgaki et al., 2011; Greene and Copp, 2014; Nychyk et al., 2022). Failure in these processes can collectively lead to openings in the neural tube which can expose the developing tissue, including central nervous system, to the extracellular environment (Greene et al., 2009; Nikolopoulou et al., 2017). Based on the etiology, genetics and site of closure disruption, neural tube defects can present with a range of characteristics and severities. Open NTDs, the most severe variations of the defect, arise from a failure in primary neurulation and include disrupted mechanisms during convergent extension (Greene and Copp, 2014). The most common defects associated with the open NTD group are craniorachischisis, where both the cranial region and spinal cord remain exposed, anencephaly, where the cranial portion of the neural tube fails to close, and open spina bifida, where a portion of the spinal cord remains exposed. Closed NTDs, are relatively milder and result from failures in secondary neurulation (Greene and Copp, 2014). These broadly lead to skin covered protrusions or gaps in the spine.

NTDs remain one of the most common groups of embryonic defects, affecting approximately 1 in 1000 Canadians (Greene et al., 2009; De Wals et a., 2007). These individuals suffer from a range of symptoms including compromised motor function, incontinence, balance issues, hydrocephalus and impaired cognitive function (Greene and Copp, 2014). A current mitigating strategy is to prevent NTDs through nutritional folate supplementation; this has been effective in most of the population, though some folate-resistant etiologies contribute to their continuing prevalence (Greene and Copp, 1997; De Wals et al., 2007; Cavalli and Ronda, 2017).

The cellular movements which comprise convergent extension require multiple cellular and molecular mechanisms to facilitate patterned intercalations (reviewed in Shindo, 2018; Sutherland et al., 2020). These mechanisms show slight variation across different models and tissue lineages. Over the past decade, work in different model organisms has uncovered two cellular behaviors by which convergent extension can be achieved (Figure 1.1). The first is defined by a cell-crawling movement, that is mediated by bipolar membrane protrusions (Keller, 2002). Originally observed in the mesoderm derived cells of *Xenopus*, the protrusions provide traction as cells cross the extra cellular matrix and intercalate with each other (Keller et al., 1985). A second movement is seen in neuroepithelia and the *Drosophila* germband (Irvine and Wieschaus, 1994; Bertet et al., 2004; Zallen and Wieschaus, 2004). Here, cell-cell boundaries contract along the dorsoventral axis and expand along the anterior-posterior axis in an ordered manner to achieve convergent extension, transitioning from a series of V-shaped junctions to a set of T-junctions. During convergent extension by junction contraction in the developing neural tube and epithelium, transient multicellular rosette structures that share a common vertex are formed (Blankenship et al., 2006; Lienkamp et al., 2012; Williams et al., 2014; Gredler and Zallen, 2023). These require contractile forces generated by actomyosin that drive the shrinking and elongation of cell-cell junctions (Harding et al., 2014; Zhou et al., 2022). Sequential assembly of rosettes is thought to coordinate junctional exchanges throughout collective cell movements (Christodoulou et al., 2018; Gredler and Zallen, 2023).

Recent work by several groups have shown that while the two behaviors can function independently, efficient intercalation in many tissues requires both cell-crawling and contraction-based mechanisms (Sun et al., 2017; Weng et al. 2022). During convergent extension in the germband of the developing *Drosophila* embryo, cells first extend via their bilateral protrusions before meeting, after which their cell-cell boundaries contract and form rosettes as in the later model. This work has been supported in both *Xenopus* mesoderm and mouse neural epithelia tissue (Shindo and Wallingford, 2014; Williams et al., 2014). Both movements require asymmetric distribution of actin. During cell crawling, actin is enriched at the mid-cell body and protruding cell boundaries in a similar manner to lamellipodia (Skoglund et al., 2008; Kim and Davidson, 2011). Likewise, during cell-cell junction contraction, two populations of actomyosin becomes asymmetrically localized (Martin et al., 2009; Munjal et al., 2015). The more superficial population forms a “node and cable” network, while a second population of actin extends along

contracting medial-lateral junctions (Skoglund et al., 2008; Kim and Davidson, 2011; Weng et al. 2022). The dynamics of these three populations of actin regulates the rate and overall force required for intercalation. Although both behaviors require asymmetric actin dynamics, they are regulated independently. Cell-crawling requires the GTPase RAC and the kinase SRC42A, while junctional contraction requires myosin II (Sun et al., 2017). Tension-based feedback between cells and contracting junctions is required for the coordination of behaviors (Weng et al. 2022). This is controlled by the expression of adhesive proteins within intercalating tissues. During *Xenopus* gastrulation, for example, Arvcf catenin is required for efficient convergent extension within mesodermal cells without effecting individual behaviors that only require crawling or contraction (Huebner et al., 2022; Weng et al. 2022).

1.3 Regulation of Collective Cell Movements

The diverse and complex contexts which many collective cell movements take place suggest that tight regulation of the process is required. Given the importance of cytoskeletal movements to collective cell movements, and specifically convergent extension. Specifically, several ligand mediated pathways and transcription factor cascades influence the localization of actomyosin contraction, either at a subcellular or regional level, or its timing in relation to milestones during embryonic development. These subsequent pathways will be discussed in terms of their relation to influencing the timing, subcellular localization or regionalization.

1.3.1 Canonical WNT Signalling

Previous study of CE has shown that WNT signalling, intracellular pathways that are initiated through a set of secreted WNT ligands, play important roles across several models of CE (Rochard et al., 2016; Zhao et al., 2022). These pathways are activated under physiological contexts in which ligands bind and activate the transmembrane receptor Frizzled (Fz) (reviewed in Liu et al., 2022; Hayat et al., 2022). WNT signaling can be divided into two main branches based on participation of the transcriptional cofactor β-catenin (Figure 1.2). The canonical signalling

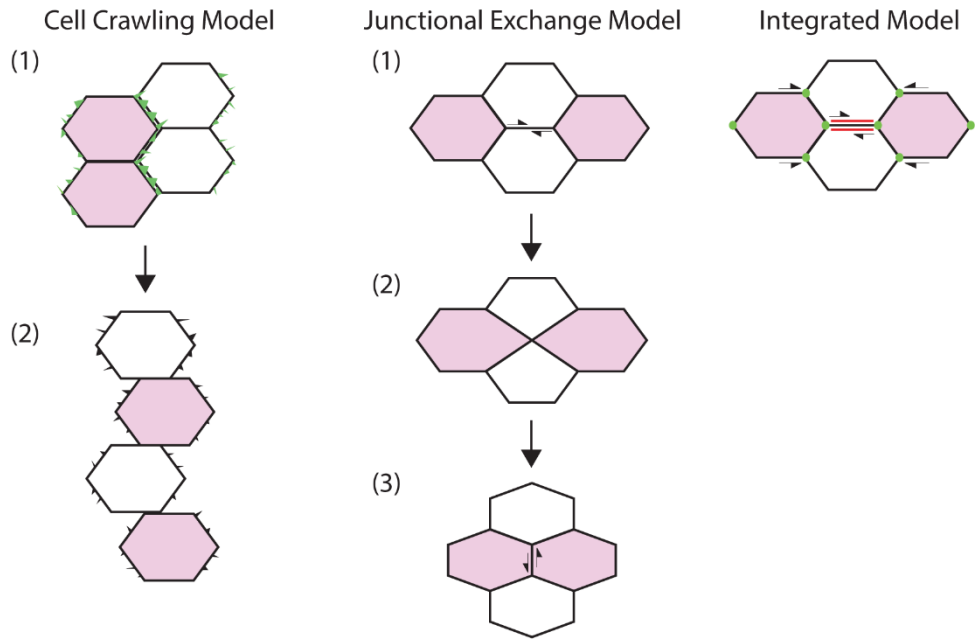

Figure 1.1: Convergent extension is predominantly driven by two cellular behaviors. In the first or "cell crawling model," cells exert traction upon each other and the extracellular matrix through actin rich protrusions (1). This drives intercalation between the cells (2). In the "junctional exchange model", the engagement of actomyosin machinery at specified medial-lateral junctions (1) contract cells to a common vertex (2). These then resolve as a relative anterior-posterior is expanded to rearrange cells (3). In most modern integrated models, these movements are commonly coincidental. Green structures indicate actin rich protrusions, while the red lines indicate contracting actomyosin.

pathway utilizes β-catenin, while non-canonical signalling, the planar cell polarity (PCP) or WNT/$Ca2^{+}$, does not. In the absence of WNT ligand binding cytoplasmic β-catenin is targeted by a destruction complex assembled from Axin, glycogen synthase kinase 3 (GSK3), adenoma polyposis coli (APC) and casein kinase 1 (CK1) (Schaefer et al., 2018; Lui et al., 2022). The complex binds and phosphorylates β-catenin, which targets it for degradation and keeps it from accumulating in the nucleus. Binding of WNT ligands, alleviates this block. WNT ligands produced from either local or distant sources reach the cell membrane where they bind to Frizzled, along with pathway specific co-receptors including ror/ryk and LDL receptor-related proteins 5 or 6 (LRP5/6) (Schaefer et al., 2018; Ren et al., 2021). In the presence of WNT ligands, Frizzled induces a conformational change that phosphorylates the cytoplasmic protein Dishevelled (Dsh/Dvl). Dishevelled then recruits the destruction complex, preventing β-catenin degradation

(Stamos and Weis, 2013; Mukherjee et al., 2018; Schaefer et al., 2018). This allows the cytosolic β-catenin to transpose into the nucleus where it binds and recruits the T-cell factor (TCF)/lymphoid enhancer factor 1 (LEF1) transcriptional complex (Behrens et al., 1996; Cadigan and Waterman, 2012). Nuclear β-catenin may also act independently of TCF/LEF1, diversifying its targets (Doumpas et al., 2019; Mukherjee et al., 2022).

Canonical WNT/β-catenin signaling plays a diverse range of roles during development, including in cell proliferation, fate decisions and morphogenesis (Hayat et al., 2022). This includes a well-established role during of axial establishment in the neuroectoderm (Hierholzer and Kemler, 2010; Range et al., 2013; Shi et al., 2024). Previous studies have shown that several components of the canonical pathway facilitate convergent related defects. This includes leucine zipper tumor suppressor 2 (LZTS2*)*, WNT co-receptor LRP6 and LEF transcription factors XLEF-1 and XTCF-3 (Kühl et al., 2001; Li et al., 2012; Zhao et al., 2022). Loss of *Lzts2, Xlef-1* and *Xtcf-3* during *Xenopus* gastrulation results in shorter dorsalized embryos (Kühl et al., 2001; Li et al., 2012). LZTS2 regulates activity of the canonical pathway by reducing nuclear pools of β-catenin (Li et al., 2012). This, in-turn, leads to mis regulation of BMP and STAT3 signaling, reduced levels of the canonical effectors *Squint/Cyclops* and the non-canonical WNT ligands *Wnt5 and Wnt11.* XLEF-1 and XTFC-3 are LEF/TCF family members which facilitate different transcriptional responses to β-catenin (Kühl et al., 2001). XLEF-1, like its murine homolog LEF-1, promote expression of canonical pathway genes, while XTCF-3 acts as a transcriptional repressor (Pukrop et al., 2001). Injection of RNA for XTCF-3 or one if its target genes, the TGF-β component, Xnr-3 is sufficient to alleviate defects in a dominant negative copy of LEF-1 (LEFΔβBD) (Kühl et al., 2001). XTCF-3 RNA cannot rescue LEFΔβBD but does have an inhibitory effect on convergent extension. Similarly, LRP6 is required during mouse neurulation to facilitate closure of the neuropore (Zhao et al., 2022). Maternal supplementation with a β-catenin agonist is sufficient to reduce spinal NTDs caused by the conditional ablation of LRP6. The role that canonical WNT signalling plays during convergent extension may involve crosstalk with non-canonical WNT/PCP pathways, consistent with antagonistic interactions which have previously been described (Sato et al., 2010). This includes inhibition of non-canonical WNT activity by β-catenin-mediated BMP signaling or the canonical WNT co-receptor LRP6 (Bryja et al., 2009; Li et al., 2012). During Xenopus gastrulation, WNT/β-catenin signaling through XLEF-1 and XNR-3 is also antagonised by WNT/Ca^{2+} activation (Kühl et al., 2001).

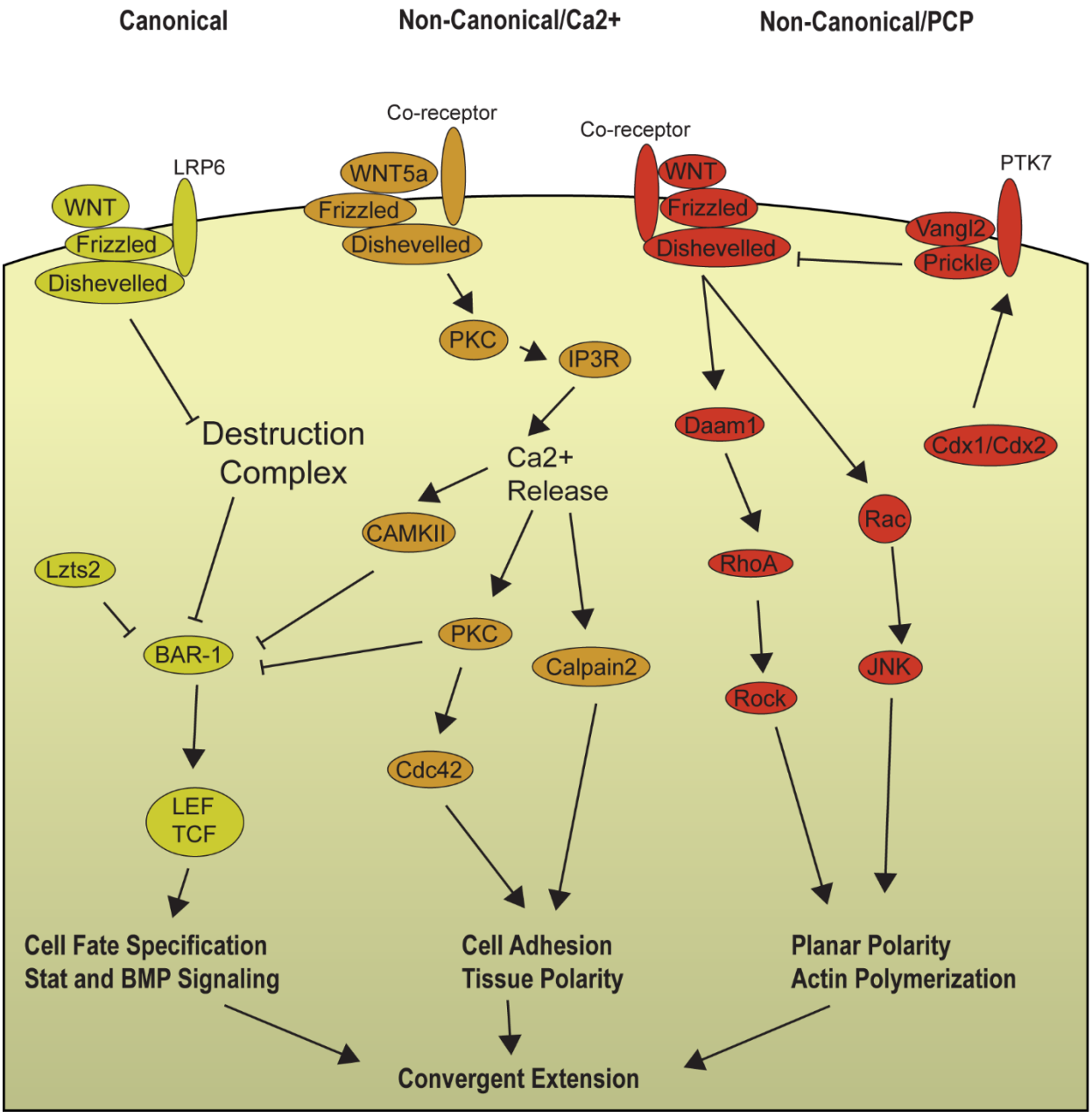

Figure 1.2: Simplified WNT signaling pathways involved in convergent extension.

1.3.2 Non-Canonical WNT/PCP Signalling

The non-canonical branch of WNT signalling, includes several pathways which do not include β-catenin; however, few are as ubiquitous as the planar cell polarity (PCP) pathway (reviewed in Hayat et al., 2022; Qin et al., 2023). First characterised in Drosophila wing hair development, this pathway is conserved throughout the eukaryotes and plays roles in epithelial development, collective cell migration, ciliogenesis and cell fate (Gubb and Garcia-Bellido, 1982; Cui et al., 2013; Hayes et al., 2013; B öttcher et al., 2021). Work in the *Drosophila* epithelium has highlighted that the PCP pathway mediates asymmetric signalling through a core set of five conserved proteins (Tissir and Goffinet, 2010; Davey and Moens, 2016; Wang et al., 2019). These include the proteins: Frizzled, Dishevelled, Van Gogh (Vang), Prickle (Pk) and the cadherin-like receptor Flamingo (Fmi/Celsr). During WNT signalling, binding of a WNT ligand to the frizzled leads to the recruitment and phosphorylation of Dishevelled and activation of downstream effectors including those that regulate cytoskeletal dynamics (Hayat et al., 2022). These include Rac1, Profilin and RhoA (Tanegashima et al., 2008; Lindqvist et al., 2010; Dworkin et al., 2011; Cavanaugh et al., 2020). This recruitment is regulated through inhibition by Vang, its co-receptor PTK7 and Prickle (Jenny et al., 2005).

PCP has a well described role in regulating convergent extension across multiple models including gastrulation and neural tube development (Walck-Shannon and Hardin, 2014; Shindo et al., 2018; Wang et al., 2019). To date, most human mutations that cause defects in primary neurulation target PCP genes (reviewed in Murdoch et al., 2014; Wang et al., 2019). Mutation of multiple PCP components results in disrupted convergent extension, characterised by shortened neural tubes and defective embryo morphology in mice (Curtin et al., 2003; Lei et al., 2019). Similarly, in *Xenopus*, mutations in WNT ligands or the Vang, Prickle and Dishevelled homologs all lead to convergent extension defects and failure of the neural tube to develop properly (Hamblet et al., 2002; Wallingford and Harland, 2002). Control of cell intercalations appears to be facilitated by the polarized distribution of PCP components. In *Xenopus*, WNT mediated phosphorylation and Vangl2 anterior polarization in the neural tube is required for its closure (Ossipova et al., 2015). A similar pattern is observed in the chicken neuroepithelium, where Celsr1 asymmetry in is needed to properly coordinate myosin (Nishimura et al., 2012; Ossipova et al., 2015). Several key factors are downstream of PCP signalling and likely play a

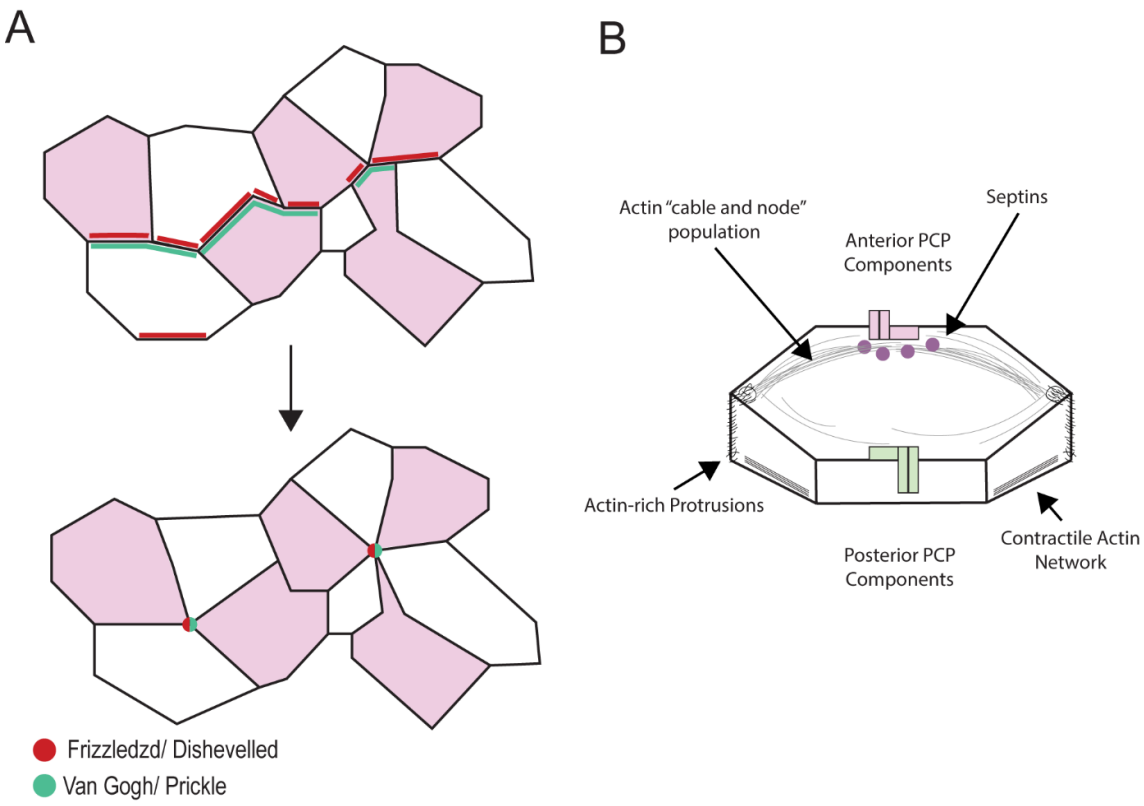

Figure 1.3: Polar arrangement of WNT/PCP pathway components during cell intercalation. (A) Schematic of tissue undergoing cell intercalations and formation of a multicellular rosette, PCP components preferentially associate with contracting junctions and rosette foci. Green and red highlight polarized PCP components. (B) Schematic of a cell undergoing intercalation. Grey highlights three population of actin: actin-rich protrusions, the "node and cable" system and medial-lateral actomyosin. Asymmetric distribution of WNT/PCP components and is facilitated by other proteins like the septins, which mediates the activity and distribution of both the "node and cable" and medial-lateral actin populations.

role in convergent extension, including the Rho/ROCK pathway, Rac, Src and Shroom (Marlow et al., 2002; Habas et al., 2003, Tahinci and Symes, 2003; Jenny et al., 2005; Chen et al., 2018; Andreeva et al., 2014; McGreevy et al., 2015).

Studies into PCP components suggest that the pathway regulates convergent extension through both cell autonomous and non-autonomous mechanisms, which include patterning of asymmetric junctional components and activation of contractile activity (Shindo and Wallingford, 2014; Devitt et al., 2024; Weng et al., 2025) (Figure 1.3). During *Xenopus* gastrulation, mesodermal cells express a medial-lateral and superficial "node and cable" population of actin,

which facilitate intercalation (Shindo and Wallingford, 2014; Devitt et al., 2024). Both populations are polarized in different regards. At shortening junctions, PCP components colocalize with actomyosin and are required for properly timed contractions (Shindo and Wallingford, 2014; Butler and Wallingford, 2018). The "node and cable" population displace an anterior-posterior polarization which is lost when Vangl2 expression is perturbed (Devitt et al., 2024). These roles are in-part facilitated by the septins, a family of cytoskeletal-like proteins which are similarly polarized (Shindo and Wallingford, 2014; Devitt et al., 2024). This maintains the function of the pathway in establishing polarity within Drosophila epithelial cells (Mitchell et al., 2009).

The regulatory role that PCP components exert over collective cell movements also reflect their widespread and varied crosstalk, both regulating and being regulated by other pathways. PCP signaling regulates several other signalling cascades, including the canonical WNT signalling pathway, WNT/Ca2+ pathway and the apicobasal polarity (ABP) pathway (Kühl et al., 2001; Choi and Ham, 2002; Murdoch, 2003; Montcouquiol et al., 2003; Bryja et al., 2009; reviewed in Qin et al., 2023). PCP components are frequently regulated by factors that influence regional identity, temporal dynamics and establish gradients within developing tissues. This includes an important role for the CDX family of *caudal* transcription factors, which establish the axis of the developing embryo and coordinate cell-fate and morphogenesis (van den Akker et al., 2002; Zhu and Lohnes, 2022). As part of this role, CDX1 and 2 are required for convergent extension and play a role in promoting the expression of PTK7 (Savory et al., 2011).

1.3.2.1 PCP Interacting Pathways

Several studies have indicated that fibroblast growth factor (FGF) signalling, which involves extracellular FGF ligands and tyrosine kinase FGF receptors, may regulate CE during neurulation. This includes observations that a reduction in FGF signaling during *Xenopus* and *Drosophila* gastrulation, either through ligand reduction or overexpression of FGF antagonists, leads to embryonic defects (Nutt et al., 2001; Chung et al., 2005). FGF is likewise required for early convergent extension movements in the chick embryo (Lee et al., 2022). These activities intersect with many components of the cytoskeleton directly or through other signaling pathways. Loss of FGF signaling during early embryogenesis is associated with decreased cell protrusions, consistent with a role in the crawling mode of cell intercalation (Chung et al., 2005). FGF activity is associated with the regulation of neurotrophin NRH, the ankyrin repeats domain protein 5

(Anr5), paraxial protocadherin (Papc) and is regulated by the TGF-β protein XNR3 (Chung et al., 2005). Regulation by XNR3 suggests that FGF signalling is at least partially influenced by the WNT/β-catenin pathway (Kühl et al., 2001). Similarly, multiple lines of evidence link FGF activity with the WNT/PCP pathway. FGF expression is required for the correct localization of Dishevelled during notochord formation in *Ciona intestinalis* (Shi et al., 2009). Papc functions through the PCP effectors Rho A and JNK (Unterseher et al., 2004; Chung et al., 2005; Kraft et al., 2012). Taken together, FGF signaling may help regulate WNT signaling during early convergent extension movements, including those that utilize cell crawling.

The finding that FGF and canonical WNT/β-catenin signaling both involve Xnr3, suggest that Nodal/TGF-β may act as a central hub for communication between FGF signaling and the different routes of WNT signalling (Kühl et al., 2001). This aligns with data suggesting that Nodal/TGF-β and WNT/PCP signaling function together during CE in Zebrafish gastrulation (William and Solnica-Krezel, 2020). TGF-β is required both cell-autonomously and non-autonomously, in part, though asymmetric signaling. Similar phenotypes result from loss of transcription factor *Zic3*, which functions upstream of the TGF-β ligand *Nodal* and is required for left-right asymmetry (Cast et al., 2013). Asymmetric signaling promote cell polarity, which together with WNT/PCP, extend the neural plate and blastoderm explants.

BMP signalling and its effectors have been found in studies of convergent extension primarily during gastrulation (Myers et al., 2002; Tucker et al., 2008; Yoon et al., 2021). Mutation of BMP ligands, the receptor *Alk8* or BMP agonist *chordin*, disrupt convergence and extension movements and lead to gastrulation defects (Myers et al., 2002; Tucker et al., 2008). The pathway functions through the establishment of both temporal and special activity gradients. BMP signaling functions downstream of WNT/Ca^{2+}, where it is inhibited by β-catenin activity and interacts with certain heparan sulfate proteoglycans during gastrulation movements in *Xenopus* (Ohkawara et al., 2003). This pathway results in the differential transcription of Smad target genes; including negative regulation of the non-canonical PCP *Wnt11* and *Wnt5a*, as the Xenopus Rho GEF *Arhgef3.2* (Myers et al., 2002; Yoon et al., 2021).

A similar role has been reported for the JAK/STAT signaling cascade, which requires the transiently activated transcription factor signal transducer and activator of transcription (STAT) (Gu et al., 2020). *Xenopus* embryos with disrupted *Stat3* activity develop defects during

gastrulation including a shortened anteroposterior axis, characteristic of CE (Yamashita et al., 2002). *Drosophila* embryos similarly show defects in germband extension (Bertet et al., 2009). JAK/STAT signaling has been shown to intersect with multiple mechanisms which are important for regulation of CE. It is unclear if it connects the same mechanism across multiple tissue types or models. WNT/β-catenin activity regulates *Stat3* signaling during Xenopus gastrulation, placing it downstream of the canonical pathway (Liu et al., 2017). Similarly, during gastrulation in Zebrafish, STAT3 activates non-canonical/PCP signaling through its effector RhoA (Miyagi et al., 2004). In epithelial cells during *Drosophila* germband extension, JAK/STAT regulates actomyosin localization through recruitment of myosin II (Bertet et al., 2009). This function requires both Rho and the cytoskeletal associated protein WASP.

The Shroom family comprises a group of 4 members (Shroom1-4) which contain a PDZ domain and bind to actin (Liu et al., 2024). Previous work has shown that Shroom proteins, particularly Shroom3 in mammals, are required in several models to facilitate CE and apical constriction (Hildebrand and Soriano, 1999; Haigo et al., 2003; Bolinger et al., 2010). These two activities are required for neurulation and subsequent loss of Shroom3 in mice results in failure of neural tube closure and subsequent cranial NTDs (Hildebrand and Soriano, 1999). The activities of Shroom proteins function predominantly through the cytoskeleton and junctional proteins which are responsible for cell adhesion. During neural tube closure, Shroom3 displays asymmetric localization dependent upon interaction with Dishevelled2 (McGreevy et al., 2014). This activity requires PCP signaling, with loss of Shroom3 and Vangl2 or Wnt5a increasing CE related defects. Shroom3 then binds to the Rho kinase Rock, and recruits phosphorylated myosin (Hildebrand, 2005; Nishimura and Takeichi, 2008). The relationship between Rock and Shroom is also observed to regulate actomyosin and rosette dynamics in Drosophila (Simões et al., 2004). This activity synergises with additional interactions between Shroom proteins and F-actin or junctional components including E-cadherin (Hildebrand and Soriano, 1999; Hildebrand, 2005; Bolinger et al., 2010). As Shroom3 expression is limited to limited to the neuroepithelium in both Xenopus and mice, these functions may be tissue specific (Hildebrand and Soriano, 1999; Lee et al., 2009).

The E3 ubiquitin ligase *Mindbomb1* plays a canonical role in Notch/Delta signaling by controlling the amount of Delta/Serrate/Lag2 (DSL) ligand through endocytosis (Borgne et al., 2005; Cao et al., 2024). Injection of a *Mib1* morpholino disrupts CE and reduces the extension of

Zebrafish gastrulation, leading to a widened notochord (Saraswathy et al., 2019). This role may be independent of Notch/Delta signaling and instead seems to require the WNT/PCP pathway. Expression of RhoA has been shown to rescue Mib1 morpholino defects. Mib1 genetically interacts with Wnt5b to regulate the PCP pathway through Ryk endocytosis.

Convergent Extension-Independent Regulation of Neural Tube Development

The above mechanisms function in parallel to additional non-convergent extension roles of PCP signalling within the developing embryo. For example, glycosaminoglycan (GAG) synthesis genetically interacts with PCP components in the developing murine neural tube (Nychyk et al., 2022). Disruption of GAG synthesis when paired with heterozygous *Lp*, resulted in failure of primary neurulation events and the presence of cranial NTDS. These defects, however, do not reflect the failure in neuroepithelial convergent extension found in homozygous *Lp* mutants as midline extension and the length-to-width ratio of embryos remaining normal. Rather the NTDs appear to result from altered neural plate morphology and somite development, which affect neural fold bending (Nychyk et al., 2022). Similarly, the PCP effectors *Inturned* and *Fizzy* are involved with neurulation, with loss of either resulting in NTDs (Heydeck and Lui, 2011). Mutation in either of these two genes, however, reflects a role for the effector in ciliogenesis rather than convergent extension (Heydeck and Lui, 2011; Vogel et al., 2012; Zilber et al., 2013). This demonstrates the diversity of processes which the PCP pathway regulates.

1.3.3 WNT/Ca^{2+} signaling

In addition to signaling through the PCP pathway, WNT activity can facilitate CE through a non-canonical mechanism that involves internal Ca^{2+} stores (reviewed in Hayat et al., 2022; Qin et al., 2023). Unlike canonical WNT or non-canonical WNT/PCP signaling, the WNT/Ca^{2+} signalling is primarily activated by a single WNT/Frizzled pair, *Wnt5a* and the Frizzled receptor *Fzd2* (Slusarski et al., 1997). Activation of Fzd2 recruits a G protein subunit which is responsible for promoting the activity of phospholipase C (PLC) (McQuate et al., 2017). The roles of WNT/Ca^{2+} signaling are predominantly mediated through the activity of PLC, which generates inositol triphosphate (IP3) and diacylglycerol (DAG) (Brown et al., 2008; Vazquez-Manrique et al., 2008). IP3 binds to an inositol triphosphate receptor and triggers intracellular Ca^{2+} release from the endoplasmic reticulum (Berridge, 1993). These intermediaries bind and activate a set of mechanisms. DAG and Ca^{2+} stimulate the activity of protein kinase C (PKC) which triggers actin

polymerization through the GTPase cell–division cycle 42 (CDC42) (Choi and Han, 2002; Schlessinger et al., 2007). Changes to Cdc42 expression block CE movements in Xenopus embryos undergoing gastrulation (Choi and Han, 2002). This may involve changes to cell adhesion, though Cdc42 has additional functions which could facilitate its role (Choi and Han, 2002; Walck-Shannon et al., 2016; Schlessinger et al., 2007). Intracellular Ca^{2+} levels also drive transcriptional responses, though the impact of these on convergent extension is less certain. As Ca^{2+} is released it binds to calcineurin and CAMKII. Calcineurin activates the transcription factor nuclear factor of activated T cells (NFAT), which promotes transcription but has not been associated with convergent extension (Heit et al., 2006). CAMKII stimulates a pathway which results in phosphorylation and inhibition of TCF, which antagonizes canonical WNT signaling during CE (Kühl et al., 2001). A mechanism, which involves the protease Calpain2 and Dact scaffolding proteins also regulates convergent extension (Zanardelli et al., 2013; Carroll et al., 2024). Pharmacological or genetic inhibition of Calpain activity is sufficient to impair medial-lateral intercalations and animal cap elongation in Xenopus (Zanardelli et al., 2013).

The roles that WNT/Ca^{2+} signaling plays during convergent extension suggest that tight regulation of the pathway is required. During *Xenopus* gastrulation either overexpression of WT Cdc42 or a dominant negative construct are both able to interfere with the process (Choi and Han, 2002). Similarly, Wnt5a and Calpain2 show a reciprocal relationship that is often associated with highly regulated mechanisms (Zanardelli et al., 2013). This aligns with previous research, showing that junctional contractions during CE are patterned by transient Ca^{2+} oscillations (Cogram et al., 2004; Politi et al., 2006; Mound et at al., 2017). Disruption of Ca^{2+} signalling is sufficient to decreased axial elongation and convergent extension (Wallingford et al., 2001; Westfall et al., 2003). Thus, WNT/Ca^{2+} signaling may play a role in propagating the tightly regulated Ca^{2+} oscillations which are required for collective cell movements.

1.3.4 PCP Independent Regulation of Collective Cell Movements

One notable exception to the importance of PCP regulation during CE, is found during germband extension in *Drosophila*. Here, loss of Frizzled receptors or Dishevelled is insufficient to significantly disrupt extension of the tissue, suggesting that CE is regulated independently of PCP activity (Zallen and Wieschaus, 2004). Instead, this process is believed to be mediated through the *Pair-wise* family, as well as the receptors *toll-2*, *toll-6* and *toll-8* (Irvine and

Wieschaus, 1994; Zallen and Wieschaus, 2004; Paré et al., 2014). Expression of Pair-wise family members and Toll receptors creates a positional code which patterns Myosin II and PAR-3 to direct convergent extension. Given that the PCP pathway still regulates polarity and asymmetry of junctional proteins, this data supports that the idea that the PCP pathway may regulate mechanisms of CE in parallel to tother mechanisms (Warrington et al., 2013; Kong et al., 2017).

Nuclear Hormone Receptors

Nuclear hormone receptors (NHRs) are a group of transcriptional regulators that facilitate diverse roles throughout development, this includes roles in cell migration proliferation, gastrulation and mammalian neurulation (Duncan et al., 1997; Wendling et al., 1999; Chomez et al., 2000; Barreto et al., 2003; Bhattacharya and Starz-Gaiano, 2024). The activity of most NHRs is regulated through the binding of ligands, though a subset of receptors are considered "orphans" for which no ligand is known (reviewed in Weikum et al., 2018; Tao et al., 2020). NHRs can be grouped into six subfamilies based on sequence conservation and the type of ligands that they bind to. These families are incredibly diverse, facilitating cellular responses to steroid and lipophilic metabolites as well as signaling pathways through orphan receptors (Weikum et al., 2018). Most NHRs from all families share a similar structural composition comprised of 5 domains (Figure 1.4A). These include a disordered N-terminal domain, DNA binding domain, hinge domain and ligand binding domain (Helsen et al., 2012; Rastinejad et al., 2013; Weikum et al., 2018). Within the N-terminal and ligand binding domains, two activation function surfaces (AF-1 and AF-2) are important to the interaction of NHRs with co-repressors and -activators (Teotico et al., 2008; Weikum et al., 2018). Receptors can also be grouped based on common mechanisms (Figure 1.4B). Briefly, type 1 receptors normally localize to the cytoplasm but translocate to the nucleus upon ligand binding. The other three types of receptors localize to the nucleus and switch between repressive and activation of genes based on the binding of their ligands; these types differ in the types of complexes they form and the types of sites that they recognize (Weikum et al., 2018).

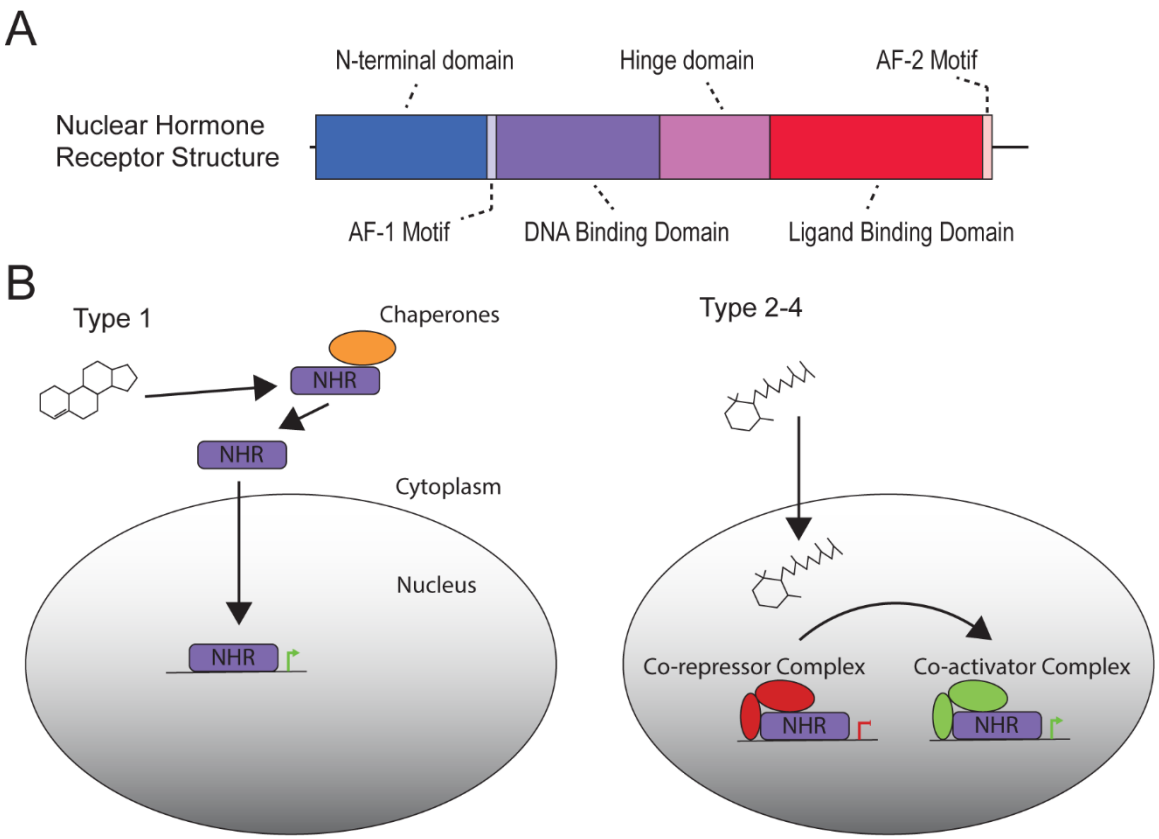

Figure 1.4: Nuclear hormone receptor (NHR) structure and mechanism of action. (A) The NHR family shares a core structure which consists of several domains. Within the N-terminal domain and ligand binding domain are AF-1/2 motifs which commonly associate with binding of coactivators and corepressors. (B) NHRs can work through 4 mechanisms; in the first binding of a ligand (ex. androgen) leads to the translocation of a cytosolic NHR, which facilitates its activity. In the other three mechanisms, a ligand (ex. retinoic acid) enters the nucleus and facilitates the exchange of complexes that regulate receptor activity. Receptors which function through this mechanism, can function as monomers, homodimers or heterodimers.

One subgroup of NHRs with important roles in neurulation and CE are the retinoic acid receptor (RAR) family. These receptors bind the extracellular metabolite all-trans-retinoic acid (conventionally referred to as retinoic acid or RA), which is synthesized from vitamin A (Cunningham and Duester, 2015). Inhibition of RA signaling, either through pharmacological or genetic disruption of the biosynthetic pathway, results in delayed gastrulation and decreased elongation of Xenopus embryos and growth defects in mouse embryos (Mic et al., 2002; Gur et al., 2022; Koch et al., 2025). In particular, the neural tube displays morphological defects and

mispositioning of cytoskeletal and junctional elements (Wilson et al., 2003). Similar results in Xenopus embryos lacking the enzyme short-chain dehydrogenase/reductase 3, which attenuates RA synthesis, show that embryos display defective CE (Kam et al., 2013). While retinoic acid signaling intersects the noncanonical WNT/PCP pathway, though the molecular mechanism through which it mediates gastrulation and neurulation have not been fully described. During both gastrulation and neurulation, RAR function includes activation of transcription factors which regulates components of WNT/PCP signaling (Houle et al., 2003; Savory et al., 2011; Gur et al., 2022). This signaling pathway compliments CE-independent functions of RARs, including the regulation of hindgut endoderm proliferation and axial segmentation, which contribute to its role during development (Chen et al., 1995; Onai et al., 2009; Cunningham and Duester, 2015).

1.3.5 Inositol Phosphate Metabolism

Inositol phosphates, a class of metabolites which are derived from the 6-carbon sugar inositol, have a wide range of intracellular roles (reviewed in Tsui and York, 2010; Greene et al., 2017; Tu-Sekine and Kim, 2022). These include participation in prominent intracellular signaling pathways and regulation of rRNA synthesis, mRNA export, ciliogenesis, ion channel function and vesicle trafficking (Norris et al., 1995; York et al., 1999; Hanakahi et al., 2000; Yang et al., 2001; Høy et al., 2002; Brehm et al., 2013; Gao and Wang, 2007; Otto et al., 2007; Sarmah et al., 2007; Maag et al., 2011). Intracellular IP derivatives can also act through regulation of cation stores and form complexes that modulate metabolism within the cellular environment (Kumar et al., 2010; Tu-Sekine and Kim, 2022). Through these roles, inositol derivatives regulate several developmental processes, including left-right organ asymmetry in zebrafish, neuronal differentiation, migration of the tracheal branches in *Drosophila,* and mammalian neurulation (Sarmah et al., 2007; Frederick et al., 2005; Wilson et al., 2009; Loss et al., 2013; D'Souza et al., 2020; Ucuncu et al., 2020).

Inositol is metabolized through biosynthesis pathways, which make use of dietary sources of myo-inositol, alternative synthesis from glucose and an elaborate pathway of kinases and phosphatases (Figure 1.5). The first or "lipid dependent pathway", involves incorporation of inositol into the lipid phosphotydylinositol (PI) (Shewan et al., 2011). Phosphatidylinositol are important intracellular signals on their own and forms the basis of glycosylphosphatidylinositol (GPI) anchors (reviewed in Kinoshita and Fujita, 2016; Hammond and Burke, 2020). One

important step in the PI biosynthesis is production of the membrane lipid phosphatidylinositol 4,5-bisphosphate (PIP2), a precursor for phosphatidylinositol 3,4,5-triphosphate (PIP3). Under physiological conditions, including during WNT/Ca^{2+} signalling, PIP2 is cleaved by Phospholipase C (PLC) to release inositol triphosphate (IP3) along with diacylglycerol (DAG) into the cytoplasm (Brown et al., 2008; Vazquez-Manrique et al., 2008). A second, recently characterised "lipid-independent" or "cytosolic" pathway involves direct phosphorylation of myo-inositol (Desfougeres et al., 2019). Here, glucose-6-phosphate or dephosphorylated myo-inositol phosphate can be converted into IP3 through two enzymes, inositol 3-phosphate synthase and inositol tetrakisphosphate 1-kinase. This mechanism is favored under conditions that reduce inorganic phosphate levels (Desfougeres et al., 2019). IP3 can be further phosphorylated into other inositol phosphate species that serve as intercellular signals, including inositol hexaphosphate (IP6) and the inositol phyrophosphates (Menniti et al., 1993; Stephens et al., 1993; Fridy et al., 2007; González et al., 2010; Márquez-Moñino et al., 2024). Catabolism of inositol hexaphosphate by Multiple Inositol Polyphosphate Phosphatase (MINPP1), and several 1- and 5-phosphotases can subsequently recycle myo-inositol levels (Trung et al., 2022). The most abundant intracellular inositol phosphate species is IP6, though exact concentrations can vary between cell types and organisms (Letcher et al., 2008; Qui et al., 2020)

Inositol is a potent regulator of neural tube development, suggesting that it may play a role in convergent extension (Figure 1.6). Inositol deficiency leads to cranial NTDs among WT mice and is enhanced in *curly tail*, a genetic model for folate-resistant NTDs which possesses a hypomorphic mutation in the *grainyhead-like-3* transcription factor (Cockroft et al., 1992; Gustavsson et al., 2007; Burren et al., 2009; Leung et al., 2024). Conversely, supplementation of *curly tail* mice with inositol is sufficient to significantly reduce NTDs (Greene and Copp, 1997). Several mechanisms currently describe the role of inositol metabolism during neurulation and potentially link the pathway to convergent extension. First, neural tube defects appear frequently in mice with mutations that disrupt the synthesis of phosphoinositides and proteins with GPI anchors (Piedrahita et al., 1999; Jacoby et al., 2009; Lukacs et al., 2019; Voigt et al., 2025).

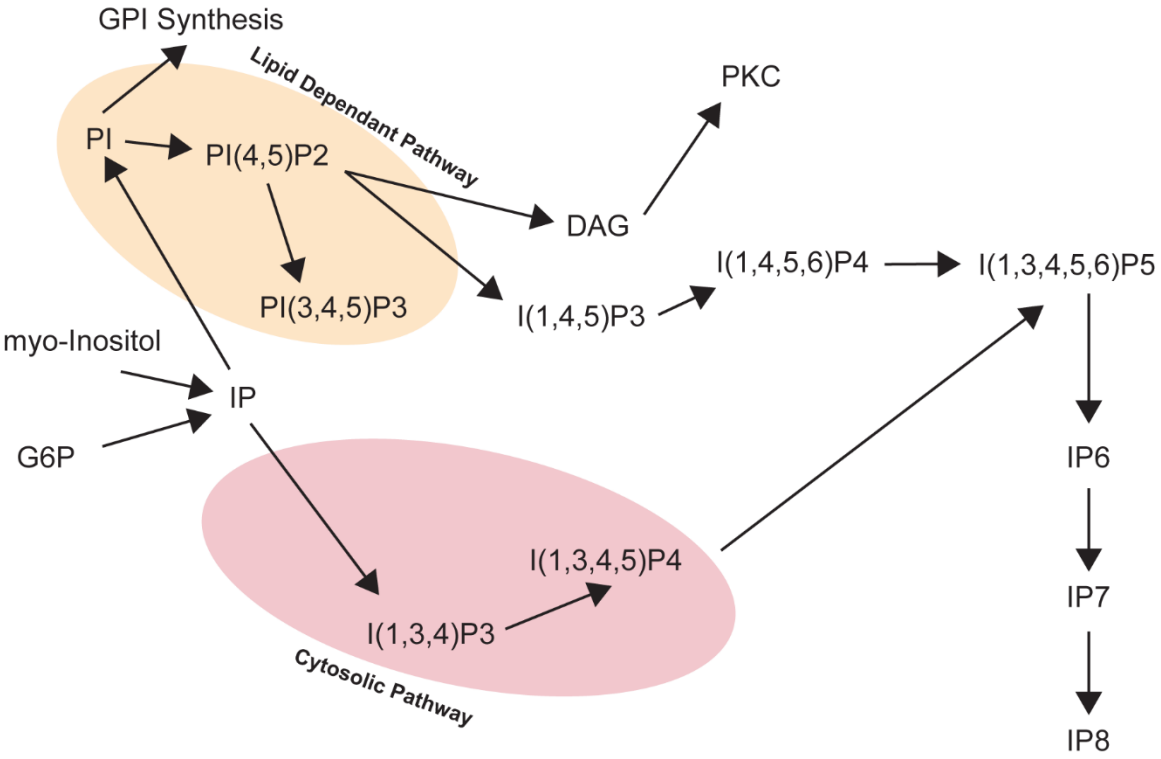

Figure 1.5: The inositol metabolic pathway. Prominent metabolites produced by inositol and phosphatidylinositol phosphate kinases are shown. Light and dark orange highlight lipid and cytosolic portions of the pathway that produce inositol pentakisphosphate.

These groups have a wide range of functions in regulation of cytoskeletal proteins and roles in cell-cell intercalation (Ahrens et al., 2009; Xie and Bankaitis, 2022). This includes regulation of actomyosin networks by PIP2 and PIP3 through the kinase AKT, GTPase Rac, Cdc42 and trafficking of PCP components (Montero et al., 2003; Miao et al., 2022; Xie and Bankaitis, 2022; Hou et al., 2025) (Figure 1.6A). PIP2 and PIP3 additionally interact with other portions of the inositol phosphate pathway under various contexts. Inositol polyphosphate multikinase (IPMK) can bind and phosphorylate PIP2 (Maag et al., 2011; Blind et al., 2012). Inositol phosphate species, including IP6, can competitively bind and inhibit PIP3 interactions or one of its downstream targets AKT (Chakraborty et al., 2010; Chen et al., 2017). Secondly, inositol metabolism plays a critical role in the WNT/Ca^{2+} pathway (Figure 1.6B). Hydrolysis of PIP2 at the cell membrane releases DAG and IP3. DAG is thought to be a potent stimulator of PKC activity, which in-turn, upregulates expression of the retinoic acid receptor β as well as promotes Cdc42-dependent actin polymerization (Greene and Copp, 1997; Garcia-Bermejo et al., 2002). Retinoic acid receptor β, a

member of the nuclear hormone receptor family, has previously been shown to regulate convergent extension and cell proliferation (Yamada, 1994; Chen et al., 1995; Greene and Copp, 1997; Kam et al., 2013). The hydrolysis of PIP2 also releases IP3, along with DAG, which binds to its receptor and triggers intracellular calcium release from the endoplasmic reticulum (Miyakawa et al., 2001). This event is critical to WNT/Ca^{2+} signalling and, as previously discussed, likely contributes to activation of actomyosin and adhesion dynamics at cell junctions (Wallingford et al., 2001).

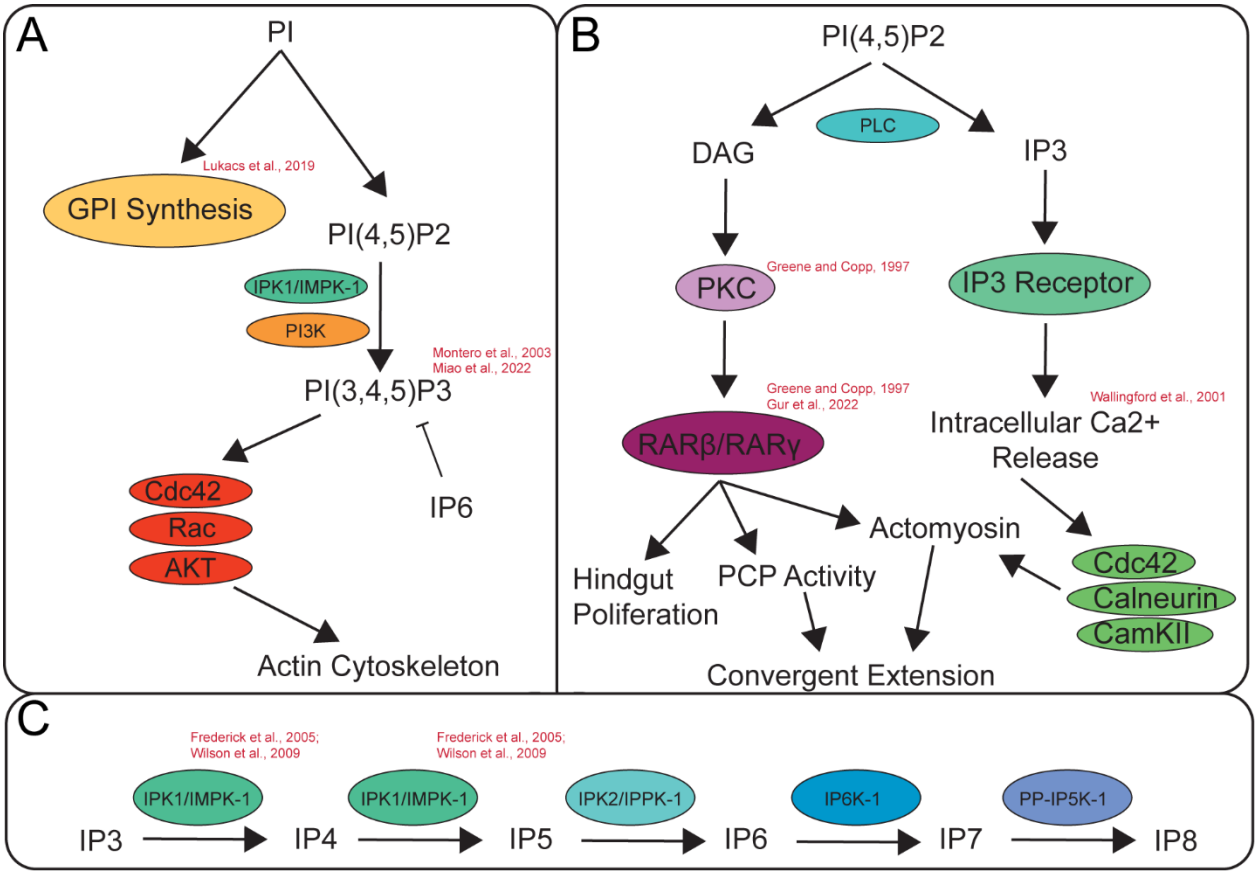

Figure 1.6: Phosphatidylinositol phosphate and inositol phosphate metabolism interact with neural tube development and convergent extension at multiple points. (A-D) Schematic of mechanisms which regulate convergent extension, neural tube development or interact with the cytoskeleton. Red citations highlight studies which have evidence linking disruption with developmental defects. (A) Phosphatidylinositol is a major component of GPIs, PIP2 and PIP3. PIP3 has been shown to interact through multiple proteins with the cytoskeleton. (B) PIP2 hydrolysis during WNT/CA^{2+} signaling produces both DAG and IP3 which can affect multiple pathways involved with convergent extension. (C) Inositol phosphate metabolism requires multiple kinases to progressively phosphorylate IP3. Of these *IPMK-1/IPK1* has been implicated in neural tube defects.

In addition to the relatively well described mechanisms through which DAG and IP3 regulate neurulation and convergent extension, if and how more phosphorylated forms of inositol regulate the process is still poorly explored. Several lines of evidence suggest that IP5 or IP6 are important for neural tube closure. Mice with disruption of inositol metabolism through reduction of inositol polyphosphate multikinase (*Ipmk*) or inositol triphosphate 5,6- kinase (*Itpk1*) display lethality during neurulation (Frederick et al., 2005; Wilson et al., 2009). These two enzymes are responsible for the phosphorylation of IP3 species to IP5 (Figure 1.6C). Arrested embryos in these mutants show features which are consistent with failed neural tube development, including abnormal neural tube morphology, a shortened anterior-posterior axis and exencephaly (Frederick et al., 2005; Wilson et al., 2009). Both proteins are also expressed within the developing neural tube. *Ipmk* is expressed throughout the neural tube by E8.5 (Frederick et al., 2005). Similarly, analysis of ITPK1 expression between E8.5 and E12.5 shows that it can be found throughout the neural tube, including the neural epithelium and paraxial mesoderm (Wilson et al., 2009). Genomic characterisation of human populations has also identified single nucleotide polymorphisms (SNPs) in inositol triphosphate 5/6- kinase as risk factors for NTDs (Guan et al., 2014; Guan et al., 2023). Given the diversity of mechanisms which inositol phosphates participate in and the lack of evidence for direct convergent extension defects in these mutants, however, the role of higher inositol phosphates during embryogenesis and neurulation remains unclear.

1.4 The *C. elegans* VNC as a Model for Convergent Extension

1.4.1 *C. elegans* as a Model Organism

For the past 50 years, the free-living soil nematode *Caenorhabditis elegans* (*C. elegans*) has been a common model organism for biological and genetic studies (Brenner, 1974). Several features contribute to their usefulness, including: a relatively small size, transparent body, large number of progeny and short lifespan. Nematodes develop through a series of larval stages (L1-L4), reaching maturity within 3 days at room temperature (Figure 1.7). In addition, the majority of *C. elegans* are hermaphrodites, which allows for the self-propagation of experimental strains. The adult hermaphrodite contains 959 cells, which develop along stereotypical lineages and can be tracked from early embryogenesis (Sulston et al., 1983; Aydin et al., 2010; Maduro et al., 2010). Of these cells, about a third form the hermaphrodite nervous system (White et al., 1986).

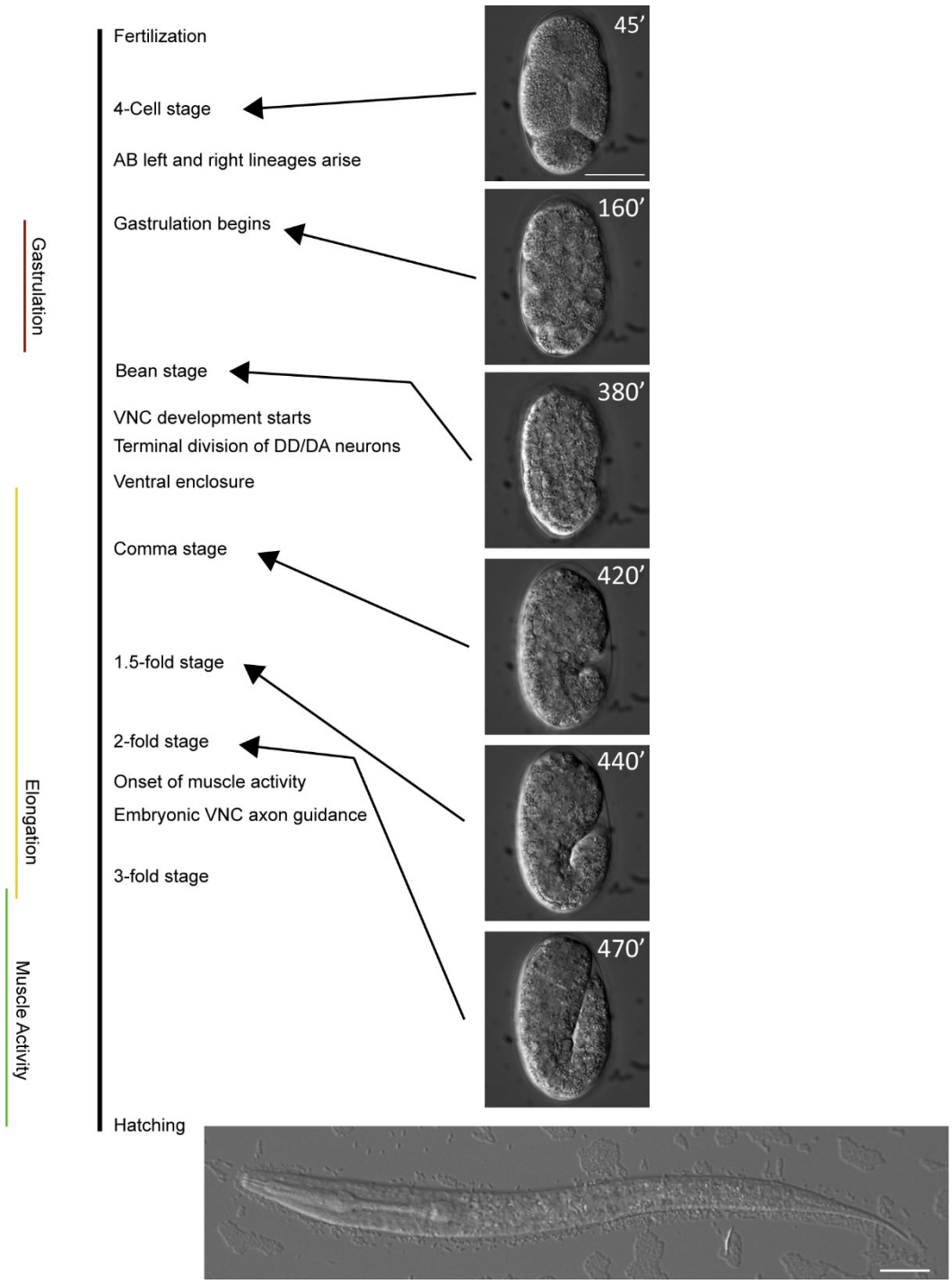

Figure 1.7: Timeline of *C. elegans* embryonic development. The major stages and processes of embryonic development are shown in from fertilization until hatching. Brightfield images taken from a timelapse demonstrate the appearance of the embryo at their relative stages. The time from fertilization is indicated in the top right of each image. Scale bar = 20um.

Prior research has fully sequenced the nematode genome, provided a complete map of synaptic connections and an extensive list of cell fate markers for different populations of neurons (*C. elegans* Sequencing Consortium, 1998; Cook et al., 2019, Yemini et al., 2020; Mulcahy et al., 2022; Poole et al., 2024). This work has also illustrated that 40% of the worm genome has functional orthologs in mammals (*C. elegans* Sequencing Consortium, 1998).

Nematodes are particularly amenable to genetic manipulation, through either the introduction of transgenic arrays or gene editing. Their genome encodes approximately 19,500 protein encoding genes (Hillier et al., 2005). Specific genes can be knocked out permanently with CRISPR/Cas9 methods or in a conditional, tissue-specific manner using ligand regulated degradation systems (Dickinson and Goldstein, 2016; Au et al., 2019; Ashley et al., 2021). Similarly, these methods can also be used to express fluorescent proteins to label cellular or sub-cellular structures (Dickinson and Goldstein, 2016). The transparency of nematodes allows for *in-vivo* imaging, such as fluorescence time lapse microscopy. Forward genetic approaches, such as mutagenesis screens, are equally essential tools during nematode research (Jorgensen and Mango, 2002; Lehrbach et al., 2017). These take advantage of the rapid nematode life cycle and large amount of progeny to identify alleles of interest. One commonly used protocol involves introducing point mutations into germ cells by soaking L4 stage worms in ethyl methanesulfonate. The large number of progeny from these mutagenized worms can then be screened to identify genes that affect a phenotype of interest. The ease of genetic manipulation and transparency of nematodes allows most research to be conducted *in-vivo*.

1.4.2 VNC Morphogenesis and Structure

The ventral nerve cord (VNC) of *C. elegans* is a tract of neurons that runs along the ventral side of worm in an anterior-posterior configuration (White et al., 1976) (Figure 1.8A). The VNC is comprised of 22 embryonically derived motor neurons, with an additional 75 that arise post-embryonically (White et al., 1976; Sulston, 1976; Sulston et al., 1983; Zhen and Samuel, 2015). At hatching, this includes three classes of motor neurons, 6 DD, 9 DA and 7 DB (Li et al., 2022). DA and DB neurons express the excitatory neurotransmitter acetylcholine, whereas the DD neurons express inhibitory GABA. Anterior and posterior located neurons of the VNC form ganglia with two main sets of interneurons (Emmons, 2024). DD1, DB1, DB2 and DA1, in the anterior are part of the retrovesticular ganglion (RVG), while DD6, DA8 and DA9 in the posterior,

are in the pre-anal ganglion (PAG) (White et al., 1976; Sulston et al., 1983; Emmons, 2024). These identities are established based on a combination of transcriptions factors, prominently from the homeobox (HOX) and NHR families, which segment the anterior, mid-body and posterior domains of the nerve cord (Taylor et al., 2021; Smith et al., 2024; Smith and Kratsios, 2024). Most neurons in the VNC form motor neuron units (typically comprised of 1 neuron from each sub-class), which innervate wall muscles on opposing sides and facilitate sinusoidal motion (Zhen and Samuel, 2015; Olivares et al., 2021). Recent molecular characterization and RNA sequencing has shown that by the L4 larval stage, VNC neurons can be further classified into 11 subclasses (Taylor et al., 2021; Smith et al., 2024). The molecular differences between these subclasses helps to define their connectivity, for example slight differences between with the unique synaptic pattern of DA1 (located in the RVG), DA2-DA5, and DA9 (located in the PNG).

Most neurons in *C. elegans*, including those of the VNC, are descendants of the AB blastomere (Sulston et al., 1983). This cell eventually divides into the posterior precursor neurons ABpl and ABpr, which establish the left and right sides of the VNC. Specification of neuronal precursors from these lineages require the activity of proneural transcriptions factors, which include the basic Helix-Loop-Helix transcription factor CND-1 and HOX transcription factor CEH-13, homologs of *NeuroD1* and *Labial*, respectively (Fox et al., 2005; Aquino-Nunez et al., 2020; Poole et al., 2024; Smith et al., 2024). Loss of either CND-1 or CEH-13 results in misspecification of neurons that become part of the VNC, including a loss of DD neurons (Aquino-Nunez et al., 2020). Following involution of mesodermal tissue during gastrulation, at around 200 minutes post-fertilization, morphogenesis of the VNC begins (Figure 1.8C and D) (Shah et al., 2017). Left and right precursors of the VNC begin to undergo a series of asymmetric cell divisions that give rise to the three embryonic subtypes. As the terminal divisions of these neuronal precursors finish, their cell bodies begin to move towards the midline of the embryo. Prior to reaching the midline, VNC neuron precursors undergo an initial series of junctional contractions and cell intercalations. These arrange DA and DD neuron precursors into an alternating pattern; wherein DD precursors are flanked by DA neurons toward the outside of the embryo (Figure 1.8D) (Shah et al., 2017). Additionally, a subset of the DB precursors become located dorsally to DA and DD precursors. Neuronal movements occur at the same time as the

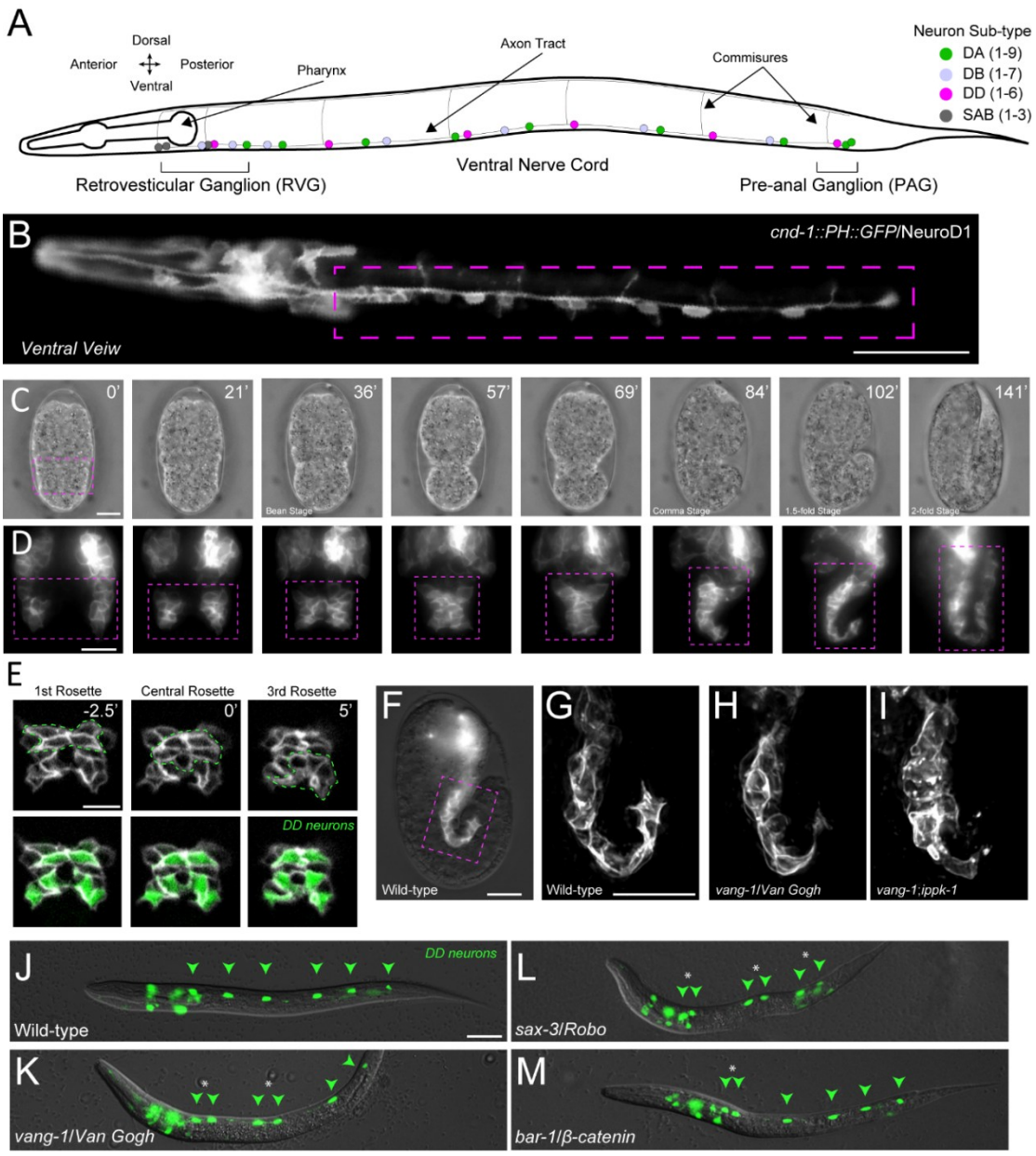

Figure 1.8: Ventral nerve cord assembly in *C. elegans*. (A) Schematic of the larval VNC. (B) Ventral view of the VNC using *cnd-1::PH::RFP* which is expressed within most DD and DA neurons. (C-D) Timelapse of VNC development showing (C) brightfield images of the embryo and (D) *cnd-1::PH::RFP* expressing cells. The magenta boxes show the approximate area of the VNC. (E) Sequential rosettes mediate VNC development. A hashed green line indicates the site of rosettes. Bottom panels: DD neurons express OP395. (F-I) VNC at 1.5-fold stage in WT (F-G), *vang-1* (H) and a double mutant (I) showing disrupted VNC development. The magenta hashed box in (F) indicates the placement of the VNC. (J-M) DD neurons in WT and mutant larvae expressing a reporter (*ynIs37[flp-13p::GFP]*) for DD neurons. Scale bar for embryos = 20um. Scale bar for larvae = 20um.

migration and constriction of ventral epithelial cells at the midline, which lies ventral to the developing neural tissue (George et al., 1998; Wernike et al., 2016). Data suggests that the two processes may influence each other (Wernike et al., 2016). Indeed, blocking cell division or disruption of non-muscle myosin in neuron precursors alters ventral epithelial development.

Upon reaching the midline, neurons of opposing sides undergo a series of coordinated cell-cell junctional arrangements which constrict mediolateral junctions. This movement allows subsets of neuron precursors to form multicellular rosette-like arrangements, where 5 or 6 cells meet at a common vertex (Shah et al., 2017). Rosettes form and resolve sequentially along the midline from anterior to posterior (Figure 1.8E). The resolution of rosettes helps to dive convergent extension and reorient neuronal precursors. As a result, the VNC constricts along the mediolateral axis and extends along the anteroposterior axis. As the worm elongates, DB neuroblasts radial intercalate into the tract. This latter part of VNC elongation, taking place from 1.5- to 2-fold stage onward, occurs during elongation of the embryo, outgrowth of axons and the onset of muscle activity (Figure 1.8F-I). By the time of hatching, the VNC consists of a single tract of cell bodies with a stereotypical order and spacing (Shah et al., 2017; Saharkhiz et al., 2025).

Table 1.1: Relevant alleles found in a forward genetic screen for VNC neuron distribution (A. Colavtia, unpublished).

Gene	Orthologue	Alleles Identified	Role
vang-1	VANGL	2	Non-Canonical WNT/PCP Signaling
prkl-1	PRICKLE	2	Non-Canonical WNT/PCP Signaling
sax-3	ROBO	2	Non-Canonical WNT/PCP Signaling
bar-1	B-Catenin	3	Canonical WNT/Notch Signaling
pry-1	AXIN	1	Canonical WNT/Notch Signaling
ippk-1	IPPK/IP5K	1	Inositol Phosphate Metabolism
pal-1	CDX1/CDK2	3	Homeobox TF
sex-1	RAR/ROR/REV-ERB	3	Nuclear hormone receptor

1.4.3 Regulation of VNC Morphogenesis as a Model to Study Collective Cell Movements

Two groups of genes are important for the arrangement and spacing of VNC neurons during embryonic morphogenesis. The first group of genes regulate rosette-mediated convergent extension during the intercalation of VNC precursors at the midline (Shah et al., 2017). These include components of the PCP pathway in the VNC assembly process (Shah et al., 2017). Loss of the core PCP components VANG-1/Van Gogh and PRKL/Prickle resulted in lengthened multicellular rosette lifetimes and delays of terminal cell-cell intercalations (Figure 1.8J-M). Rosette lifetime and neuron distribution defects are enhanced by mutation of the *Robo* homolog SAX-3, a receptor that is known for its role in axon guidance (Zallen et al., 1998; Shah et al., 2017; Alan et al., 2018). *sax-3* and *vang-1* double mutants are substantially worse, with central rosettes that have a lifetime more than 4-fold longer than that of WT embryos and 2-fold longer then in either individual mutant (Shah et al., 2017). These delays produce a significantly shortened VNC with most neuronal cell bodies displaced in the anterior half of the worm at hatching. Interestingly, while *Slit*, the ligand for Robo, has been implicated in collective cell movements, including CE during zebrafish gastrulation, the extent of a conserved function is unclear (Yeo et al., 2001; Challa et al., 2005; Giovannone et al., 2012). Mutation of the *Slit* homolog, *slt-1* fails to perturb VNC assembly. This suggests that in nematodes the involvement of SAX-3 is independent of its role as a receptor for SLT-1 and functions cooperatively with PCP signalling during VNC assembly.

Mutation in several genes also suggest that left-right asymmetry of the VNC during embryogenesis contributes to neuron arrangement and position (Chan et al., 2025). Mutation in the β-catenin homolog *bar-1* or the *Axin* homolog *pry-1* leads to displacement of anterior DA, DB and DD neuron cell bodies (Figure 1.8J-M) (Evans, 2018; Chan et al., 2025). The role of β-catenin during VNC development involves asymmetry, as BAR-1 is only expressed in right-originating DA and DD neurons. Rather than functioning through the canonical WNT pathway, BAR-1 is instead regulated by Notch dependant expression of PRY-1 in left-originating motor neurons. Loss of WNT signalling in the mutant allele of *mig-14*/Wntless, which is required for the secretion of WNT ligands, does not phenocopy *bar-1* mutants (Chan et al., 2025). Instead, loss of Notch/LIN-12 or C Promoter Binding factor (CBF1)/LAG-1, results in decreased PRY-1 and symmetric expression of BAR-1 (Chan et al., 2025).

1.5 Study Objectives and Rational

Convergent extension is important in the morphogenesis of the VNC in *C. elegans*. Early VNC development shares multiple commonalities with mammalian neural tube development including several components from both the canonical/β-catenin, Notch and non-canonical/PCP pathways. Despite these findings, the genetic landscape required for early VNC development and convergent extension is still relatively poorly understood in comparison to other models. What other signaling pathways and mechanisms pattern canonical and non-canonical WNT signaling spatially within the VNC or temporally during late embryogenesis? Utilizing the embryonic VNC, this thesis aims to explore regulatory pathways that function during development, with a focus on components which may be conserved between nematodes and other models.

To identify cellular and molecular mechanisms that are required for embryonic development of the VNC, a screen for mutants that disrupted the equidistant position of DD neurons was performed (Colavtia, unpublished; Table 1.1). This screen identified alleles which contain mutations in genes that have previously been associated with VNC morphogenesis. Additionally, several alleles found in this genetic screen contain mutations in the genes *ippk-1* and *pal-1*. *ippk-1* encodes a kinase that is orthologous to the mammalian inositol pentakisphosphate kinase 1 (IPPK1/IP5K) (Figure 1.9). Inositol phosphate production has been shown to be involved with nematode development and membrane biology, however, in comparison to its mammalian homolog the role of IPPK-1 is poorly characterized (Vazquez-Manrique et al., 2008; Lowry et al., 2015; Yang et al., 2021). *pal-1* encodes a *caudal* homologue with similar roles to the mammalian CDX family (Figure 1.10). This includes roles in regulating cell fate determination during early embryogenesis and in cell migration (Hunter and Kenyon, 1996; Edgar et al., 2001; Maduro et al., 2005; Gilbert et al., 2020). The alleles of *ippk-1* and *pal-1* found in the screen produce robust and severe displacement of neuronal cell body positions along the VNC. Disruption of *ippk-1* resembles defects observed in *sax-3* and *vang-1* loss-of-function mutants. The defects observed in *pal-1* mutants also resemble another set of alleles found in the genetic screen, caused by mutations in the nuclear hormone receptor *sex-1*, as both severely affect posterior DD type motor neurons. Our study seeks to explore the role of the inositol phosphate kinase *ippk-1* and caudal transcription factor *pal-1* play in the developing VNC of *C. elegans*.

In line with this rational, this dissertation pursued several objectives:

1. Characterize the impact of disrupting *ippk-1* or *pal-1* during VNC assembly.

2. Determine if either gene interacts with the PCP pathway or SAX-3.
3. Explore the role of *ippk-1* in neuronal progenitor movements during assembly of the VNC.
4. Investigate the potential interaction between *sex-1* and *pal-1*.

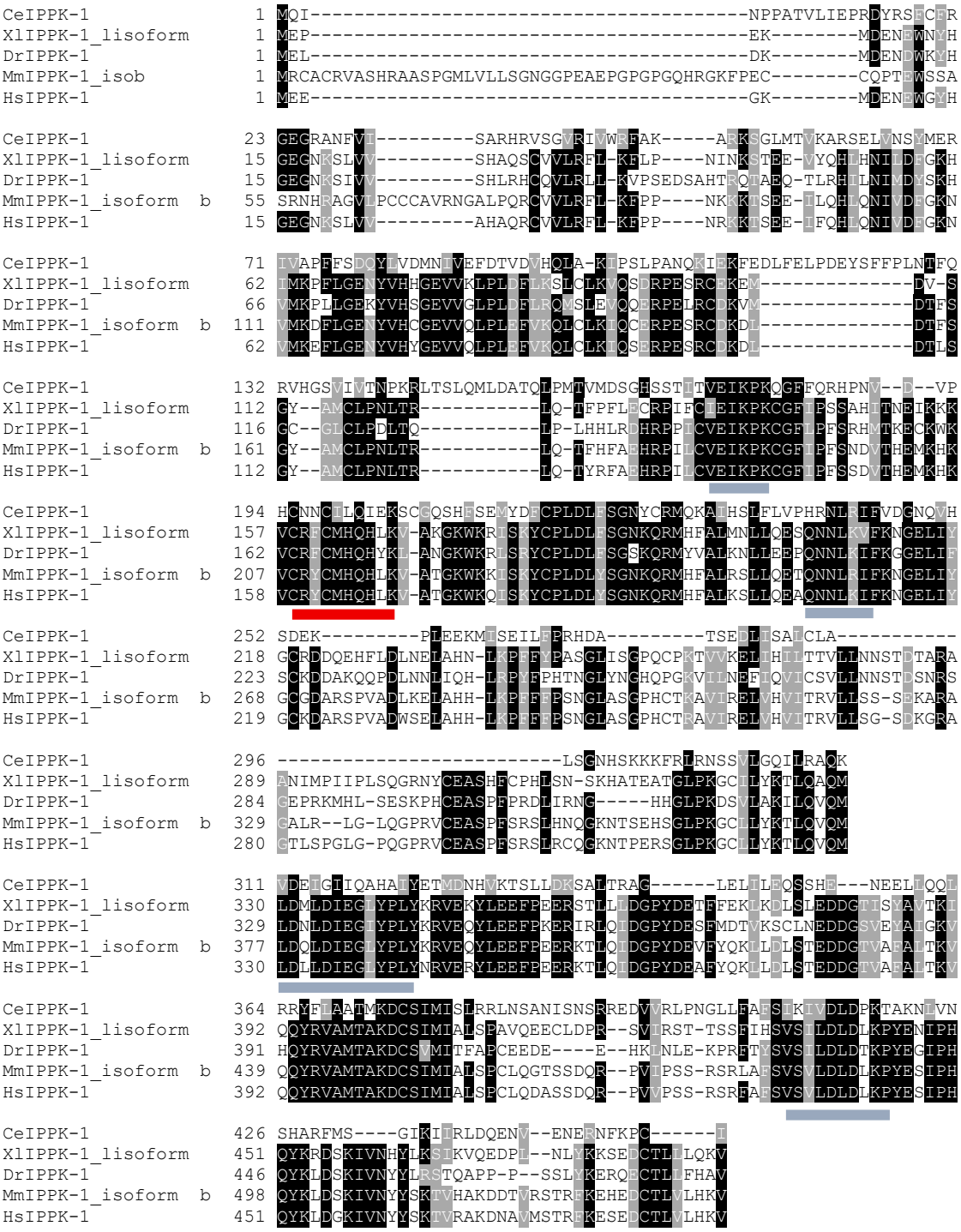

Figure 1.9: Sequence Alignment of IPPK-1 in *C. elegans* (Ce) with its *X. lavis* (Xl), *D. rerio* (Dr), *M. musculus* (Mm), and *H. sapiens* (Hs) homologs. Shading indicates nucleotide similarities. The blue line indicates the kinase domain. The red line indicates the motif involved in inositide recognition. The blue lines indicate domains involved in ligand binding. Sequence alignment preformed using T-Coffee v11 (Notredame et al., 2000; Tommaso et al., 2011) and Boxshade v3.3 (https://junli.netlify.app/apps/boxshade/). Domains were labelled based on González et al., 2010.

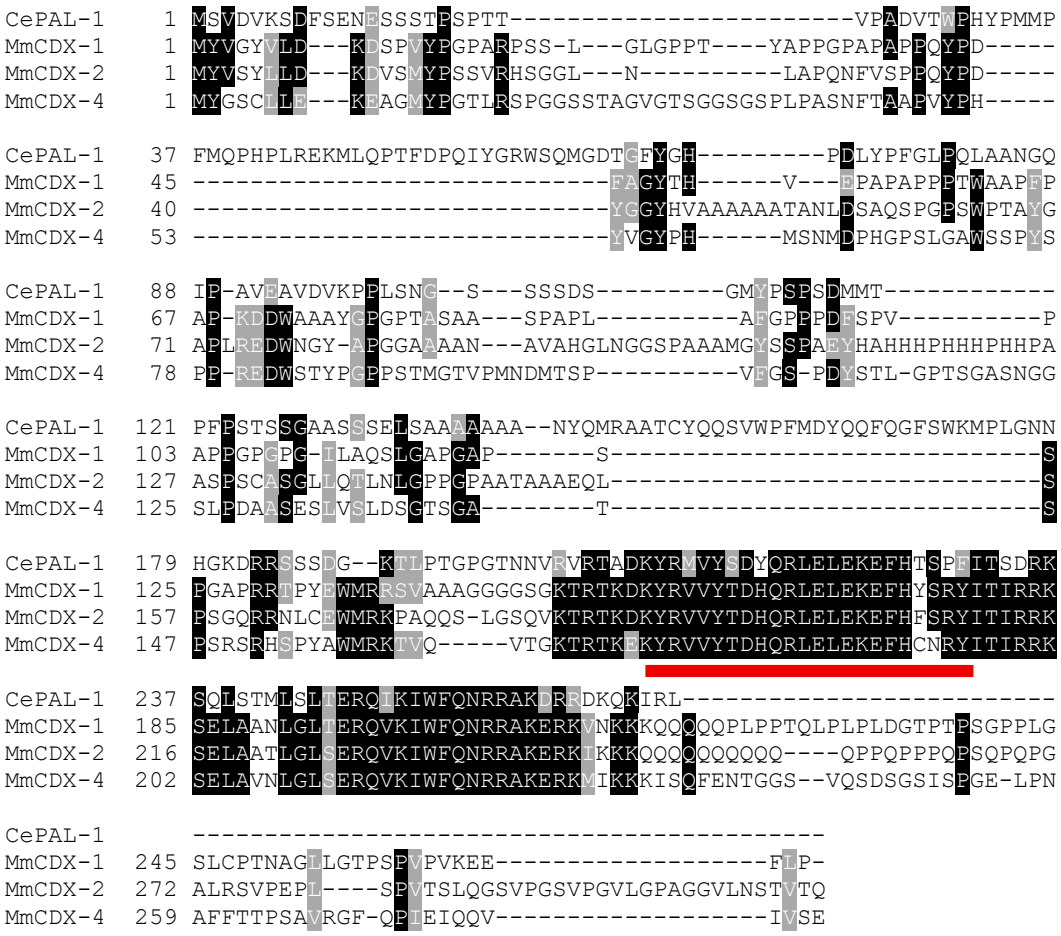

Figure 1.10: Sequence Alignment of PAL-1 in *C. elegans* (Ce), with Cdx1, Cdx2 and Cdx4 in *M. musculus* (Mm). Shading indicates nucleotide similarities. The red line indicates the homeobox domain. Sequence alignment preformed using T-Coffee v11 (Notredame et al., 2000) and Boxshade v3.3 (https://junli.netlify.app/apps/boxshade/). Domain prediction was preformed using NCBI Conserved Domain Search (Wang et al., 2023).

Chapter 2: Manuscript #1 - IPPK-1 and IP6 Contribute to Ventral Nerve Cord Assembly in *C. elegans*

IPPK-1 and IP6 contribute to ventral nerve cord assembly in C. elegans

Nathaniel Noblett[a,b], Tony Roenspies[a], Chloe B. Kirezi[a,b], Clover Stubbert[c,d], Stephane Flibotte[e], Pavak K. Shah[c,d,f], Antonio Colavita[a,b,g] ,*

[a]Neuroscience Program, Ottawa Hospital Research Institute, Ottawa, ON, Canada
[b]Department of Cellular and Molecular Medicine, University of Ottawa, Ottawa, ON, Canada
[c]Department of Molecular, Cell and Developmental Biology, University of California, Los Angeles, CA, USA
[d]Molecular Biology Institute, University of California, Los Angeles, CA, USA
[e]UBC/LSI Bioinformatics Facility, University of British Columbia, Vancouver, BC, Canada
[f]Institute for Quantitative and Computational Biosciences, University of California, Los Angeles, CA, USA
[g]University of Ottawa Brain and Mind Research Institute, Ottawa, ON, Canada
[*]**Corresponding Author:** Antonio Colavita colavita@uottawa.ca

Abstract

Inositol phosphates (IPs) are essential for the development and function of the nervous system. Loss-of-function studies, which demonstrate the importance of specific IP isomers, show their critical role in proper neural tube formation. In this study, we show that inositol pentakisphosphate 2-kinase (IPPK-1), the kinase that phosphorylates IP5 to generate IP6, is involved in assembling the ventral nerve cord (VNC) in C. elegans. We show that mutations in ippk-1 lead to the mispositioning of motor neurons along the VNC of newly hatched larvae. These positioning defects reflect disruption of VNC assembly during embryogenesis, as VNC neuronal progenitors in ippk-1 embryos display a more compact organization after arising on the left and right sides of the embryo, delays in rosette-mediated convergent extension, and defects in cell intercalation. We further show that injection of exogenous IP6 into the gonads of ippk-1 mutants can rescue both embryonic and neuron positioning defects. Our findings indicate that IP isomers, particularly IP6, are important for ventral nerve cord formation in C. elegans. Along with their role in neural tube formation in vertebrates, these results suggests that IP isomers play an ancient role in central nerve cord development.

Introduction

Inositol phosphates and polyphosphates, groups of metabolites produced through the progressive phosphorylation of inositol triphosphate (IP3), are central players in a diverse range of cellular processes. These include the regulation of ion channel activity, cell migration,

exocytosis, developmental timing and the establishment of left-right asymmetry (Efanov et al., 1997; Yang et al., 2001, 2021; Sarmah et al., 2005; Jadav et al., 2016; Rao et al., 2015). These functions are essential for proper embryogenesis and organogenesis during development (Yang et al., 2021; Frederick et al., 2005; Boitano et al., 1992; Seeds et al., 2015). In the developing nervous system, the activity of inositol phosphate and polyphosphate kinases regulate several aspects of brain development and function (Loss et al., 2013; Park et al., 2019a, 2019b; Ahmed et al., 2015; Wilson et al., 2009). Regulation of inositol phosphate levels, specifically inositol pentakisphosphate (IP5) and inositol hexaphosphate (IP6), are important for neuronal survival and differentiation (Loss et al., 2013; Ucuncu et al., 2020). Additionally, loss of inositol hexaphosphate kinases lead to impaired brain development due to neuronal migration, morphology and synapse formation defects (Rojas et al., 2019; Fu et al., 2015, 2017).

Neural tube defects, caused by a failure of the neural plate to fold, fuse or undergo canalization during neurulation, are highly prevalent congenital abnormalities (reviewed in Greene et al., 2017; Nikolopoulou et al., 2017). Disrupting inositol phosphate metabolism, either through deprivation of dietary inositol or introducing loss-of-function mutations in IP synthesis enzymes, results in or exacerbates cranial neural tube defects (NTDs) (Wilson et al., 2009; Cockroft et al., 1992; Greene and Copp, 1997). Several studies have also described functions for highly phosphorylated forms of inositol during neural tube closure. Loss of inositol-tetrakisphosphate 1-kinase (ITPK1) and inositol polyphosphate multikinase (IPMK), kinases required for the production of IP5 and its derivatives, results in lethality around the neurulation stage in mice and has been linked to an increase in NTD cases in humans (Wilson et al., 2009; Frederick et al., 2005; Guan et al., 2014; Verbsky et al., 2005a).

While numerous genes have been implicated in the development of NTDs in vertebrates, a key category are those that encode for proteins involved in convergent extension. This morphogenetic process is marked by the constriction of cell-cell junctions and cell intercalation that act to narrow a tissue along one axis and lengthen it along another (reviewed in Sutherland et al., 2020). Coordination of convergent extension across the neural tube is a prominent driver of early neurulation, which depends on the closure of neuroepithelial folds. Failure of this process can lead to severe NTDs in vertebrates (Wallingford and Harland, 2002; Goto and Keller, 2002). Components of the conserved Wnt-planar cell polarity (PCP) pathway, such as VANGL1/2 and

their orthologues, play important roles in coordinating convergent extension in mice (Lei et al., 2019; Curtin et al., 2003; Murdoch et al., 2003), *Xenopus* (Wallingford and Harland, 2002; Williams et al., 2014; Butler and Wallingford, 2018) and zebrafish (Ciruna et al., 2006; Reynolds et al., 2010). Besides PCP signaling, junctional contraction during convergent extension are also controlled by transient Ca^{2+} oscillations resulting from the interaction between inositol triphosphate (IP3) and its receptor (Cogram et al., 2004; Politi et al., 2006, Mound et et al., 2017). In support of this, reducing Ca2+ waves through pharmacological or genetic means impairs axial elongation and disrupts convergent extension (Wallingford et al., 2001; Westfall et al., 2003). However, the role that more highly phosphorylated forms of inositol play during neural tube development remains poorly understood.

In *C. elegans*, convergent extension movements are involved in the early assembly of the ventral nerve cord (VNC) (Shah et al., 2017). The VNC runs along the anterior-posterior (AP) axis of the worm and is comprised of three classes of motor neurons (DD, DA and DB) at hatching. During embryogenesis, neuronal progenitors born on the left and right sides of the embryo, undergo cell-cell intercalations, including processes driven by the formation and resolution of multicellular rosettes, to converge toward and extend along the midline. Following this, progenitor cell bodies are positioned along the AP axis in a predominantly single-file formation. This process involves VANG-1/Van Gogh and SAX-3/Robo-mediated regulation of cell-cell intercalations (Shah et al., 2017). Loss of VANG-1 or SAX-3 signaling delays rosette resolution and, subsequently, the single-file intercalation of progenitors at the midline. However, simultaneous disruption of both pathways leads to a more severe convergent extension defect, which, in the most extreme cases, results in the anterior displacement of most motor neuron cell bodies in the VNC at hatching (Shah et al., 2017).

In this study, we explore the role of *ippk-1*, the gene encoding the worm orthologue of mammalian inositol-pentakisphosphate 2-kinase (IPPK/IP5K), in VNC assembly. IPPK is an enzyme in the IP biosynthesis pathway responsible for phosphorylating IP5 to generate IP6 (Verbsky et al., 2002). Our study reveals that the loss of *ippk-1* results in the mispositioning of motor neuron cell bodies within the VNC of newly hatched worms. Disruption of the worm orthologue of IPMK also produces a similar phenotype. Examination of VNC morphogenesis in *ippk-1* mutant embryos uncovered a more compact organization as VNC neuronal progenitors

from the left and right sides migrated toward the midline. Additionally, we observed defects related to abnormal convergent extension, including delays in rosette resolution, persistent cell contacts after midline intercalation, and reduced VNC extension by the 1.5-fold stage. Motor neuron positioning defects in newly hatched worms, a consequence of abnormal VNC development during embryogenesis, were rescued by the addition of exogenous IP6. These findings highlight the importance of IP biosynthesis pathways and polyphosphorylated IPs in the development of central nerve cords.

Results

IPPK-1 is required for proper positioning of DD neurons along the VNC

At hatching, the VNC contains three classes of motor neurons (6 GABAergic inhibitory DD, 9 cholinergic excitatory DA, and 7 cholinergic excitatory DB) arranged in repeating DD-DA-DB motor pools responsible for sinusoidal locomotion (Lu et al., 2022). The cell bodies of these neurons are stereotypically positioned along the VNC (Saharkhiz et al., 2024). We have previously shown that loss of planar cell polarity genes like *vang*-1/VANG result in VNC assembly defects during embryogenesis which manifest as mispositioned motor neurons in L1 larvae (Shah et al., 2017). To identify new genes involved in neuron positioning, we performed a genetic screen (A. Colavita, unpublished results) using the DD-specific reporter *ynIs37[flp-13p::GFP]* (a gift from Dr. Chris Li, CCNY) and identified *zy65*. Whole genome sequencing revealed *zy65* to be a mutation in *ippk-1*, the sole *C. elegans* orthologue of inositol-pentakisphosphate 2-kinase (IPPK), a kinase in the IP biosynthesis pathway that catalyzes the conversion of IP5 to IP6 (Figure 2.1A and B). *ippk-1(zy65)* contains an A to T nucleotide change in the consensus splice acceptor site of exon 6 that is predicted to affect splicing of the *ippk-1* transcript (Figure 2.1A).

IPPK-1 was previously shown to be essential for larval growth and in the maintenance of adult germline membrane architecture (Lowry et al., 2015). Our findings indicate an additional role in VNC development. In newly hatched animals, DD motor neurons display an approximately equidistant spacing along the VNC. In *zy65* mutants, DD neurons are located at more anterior positions compared to wild type (WT) animals (Figure 2.1C and D). This

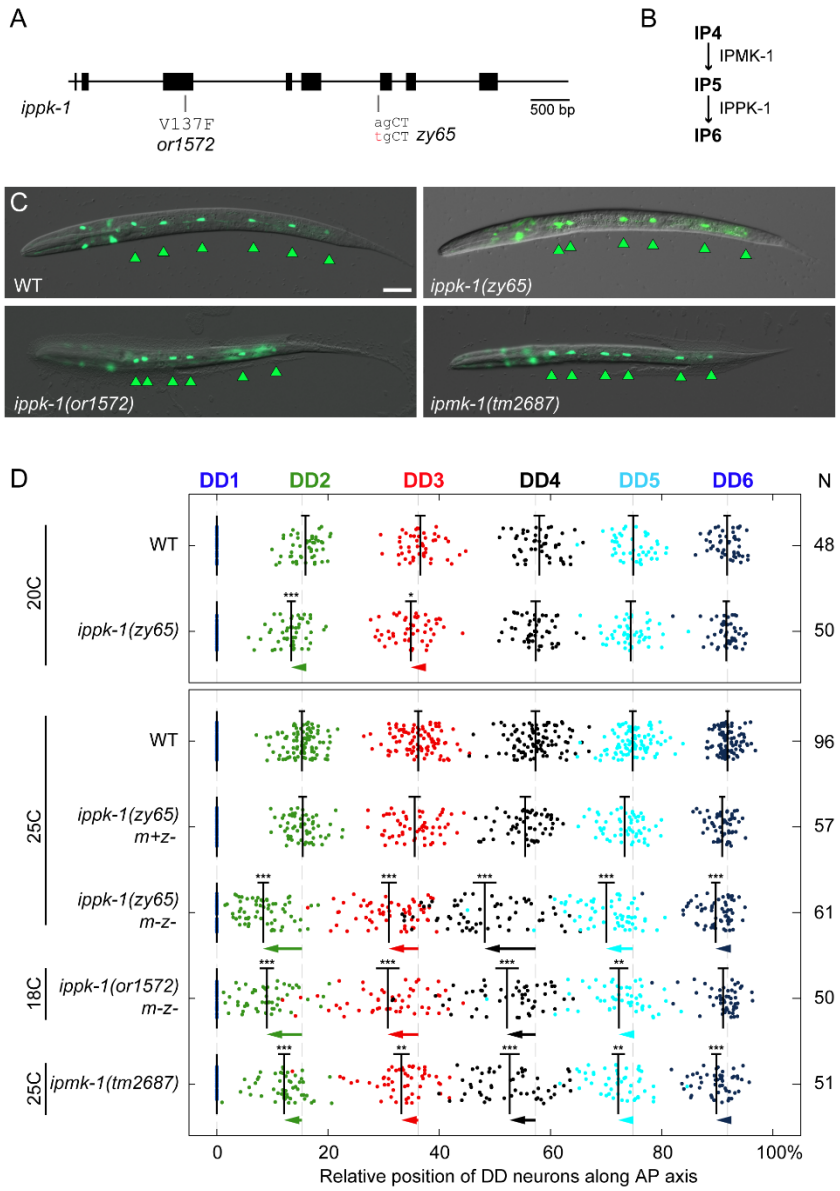

Figure 2.1: *ippk-1* mutants display DD neuron spacing defects. (A) Diagram of the *ippk-1* genomic region labeled with alleles used in this study. (B) Kinase cascade pathway involved in phosphorylating IP4 and IP5 to produce IP6. (C) Representative images of DD positions in WT, *ippk-1* and *ipmk-1* mutants, visualized using the DD-specific *flp-13p::GFP* reporter. Arrowheads mark DD neurons. Scale bar = 20 µm. (D) Quantification of DD2–DD6 mean positions relative to DD1 in L1 stage WT and mutant worms. Neurons (colour coded as indicated along top and numbered in sequence from anterior to posterior) are plotted along the AP axis, where DD1 and anus mark the 0 % and 100 % positions respectively. m = maternal, z = zygotic. Means and 95 % confidence intervals are indicated for each neuron. Animals scored (N) indicated on the right. Statistics: One-way ANOVA with Dunnett's post-hoc test against the corresponding WT neuron, except for strains scored at 20 °C, where a two-tailed *t*-test with Welch's correction was used. $*p < 0.05$, $**p < 0.01$, $***p < 0.001$. Arrows indicate the size of the shift from the WT mean for all neurons where $p > 0.05$.

phenotype is temperature sensitive as there is a significant increase in the penetrance of anteriorly shifted DD neurons when animals are incubated at 25 °C compared to 20 °C (Figure 2.1D). We also found that DD position defects are maternally rescued indicating a role for maternally derived IPPK-1 or its product IP6 (Figure 2.1D). To determine if the changes in neuron position are unique to DD neurons or shared by other motor neuron classes, we also examined DB neurons using an mScarlet knock-in at the *vab-7* locus (Saharkhiz et al., 2024) (Supplemental Figure 2.1). DB neurons were also mispositioned more anteriorly in *zy65* mutants, indicating a more general role in motor neuron positioning.

Two observations confirm that the *ippk-1* gene is responsible for the observed motor neuron position defects. First, the position defects in *ippk-1(zy65)* were rescued by expressing the *ippk-1* cDNA from either the *ippk-1* promoter or a heterologous *unc-33* promoter (Supplemental Figure 2.2). Second, *ippk-1(or1572)*, a temperature-sensitive allele from the Lowry et al. (2015) study, also displayed similar anterior shifts in DD cell body positions (Figure 2.1C and D). As *or1572* exhibited sterility and larval arrest at temperatures above 20 °C, it was scored at 18 °C to ensure the production of viable larvae. *ippk-1(zy65*) worms also displayed sterility and epidermal morphology defects, similar to those in *ippk-1(or1572)*, when grown at the restrictive temperature. 9.5 % (N = 116) of post-comma stage embryos and 17.4 % (N = 135) of larvae displayed epidermal morphology defects characterized by a lumpy appearance, with lumps mostly in the posterior (Supplemental Figure 2.3). Notably, loss of upstream components required for the generation of inositol triphosphate (IP3) have been reported to show similar defects in both embryonic and larval stages (Vázquez-Manrique et al., 2008).

Since IPPK-1 acts in an IP synthesis pathway with several other kinases, we also asked if loss of another kinase in this pathway would also disrupt DD positioning. IPMK phosphorylates both IP3 and IP4 to produce IP5 (Saiardi et al., 1999; Odom et al., 2000) (Figure 2.1B). *ipmk-1* is the only *C. elegans* orthologue of IPMK. Unlike *ippk-1*, which is an essential gene, the *ipmk-1(tm2687)* deletion allele (Mitani, 2017), a probable null, is viable (Yang et al., 2021). We found that *tm2687* displayed DD position defects similar to those in *ippk-1* mutants (Figure 2.1C and D). As human IPPK has been shown to play additional non-catalytic roles unrelated to IP synthesis (Brehm et al., 2013), these findings indicate that an intact IP kinase cascade is important for proper DD positioning in the VNC.

Ippk-1 is expressed at low levels, except in the spermatheca

To determine where *ippk-1* is expressed, we generated a transcriptional reporter and tagged the endogenous *ippk-1* locus with GFP (Supplemental Figure 2.4). The transcriptional reporter was made using approximately 3 kb of *ippk-1* promoter fused to GFP (Supplemental Figure 2.4A). Expression from a transgenic array was observed in pharynx, intestine, spermatheca, and a subset of head, tail and ventral cord neurons (Supplemental Figure 2.4B-D). Two GFP knock-in strains were made, with GFP inserted at either the N or C-terminus of *ippk-1*, using the CRISPR/Cas9 homology-directed repair approach described in Dickinson et al. (2015). This approach utilizes a selection cassette (SEC) containing a GFP reporter, followed by a loxP-flanked stop cassette which allows transcriptional read-through past the reporter only upon Cre recombinase-mediated SEC excision. The N-terminal insertion can therefore function as a transcriptional reporter prior to SEC excision. In contrast to the transcriptional reporter, the *ippk-1(zy100[GFP::loxP-stop-loxP::IPPK-1])* strain, which reflects endogenous promoter activity, showed strong expression only in the spermatheca (Supplemental Figure 2.4E). Likewise, both the N-terminal (*zy101*) and C-terminal (*zy102*) GFP knock-ins appeared to show protein expression only in the spermatheca (Supplemental Figure 2.4F). With the exception of the spermatheca, we did not observe expression in other areas of the somatic gonad or germline, where we might have expected it, given its role in germline architecture and gonad arm morphology (Lowry et al., 2015). These observations suggests that *ippk-1* expression may be below the detection limit of our methods, which is consistent with single-cell transcriptome data showing generally low abundance of *ippk-1* transcripts except in the spermatheca (Taylor et al., 2021; Packer et al., 2019).

IPPK-1 acts in concert with VANG-1 and SAX-3 to position DD neurons in the VNC

We previously demonstrated that the PCP pathway protein VANG-1 and the Robo receptor SAX-3 function in parallel to ensure proper motor neuron cell body positioning in the VNC of newly hatched worms. Simultaneous deletion of both *vang-1* and *sax-3* leads to the highly penetrant displacement of motor neuron cell bodies toward the anterior, which is more

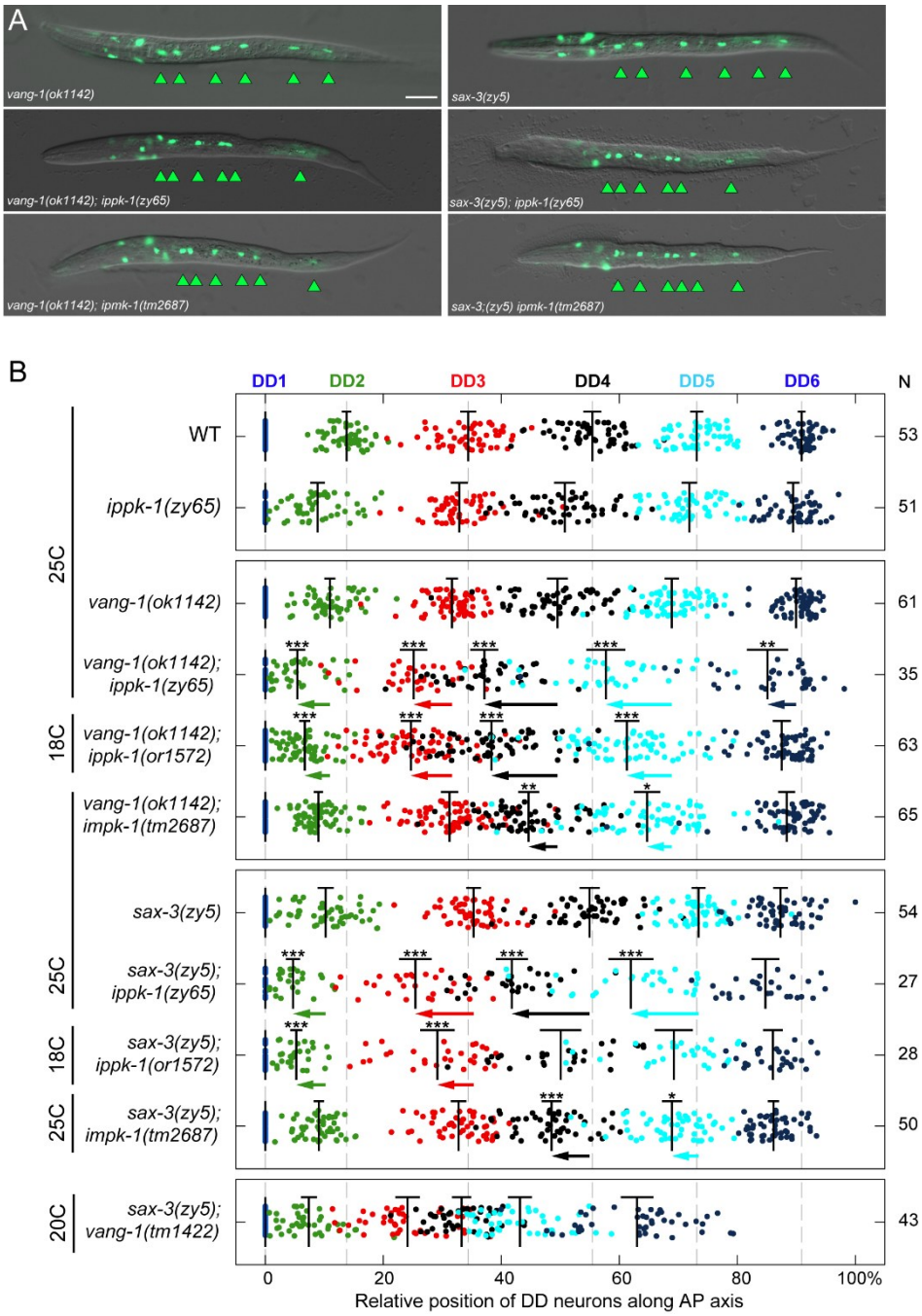

Figure 2.2: DD position defects are more severe in *vang-1; ippk-1* and *sax-3; ippk-1* double mutants compared to single mutants. (A) Representative images and (B) quantification of mean DD neuron position relative to DD1 in *vang-1* and *sax-3* single mutants or in combination with ippk-1 and ipmk-1 mutants. The *vang-1(tm1422) sax-3(zy5)* DD position data, included for comparison, is from Saharkhiz et al. (2024). Scale bar = 20 µm. Means, 95 % confidence intervals and plot format as in Fig. 1D. Statistics: One-way ANOVA with Tukey's post-hoc test. The significance of each neuron across all double mutants is shown relative to the position of its constituent *vang-1(ok1142)* or *sax-3(zy5)* single mutant. $*p < 0.05$, $**p < 0.01$, $***p < 0.001$. Arrows indicate the size of the mean position shift in double mutants compared to the relevant *vang-1* or *sax-3* single mutant where $p > 0.05$.

severe than the defect caused by loss of either gene alone (Figure 2.2) (Shah et al., 2017). This striking anterior displacement is the result of a severe disruption of convergent extension movements as neuronal progenitors undergo mediolateral convergence and anterior-posterior extension to form the VNC during embryogenesis (Shah et al., 2017). To investigate genetic interactions between *ippk-1* and these pathways, we examined DD neuron positions in *ippk-1* double mutants with *vang-1* and *sax-3*. We found that double mutants containing *ippk-1(zy65)* displayed significantly stronger anterior shifts, at one or more DD neuron cell body positions, compared to *vang-1* and *sax-3* single mutants (Figure 2.2). A similar, albeit milder, increase in severity was also observed in *vang-1; ipmk-1* and *sax-3; ipmk-1* double mutants (Figure 2.2). Interestingly, although *vang-1* and *sax-3* double mutants containing *ippk-1(zy65)* displayed similar shifts in DD positions, double mutants containing *ippk-1(or1572)* displayed stronger shifts in the *vang-1* mutant background than in the *sax-3* background. This difference appeared to be absent in *ipmk-1* double mutants, suggesting that the *zy65* and *or1572* lesions disrupt IPPK-1 protein function in different ways, with *or1572* likely retaining more kinase activity. However, in all cases, *ippk-1* double mutants with *vang-1* and *sax-3* did not exhibit the more severe anterior displacements found in *vang-1; sax-3* double mutants, most pronounced in DD6, which are indicative of a major perturbation of convergent extension (Figure 2.2B). Overall, these results are consistent with an *ipmk-1* and *ippk-1* containing IP pathway acting, at least in part, in parallel with *vang-1* and *sax-3* to promote proper motor neuron positioning in the VNC.

***Ippk-1* mutants display defective organization of DD and DA progenitors at midline contact.**

During embryogenesis, DD and DA progenitors from both the left and right sides, form tightly juxtaposed groups that migrate towards the midline, where they intercalate to establish the presumptive VNC (Shah et al., 2017). To begin to understand how *ippk-1* regulates VNC formation during this stage, we performed time-lapse microscopy using a *cnd-1p::PH::mCherry* reporter to label the membranes of DD and DA progenitors (specifically, DD1-6 and DA1-5) (Figure 2.3A). In *ippk-1* mutants, we found that these progenitors appeared more disorganized and compact as they moved toward the midline (Figure 2.3B). To quantify tissue compactness, we measured the combined area occupied by the progenitors on the left and

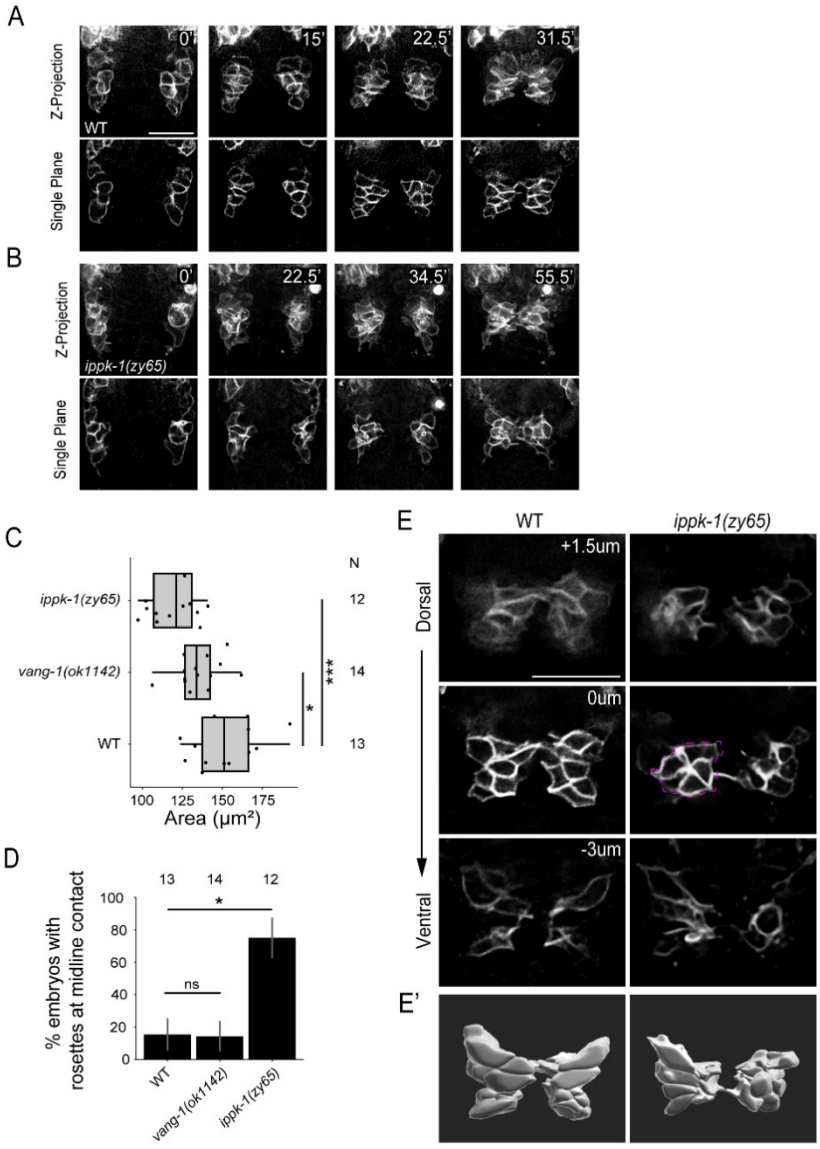

Figure 2.3: *ippk-1* mutants display defective organization of DD and DA neuronal progenitors prior to midline contact. (A–B) Time-lapse fluorescence single plane images and maximum-intensity projections showing the migration of a subset of DD and DA progenitors, labeled (membranes) with *cnd-1p::PH::mCherry*, from left and right sides toward the midline in (A) WT and (B) *ippk-1(zy65)* embryos. Scale bars = 10 µm. (C) Box plot showing the combined area of left and right *cnd-1p*-labeled VNC progenitors at midline contact. Tails indicate min and max. (D) Plot showing the proportion of embryos containing at least one rosette among VNC progenitors at midline contact. Error bars indicate SEP. (E) Z-slices arranged from dorsal to ventral from a representative WT and *zy65* embryo showing *cnd-1p*-labeled VNC progenitors at midline contact, revealing the more compact organization and the presence of a rosette (dotted magenta outline) in the *zy65* embryo. (E′) 3D reconstruction of VNC progenitors in E. Statistics: (C) Chi-squared test with Monte Carlo simulation for 10,000 replicates, followed by a pairwise analysis using Fisher's exact test with Monte Carlo simulation for 10,000 replicates and adjustments with Holm corrections, (D) ANOVA with Dunnett's post-hoc test against WT. $*p < 0.05$, $**p < 0.01$, $***p < 0.001$.

right sides in each embryo at the time of midline contact. We found that in *ippk-1(zy65)* mutants, this area was significantly smaller (119.1 μm^2) (N = 12, $p < 0.0001$) compared to WT (151.8 μm^2) (N = 13) (Figure 2.3C).

To ascertain whether the more compact organization resulted from changes in cell number or fate, we counted the number of *cnd-1* promoter-labeled progenitors at the embryonic bean stage and in L1 animals using terminal cell fate markers. We found a slight reduction ($p = 0.0131$) in the number of progenitors at the bean stage, with an average of 20 *cnd-1*-labeled cells (N = 16) in WT and 19 (N = 19) in *ippk-1* mutants (Supplemental Figure 2.5A). However, the number of terminally differentiated DD, DA, and DB neurons in L1 animals remained unchanged (Supplemental Figure 2.5B), suggesting that the more compact organization in *ippk-1* mutants is not due to a reduction in progenitor number or cell fate defects.

Closer examination of the left and right progenitor groups to better understand their organization revealed differences in the presence of multicellular rosettes, structures where the junctions of five or more cells meet at a common vertex, between *ippk-1* mutants and WT. In *ippk-1(zy65)* mutants, 75 % of embryos displayed a rosette at the time of midline contact (N = 12, $p = 0.01294$), compared to 15.4 % in WT (N = 13) embryos (Figure 2.3D and E). These ectopic rosettes may therefore underlie some aspect of the disorganization and compactness seen in these progenitors during their migration to the midline. As progenitor groups in WT embryos typically show rosettes prior to midline contact, we cannot rule out that a proportion of these may be persistent instead. These rosettes appear to be a distinct feature of *ippk-1* mutants, as *vang-1(ok1142)* mutants did not show a greater proportion of rosettes at midline contact (N = 14, $p > 0.9999$) compared to WT (Figure 2.3D). To determine whether *ippk-1* plays a role in VANG-1 localisation, which we have previously shown to be localised to cell junction vertices (Shah et al., 2017), we examined an endogenous mNG::VANG-1 knock-in in both WT and *ippk-1* backgrounds but detected no obvious differences in localisation (Supplemental Figure 2.6). These observations suggests that IPPK-1 and its product IP6 are important for inhibiting rosette formation or promoting rosette resolution prior to VNC progenitor intercalation at the midline.

Ippk-1 mutants display defects in convergent extension

Shortly after meeting at the midline, DD and DA progenitors from the left and right contribute to the formation of multicellular rosettes (Shah et al., 2017). The resolution of these

rosettes sequentially from anterior to posterior is part of the convergent extension process, which narrows the tissue along the mediolateral axis and elongates it along the anterior-posterior axis. By the 1.5-fold stage, single-cell intercalations result in a stereotypical pattern of DD and DA neurons, aligned in a mostly single file along the developing VNC (Shah et al., 2017).

Our previous study indicated that the loss of PCP pathway components, like VANG-1, delays rosette resolution or causes unstable resolution, where rosettes partially resolve and then reform. These defects disrupt convergent extension and the normal intercalation of cells at the midline (Shah et al., 2017). To determine whether *ippk-1* regulates rosette dynamics, we performed time-lapse microscopy using our *cnd-1p::PH::mCherry* membrane marker to label DD and DA progenitors and measured the lifetime of the centrally positioned rosette formed when these cells meet at the midline. Rosette lifetimes were defined as the time from initial formation to resolution. For unstable resolutions, rosette lifetimes were measured from formation to final resolution. In WT, the centrally located rosette resolves within 3.3 min (median) after

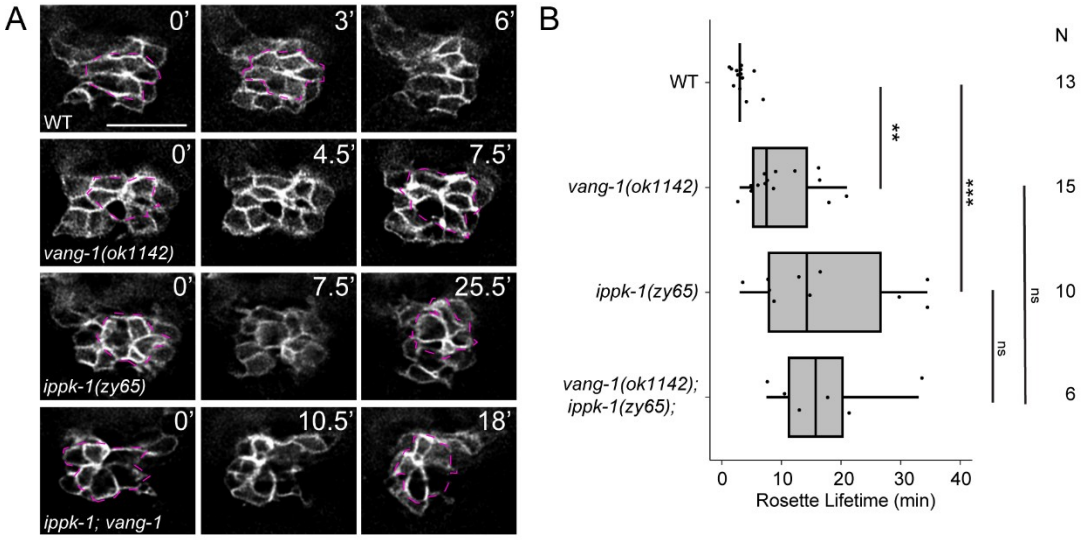

Figure 2.4: *ippk-1* mutants display defects in central rosette resolution. (A) Examples of rosette resolution dynamics in WT and mutant VNC progenitors labeled with *cnd-1p::PH::mCherry*. Cells participating in a rosette are outlined with a dotted magenta line. (B) Quantification of central rosette lifetime. Box plot tails indicate min and max. Statistics: Kruskal-Wallis with Dunn's post-hoc test. $*p < 0.05$, $**p < 0.01$, $***p < 0.001$. Scale bars = 10 μm.

formation. In *ippk-1(zy65)* mutants, the median rosette lifetime increased to 17.1 min ($p = 0.0003$) (Figure 2.4A and B). As a comparison, we also measured rosette lifetime in *vang-1* mutants and showed that the median resolution time was 9.8 min ($p = 0.0082$) (Figure 2.4B). Interestingly, *vang-1(ok1142); ippk-1(zy65)* double mutants (17.2-min median) did not show a significant increase in rosette lifetime compared to *zy65* single mutants ($p > 0.9999$). This finding is consistent with *ippk-1* and *vang-1* acting in a common pathway to regulate rosette resolution dynamics.

The outcome of single cell intercalation and effects on VNC extension were assessed at the 1.5-fold stage using *unc-30p::GFP* to label DDs (cytoplasm) and *cnd-1p::PH::mCherry* to label DD and DAs (membrane). At this stage, most DD and DA progenitors have intercalated into a single file with some of DD1-4 and DA2-5 displaying a stereotypical alternating DD DA pattern (WT in Figure 2.5A). We defined an embryo with a cell intercalation defect as one containing at least one abnormal DD-DD cell contact instead of a DD-DA contact. Not surprisingly, given the earlier organization and rosette resolution defects, we found a significant number of single cell intercalation defects in *ippk-1(zy65)* (36.5 %) ($N = 52$, $p = 0.0069$) and *ippk-1(or1572)* (50 %) ($N = 32$, $p = 0.0004$) mutants compared to WT (7.7 %) ($N = 52$) (Figure 2.5A and B). *ipmk-1* mutants showed a modest increase at 28.2 % ($N = 39$, $p = 0.0912$) in single cell intercalation defects compared to WT, although this difference was not statistically significant.

To determine if loss of *ippk-1* affected VNC extension at the 1.5-fold stage, we calculated a VNC extension index, defined as the length the VNC extends past the apex of the embryonic fold divided by the overall embryo length (Figure 2.5C). In WT animals, this index is 0.17, whereas it showed a slight but significant decrease to 0.12 in *ippk-1(zy65)* mutants ($p < 0.0001$), indicating a shorter posterior extension (Figure 2.5C). However, neither *ippk-1(or1572)* nor *ipmk-1(tm2687)* mutants showed a significant change. Interestingly, within the scored *or1572* embryos, one exhibited an unusually long posterior extension, though the reason for this remains unclear. *vang-1* mutants also showed a small but significant decrease in the extension index to 0.14 ($p = 0.0069$). In *vang-1; ippk-1* double mutants, this index decreased even further to 0.09 ($p < 0.0001$) and was smaller than *vang-1* ($p < 0.0348$) but not significantly different than *ippk-1* single mutants ($p < 0.9999$) (Figure 2.5C). This result is consistent with the rosette lifetime findings, suggesting that *ippk-1* and *vang-1* may function in a common pathway. Together, defects

in rosette resolution, single cell intercalation and posterior VNC extension are consistent with the involvement of *ippk-1* in convergent extension during VNC assembly.

Septins UNC-59 and UNC-61 are involved in proper positioning of DD neurons

Septins are a family of GTPase proteins associated with the cytoskeleton that function as critical regulators of convergent extension in *Xenopus* (Shindo and Wallingford, 2014). This, together with evidence that septins and IP6 bind each other *in vitro* (Yin et al., 2016), led us to ask whether septins also contribute to proper neuronal cell body positioning in the VNC. The *C. elegans* genome contains two septin genes, *unc-59* and *unc-61* (Nguyen et al., 2000), both of which are expressed in VNC neurons, where they have been implicated in axon guidance (Finger et al., 2003). To test their role in neuronal positioning, we examined *unc-59(tm1939)* and *unc-61(e228)*, two strong loss-of-function alleles (Nguyen et al., 2000; Jovelin and Cutter, 2016), for shifts in mean DD neuron position. Both *unc-59* and *unc-61* mutants showed disrupted equidistant spacing of DD neurons along the VNC (Supplemental Figure 2.7A). However, loss of *unc-59* causes significantly stronger anterior shifts in DD neuron positions than loss of *unc-61* (Supplemental Figure 2.7B). *unc-61* mutants do not exhibit significant anterior shifts in the mean positions of DD neurons compared to WT, but defects become apparent when assessing the distribution of individual neurons along the VNC, particularly the position of DD2 (Supplemental Figure 2.7). *unc-59* and *unc-61* mutants exhibit anterior position shifts similar to those observed in *ippk-1* mutants, but the defects are much less severe (Supplemental Figure 2.7B). These findings are consistent with IP signaling and septins acting together to ensure proper motor neuron positioning in the VNC, but further investigation is needed to determine whether septin defects reflect impaired convergent extension and whether they function in a shared pathway.

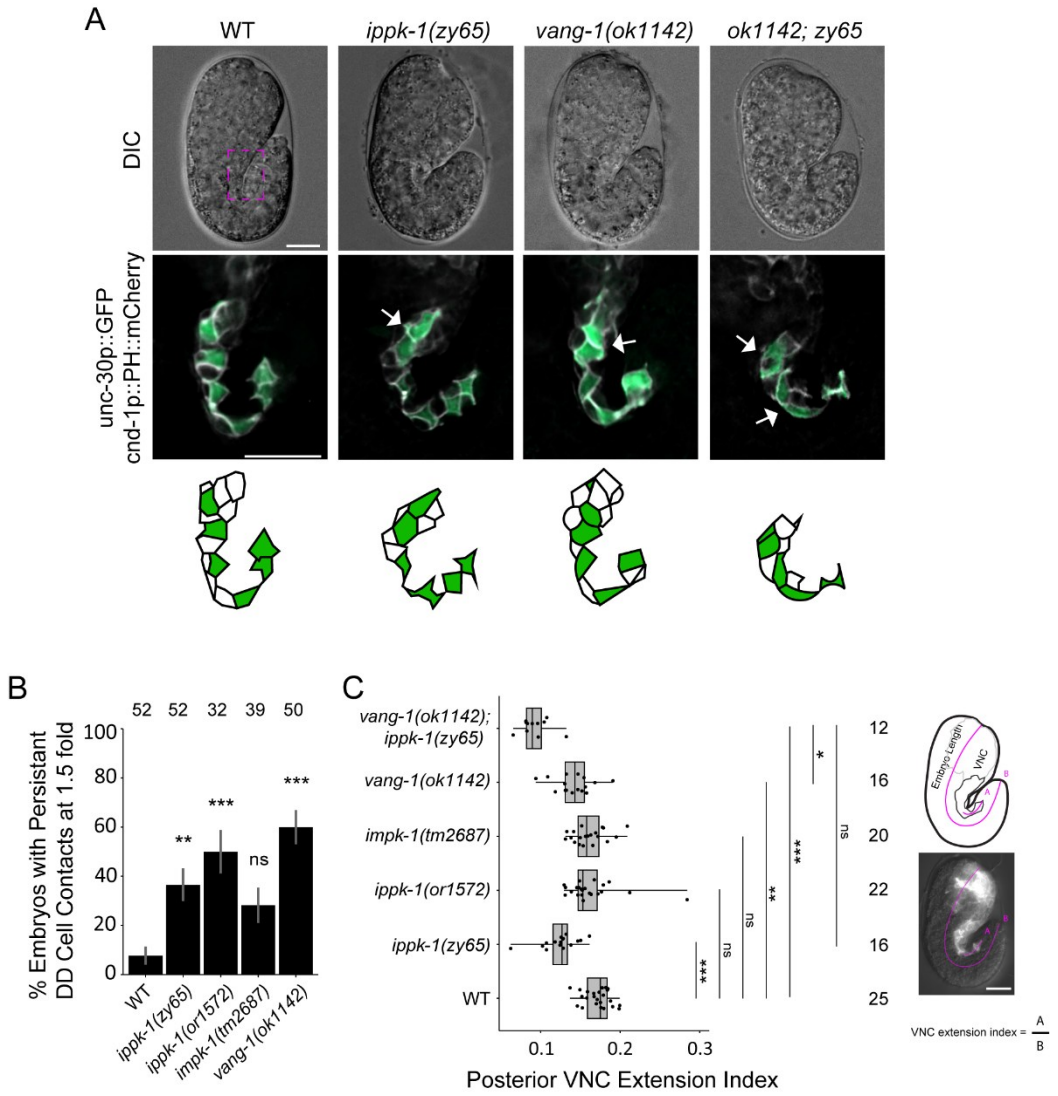

Figure 2.5: ippk-1 mutants display neuron intercalation and VNC extension defects. (A) Brightfield images of embryos and corresponding deconvolved fluorescence images of the VNC at 1.5 fold in WT and mutants, with the cytoplasm of DD neurons labeled with *unc-30p::gfp* and the membranes of DD and DA neurons labeled with *cnd-1p::PH::mCherry*. The magenta box indicates the approximate area of the middle panels. Schematics of the corresponding middle panel VNC show DD neurons highlighted in green. (B) Quantification of persistent DD cell contacts in WT and mutant embryos. Error bars indicate SEP. Statistics: Chi-squared test, followed by a pairwise analysis using Fisher's exact test adjusted with Bonferroni corrections. (C) Quantification of the posterior VNC extension index in WT and mutant embryos, relative to total embryo length. Tails indicate min and max. Panels show an image and corresponding schematic of a WT embryo with magenta lines indicating the lengths measured to calculate index. Statistics: (B) Chi-squared test with Monte Carlo simulation for 10,000 replicates, followed by a pairwise analysis using Fisher's exact test with Monte Carlo simulation for 10,000 replicates and adjustments with Holm corrections, (C) Kruskal-Wallis with Dunn's post-hoc test, significance compared to WT is shown. $*p < 0.05$, $**p < 0.01$, $***p < 0.001$. Scale bars = 10 μm.

Exogenous IP6 is sufficient to rescue *ippk-1* defects

In the IP kinase cascade, IPPK-1 phosphorylates IP5 to generate IP6. As a result, we explored whether the introduction of exogenous IP6 could mitigate the phenotypes associated with *ippk-1(zy65)*. To examine this, we performed microinjections of either IP6 (phytic acid) or a control solution (H_2O) into the gonads of *ippk-1(zy65)* worms and subsequently evaluated their progeny for signs of rescued left and right embryonic DD DA organization and larval DD neuron cell body position defects. Measurement of IP6 levels in different cells and organisms suggested that endogenous concentrations ranged from 10 μM to 100 μM (Szwergold et al., 1987; Freund et al., 1992; Veiga et al., 2006). Consequently, we tested both 10 μM–100 μM IP6 concentrations to assess their potential to rescue *ippk-1* mutants.

Injection of IP6 into *ippk-1(zy65)* mutant mothers restored the organization of *cnd-1*-labeled left and right-side DD and DA progenitors, as determined by scoring ectopic rosettes. *zy65* mutants with ectopic rosettes were reduced from 58.1 % (N = 31) to 11.8 % (N = 34) ($p = 0.0002$) in F1 progeny of mothers injected with 100 μM IP6 (Figure 2.6A and B). Similarly, exogenous IP6 was able to rescue DD neuron positioning defects in L1 and L2 larvae.

In WT, the six DD neurons, visualized with a *flp-13p::GFP* reporter, are typically equidistantly spaced along the VNC, whereas in *zy65* mutants, they are anteriorly displaced. For simplicity, we only assessed the spacing between DD1 and DD2, considering it defective if they were within one cell diameter of each other. In F1 progeny, the proportion of *zy65* mutants with DD1 DD2 spacing defects decreased significantly from 94.1 % (N = 51) to 37.9 % (N = 87) and 23.5 % (N = 68) when mothers were injected with 10 μM or 100 μM IP6, respectively (both $p < 0.0001$) (Figure 2.6C and D). Injection of IP6 into WT animals did not result in significant ectopic rosette or DD spacing defects in their progeny. As a specificity test, we injected 100 μM IP6 into *vang-1* mutant mothers and observed no rescue of DD1 DD2 spacing defects in the F1 progeny (Figure 2.6D). This indicates that exogenous IP6 specifically corrects defects associated with IPPK-1 function. These findings show that IP6, the downstream product of IPPK-1, is sufficient to rescue *ippk-1* defects, suggesting that these defects result from an IP6 deficiency.

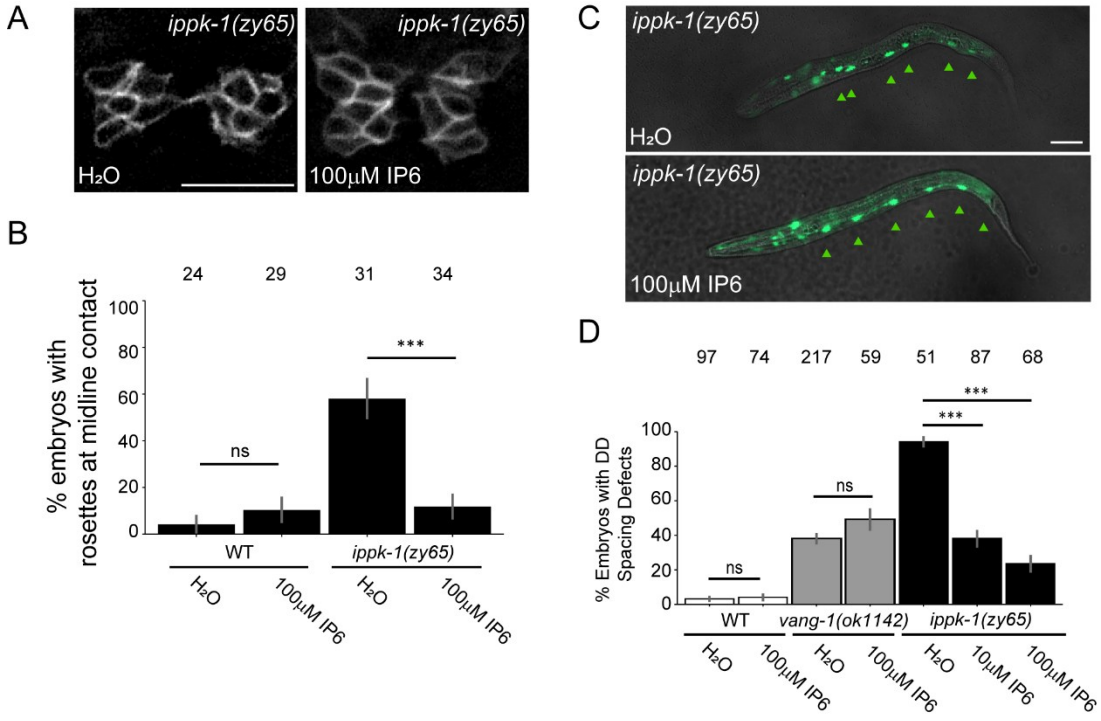

Figure 2.6: Exogenous IP6 is sufficient to rescue *ippk*-1 VNC defects. (A) Representative images of VNC progenitors at the stage of midline contact in *ippk-1(zy65)* embryos, showing rescue of organization defects following injection with either H_20 or IP6 (dissolved in H_20). Scale bar = 10 μm. (B) Plot showing the proportion of embryos in which VNC progenitors form at least one rosette at midline contact. (C) Representative images of DD neurons in *ippk-1(zy65)* larvae showing rescue of position defects after injection with IP6. Arrowheads mark DD neurons. Scale bar = 20 μm. (D) Quantification of the proportion of WT and mutant larvae displaying a DD1 DD2 spacing defect. For both B and D, error bars indicate SEP. Statistics: (B) Fisher's exact test. (D) Control and treatment groups for WT and *vang-1(ok1142)* were compared using Fisher's exact test. *ippk-1(zy65)* strains were compared using a Chi-squared test with Monte Carlo simulation for 10,000 replicates, followed by a pairwise analysis using Fisher's exact test with Monte Carlo simulation for 10,000 replicates and adjustments with Holm corrections.

Discussion

IP molecules, through their regulation of basic cellular processes, play essential roles during animal embryonic development (Seeds et al., 2015; Frederick et al., 2005; Sarmah et al., 2005; Verbsky et al., 2005a). The pathway for IP synthesis involves a cascade of inositol kinases that sequentially phosphorylate one of six hydroxyl positions in the inositol ring. It typically commences with phospholipase C (PLC) and phosphoinositide phosphatidylinositol (4,5)-bisphosphate (PIP2)-derived IP3, ultimately leading to the production of IP6, as well as the higher

inositol pyrophosphates IP7 and IP8 (Laha et al., 2021; Majerus, 1992). Inositol-pentakisphosphate 2-kinase (IPPK) is the rate limiting kinase that converts IP5 to IP6, by phosphorylating IP5 at the 2 hydroxyl position of the inositol ring (Verbsky et al., 2002, 2005b). In this study, we show that the *C. elegans* orthologue IPPK-1 and its product IP6 are important for proper ventral nerve cord (VNC) morphogenesis.

IPPK-1 in *C. elegans* has previously been shown to be essential for the formation and maintenance of germline membrane architecture (Lowry et al., 2015). We found that IPPK-1 is also important for multiple aspects of the morphogenetic process that leads to the narrowing and elongation of neuronal progenitor tissue as its constituent cells move towards and intercalate at the midline to form the VNC. The loss of *ippk-1* disrupts this process in several ways. First, the DD and DA progenitor assemblies arising on the left and right sides of the embryo are more compact and disorganized as they converge toward the midline. This abnormal tissue morphology may, in part, result from a significant increase in ectopic rosettes, structures where five or more cells meet at a common vertex, within these assemblies. Second, *ippk-1* mutants display delays in resolving the multicellular rosettes that form when the left and right VNC progenitors meet at the midline. Rosette dynamics are important drivers of convergent extension, as they reorient progenitors from the left and right to align along the anterior-posterior axis. And third, defects in midline intercalation that result in motor neuron cell body mispositioning along the developing VNC at the 1.5-fold stage of embryonic development. Collectively, these defects contribute to the anterior displacement of VNC motor neurons observed in *ippk-1* mutants at hatching.

In metazoans, IP kinases are classified into four groups: IPK, ITPK, IPPK, and PPIP5K, with the IPK group further subdivided into ITP3K, IPMK and IP6K (Laha et al., 2021). Some of these kinases, like ITPK and IPMK are multifunctional and phosphorylate more than one IP ring position (Odom et al., 2000; York et al., 1999). The *C. elegans* genome encodes one orthologue each of ITP3K, IPMK, IPPK and PPIP5K and three orthologues of IP6K. IPMKs catalyze the stepwise phosphorylation of the 6 and 3 hydroxyl positions of IP3 and IP4 respectively to generate IP5. Loss of the *C. elegans* IPMK (*ipmk-1)* leads to phenotypic traits like those caused by *ippk-1* loss, including intercalation defects and neuron position defects in newly hatched larvae. This finding, coupled with the rescue of *ippk-1* defects by the exogenous addition of IP6, indicates that

VNC defects in *ippk-1* mutants are caused by disruption of IP metabolism and not some other factor independent of its catalytic activity.

Surprisingly, the defects in *ipmk-1* were generally milder than those of *ippk-1*, even though we used a deletion allele expected to result in a strong loss of function and, therefore, would be expected to strongly disrupt IP5 production. In vertebrates, the ability of ITPK, acting through an alternative PLC-independent pathway, to sequentially phosphorylate hydroxyl positions on IP1 through IP4 to generate IP5, could potentially compensate for the loss of IPMK (Desfougères et al., 2019). However, in contrast to vertebrates, *C. elegans* and several other lower species do not possess a member of the ITPK family (Laha et al., 2021). One possibility is that in *C. elegans*, another IP kinase has an IP binding pocket that enables it to bind and phosphorylate IP4 molecules. A possible candidate for such a multifunctional kinase might be LFE-2, the ITP3K orthologue. Supporting this idea, the simultaneous loss of both *ipmk-1* and *lfe-2* is lethal, even though each gene, when mutated individually, does not affect viability (Yang et al., 2021).

In a previous study, we found that VANG-1 and PRKL-1, core components of the planar cell polarity pathway (PCP), and SAX-3, a Robo receptor, act in parallel pathways to regulate convergent extension during VNC assembly (Shah et al., 2017). Disruption of these pathways individually leads to cell intercalation defects and prolonged rosette resolution times, which may contribute to the anterior neuron displacement observed in the mutants. However, simultaneous loss of both pathways results in a more severe disruption of rosette-mediated convergent extension. For example, in our previous study, we found that in wild type, the central rosette that forms at the midline resolves in less than 4 min, compared to approximately 20 min in *sax-3* and *prkl-1* single mutants and greater than 50 min in *sax-3; prkl-1* double mutants (Shah et al., 2017). This long delay in the double mutant before midline intercalation, during which time the embryo continues to undergo elongation into a more wormlike shape, likely explains why, at hatching, nearly all motor neuron cell bodies are abnormally positioned in the anterior half, rather than being evenly distributed along the VNC.

Loss of *ippk-1*, like loss of *vang-1*, results in defects consistent with impaired convergent extension, similar to those of *vang-1* mutants, including rosette resolution delays, incorrect cell contacts following midline intercalation, and anterior displacement of motor neurons in newly hatched worms. We found that the average rosette delay phenotype of *vang-1; ippk-1* double

mutants was not significantly different from that observed in the single mutants. This suggests that *ippk-1* and *vang-1* may act within a common pathway to ensure timely rosette resolution. However, the involvement of independent pathways cannot be excluded, as the *ippk-1* mutants used in the double mutants likely retain substantial IP5 kinase activity, given that complete loss of function is lethal. Consequently, the full extent of *ippk-1* involvement in VNC assembly remains unclear and we cannot rule out the possibility that a complete lack of IPPK-1 leads to the severe disruption of convergent extension observed in PCP and Robo double mutants.

Interestingly, despite similar rosette lifetimes in embryos, *vang-1; ippk-1* double mutants exhibited more pronounced anterior shifts in DD neuron cell body positions in larvae compared to single mutants. This observation suggests that proper neuronal positioning in the VNC may rely on both rosette-dependent and rosette-independent mechanisms. Indeed, much remains to be understood about VNC assembly, particularly the molecular and cellular processes that ensure the proper spacing and stereotypical organization of the three motor neuron classes, DD, DA, and DB, present in the VNC of L1 larvae.

The role that IPPK-1 plays in VNC development is interesting given the evidence highlighting the importance of IP metabolism in neural tube formation. Several studies have shown that disruptions in IP kinases are associated with neural tube defects. Notably, loss of mammalian ITPK1 leads to embryos that develop neural tube defects of varying severity, including spina bifida and exencephaly (Wilson et al., 2009). A similar pattern is observed in mutants for the mammalian IPMK/IPK2; although embryos arrest around E9.5, they exhibit multiple morphological abnormalities, including abnormal folding of the neural tube (Frederick et al., 2005). ITPK polymorphisms have been associated with an increased prevalence of neural tube defects and are correlated with lower maternal plasma IP6 levels (Guan et al., 2014). Similarly, reduced maternal myo-inositol levels are associated with an increased risk of spina bifida (Groenen et al., 2003). However, IPPK has not been directly linked to neural tube defects, as loss of *Ippk* in mouse models leads to early embryonic defects that prevent a thorough analysis of neural tube development (Verbsky et al., 2005a). It is important to note, though, that all three genes are expressed in the developing neural tube (Wilson et al., 2009; Frederick et al., 2005; Verbsky et al., 2005a), consistent with their shared role in IP metabolism.

Convergent extension is a key driver of neural tube formation in chordate species. In mice, mutations in genes associated with PCP, which are key regulators of convergent extension, are closely linked to failed neurulation (Lesko et al., 2021; Williams et al., 2014; Blankenship et al., 2006). Convergent extension and neural tube development in mice are, in part, driven by the regulation of junctional dynamics, including the formation and resolution of multicellular rosettes (Williams et al., 2014). In other animals, convergent extension has been shown to depend on localised junctional dynamics, which require the asymmetric distribution of PCP proteins (Shindo et al., 2019; Butler and Wallingford, 2018). IP6 and its derivatives have been previously shown to interact with several membrane and cytoskeletal proteins both *in vitro* and *in vivo* during cell migration and adhesion (Cheng and Andrew, 2015; Fu et al., 2017; Schröterová et al., 2018; Rojas et al., 2019; Bhat et al., 2024). Given the importance of cytoskeleton dynamics in collective cell movements, the production of these metabolites may play a role in facilitating membrane dynamics. Supporting this idea, loss of *ippk-1* disrupts the complex membrane architecture of the germline, which relies on membrane remodeling during oogenesis (Lowry et al., 2015).

Another potential connection between IP6 and convergent extension is the septin family, a group of cytoskeletal proteins with GTPase activity that form filamentous structures involved in membrane dynamics and cellular organization (reviewed in Woods and Gladfelter, 2021). Septins are critical to the distribution, polarity and dynamics of multiple populations of actin within tissues undergoing convergent extension (Shindo and Wallingford, 2014; Devitt et al., 2024). They also co-localize and function alongside PCP components, including Vangl2 and Prickle2, influencing the distribution of actin rich cables along the anterior-posterior axis (Devitt et al., 2024). Evidence for a potential physical interaction between septins and IP6 was shown using an IP6-containing affinity tag in a colon cancer cell line, which also identified targets associated with intercellular transport and the cytoskeleton (Yin et al., 2016). Our finding that loss of the *C. elegans* septins encoded by *unc-59* and *unc-61*, especially *unc-59*, causes motor neuron cell body positioning defects similar to, though less severe than, those in *ippk-1* mutants further supports this notion and suggests that more research may be warranted to determine whether the IP pathway and septins cooperate to regulate convergent extension.

The production of IP6 may also facilitate convergent extension more broadly through the regulation of endocytosis. Several types of inositol phosphates and pyrophosphates bind to

components of vesicle transport pathways, including AP-1/2/3, PIP2, and dynamin, where they facilitate both exocytosis and endocytosis in diverse situations (Voglmaier et al., 1992; Høy et al., 2002; Li et al., 2022). Endocytosis is essential for convergent extension movements, as evidenced by defects in intercalation and tissue extension when dynamin function is disrupted (Jarrett et al., 2002; Levayer et al., 2011). One way this occurs is through internalization of Frizzled and Ryk receptors during gastrulation, which promotes or redirects PCP signaling to support proper convergent extension (Brinkmann et al., 2016; Lee et al., 2016; Saraswathy et al., 2022).

Conclusions

Overall, our findings implicate IPPK-1 and its metabolite IP6 in coordinating the organization and timing of cell intercalations during VNC assembly. Together with the involvement of IP kinases in vertebrate neural tube formation, this suggests that IP metabolism plays an evolutionarily conserved role in central nerve cord development. Considering the crucial role of convergent extension in this process, it will be important to elucidate the precise mechanism through which IP6 or other inositol phosphates regulate this morphogenetic event.

Materials and Methods

Strains and culture conditions

Strains were maintained on NGM plates at 20 °C, except for temperature-sensitive strains, which were maintained at 18 °C. The Bristol N2 strain was used as wild type (WT), along with the following alleles and transgenes: LGI: *unc-59(tm1939)*. LGII: *ippk-1(zy65), ippk-1(zy100[GFP::SEC::ippk-1]), ippk-1(zy101[GFP::ippk-1]), ippk-1(zy102[ippk-1::GFP]), ippk-1(or1572), unc-4(syb1658[unc-4::GFP])*. LGIII: *ynIs37[flp-13p::gfp], vab-7(st12267[vab-7::GFP])*. LGIV: *ipmk-1(tm2687)*. LGV: *unc-61(e228)*. LGX: *sax-3(zy5), vang-1(ok1142), zyIs36[cnd-1p::PH::mCherry myo-2p::mCherry], zy115[mNG::vang-1]*. Unassigned linkage: *zyIs40[unc-30p::GFP; cnd-1p::PH::mCherry myo-2p::mCherry]*.

Whole genome sequencing and GFP insertion into the endogenous *ippk-1* gene

zy65 was identified in a genetic screen for DD neuron position defects (A Colavita, unpublished) and outcrossed at least 3 times. The mutation in the *zy65*-containing strain was identified by whole genome sequencing as described in Noblett et al. (2019). Sanger sequencing (performed at OHRI Stemcore) was used to genotype *zy65* in single and compound mutants, using the primers N22 and N23 (Table S1).

Table 2.1: Key resources used in *ippk-1* experiments

Reagent or resource	Source	Identifier
Chemicals, Peptides, and Recombinant Proteins		
Phytic acid sodium salt hydrate	Sigma-Aldritch	P0109; CAS:14306-25-3
Levamisol hydrochloride	Millipore Sigma	31742; CAS:16595-80-5
Bacterial and Virus Strains		
E. coli: OP50	*Caenorhabditis* Genetics Center (CGC)	WBStrain00041969
Experimental Models: Organisms/Strains		
C. elegans: N2 (wild isolate)	CGC	
C. elegans: *ippk-1(zy65)* II	This study	N/A
C. elegans: *ippk-1(or1572)* II	CGC, Lowry et al., 2015.	EU2908 WBVar00241916
C. elegans: *ippk-1(zy100[GFP::SEC::IPPK-1])* II	This study	N/A
C. elegans: *ippk-1(zy102[IPPK-1::GFP])* II	This study	N/A
C. elegans: *ynIs37[flp-13p::gfp]* III	CGC	NY2037 WBStrain00029158
C. elegans: *ipmk-1(tm2687)* IV	Dr. Shohei Mitani, National BioResource Project (NBRP)	N/A
C. elegans: *sax-3(zy5) X*	Shah et al., 2017	N/A
C. elegans: *vang-1(ok1142) X*	CGC	RB1125 WBStrain00031829
C. elegans: *zyIs36(cnd-1::PH::mCherry; myo-2p::mCherry) X*	Antonio Colavita, Shah et al., 2017	N/A
C. elegans: *zyIs40(unc-30p::gfp; cnd-1::PH::mCherry)* Unassigned linkage	This study	N/A
Plasmids		
pPD95.77	Andrew Fire	Addgene #1000000001
pDD282	Dickinson et al., 2015	Addgene #66823
pDD162	Dickinson et al., 2013	Addgene #47549
pAC422	This study	N/A
pAC425	This study	N/A
pAC426	This study	N/A
pCFJ90	Frøkjær-Jensen et al., 2008	Addgene #19327
Oligonucleotides		
DNA Oligonucleotides	Eurofins	See Table S1 for sequences.
Software and Algorithms		
Zeiss Zen 3.2	Zeiss	https://www.zeiss.com/microscopy/en/products/software/zeiss-zen.html
Graphpad Prism 10	Graphpad Software	https://www.graphpad.com/scientific-software/prism/
Imaris 10	Oxford Instruments	https://imaris.oxinst.com/

Two separate strains were generated in which GFP was inserted at either the N-terminus or the C-terminus of the endogenous *ippk-1* gene using the CRISPR/Cas9 homology-directed repair (HDR) approach described in Dickinson et al. (2015). Target sites for N-terminal and C-terminal insertion were generated using the IDT guide RNA design tool at idtdna.com/site/order/designtool/index/CRISPR_SEQUENCE. Guide sequences were inserted into the Cas9–sgRNA plasmid (pDD162, Addgene #47549) using the NEB Q5 Site-Directed Mutagenesis Kit. The HDR plasmid containing *ippk-1* homology arms and the GFP and selection cassette (pDD282, Addgene #66823) was made using Gibson Assembly as described in Dickinson et al. (2015). The *mNG::vang-1* knock-in was made using the same approach (pDD268, Addgene #132523). All primers, including sgRNA primers, are listed in Table S1.

Reporter and rescue constructs

ippk-1p::GFP (pAC420) was made by amplifying a 2974 bp fragment of the *ippk-1* promoter from N2 genomic DNA using primers 18 and 19 (Table S1) and inserting it between the *Sph*I and *Bam*HI sites of pPD95.77 (from Dr. Andrew Fire Lab *C. elegans* Vector Kit). GFP::IPPK-1 was made using Gibson Assembly (New England Biolabs) by combining fragments from cDNA clones yk1067e07 and yk1209d01 (kindly provided by Yuji Kohara, National Institute of Genetics, Japan) and pPD95.77 using primers N12-N17 (Table S1). The resulting construct (pAC422) contained a 2246 bp *ippk-1* cDNA, which was comprised of a 1365 bp open reading frame and an 881 bp 3' untranslated region, inserted in-frame with GFP. The *ippk-1p::GFP::IPPK-1* construct (pAC426) was made by amplifying the 2974 bp *ippk-1* promoter with primers N18 and N19 (Table S1) and inserting it between the *Sph*I and *Bam*HI sites of pAC422. The unc-33p:GFP::IPPK-1 construct (pAC425) was made by amplifying the 1961 bp *unc-33* promoter from N2 genomic DNA using primers N20 and N21 (Table S1) and inserting it between the *Sph*I and *Bam*HI sites of pAC422. Germline transformation was performed using standard methods (Mello et al., 1991) by injecting constructs at 1–5 ng/µl along with 2.5 ng/µl of *myo-2p::mCherry* (pCFJ90, Addgene #19327) and pBluescript KS (Stratagene) to a total DNA concentration of 100 ng/µl.

Microscopy and image analysis

For static and timelapse imaging of live embryos, L4 worms were grown at 25 °C, except for *ippk-1(or1572)* which was grown at 18 °C, until gravid. Static imaging was used to quantify

the posterior extension of the VNC, presence of persistence-cell contacts and to determine the number of *cnd-1* positive VNC progenitors. Embryos were imaged at 63× magnification using a Zeiss Imager M2, Colibri7 LED source, AxiocamHR camera and Zen V3.2 software.

Tissue measurements were taken with a z-projection of 42 slices with 0.25 µm slice width, in a *zyIs36 [cnd-1p::PH::mCherry]* background. Images were processed using a maximum intensity projection prior to analysis. The length of each embryo was measured down the midline starting at the tip of the mouth to the end of the tail. The posterior portion of the VNC was measured starting at the point where it transected the intestinal valve to the end of DD6 (Martin et al., 2016). All images were acquired with an RFP exposure time of 700–900ms at 30 % intensity. Images for cell determination counts were taken with the same conditions across the width of the VNC using a 0.5 µm slice width. All *cnd-1* positive neurons within the area of the VNC were counted. A representative image of the midline defects was also taken using these settings (Fig. 3E) (Fig. 4C and D) and deconvolved using the constrained iterative algorithm on Zeiss Zen V3.2. Persistent-cell contact images were taken in a *zyIs40 (unc-30p::GFP cnd-1p::PH::mCherry)* background, with a GFP exposure time of 50ms at 15 % intensity and mCherry exposure as above. Images were taken over a z-projection of 1-15 slices with 0.5 µm slice width. We defined an embryo with a cell intercalation defect as one containing at least one abnormal persistent DD-DD cell contact instead of a DD-DA contact.

Embryos used for time-lapse imaging were collected from plates using a capillary attached to glass pipette, mounted in a 3 µL drop of M9 containing approximately fifty 25 µm diameter polystyrene beads (Polyscience Inc.) and sealed under a coverslip using Vaseline. Fluorescence time-lapse imaging was performed at 63× magnification using the above microscope configuration with a Zeiss SVB1 microscope signal distribution box/*TTL* trigger cable-controlled camera shutter to minimize excitation light induced phototoxicity. Images of bean stage embryos were acquired at 1.5-min intervals, for approximately 60-min, across a z-projection of 5–15 slices with 0.5 µm between slices. 2x2 binning was used to further minimize the required exposure times during timelapse for rosette timing measurements. Timelapse images were taken in a *zyIs36 [cnd-1p::PH::mCherry]* background, with an *mCherry* exposure time of 400ms at 10 % intensity. The images were deconvolved using the iterative constrained algorithm on Zen 3.2. Measurements of VNC area were preformed on maximum intensity projections of the deconvolved images. Rosette

duration was determined as performed in Shah et al. (2017). Images included in each figure were processed using Zeiss Zen V3.2 and Photoshop. Adjustments were made to the brightness-contrast of each image to standardize representative phenotypes to be easily visible. Deconvolution, using the iterative constrained algorithm on Zen 3.2, was preformed on a representative image of WT and *ippk-1(zy65)* VNC cells at the midline. 3D reconstructions were made by manually tracing cell outlines in Imaris (Oxford Instruments).

Fluorescence images of mNG::VANG-1 were acquired using a Visitech iSIM, coupled to an Olympus IX83 using an Olympus UPLSAPO60XS2 silicone oil immersion objective. The objective correction collar was adjusted for a coverslip thickness of 0.17 and embryos were mounted on high precision coverslips (Marienfeld) in approximately 2 µL of M9 buffer in which 20 µm diameter polystyrene microspheres (Polysciences) were diluted to a concentration of approximately 100 per µL. Images were acquired using Hamamatsu ORCA-Fusion (C14440-20UP) cameras and aligned across channels using multicolored fluorescent beads (Invitrogen Tetraspeck Microspheres, 0.1 µm). Images were acquired using micro-manager and cropped and arranged for visualization, including background subtraction of the median of a 50 × 50 pixel neighbourhood placed adjacent to but outside the embryo, using Fiji (Schindelin et al., 2012).

Quantification of neuron number and position in larvae

Eight to ten L4 stage larval worms were transferred to seeded NGM plates and grown at 25 °C overnight with the exception of *ippk-1(or1572)*, which was grown at 18 °C. L1 stage progeny from these plates were mounted on 2 % agarose pads using 200 µM levamisole (31742, Sigma). DD and DB neuron positions were measured as described in Shah et al. (2017). DD neurons were visualized with *ynIs37[flp-13p::GFP]* and DB neurons with *vab-7(zy142[vab-7::mNG::T2A::mScarlet-I::H2B])* (Saharkhiz et al., 2024). Briefly, neurons were scored by measuring the position of each along the worm using the curve (spline) tool (Zen 3.2). These positions were then converted into mean percentage locations using DD1 or DB1 as 0 % and the anus as 100 %. Each percentage location was plotted using base R, version 4.4.2 (R Core Team, 2019) and geom_jitter from the ggplot2 suite (Wickham, 2009).

Individual DD, DA and DB neuron counts were scored at 20× magnification using *ynIs37[flp-13p::gfp]* (a gift from Dr. Chris Li, CUNY), *unc-4(syb1658[unc-*

4::GFP]) and *vab-7(st12267[vab-7::EGFP]* reporters respectively. Zeiss Zen 3.2 was used for image analysis.

Exogenous IP6 rescue

IP6 (phytic acid sodium salt hydrate, P8810, Sigma) was dissolved in ddH_20 to prepare 0.1 μM, 10 μM and 100 μM solutions. These concentrations were chosen, as they cover a range which has been quantified from mammalian and non-mammalian sources (Szwergold et al., 1987; Freund et al., 1992; Veiga et al., 2006). WT, *ippk-1(zy65)* and *vang-1(ok1142)* worms were grown at 18 °C (*zy65*) or 20 °C (WT and *ok1142*) and transferred to 25 °C at 5–6 h prior to injections. Young adult worms were then injected with IP6 solution into both gonad arms and allowed to recover for 1 h. Healthy survivors were singled onto seeded NGM plates overnight at 25 °C. Hatched larvae or embryos were mounted on the subsequent morning on 2 % agarose pads. L1 and L2 stage worms were scored for the proximity of two or more neurons within a distance of one cell body. Ventral mounted embryos were scored for a shift in the initial meeting of cells towards the posterior of the embryo (as described above). Progeny from independent worms were pooled for statistical analysis.

Statistics

Larval and embryo measurements were compared across populations with the indicated number of individuals. Statistical tests and parameters used to determine significance are indicated in each figure legend. All non-categorical data was assessed for normality when determining the appropriate statistical tests. If the datasets being tested passed the Shapiro–Wilk test, they were analyzed using either Welch's T-test or analysis of variance (ANOVA), as appropriate. Groups that failed to pass the test were compared using the Mann-Whitney *U* test or Kruskal-Wallis test, as appropriate. Graphpad Prism 10 was used for statistical analysis, with the exception of Chi-squared tests followed by post hoc analysis which used base R, version 4.4.2 (R Core Team, 2019).

Credit authorship contribution statement

Nathaniel Noblett: Writing – review & editing, Writing – original draft, Visualization, Methodology, Investigation, Formal analysis. **Tony Roenspies:** Resources, Investigation. **Chloe B. Kirezi:** Investigation. **Clover Stubbert:** Investigation. **Stephane Flibotte:** Investigation. **Pavak K. Shah:** Writing – review & editing, Funding acquisition. **Antonio Colavita:** Writing – review & editing, Writing – original draft,

Supervision, Resources, Project administration, Methodology, Funding acquisition, Formal analysis, Conceptualization.

Funding

This work was supported by the National Institutes of Health [grant number R35GM151199] (PKS); and the Canadian Institutes of Health Research [grant numbers 123513 and 156160] (AC).

Acknowledgements

We thank Dr. Shohei Mitani for *ipmk-1(tm2687)* and *unc-59(tm1939)*, Dr. Yuji Kohara for *ippk-1* cDNAs, and Dr. Chris Li for *ynIs37*. We also thank Saber Saharkhiz for comments on the manuscript. Some strains were provided by the *Caenorhabditis* Genetics Center, which is funded National Institutes of Health Office of Research Infrastructure Programs (P40 OD010440). Gene information, including genomic data, was accessed through WormBase. The authors acknowledge the Cell Biology and Image Acquisition Core (RRID: SCR_021845) funded by the University of Ottawa, Ottawa, Natural Sciences and Engineering Research Council of Canada, and the Canada Foundation for Innovation. We would also like to acknowledge the assistance of StemCore Laboratories Genomics Core Facility (OHRI, uOttawa), RRID:SCR_012601.

Supplemental Figures

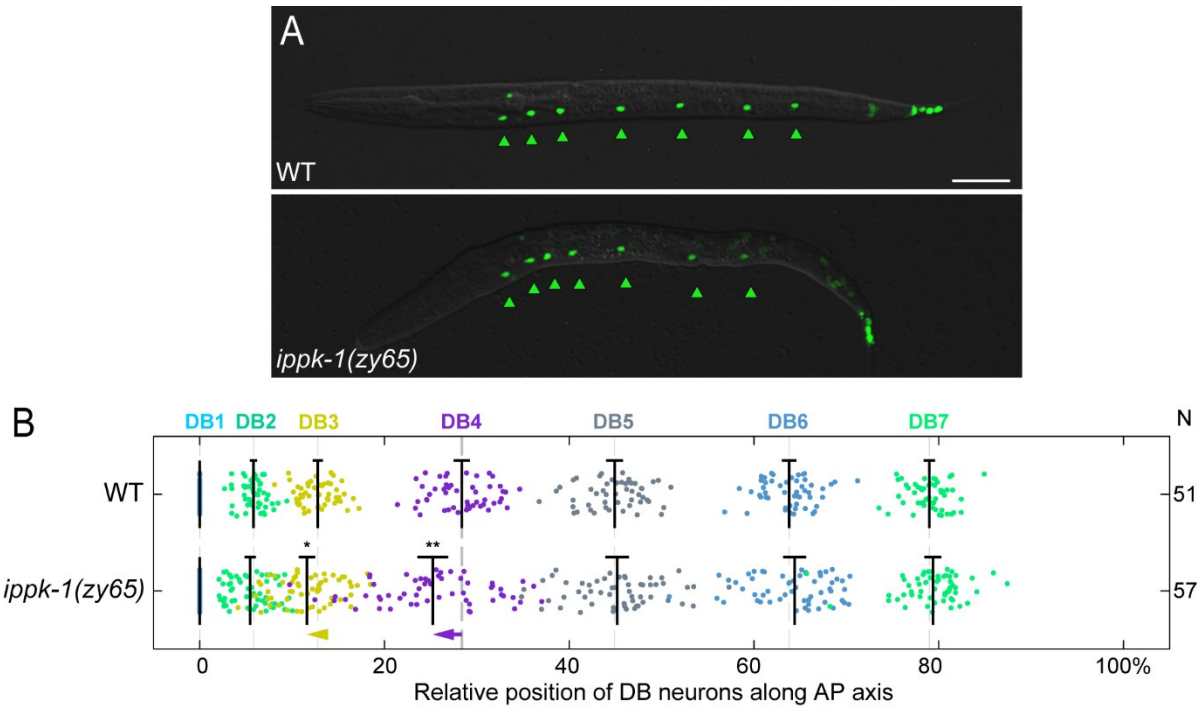

Supplemental Figure 2.1: *ippk-1* mutants show defects in DB neuron positioning. (A) Representative images of DB neuron positions in WT and ippk-1 mutants, visualised using the DB-specific *vab-7(zy142[vab-7::mNG::T2A::mScarlet-I::H2B])*. Arrowheads mark DB neurons. Scale bar = 20µm. (B) Quantification of the mean position of DB2-DB7 neurons relative to DB1 in L1 stage WT and mutant worms. Neurons (colour coded as indicated along top and numbered in sequence from anterior to posterior) are plotted along the AP axis, where DB1 and anus mark the 0% and 100% positions respectively. Means and 95% confidence intervals are indicated for each DB2-7 neuron. Animals scored (N) are indicated on the right. Statistics: Two-tailed T-test was used, Welch's correction. *p0.05.

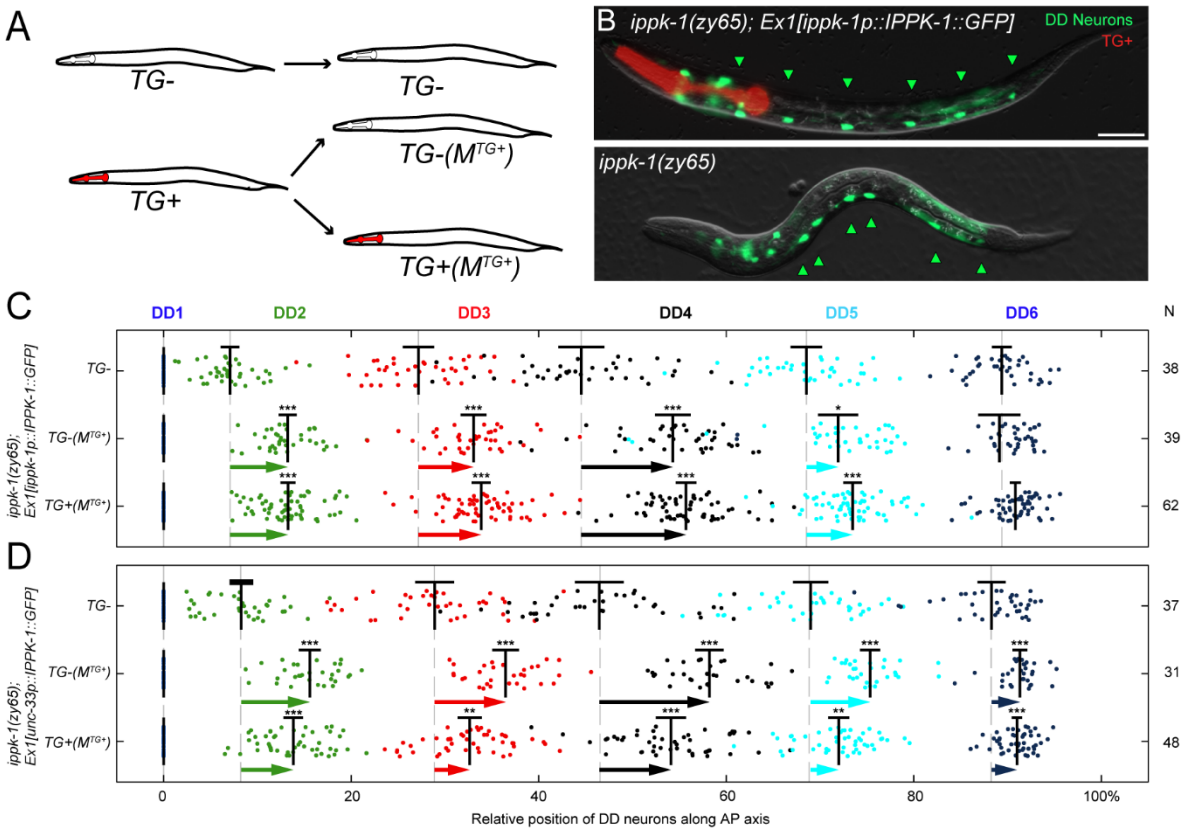

Supplemental Figure 2.2: Rescue of *ippk-1(zy65)* DD neuron position defects with *ippk-1* and *unc-33* promoter driven *ippk-1*. (A) Schematic of the transgene (TG) rescue experiment showing parental (P) and first (F1) generations, along with the presence or absence of TG maternal rescue (MTG+ or MTG-). (B) Representative images of DD positions in *ippk-1(zy65)* mutants with or without an extrachromosomal array carrying the IPPK-1 cDNA transgene and a *myo-2p::mCherry* pharyngeal muscle marker. DD neurons (arrowheads) are labeled using the DD-specific *flp-13p::GFP* reporter. Scale bar = 20µm. (C-D) ippk-1(zy65) DD position defects are maternally rescued when ippk-1 is expressed from an ippk-1 or pan-neuronal unc-33 promoter. Quantification of DD2–4 positions relative to DD1 in L1 worms of the indicated genotype. Neurons (colour coded as indicated along top) are plotted along the AP axis, where DD1 and anus mark the 0% and 100% positions respectively. Means and 95% confidence intervals are indicated for each DD2-6 neuron. Animals scored (N) are indicated on the right. Statistics: One-way ANOVA with Dunnett's post-hoc test against the corresponding WT neuron. *p0.05, **p0.05, ***p<0.001. Arrows show the size of the shift from the mean DD neuron positions found in a TG- *ippk-1(zy65)* mutant for all neurons where p<0.05.

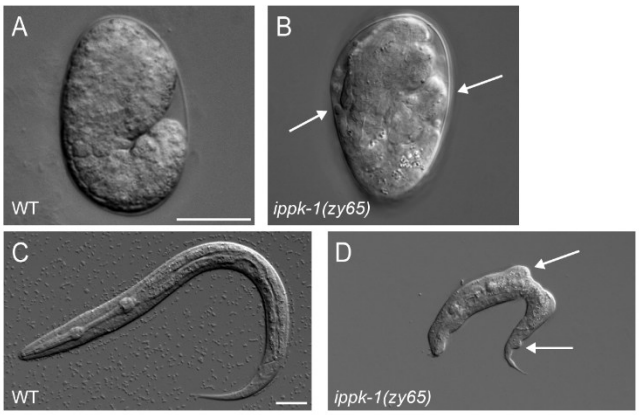

E

Mutant	# embryos (N)	% embryos with epidermal protrusions	# larvae (N)	% larvae with epidermal protrusions
WT*	76	0	79	0
*ippk-1(or1572)**	79	38.0	89	32.6
WT	75	0	65	0
ippk-1(zy65)	116	9.5	135	17.4
vang-1(ok1142)	93	0	67	0
ippk-1(zy65);vang-1(ok1142)	128	23.4	136	38.2
sax-3(zy5)	99	5.0	97	9.3
ippk-1(zy65);sax-3(zy5)	113	32.7	153	60.8

Supplemental Figure 2.3: Epidermal morphology defects in ippk-1(zy65) mutants. (A-B) Representative image of (A) WT and (B) an *ippk-1(zy65)* embryos with epidermal protrusions (arrows). Scale bar = 10µm. (C-D) Representative image of (C) WT and (D) an *ippk-1(zy65)* larvae with epidermal protrusions (arrows). Scale bar = 20µm. (E) Quantification of epidermal defects in WT and mutant embryo and larvae.

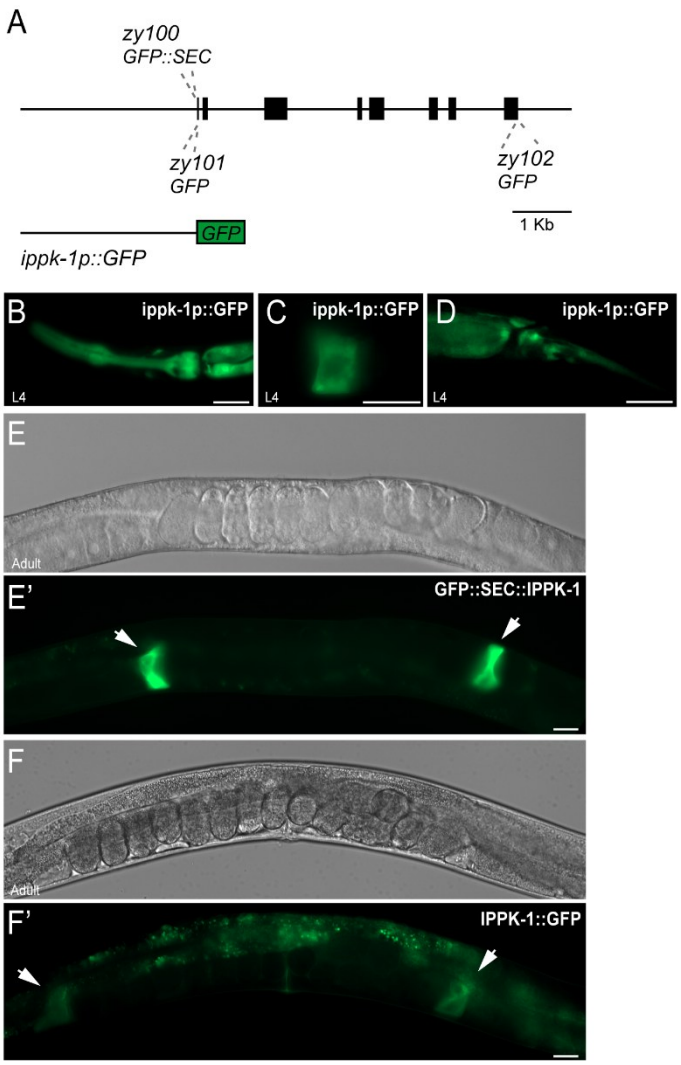

Supplemental Figure 2.4: ippk-1 expression. (A) Schematic showing the ippk-1 GFP transcriptional reporter and GFP knock-ins into the endogenous ippk-1 gene. (B-D) Representative images of expression from an ippk-1p::GFP transgene containing ~3kb of promoter sequence. Expression is detected in (B) pharynx, (C) spermatheca, and (D) tail cells. Endogenous ippk-1 expression in adults from (E) zy100[GFP::SEC::IPPK-1] and (F) zy102 [IPPK-1::GFP] showing strong expression in spermatheca (white arrows). Corresponding Nomarski image above fluorescence image. Scale bar = 20μm.

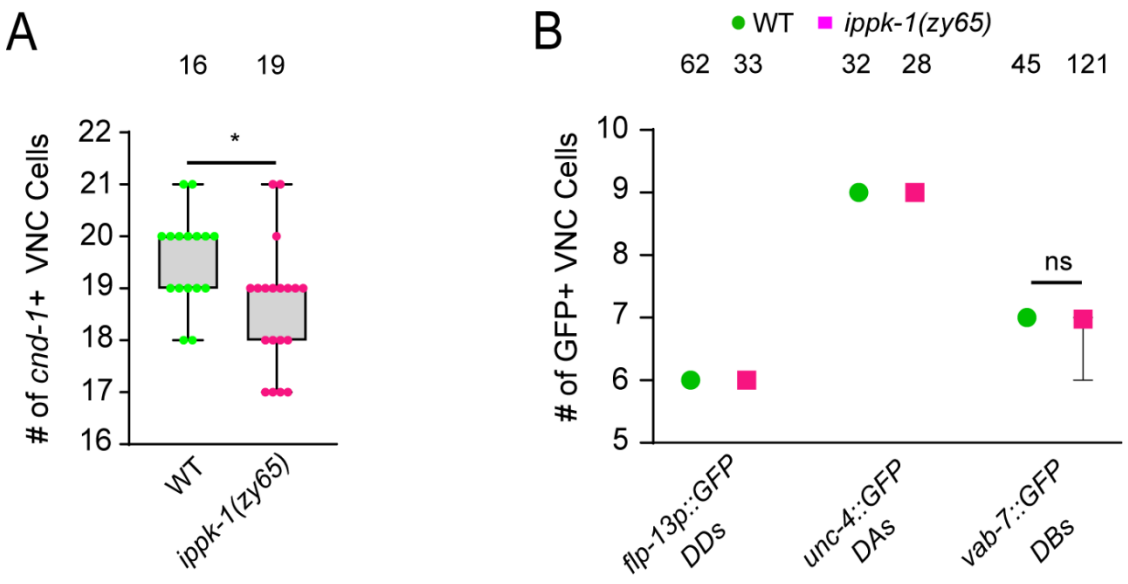

Supplemental Figure 2.5: *ippk-1* mutants do not affect VNC progenitor numbers or terminal cell fates. (A) Quantification of the number *cnd-1p::PH::mCherry* expressing VNC progenitors in late bean stage WT and *ippk-1(zy65)* mutants. (B) Quantification of the number of DA, DB and DD neurons in L1 WT and *ippk-1(zy65)* mutants. Statistics: (A) Mann-Whitney U test. (B) The number of larval DD and DA neurons were identical between WT and ippk-1(zy65) and thus no p-value can be provided. *p<0.05.

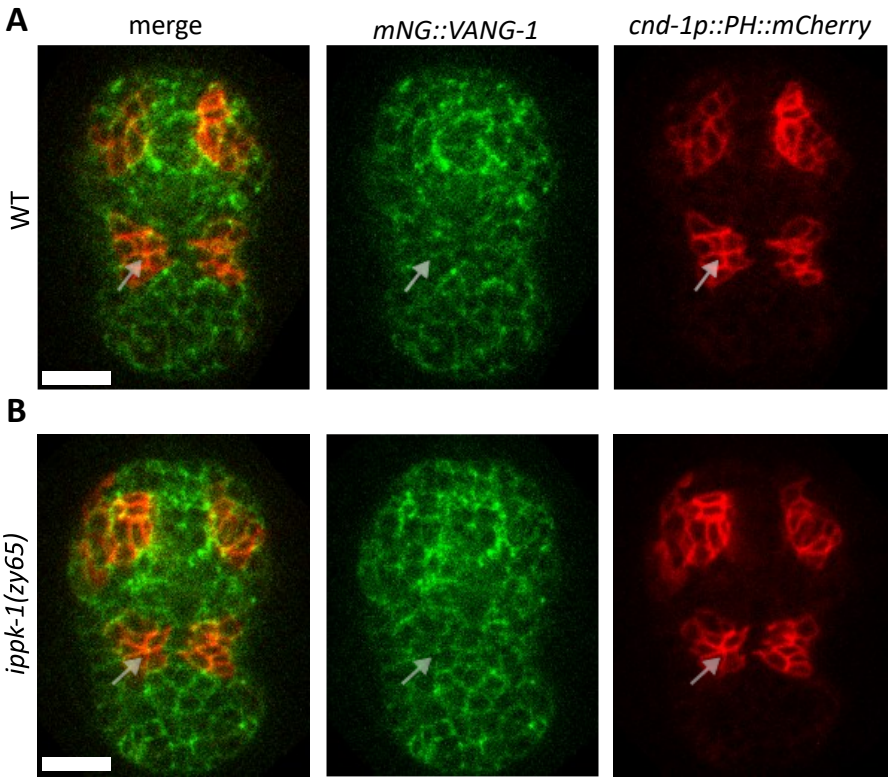

Supplemental Figure 2.6: ippk-1 mutants do not affect VANG-1 localisation to cell vertices. Representative images of mNG::VANG-1 in a (A) WT and (B) ippk-1(zy65) bean stage embryo showing localisation at cell junction vertices (arrow). Cell junctions are labeled with cnd-1p:: PH::mCherry. Scale bar = 10μm.

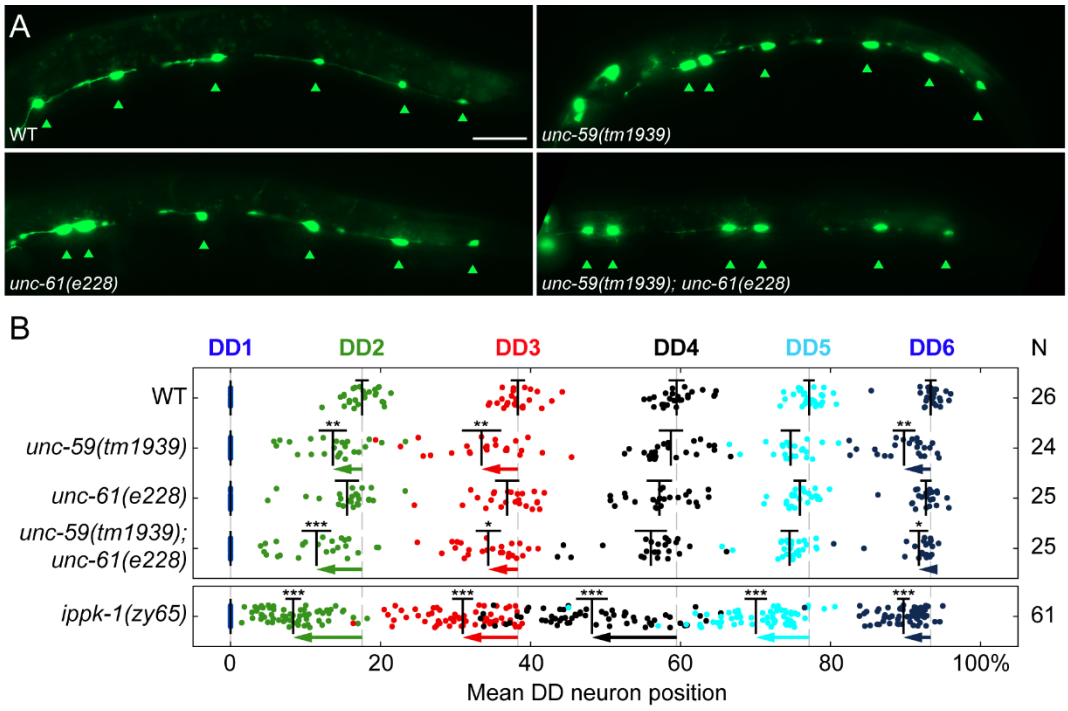

Supplemental Figure 2.7: Septin mutants show defects in DD neuron positioning. (A) Representative images of DD neuron positions in WT, *unc-59(tm1939)*, *unc-61(e228)*, and double mutants, visualised using the DD-specific *ynIs37[flp-13p::gfp]* reporter. Arrowheads mark DD neurons. Scale bar = 20µm. (B) Quantification of DD2-DD6 mean positions relative to DD1 in L1 stage WT and mutant worms. Neurons (colour coded as indicated along top and numbered in sequence from anterior to posterior) are plotted along the AP axis, where DD1 and anus mark the 0% and 100% positions respectively. Means and 95% confidence intervals are indicated for each neuron. Animals scored (N) indicated on the right. *ippk-1(zy65)* positions from Figure 1 is shown in the bottom box for comparison. Statistics: one-way ANOVA with Tukey's post-hoc test. The significance of each neuron is shown relative to WT. *p0.05, **p0.05, ***p<0.001. Arrows show the size of the shift from the mean DD neuron positions found in WT for all neurons where p<0.05.

Supplemental Table 2.1 - Oligonucleotides used in *ippk-1* experiments

Oligo #	DNA Oligos Sequence (5' – 3')	Source	Use
N1	AAATGGCCAAATTAAATGCAGTTTTAGAGCTAGAAATAGCAAGT	Eurofins	sgRNA for *ippk-1::GFP* knock-in
N2	CAAGACATCTCGCAATAGG	Eurofins	sgRNA universal reverse primer
N3	ACGTTGTAAAACGACGGCCAGTCGCCGGCAGGTCATATTTCGGCG GATGT	Eurofins	5' Repair template for *ippk-1::GFP* knock-in
N4	CATCGATGCTCCTGAGGCTCCCGATGCTCCAATGCACGGCTTAAAA TTTCGC	Eurofins	5' Repair template for *ippk-1::GFP* knock-in
N5	CGTGATTACAAGGATGACGATGACAAGAGATAATTTGGCCATTTTT TGCATCAA	Eurofins	3' Repair template for *ippk-1::GFP* knock-in
N6	GGAAACAGCTATGACCATGTTATCGATTTCAGGAAATTGGAAATG TACGTGG	Eurofins	3' Repair template for *ippk-1::GFP* knock-in
N7	GAGGATTAATCTGCATTTTCGTTTTAGAGCTAGAAATAGCAAGT	Eurofins	sgRNA for *GFP::ippk-1* knock-in
N8	ACGTTGTAAAACGACGGCCAGTCGCCGGCAGTTTCCGCAGAATCC CCATC	Eurofins	5' Repair template for *GFP::ippk-1* knock-in
N9	TCCAGTGAACAATTCTTCTCCTTTACTCATTTTCGGGTGGTTTTGGT GAG	Eurofins	5' Repair template for *GFP::ippk-1* knock-in
N10	CGTGATTACAAGGATGACGATGACAAGAGAATGCAGATTAATCCT CCTGCA	Eurofins	3' Repair template for *GFP::ippk-1* knock-in
N11	TCACACAGGAAACAGCTATGACCATGTTATCCACGAGGGGCATTT CAAAT	Eurofins	3' Repair template for *GFP::ippk-1* knock-in
N12	ACTATACAAAATGCAGATTAATCCTCCTG	Eurofins	GFP:IPPK-1 Fragment 1
N13	TCCATGTACCCTTTGGAATGTGTTCAGTG	Eurofins	GFP:IPPK-1 Fragment 2
N14	CATTCCAAAGGGTACATGGATCGGTTATTG	Eurofins	GFP:IPPK-1 Fragment 3
N15	GCCGACTAGTAAAATGCGATATACATTCATTATTG	Eurofins	GFP:IPPK-1 Fragment 4
N16	ATCGCATTTTACTAGTCGGCCGTACGGG	Eurofins	GFP:IPPK-1 Fragment 5
N17	TAATCTGCATTTTGTATAGTTCATCCATGCCATGTG	Eurofins	GFP:IPPK-1 Fragment 6
N18	ATAGCATGCAATACTAAATTAGCCAGAGGCG	Eurofins	Amplify the ippk-1 promoter
N19	TTAGGATCCTTTCGGGTGGTTTTGGTGAGT	Eurofins	Amplify the ippk-1 promoter
N20	ATAGCATGCTAGCAAGAAGCCAGCAAGAAG	Eurofins	Amplify the cnd-1 promoter
N21	TTAGGATCCTTTCCAGTGATGTCCGCCAAC	Eurofins	Amplify the cnd-1 promoter
N22	CATTTTGCTCTTGGAATAACGCA	Eurofins	Sequence *ippk-1(zy65)*
N23	TTTGTCCAGGAGGCTTGTCT	Eurofins	Sequence *ippk-1(zy65)*
N24	GTTGACGTACATCAGCTCGC	Eurofins	Sequence *ippk-1(or1572)*
N25	TGGACACACAGAATAAGCGC	Eurofins	Sequence *ippk-1(or1572)*
N26	TCTCCACCCAAAACTCAGGA	Eurofins	Genotype *ipmk-1(tm2687)*
N27	CACCTCTGAACCTATACCGCT	Eurofins	Genotype ipmk-1(tm2687)
N28	ACCCTGCAATATCCGGTTCA	Eurofins	Genotype *ipmk-1(tm2687)*
N29	TTCACCTTGACAACGCCAGA	Eurofins	Genotype *vang-1(ok1142)*
N30	GGCATGATGACTAGCCCACAA	Eurofins	Genotype *vang-1(ok1142)*
N31	TGTGACAGGGAAAAGTGGAC	Eurofins	Genotype *vang-1(ok1142)*
N32	TTCCTGTGATTGTCATTGTTGC	Eurofins	Genotype *sax-3(zy5)*
N33	TCGATCGAGATCGTCTTCCA	Eurofins	Genotype *sax-3(zy5)*

References

Ahmed, I., Sbodio, J.I., Harraz, M.M., Tyagi, R., Grima, J.C., Albacarys, L.K., Hubbi, M.E., Xu, R., Kim, S., Paul, B.D., Snyder, S.H., 2015. Huntington's disease: neural dysfunction linked to inositol polyphosphate multikinase. Proc. Natl. Acad. Sci. 112 (31), 9751–9756. https://doi.org/10.1073/pnas.1511810112.

Bhat, S.A., Malla, A.B., Oddi, V., Sen, J., Bhandari, R., 2024. Inositol hexakisphosphate kinase 1 is essential for cell junction integrity in the mouse seminiferous epithelium. Biochim. Biophys. Acta Mol. Cell Res. 1871 (1), 119596.

Blankenship, J.T., Backovic, S.T., Sanny, J.S., Weitz, O., Zallen, J.A., 2006. Multicellular rosette formation links planar cell polarity to tissue morphogenesis. Dev. Cell 11 (4), 459–470.

Boitano, S., Dirksen, E.R., Sanderson, M.J., 1992. Intercellular propagation of calcium waves mediated by Inositol Trisphosphate. Science 258 (5080), 292–295. https:// doi.org/10.1126/science.1411526.

Brehm, M.A., Wundenberg, T., Williams, J., Mayr, G.W., Shears, S.B., 2013. A noncatalytic role for inositol 1,3,4,5,6-pentakisphosphate 2-kinase in the synthesis of ribosomal RNA. J. Cell Sci. 126 (2), 437–444. https://doi.org/10.1242/jcs.110031.

Brinkmann, Eva-Maria, Mattes, Benjamin, Kumar, Rahul, Hagemann, Anja IH., Gradl, Dietmar, Scholpp, Steffen, Steinbeisser, Herbert, Kaufmann, Lilian T., Ozbek, ¨ Suat, 2016. Secreted frizzled-related protein 2 (sFRP2) redirects noncanonical wnt signaling from Fz7 to Ror2 during vertebrate gastrulation. J. Biol. Chem. 291 (26), 13730–13742.

Butler, M.T., Wallingford, J.B., 2018. Spatial and temporal analysis of PCP protein dynamics during neural tube closure. eLife 7, e36456. https://doi.org/10.7554/ eLife.36456. Cheng, Y.L., Andrew, D.J., 2015. Extracellular Mipp1 activity confers migratory advantage to epithelial cells during collective migration. Cell Rep. 13 (10), 2174–2188.

Ciruna, B., Jenny, A., Lee, D., Mlodzik, M., Schier, A.F., 2006. Planar cell polarity signalling couples cell division and morphogenesis during neurulation. Nature 439 (7073), 220–224. https://doi.org/10.1038/nature04375.

Cockroft, D.L., Brook, F.A., Copp, A.J., 1992. Inositol deficiency increases the susceptibility to neural tube defects of genetically predisposed (curly tail) mouse embryos in vitro. Teratology 45 (2), 223–232. https://doi.org/10.1002/ tera.1420450216.

Cogram, P., Hynes, A., Dunlevy, L.P.E., Greene, N.D.E., Copp, A.J., 2004. Specific isoforms of protein kinase C are essential for prevention of folate-resistant neural tube defects by inositol. Hum. Mol. Genet. 13 (1), 7–14. https://doi.org/10.1093/ hmg/ddh003.

Curtin, J.A., Quint, E., Tsipouri, V., Arkell, R.M., Cattanach, B., Copp, A.J., Henderson, D. J., Spurr, N., Stanier, P., Fisher, E.M., Nolan, P.M., Steel, K.P., Brown, S.D.M., Gray, I.C., Murdoch, J.N., 2003. Mutation of Celsr1 disrupts planar polarity of inner ear hair cells and

causes severe neural tube defects in the mouse. Curr. Biol. 13 (13), 1129–1133. https://doi.org/10.1016/S0960-9822(03)00374-9.

Desfoug`eres, Y., Wilson, M.S., Laha, D., Miller, G.J., Saiardi, A., 2019. ITPK1 mediates the lipid-independent synthesis of inositol phosphates controlled by metabolism. Proc. Natl. Acad. Sci. 116 (49), 24551–24561.

Devitt, C.C., Weng, S., Bejar-Padilla, V.D., Alvarado, J., Wallingford, J.B., 2024. PCP and Septins govern the polarized organization of the actin cytoskeleton during convergent extension. Curr. Biol. 34 (3), 615–622.

Dickinson, D.J., Pani, A.M., Heppert, J.K., Higgins, C.D., Goldstein, B., 2015. Streamlined genome engineering with a self-excising drug selection cassette. Genetics 200 (4), 1035–1049. https://doi.org/10.1534/genetics.115.178335. Efanov, A.M., Zaitsev, S.V., Berggren, P.-O., 1997. Inositol hexakisphosphate stimulates non-Ca2+-mediated and primes Ca2+-mediated exocytosis of insulin by activation of protein kinase C. Proc. Natl. Acad. Sci. 94 (9), 4435–4439. https://doi.org/ 10.1073/pnas.94.9.4435.

Finger, F.P., Kopish, K.R., White, J.G., 2003. A role for septins in cellular and axonal migration in C. elegans. Dev. Biol. 261 (1), 220–234. https://doi.org/10.1016/ s0012-1606(03)00296-3.

Frederick, J.P., Mattiske, D., Wofford, J.A., Megosh, L.C., Drake, L.Y., Chiou, S.-T., Hogan, B.L.M., York, J.D., 2005. An essential role for an inositol polyphosphate multikinase, Ipk2, in mouse embryogenesis and second messenger production. Proc. Natl. Acad. Sci. 102 (24), 8454–8459. https://doi.org/10.1073/pnas.0503706102.

Freund, W.D., Mayr, G.W., Tietz, C., Schultz, J.E., 1992. Metabolism of inositol phosphates in the protozoan paramecium: characterization of a novel inositolhexakisphosphate-dephosphorylating enzyme. Eur. J. Biochem. 207 (1), 359–367.

Fu, C., Xu, J., Li, R.J., Crawford, J.A., Khan, A.B., Ma, T.M., et al., 2015. Inositol hexakisphosphate kinase-3 regulates the morphology and synapse formation of cerebellar purkinje cells via spectrin/adducin. J. Neurosci. 35 (31), 11056–11067.

Frøkjaer-Jensen, C., Davis, M.W., Hopkins, C.E., Newman, B.J., Thummel, J.M., Olesen, S.P., Grunnet, M., Jorgensen, E.M., 2008. Single-copy insertion of transgenes in Caenorhabditis elegans. Nat. Genet. 40 (11), 1375–1383. https://doi.org/ 10.1038/ng.248.

Fu, C., Xu, J., Cheng, W., Rojas, T., Chin, A.C., Snowman, A.M., Harraz, M.M., Snyder, S. H., 2017. Neuronal migration is mediated by inositol hexakisphosphate kinase 1 via α-actinin and focal adhesion kinase. Proc. Natl. Acad. Sci. 114 (8), 2036–2041. https://doi.org/10.1073/pnas.1700165114.

Goto, T., Keller, R., 2002. The planar cell polarity gene strabismus regulates convergence and extension and neural fold closure in Xenopus. Dev. Biol. 247 (1), 165–181. https://doi.org/10.1006/dbio.2002.0673.

Greene, N.D.E., Copp, A.J., 1997. Inositol prevents folate-resistant neural tube defects in the mouse. Nat. Med. 3 (1), 60–66. https://doi.org/10.1038/nm0197-60.

Greene, N.D., Leung, K.Y., Copp, A.J., 2017. Inositol, neural tube closure and the prevention of neural tube defects. Birth defects research 109 (2), 68–80.

Groenen, P.M., Peer, P.G., Wevers, R.A., Swinkels, D.W., Franke, B., Mariman, E.C., Steegers-Theunissen, R.P., 2003. Maternal myo-inositol, glucose, and zinc status is associated with the risk of offspring with spina bifida. Am. J. Obstet. Gynecol. 189 (6), 1713–1719. https://doi.org/10.1016/S0002-9378(03)00807-X.

Guan, Z., Wang, J., Guo, J., Wang, F., Wang, X., Li, G., Xie, Q., Han, X., Niu, B., Zhang, T., 2014. The maternal ITPK1 gene polymorphism is associated with neural tube defects in a high-risk Chinese population. PLoS One 9 (1), e86145. https://doi.org/10.1371/ journal.pone.0086145.

Høy, M., Efanov, A.M., Bertorello, A.M., Zaitsev, S.V., Olsen, H.L., Bokvist, K., et al., 2002. Inositol hexakisphosphate promotes dynamin I-mediated endocytosis. Proc. Natl. Acad. Sci. 99 (10), 6773–6777.

Jadav, R.S., Kumar, D., Buwa, N., Ganguli, S., Thampatty, S.R., Balasubramanian, N., Bhandari, R., 2016. Deletion of inositol hexakisphosphate kinase 1 (IP6K1) reduces cell migration and invasion, conferring protection from aerodigestive tract carcinoma in mice. Cell. Signal. 28 (8), 1124–1136. https://doi.org/10.1016/j. cellsig.2016.04.011.

Jarrett, O., Stow, J.L., Key, B., 2002. Dynamin-dependent endocytosis is necessary for convergent-extension movements in Xenopus animal cap explants. Int. J. Dev. Biol. 46 (4), 467–473.

Jovelin, R., Cutter, A.D., 2016. Hitting two birds with one stone: the unforeseen consequences of nested gene knockouts in Caenorhabditis elegans. Worm 5 (2), e1156835. https://doi.org/10.1080/21624054.2016.1156835.

Laha, D., Portela-Torres, P., Desfoug`eres, Y., Saiardi, A., 2021. Inositol phosphate kinases in the eukaryote landscape. Adv. biol. regul. 79, 100782.

Lei, Y., Kim, S.-E., Chen, Z., Cao, X., Zhu, H., Yang, W., Shaw, G.M., Zheng, Y., Zhang, T., Wang, H.-Y., Finnell, R.H., 2019. Variants identified in PTK7 associated with neural tube defects. Mol. Gen. Genomic Med. 7 (4), e00584. https://doi.org/10.1002/ mgg3.584.

Lee, H., Lee, S.J., Kim, G.H., Yeo, I., Han, J.K., 2016. PLD1 regulates Xenopus convergent extension movements by mediating Frizzled7 endocytosis for Wnt/PCP signal activation. Dev. Biol. 411 (1), 38–49.

Lesko, A.C., Keller, R., Chen, P., Sutherland, A., 2021. Scribble mutation disrupts convergent extension and apical constriction during mammalian neural tube closure. Dev. Biol. 478, 59–75. https://doi.org/10.1016/j.ydbio.2021.05.013.

Levayer, R., Pelissier-Monier, A., Lecuit, T., 2011. Spatial regulation of Dia and Myosin-II by RhoGEF2 controls initiation of E-cadherin endocytosis during epithelial morphogenesis. Nat. Cell Biol. 13 (5), 529–540.

Li, H., Datunashvili, M., Reyes, R.C., Voglmaier, S.M., 2022. Inositol hexakisphosphate kinases differentially regulate trafficking of vesicular glutamate transporters 1 and 2. Front. Cell. Neurosci. 16, 926794.

Loss, O., Wu, C.T., Riccio, A., Saiardi, A., 2013. Modulation of inositol polyphosphate levels regulates neuronal differentiation. Mol. Biol. Cell 24 (18), 2981–2989. https://doi.org/10.1091/mbc.e13-04-0198.

Lowry, J., Yochem, J., Chuang, C.-H., Sugioka, K., Connolly, A.A., Bowerman, B., 2015. High-Throughput cloning of temperature-sensitive Caenorhabditis elegans mutants with adult syncytial germline membrane Architecture defects. G3 Genes|Genomes| Genetics 5 (11), 2241–2255. https://doi.org/10.1534/g3.115.021451.

Lu, Y., Ahamed, T., Mulcahy, B., Meng, J., Witvliet, D., Guan, S.A., Holmyard, D., Hung, W., Wen, Q., Chisholm, A.D., Samuel, A.D.T., Zhen, M., 2022. Extrasynaptic signaling enables an asymmetric juvenile motor circuit to produce symmetric undulation. Curr. Biol.: CB 32 (21), 4631–4644.e5. https://doi.org/10.1016/j. cub.2022.09.002.

Majerus, P.W., 1992. Inositol phosphate biochemistry. Annu. Rev. Biochem. 61 (1), 225–250.
Martin, E., Rocheleau-Leclair, O., Jenna, S., 2016. Novel metrics to characterize embryonic elongation of the nematode Caenorhabditis elegans. JoVE J. (109), e53712.

Mello, C.C., Kramer, J.M., Stinchcomb, D., Ambros, V., 1991. Efficient gene transfer in C. elegans: extrachromosomal maintenance and integration of transforming sequences. The EMBO journal 10 (12), 3959–3970.

Mitani, S., 2017. Comprehensive functional genomics using Caenorhabditis elegans as a model organism. Proc. Jpn. Acad. Ser. B, 93.

Mound, A., Vautrin-Glabik, A., Foulon, A., Botia, B., Hague, F., Parys, J.B., OuadidAhidouch, H., Rodat-Despoix, L., 2017. Downregulation of type 3 inositol (1,4,5)- trisphosphate receptor decreases breast cancer cell migration through an oscillatory Ca2+ signal. Oncotarget 8 (42), 72324–72341. https://doi.org/10.18632/ oncotarget.20327.

Murdoch, J.N., Henderson, D.J., Doudney, K., Gaston-Massuet, C., Phillips, H.M., Paternotte, C., Arkell, R., Stanier, P., Copp, A.J., 2003. Disruption of scribble (Scrb1) causes severe neural tube defects in the circletail mouse. Hum. Mol. Genet. 12 (2), 87–98. https://doi.org/10.1093/hmg/ddg014.

Nguyen, T.Q., Sawa, H., Okano, H., White, J.G., 2000. The C. elegans septin genes, unc59 and unc-61, are required for normal postembryonic cytokineses and morphogenesis but have no essential function in embryogenesis. J. Cell Sci. 113 (21), 3825–3837.

Nikolopoulou, E., Galea, G.L., Rolo, A., Greene, N.D.E., Copp, A.J., 2017. Neural tube closure: cellular, molecular and biomechanical mechanisms. Development 144 (4), 552–566. https://doi.org/10.1242/dev.145904.

Noblett, N., Wu, Z., Ding, Z.H., Park, S., Roenspies, T., Flibotte, S., et al., 2019. DIP-2 suppresses ectopic neurite sprouting and axonal regeneration in mature neurons. Journal of Cell Biology 218 (1), 125–133.

Odom, A.R., Stahlberg, A., Wente, S.R., York, J.D., 2000. A role for nuclear inositol 1,4,5-Trisphosphate kinase in transcriptional control. Science 287 (5460), 2026–2029. https://doi.org/10.1126/science.287.5460.2026.

Packer, J.S., Zhu, Q., Huynh, C., Sivaramakrishnan, P., Preston, E., Dueck, H., Stefanik, D., Tan, K., Trapnell, C., Kim, J., Waterston, R.H., Murray, J.I., 2019. A lineage-resolved molecular atlas of *C. elegans* embryogenesis at single-cell resolution. Science 365 (6459), eaax1971. https://doi.org/10.1126/science. aax1971.

Park, J., Longo, F., Park, S.J., Lee, S., Bae, M., Tyagi, R., Han, J.-H., Kim, S., Santini, E., Klann, E., Snyder, S.H., 2019a. Inositol polyphosphate multikinase mediates extinction of fear memory. Proc. Natl. Acad. Sci. 116 (7), 2707–2712. https://doi. org/10.1073/pnas.1812771116.

Park, J., Park, S.J., Kim, S., 2019b. Inositol polyphosphate multikinase deficiency leads to aberrant induction of synaptotagmin-2 in the forebrain. Mol. Brain 12 (1), 58. https://doi.org/10.1186/s13041-019-0480-1.

Politi, A., Gaspers, L.D., Thomas, A.P., Hofer, ¨ T., 2006. Models of IP3 and Ca2+ oscillations: frequency encoding and identification of underlying feedbacks. Biophys. J. 90 (9), 3120–3133. https://doi.org/10.1529/biophysj.105.072249.

R Core Team, 2019. R: a Language and Environment for Statistical Computing. R Foundation for Statistical Computing, Vienna, Austria. https://www.R-project.org.

Rao, F., Xu, J., Fu, C., Cha, J.Y., Gadalla, M.M., Xu, R., Barrow, J.C., Snyder, S.H., 2015. Inositol pyrophosphates promote tumor growth and metastasis by antagonizing liver kinase B1. Proc. Natl. Acad. Sci. 112 (6), 1773–1778. https://doi.org/10.1073/ pnas.1424642112.

Reynolds, A., McDearmid, J.R., Lachance, S., De Marco, P., Merello, E., Capra, V., et al., 2010. VANGL1 rare variants associated with neural tube defects affect convergent extension in zebrafish. Mech. Dev. 127 (7–8), 385–392.

Rojas, T., Cheng, W., Gao, Z., Liu, X., Wang, Y., Malla, A.P., Chin, A.C., Romer, L.H., Snyder, S.H., Fu, C., 2019. Inositol hexakisphosphate kinase 3 promotes focal adhesion turnover via interactions with dynein intermediate chain 2. Proc. Natl. Acad. Sci. 116 (8), 3278–3287. https://doi.org/10.1073/pnas.1817001116.

Saharkhiz, S., Petite, M., Roenspies, T., Perkins, T., Colavita, A., 2024. VNC-Dist: a machine learning-based pipeline for quantification of neuronal positioning in the ventral nerve cord of C. elegans. bioRxiv. https://doi.org/10.1101/ 2024.11.16.623955.

Saiardi, A., Erdjument-Bromage, H., Snowman, A.M., Tempst, P., Snyder, S.H., 1999. Synthesis of diphosphoinositol pentakisphosphate by a newly identified family of higher inositol polyphosphate kinases. Curr. Biol. 9 (22), 1323–1326. https://doi. org/10.1016/S0960-9822(00)80055-X.

Saraswathy, V.M., Kurup, A.J., Sharma, P., Pol`es, S., Poulain, M., Fürthauer, M., 2022. The E3 ubiquitin ligase mindbomb1 controls planar cell polarity-dependent convergent extension movements during zebrafish gastrulation. eLife 11, e71928.

Sarmah, B., Latimer, A.J., Appel, B., Wente, S.R., 2005. Inositol polyphosphates regulate zebrafish left-right asymmetry. Dev. Cell 9 (1), 133–145. https://doi.org/10.1016/j. devcel.2005.05.002.

Schindelin, J., Arganda-Carreras, I., Frise, E., Kaynig, V., Longair, M., Pietzsch, T., Cardona, A., 2012. Fiji: an open-source platform for biological-image analysis. Nat. Methods 9, 676–682. https://doi.org/10.1038/nmeth.2019.

Schröterová, L., Ježková, A., Rudolf, E., Caltová, K., Králová, V., Hanušová, V., 2018. Inositol hexaphosphate limits the migration and the invasiveness of colorectal carcinoma cells in vitro. Int. J. Oncol. 53 (4), 1625–1632.

Seeds, A.M., Tsui, M.M., Sunu, C., Spana, E.P., York, J.D., 2015. Inositol phosphate kinase 2 is required for imaginal disc development in Drosophila. Proc. Natl. Acad. Sci. 112 (51), 15660–15665. https://doi.org/10.1073/pnas.1514684112.

Shah, P.K., Tanner, M.R., Kovacevic, I., Rankin, A., Marshall, T.E., Noblett, N., Tran, N. N., Roenspies, T., Hung, J., Chen, Z., Slatculescu, C., Perkins, T.J., Bao, Z., Colavita, A., 2017. PCP and SAX-3/Robo pathways cooperate to regulate convergent extension-based nerve cord assembly in C. elegans. Dev. Cell 41 (2), 195–203.e3. https://doi.org/10.1016/j.devcel.2017.03.024.

Shindo, A., Wallingford, J.B., 2014. PCP and septins compartmentalize cortical actomyosin to direct collective cell movement. Science 343 (6171), 649–652.

Shindo, A., Inoue, Y., Kinoshita, M., Wallingford, J.B., 2019. PCP-dependent transcellular regulation of actomyosin oscillation facilitates convergent extension of vertebrate tissue. Dev. Biol. 446 (2), 159–167.

Sutherland, A., Keller, R., Lesko, A., 2020. Convergent extension in mammalian morphogenesis. In: Seminars in Cell & Developmental Biology, 100. Academic Press, pp. 199–211.

Szwergold, B.S., Graham, R.A., Brown, T.R., 1987. Observation of inositol pentakis-and hexakis-phosphates in mammalian tissues by 31P NMR. Biochem. Biophys. Res. Commun. 149 (3), 874–881.

Taylor, S.R., Santpere, G., Weinreb, A., Barrett, A., Reilly, M.B., Xu, C., et al., 2021. Molecular topography of an entire nervous system. Cell 184 (16), 4329–4347.

Ucuncu, E., Rajamani, K., Wilson, M.S.C., Medina-Cano, D., Altin, N., David, P., Barcia, G., Lefort, N., Banal, C., Vasilache-Dangles, M.-T., Pitelet, G., Lorino, E., Rabasse, N., Bieth, E., Zaki, M.S., Topcu, M., Sonmez, F.M., Musaev, D., Stanley, V., et al., 2020. MINPP1 prevents intracellular accumulation of the chelator inositol hexakisphosphate and is mutated in Pontocerebellar Hypoplasia. Nat. Commun. 11 (1), 6087. https://doi.org/10.1038/s41467-020-19919-y.

Vazquez-Manrique, ´ R.P., Nagy, A.I., Legg, J.C., Bales, O.A.M., Ly, S., Baylis, H.A., 2008. Phospholipase C-ε regulates epidermal morphogenesis in Caenorhabditis elegans. PLoS Genet. 4 (3), e1000043. https://doi.org/10.1371/journal.pgen.1000043.

Veiga, N., Torres, J., Domínguez, S., Mederos, A., Irvine, R.F., Díaz, A., Kremer, C., 2006. The behaviour of myo-inositol hexakisphosphate in the presence of magnesium (II) and calcium (II): protein-free soluble InsP6 is limited to 49 μM under cytosolic/ nuclear conditions. J. Inorg. Biochem. 100 (11), 1800–1810.

Verbsky, J.W., Wilson, M.P., Kisseleva, M.V., Majerus, P.W., Wente, S.R., 2002. The synthesis of Inositol Hexakisphosphate: CHARACTERIZATION of human inositol 1,3,4,5,6-PENTAKISPHOSPHATE 2-KINASE. J. Biol. Chem. 277 (35), 31857–31862. https://doi.org/10.1074/jbc.M205682200.

Verbsky, J., Lavine, K., Majerus, P.W., 2005a. Disruption of the mouse inositol 1,3,4,5,6-pentakisphosphate 2-kinase gene, associated lethality, and tissue distribution of 2- kinase expression. Proc. Natl. Acad. Sci. 102 (24), 8448–8453. https://doi.org/ 10.1073/pnas.0503656102.

Verbsky, J.W., Chang, S.C., Wilson, M.P., Mochizuki, Y., Majerus, P.W., 2005b. The pathway for the production of inositol hexakisphosphate in human cells. J. Biol. Chem. 280 (3), 1911–1920.

Voglmaier, S.M., Keen, J.H., Murphy, J.E., Ferris, C.D., Prestwich, G.D., Snyder, S.H., Theibert, A.B., 1992. Inositol hexakisphosphate receptor identified as the clathrin assembly protein AP-2. Biochem. Biophys. Res. Commun. 187 (1), 158–163.

Wallingford, J.B., Ewald, A.J., Harland, R.M., Fraser, S.E., 2001. Calcium signaling during convergent extension in Xenopus. Curr. Biol. 11 (9), 652–661. https://doi. org/10.1016/S0960-9822(01)00201-9.

Wallingford, J.B., Harland, R.M., 2002. Neural tube closure requires dishevelleddependent convergent extension of the midline. Development 129 (24), 5815–5825. https://doi.org/10.1242/dev.00123.

Westfall, T.A., Brimeyer, R., Twedt, J., Gladon, J., Olberding, A., Furutani-Seiki, M., Slusarski, D.C., 2003. Wnt-5/pipetail functions in vertebrate axis formation as a negative regulator of Wnt/β-catenin activity. Journal of Cell Biology 162 (5), 889–898. https://doi.org/10.1083/jcb.200303107.

Wickham, H., 2009. ggplot2: Elegant Graphics for Data Analysis. Springer, New York.

Williams, M., Yen, W., Lu, X., Sutherland, A., 2014. Distinct apical and basolateral mechanisms drive planar cell polarity-dependent convergent extension of the Mouse neural plate. Dev. Cell 29 (1), 34–46. https://doi.org/10.1016/j. devcel.2014.02.007.

Wilson, M.P., Hugge, C., Bielinska, M., Nicholas, P., Majerus, P.W., Wilson, D.B., 2009. Neural tube defects in mice with reduced levels of inositol 1,3,4-trisphosphate 5/6- kinase. Proc. Natl. Acad. Sci. 106 (24), 9831–9835. https://doi.org/10.1073/ pnas.0904172106.

Woods, B.L., Gladfelter, A.S., 2021. The state of the septin cytoskeleton from assembly to function. Curr. Opin. Cell Biol. 68, 105–112.

Yang, S.-N., Yu, J., Mayr, G.W., Hofmann, F., Larsson, O., Berggren, P.-O., 2001. Inositol hexakisphosphate increases L-type Ca2+ channel activity by stimulation of adenylyl cyclase. FASEB J. 15 (10), 1753–1763. https://doi.org/10.1096/fj.00-0799com.

Yang, Z.-L., Chen, J.-N., Lu, Y.-Y., Lu, M., Wan, Q.-L., Wu, G.-S., Luo, H.-R., 2021. Inositol polyphosphate multikinase IPMK-1 regulates development through IP3/calcium signaling in Caenorhabditis elegans. Cell Calcium 93, 102327. https://doi.org/ 10.1016/j.ceca.2020.102327.

Yin, M.X., Catimel, B., Gregory, M., Condron, M., Kapp, E., Holmes, A.B., Burgess, A.W., 2016. Synthesis of an inositol hexakisphosphate (IP6) affinity probe to study the interactome from a colon cancer cell line. Integr. Biol. 8 (3), 309–318.

York, J.D., Odom, A.R., Murphy, R., Ives, E.B., Wente, S.R., 1999. A phospholipase Cdependent inositol polyphosphate kinase pathway required for efficient messenger RNA export. Science 285 (5424), 96–100.

Chapter 3. Manuscript #2 - Nuclear hormone receptor regulation of PAL-1/Caudal mediates ventral nerve cord assembly in *C. elegans*

Nuclear hormone receptor regulation of PAL-1/Caudal mediates ventral nerve cord assembly in *C. elegans*.

Nathaniel Noblett[a,b], Tony Roenspies[a], Stephane Flibotte[c], and Antonio Colavita[a,b*]

[a]Neuroscience Program, Ottawa Hospital Research Institute, Ottawa, Canada
[b]Department of Cellular and Molecular Medicine, University of Ottawa, Ottawa, Canada
[c]UBC/LSI Bioinformatics Facility, University of British Columbia, Vancouver, Canada
[*]**Corresponding Author:** Antonio Colavita colavita@uottawa.ca

Abstract

The regulatory network governed by CDX/*Caudal* family transcription factors plays critical roles in shaping embryonic neural development. In *C. elegans*, we found that proper expression of *pal-1*, the *C. elegans Caudal* homologue, is required for correct positioning of motor neuron cell bodies in the first larval stage ventral nerve cord (VNC). We identified an upstream regulatory region within the *pal-1* promoter that drives *pal-1* expression in a subset of DD and DA neuronal progenitors. We also show that SEX-1, a nuclear hormone receptor, is required for motor neuron positioning in the VNC. Loss of *sex-1* results in neuronal positioning defects similar to those observed in *pal-1* mutants. This is in part due to a requirement for SEX-1 in promoting *pal-1* expression in DD and DA neuronal progenitors during VNC assembly. Double mutant analysis further suggests that *sex-1* also has *pal-1*-independent functions. Together, these findings define a transcriptional hierarchy in which the SEX-1 nuclear hormone receptor regulates the tissue-specific activity of PAL-1 to promote proper motor neuron positioning in the VNC and highlight a conserved role for NHR and CDX/Caudal family proteins in central nerve cord formation.

Introduction

The coordination of signaling cascades and positional information through transcriptional networks is essential for axial extension during embryonic morphogenesis (Collinet and Lecuit, 2021). The *Caudal* family of homeodomain transcription factors, including CDX1/2/4 in mammals and their worm homologue PAL-1, play critical roles in posterior patterning and axial extension by coordinating pathways involved in cell-fate determination, morphogenesis and regionalization (Edgar et al., 2001; van den Akker et al., 2002; Savory et al., 2011; Gilbert et al., 2020). For CDX proteins this includes the regulation of neurulation during mammalian development, a process where the neuroectoderm folds and elongates to form the neural tube (Savory et al., 2011; Zhao et al., 2014). Neurulation is partly driven by convergent extension, a morphogenetic process characterized by coordinated cell-cell intercalations along the mediolateral axis and extension along the anterior-posterior axis. Mouse embryos with mutations in both CDX1 and CDX2 exhibit typical convergent extension defects, including a reduced length-to-width ratio of the neural tube,

failure of extension, and a broadened midline of the neural plate (Savory et al., 2011). These defects lead to embryonic lethality and craniorachischisis, a severe neural tube defect (Savory et al., 2011).

CDX proteins function as a central hub for multiple signaling pathways that regulate neurulation (Wilson et al., 2003; Palmer et al., 2021; Zhao et al., 2022). This includes the direct induction of CDX1 by retinoic acid receptors (RARs) α1 and γ, two types of ligand dependent nuclear hormone receptors, as well as β-catenin, a key component of canonical WNT signaling (Houle et al., 2003; Zhao et al., 2014). During neurulation, CDX members have been linked to regulation of the Planar Cell Polarity (PCP) pathway, a key pathway involved in convergent extension (Savory et al., 2011). PCP components associated with CDX include Scribble and the transmembrane receptor PTK7 (Wehner et al., 2011; Hayes et al., 2013; Martinez et al., 2015). Both ChIP analysis and transfection assays suggest that CDX proteins directly regulate PTK7 expression (Savory et al., 2011).

In *C. elegans*, PAL-1 is involved in cell fate determination, regional identity, and morphogenesis. PAL-1 plays an early role in blastomere cell fate, including a key role in establishing the fate of descendants of the C and D blastomeres (producing primarily body-wall muscle, hypodermal cells, along with two neurons) and, along with the WNT effector POP-1 and the bZIP transcription factor SKN-1, the descendants of the E blastomere (producing intestinal cells) (Hunter and Kenyon, 1996; Maduro et al., 2005). Additionally, PAL-1 is involved in non-cell fate related functions, such as orienting epidermal seam-cell migration and alignment during development (Gilbert et al., 2020). Other defects, including delays in ventral enclosure, failed long range migration in MS cell descendants, and abnormal cleavage axis in muscle cells suggest that additional functions of a *pal-1* network remain to be explored (Edgar et al., 2001).

At hatching, the ventral nerve cord (VNC) in *C. elegans*, is comprised of 22 embryonically born motor neurons, belonging to three classes (6 GABAergic inhibitory DD, 9 cholinergic excitatory DA, and 7 cholinergic excitatory DB), that innervate body wall muscle to control sinusoidal locomotion (Lu et al., 2022). Progenitors of these neurons are born on the left and right sides of the embryo and undergo collective cell movement toward the midline where they intercalate to form the VNC. This process shares several key features with neurulation in mammals, including rosette mediated-convergent extension, asymmetric distribution of core PCP

components like VANG-1/VangL, and inositol phosphate signaling (Shah et al., 2017; Noblett et al., 2025).

Here, we describe roles for the nuclear hormone receptor (NHR) SEX-1 and the *Caudal* homologue PAL-1 in regulating proper neuronal organization of the VNC. Using alleles with tissue-specific effects on gene expression, we identified a role for *pal-1* in regulating the proper positioning of embryonically derived motor neurons in the VNC. These mutations disrupt a *pal-1* promoter region required for expression in a subset of neuronal progenitors during embryonic convergent extension movements that form the VNC. We found that SEX-1 is required for *pal-1* expression in progenitor neurons, and that restoring *pal-1* expression in these cells is sufficient to partially rescue the neuronal positioning defects in *sex-1* mutants. These findings show that nuclear hormone regulation of Caudal is important for VNC assembly. Given that NHRs and CDX/Caudal proteins contribute to neural tube formation in vertebrates (Barreto et al., 2003; Savory et al., 2011; Zhao et al., 2014; Koch et al., 2025), our findings highlight the deep conservation of mechanisms underlying central nerve cord development.

Results

Identification of a *pal-1* promoter region involved in neuronal specific expression.

The VNC at the first larval (L1) stage contains three classes of motor neurons (6 DD, 9 DA, and 7 DB). We have previously shown that loss of PCP genes, such as *vang-1*, and the Robo encoding gene *sax-3* result in VNC assembly defects during embryogenesis, which manifest as mispositioned motor neurons in L1 larvae (Shah et al., 2017). To identify new genes involved in neuron positioning, we performed a genetic screen using the DD-specific reporter *ynIs37[flp-13p::GFP]* (unpublished results). We identified two mutants, *zy43* and *zy44*, that displayed similar DD neuron positioning defects, with DD2 and DD3 positioned closer together than in wild type (WT) (Figure 3.1A). Whole genome sequencing revealed these mutations to be single nucleotide changes, one nucleotide apart, located 143 and 145 bp upstream of the *arl-6* start codon (Figure 3.1C). To determine if these changes were responsible for the neuron position defects, we used Cas9-targetted non-homologous end joining-mediated DNA repair to generate a 44 bp deletion (*zy117*) centered on the mutated region (Figure 3.1C and D). This mutant displayed similar neuron positioning defects (Figure 3.1B).

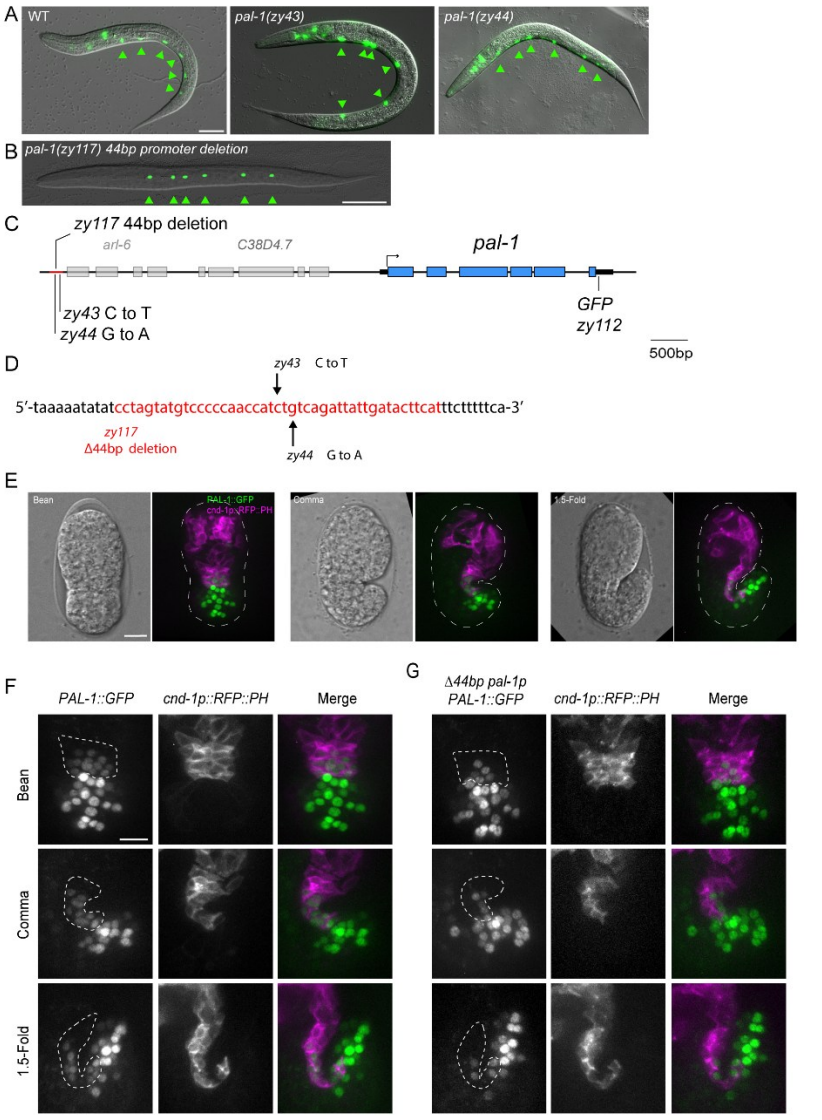

Figure 3.1: A distal promoter element regulates *pal-1* expression in DD and DA progenitors. (A-B) Representative images of DD positions in (A) WT, *pal-1(zy43)*, *pal-1(zy44)* and (B) *pal-1(zy117)* mutants. Arrowheads mark DD neurons, which are visualised using *flp-13p::GFP*. Scale bar = 20µm. (C) Diagram of the *pal-1* genomic region showing the positions of mutations used in this study. (D) The location of nucleotide changes in *zy43*, *zy44* and *zy117*. Red nucleotides highlight the deleted sequence in *pal-1(zy117)*. (E) Representative maximum intensity projections of an endogenous *pal-1::GFP* expression at three stages of embryonic development. Nomarski image indicates the morphology of the embryo. A *cnd-1p::mCherry ::PH* reporter labels the membranes of DD and a subset of DA progenitors. Scale bar = 10µm. (F) Representative maximum intensity projections show endogenous *pal-1::GFP* expression in WT and *pal-1(zy117)* mutant backgrounds. The dotted line indicates regions of interest containing expression changes. Number of embryos examined: N = 8 for WT and N = 3 for *pal-1(zy117)* at the bean stage. N = 4 for both genotypes at comma stage. N = 7 for WT and N = 6 for *pal-1(zy117)* at the 1.5-fold stage. Scale bar = 10µm.

The proximity of *zy43* and *zy44* to the *arl-6* gene led us to examine DD neuron positioning in an *arl-6* mutant, but we did not observe any defects (data not shown). These mutations were also located approximately 6.5 kb upstream of *pal-1* (Figure 3.1C), an essential gene encoding an homologue of the homeobox protein CDX/Caudal, within a region known to be required for complete rescue of *pal-1* embryonic defects (Edgar et al., 2001). The CDX family of proteins are also associated with neural tube defects in mammals, suggesting *pal-1* was a good candidate for involvement in VNC formation (Savory et al., 2011).

Because strong *pal-1* loss-of-function mutants are non-viable and display severe embryonic and larval morphology defects (Baugh et al., 2005), we asked whether the 44 bp *zy117* deletion disrupted a promoter region important for *pal-1* expression. To address this, we endogenously tagged the *pal-1* gene with a C-terminal GFP in both the WT and *zy117* background (Figure 3.1E). As previously reported, PAL-1::GFP is widely expressed in the nuclei of posterior cells from the bean to 1.5-fold stage embryo (Edgar et al., 2001). Using a *cnd-1p::mCherry::PH* reporter (*zyIs36*) to label the membranes of DD and DA neuronal progenitors, we observed that *PAL-1::GFP* was also expressed in the nuclei of a subset of DD, DA, and DB progenitors, specifically those located in the posterior VNC (Figure 3.1E and F). Based on their location, these appear to be DD3-6, DA3-6, and DB5-7. Strikingly, in the *zy117* promoter mutant, PAL-1::GFP expression was completely absent from DD and DA progenitors (Fig Figure 3.1G). Posterior tail cells and DB progenitors, which can be identified by their location outside and ventral to *cnd-1p*-labeled progenitors at the 1.5-fold stage, were not affected in *zy117* mutants. These results indicate that *zy43*, *zy44*, and the 44 bp *zy117* deletion mutant disrupt a *pal-1* promoter regulatory element required for expression in DD and DA neurons.

pal-1 promoter mutants exhibit motor neuron cell body positioning defects.

Our *pal-1* promoter mutants were identified based on defects in the positioning of DD motor neurons, one of three classes of motor neurons present in the VNC of newly hatched L1 worms. To quantify these position defects and determine if they extend to the other two classes of motor neurons, DA and DB, we utilised a two-colour reporter background in which each neuron class was uniquely labeled with a class-specific fluorescent cell fate marker at L1 (Saharkhiz et al., 2024). The nuclei of DD1-6 were labeled in red with *zySi2[unc-30p::mCherry::H2B]*, DA1-9 in green with *unc-4(zy123[unc-4::mNG])*, and DB1-7 in both red and green, detected as yellow,

with *vab-7(zy142[vab-7::mNG::T2A::mScarlet-I::H2B])*. The *unc-4* marker also labels the interneurons SABVL, SABVR, and SABD, which are located anterior to DA1. Neuron positions were normalized by setting SABVL as the anterior reference point (0%) and the rectum as the posterior reference point (100%), allowing neuron locations to be compared relative to VNC length across different animals. When plotted, neurons of each class are numbered sequentially from anterior to posterior, regardless of their terminal cell lineage identity, which may be unknown in mutant backgrounds.

DD, DA, and DB motor neurons are stereotypically positioned and arranged in a repeating pattern along the VNC. We found that the mean position of most DD neurons in *pal-1(zy117)* showed significant anterior shifts along the VNC compared to WT (Figure 3.2A and B, Supplemental Figure 3.1). Some DA and DB neurons were also mispositioned compared to WT, but these shifts were milder than the DD neuron defects and may represent secondary effects caused by the mispositioned DD neurons. Indeed, the strongest position shifts affected DD3–6, which correlates with *pal-1* expression in these neurons, while milder shifts were observed in DD1 and DD2, where expression is absent. In addition, except for DA8 and DA9, which are located opposite each other on the left and right in the preanal ganglia, the neuron classes are arranged in an alternating sequence, with no two classes adjacent to each other (Figure 3.2C-E). This pattern is significantly altered in *zy117* mutants, with some same class cell bodies more frequently adjacent to each other (Figure 3.2D and E). For example, in 21% of *zy117* larvae (N=53), the DD2 and DD3 cell bodies are adjacent with no intervening cells, compared to 0% in WT (N=51). Notably, although *pal-1* regulates cell fates (Edgar et al., 2001; Maduro et al., 2005), we did not observe any changes in DD, DA, or DB cell numbers that would indicate cell fate defects during our analysis. Overall, these results indicate that *pal-1* expression, driven by the DD-DA-specific promoter element, is primarily required for proper DD motor neuron positioning.

PAL-1 acts independently of VANG-1 and SAX-3 to position motor neurons in the VNC.

We previously showed that the PCP pathway component VANG-1 and the Robo receptor SAX-3 act in parallel to regulate motor neuron cell body positioning in the VNC of newly hatched larvae. Loss of both *vang-1* and *sax-3* causes a highly penetrant anterior displacement of motor neuron cell bodies, a defect that is synergistically more severe than in either single mutant

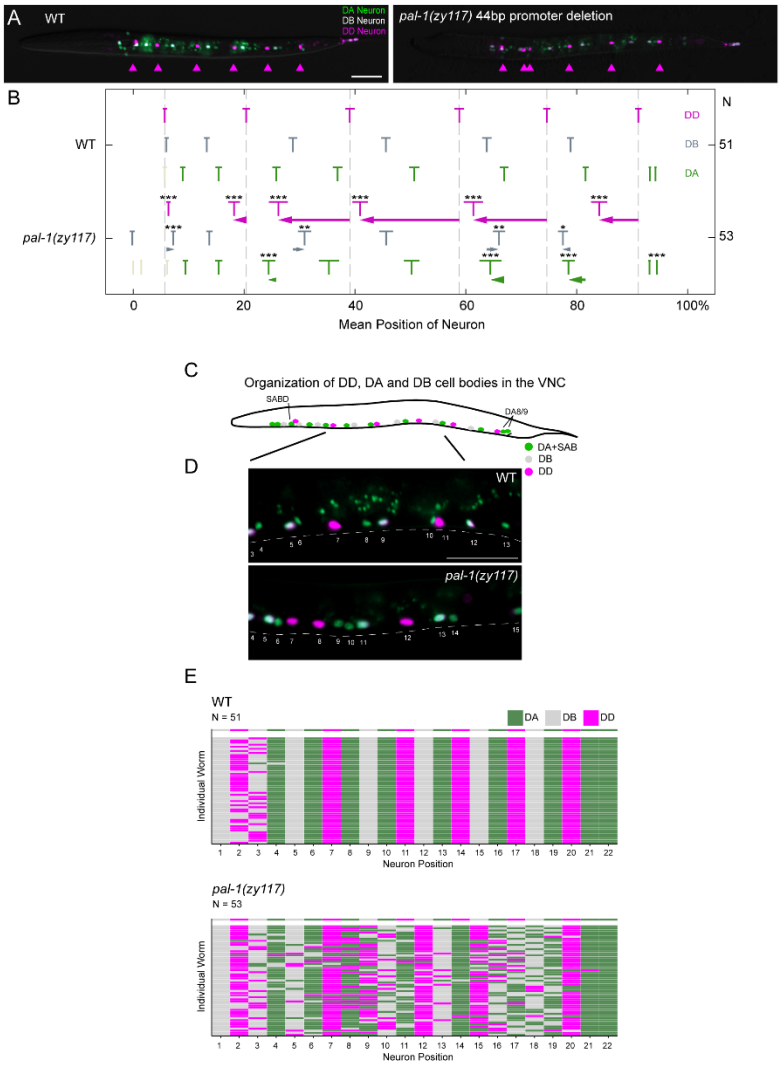

Figure 3.2: *pal-1* is required for proper motor neuron positioning in the VNC. (A) Representative images of DD, DA, and DB positions in WT and *pal-1(zy117)* mutants. DA neurons (*zy123[unc-4::mNG*) are indicated in green, DB neurons (*zy142[vab-7::mNG::T2A::mScarlet-I::H2B]*) in grey and DD neurons (*unc-30p::mCherry::H2B*) in magenta. Arrowheads mark the position of DD neurons. Scale bar = 20µm. (B) Quantification of DD, DA, and DB mean neuron position relative to the SABVL neuron and the rectum in L1 stage worms. Means and 95% confidence intervals are indicated for each neuron. Animals scored (N) indicated on the right. Hashed lines indicate the mean position of WT DD neurons. Arrows indicate the size and direction of the mean neuron position in *pal-1(zy117)* from the mean position of their WT equivalent. (C) Schematic of neuron organization in the L1 stage VNC. DA neurons in green and DD neurons in magenta. (D) Representative images showing neuron organization in WT and *pal-1(zy117)* mutants. Scale bar = 20µm. (E) Organization of DA, DB and DD neurons in WT and *pal-1(zy117)* worms. Individual boxes show the identity of the neuron in each position along the VNC with each row indicating an individual. The top row shows the stereotypical order of neurons in WT. Statistics: (B) Weltch's T-Test. *p<0.05, **p<0.01, ***p<0.001.

(Shah et al., 2017). This pronounced anterior shift reflects a major disruption of convergent extension movements among tightly juxtaposed neuronal progenitors during embryogenesis. From their birth locations on the left and right sides of the embryo, these progenitors converge mediolaterally, narrowing the tissue along the medial-lateral axis while elongating the nascent VNC along the anterior-posterior axis (Shah et al., 2017). In *vang-1 sax-3* double mutants, elongation of VNC progenitors along the anterior-posterior axis is impaired or delayed, leading to neuronal cell bodies that are positioned significantly more anteriorly than in WT.

To investigate genetic interactions between *pal-1* and these pathways, we examined the VNC positions of DD and DA neurons relative to SABVL and the rectum in *pal-1(zy117)* double mutants with *vang-1(tm1422)* and *sax-3(zy5)* (Figure 3.3A). *tm1422* is a deletion allele predicted to eliminate VANG-1 activity, whereas *zy5* is a nonsense allele expected to produce a SAX-3 protein with a truncated cytoplasmic domain (Shah et al., 2017). The *zy5* allele is used instead of the *sax-3* null allele because it exhibits significantly higher viability and fewer body morphology defects, which would otherwise interfere with measurements of neuron position. We found that the anterior shifts in the mean position of DD3-6 cell bodies along the VNC in *pal-1(zy117)* mutants were substantially more severe than those in *vang-1* and *sax-3* single mutants (Figure 3.3B and Supplemental Figure 3.2). In contrast, the anterior shifts in DA cell bodies were similar across all mutants, being relatively mild in each case. *vang-1; pal-1* double mutants exhibited significantly more severe anterior shifts in mean DD and DA neuron positions compared to either single mutant. Interestingly, in *sax-3; pal-1* double mutants, the mean position of DD cell bodies showed significantly more severe anterior shifts compared to single mutants, while only DA3 and DA4 among the DA cell bodies were significantly different from *pal-1* mutants (Figure 3.3B and Supplemental Figure 3.3). These results suggest that, at least for some aspects, *pal-1* and *vang-1* act in parallel or independent pathways to position DD and DA cell bodies. This redundancy is particularly evident in DA neurons which show a synergistic increase in the anterior shifts of mean cell body position compared to the single mutants. The findings also suggest that *pal-1* and *sax-3* act in parallel or independent pathways to position DD neurons and a subset of DA neurons. Furthermore, the similarity of the *vang-1; pal-1* cell body position phenotype to the *vang-1; sax-3* phenotype, in which convergent extension is disrupted, suggests that the downstream transcriptional targets of *pal-1* may also act to mediate convergent extension.

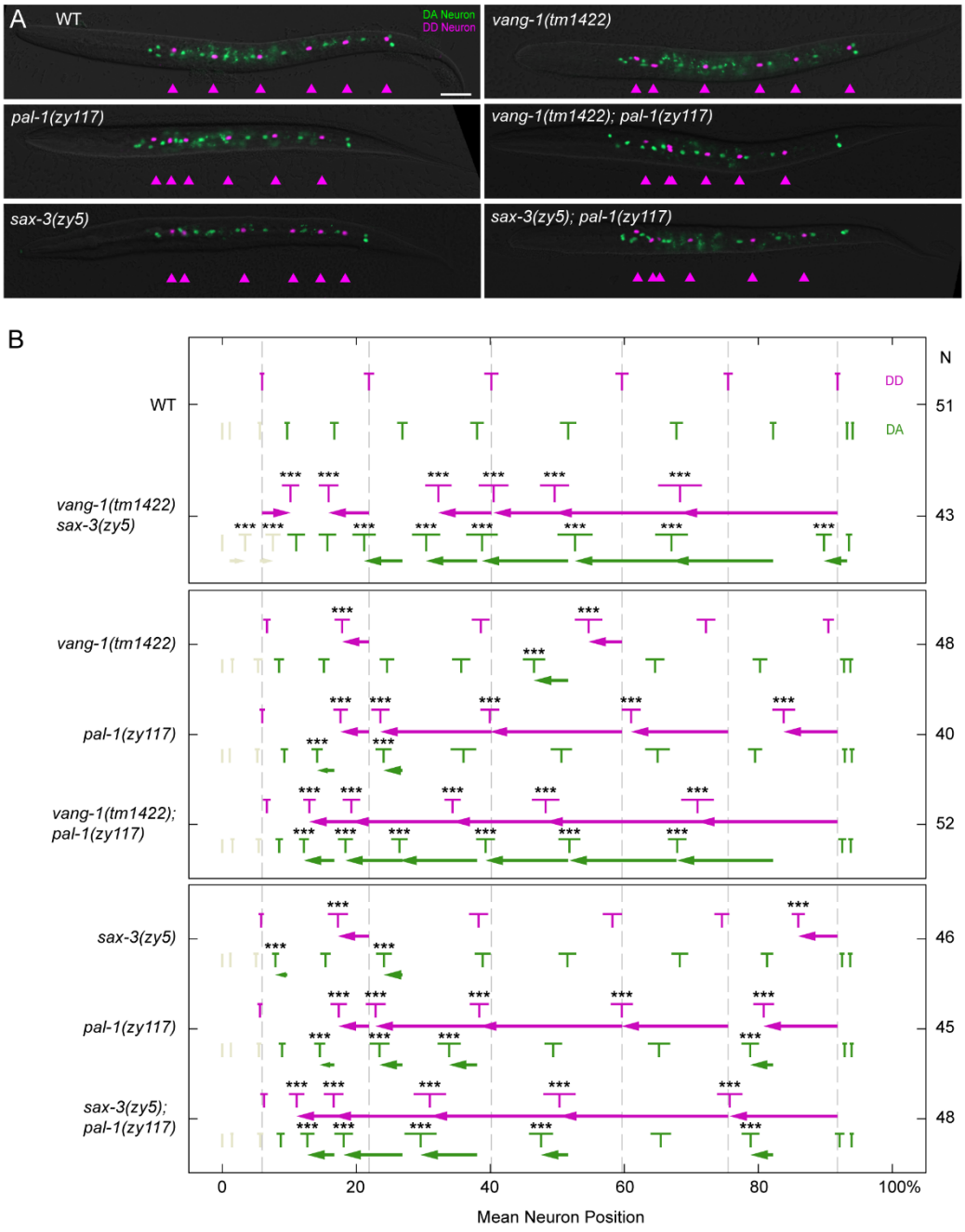

Figure 3.3: Genetic interactions between *pal-1*, *vang-1*, and *sax-3* during neuronal positioning. (A) Representative images of WT, *pal-1(zy117), vang-1(tm1422)*, *sax-3(zy5)* single and double mutants. DA neurons in green and DD neurons in magenta. Arrowheads mark the position of DD neurons. Scale bar = 20µm. (B) Quantification of DD and DA neuron position relative to the SABVL neuron and rectum in L1 stage worms. Means and 95% confidence intervals are indicated for each neuron and animals scored (N) indicated on the right. Hashed lines indicate the position of WT DD neurons. Arrows indicate the size and direction of the mean neuron position shift in each neuron compared to the mean position of their WT equivalent. Statistics: (B) one-way ANOVA with Tukey's Post-hoc Comparison. *p<0.05, **p<0.01, ***p<0.001.

***sex-1* mutants exhibit motor neuron cell body positioning defects.**

sex-1 encodes a 534-amino acid nuclear hormone receptor that was originally identified for its key role in sex determination (Carmi et al., 1998). In the same screen that identified *pal-1 zy43* and *zy44*, we also isolated a *sex-1* mutant. This mutant exhibited abnormally close spacing between the DD2 and DD3 cell bodies, similar to the defects observed in *pal-1* mutants (Figure 3.4A). This mutation, *sex-1(zy45)*, introduces a premature stop codon at amino acid W51, predicted to result in a severely truncated protein. We confirmed that *sex-1* is the causative gene by observing similar motor neuron positioning defects in two additional CRISPR/Cas9-generated *sex-1* alleles: *zy130*, a 7-nucleotide deletion that causes a frameshift after L54 and is likely a null allele, and *zy159*, a 20-nucleotide deletion that causes a frameshift after V253. These alleles were originally created for an unrelated study (unpublished). Given that *pal-1* and *sex-1* show a similar DD2–DD3 cell body proximity phenotype, we investigated the role of *sex-1* in neuronal positioning.

To better understand motor neuron positioning defects in *sex-1(zy130)* null mutants, we used our neuron class-specific reporters to measure the positions of DD and DA cell bodies in the newly hatched VNC relative to SABVL and the rectum. *sex-1* mutants show significant anterior shifts in the positions of both DD and DA cell bodies compared to WT, in contrast to *pal-1(zy117)* mutants, which primarily affect DD neurons (Figure 3.4B and C). These DD and DA cell body shifts become significantly more severe in *sex-1(zy130); pal-1(zy117)* double mutants compared to either single mutant (Figure 3.4C and Supplemental Figure 3.4). As in *pal-1* mutants, cell body position shifts in *sex-1* mutants are associated with changes to the stereotypical arrangement of motor neurons along the VNC (Figure 3.4D). However, unlike *pal-1* mutants, *sex-1* mutants also display additional organizational defects in the anterior VNC, where cell bodies are frequently mispositioned dorsally rather than aligned in a single file (Figure 3.4E and G). The proportion of dorsally mispositioned neurons increased from 5.9% in WT to 64.3% in *sex-1(zy130)* mutants ($p < 0.001$) (Figure 3.4G). Dorsally mispositioned neurons in *pal-1(zy117)* are not significantly different from WT (Figure 3.4G). Mispositioning defects in *sex-1(zy130); pal-1(zy117)* double mutants appear additive but are not significantly more severe than those in *sex-1(zy130)* alone (Figure 3.4G), consistent with *pal-1*, or at least its activity in DD and DA neurons, acting in a parallel pathway or not being involved in single file alignment.

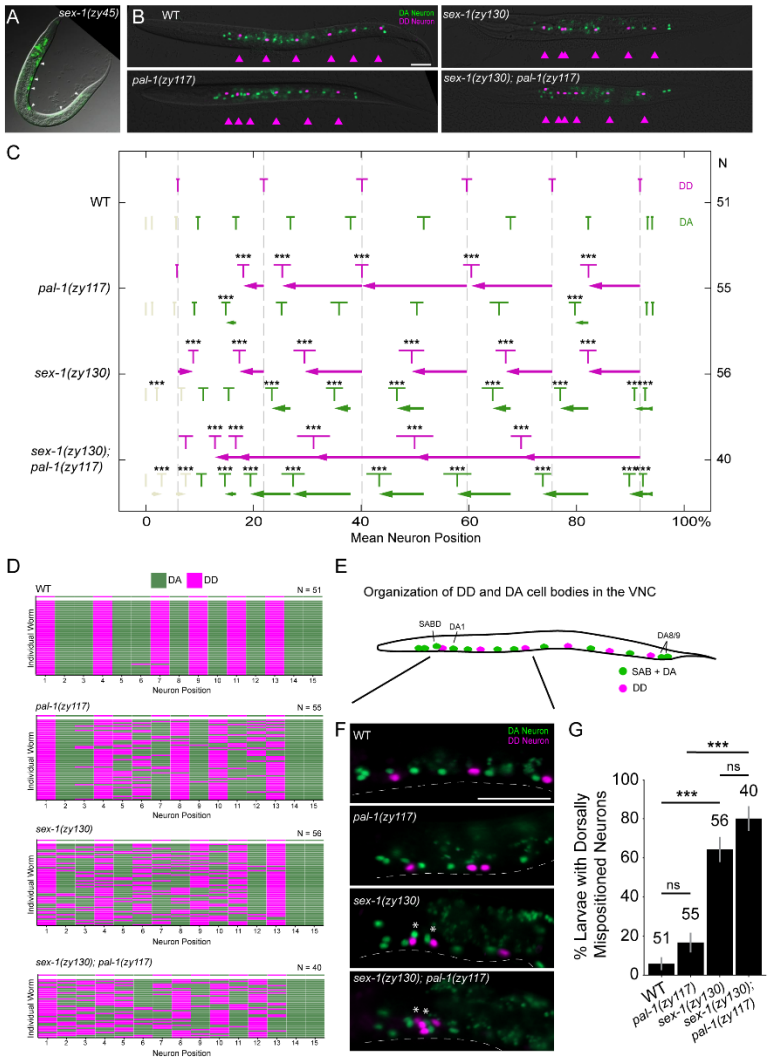

Figure 3.4: *sex-1* is required for proper motor neuron positioning in the VNC and genetic interactions with *pal-1*. (A) Representative image of DD neuron positions in *sex-1(zy45)*, visualized using *flp-13p::GFP*. (B) Representative images of WT, *pal-1(zy117)*, *sex-1(zy130)*, and double mutants showing DA neurons in green and DD neurons in magenta. Arrowheads mark the position of DD neurons. Scale bar = 20µm. (C) Quantification of DD and DA neuron position relative to the SABVL neuron and rectum in L1 stage worms. Means and 95% confidence intervals are indicated for each neuron. Animals scored (N) indicated on the right. Hashed lines indicate the position of WT DD neurons. Arrows indicate the size and direction of the mean neuron position shift in each neuron from the mean position of their WT equivalent. (D) Organization DD and DA neurons in WT and mutant worms. (E) Schematic showing DD and DA neuron organization along the VNC. (F) Representative images of anterior DA and DD neurons in *pal-1(zy117), sex-1(zy130)* and double mutants. Asterisks mark dorsally mispositioned neurons. Scale bar = 20µm. (G) Quantification of worms with dorsally mispositioned neurons at L1. Statistics: (C) one-way ANOVA with Tukey's Post-hoc Comparisons, and (G) Chi-squared test with Monte Carlo simulation for 10,000 replicates, followed by a pairwise analysis using Fisher's exact test with Monte Carlo simulation for 10,000 replicates and adjusted with Holm corrections. *p<0.05, **p<0.01, ***p<0.001.

Further research will be needed to validate these conclusions with a complete knockdown of *pal-1*, perhaps using RNAi. Together, these findings indicate that, at least for some aspects, *pal-1* and *sex-1* act redundantly or independently to position motor neurons in the VNC. Furthermore, *sex-1* plays an additional role in ensuring the single-file alignment of neurons in the anterior region of the VNC.

SEX-1 regulates PAL-1 expression in DD and DA neuronal progenitors.

Motor neuron positioning defects in the VNC of newly hatched worms indicate a disruption in the assembly of the VNC that begins at the embryonic bean stage. VNC assembly involves several distinct processes, including convergent extension of DD, DA, and DB neuronal progenitors, as well as still unknown sorting and spacing mechanisms that establish their stereotypical organization (Shah et al., 2017; Saharkhiz et al., 2024). The increased severity of neuron positioning defects in *sex-1; pal-1* double mutants compared to single mutants suggests that *sex-1* and *pal-1* may act in parallel or independent pathways during VNC assembly, though a role in the same pathway for some aspect of this process cannot be excluded. Given that both *sex-1* and *pal-1* encode transcription factors, we tested the possibility that one might regulate the expression of the other.

We first tested whether *pal-1* regulates *sex-1* expression. To do this, we knocked mNeonGreen (mNG) into the C-terminus of *sex-1* and examined its expression in WT and *pal-1(zy117)* mutant backgrounds, using our mCherry membrane reporter (*zyIs36*) to label DD and DA neurons. SEX-1::mNG was broadly expressed through the comma stage, including in the nuclei of all DD, DA, and DB progenitors (Supplemental Figure 3.5A). Its expression declined by the 1.5-fold stage, with few nuclei still showing detectable signal. No differences in SEX-1::mNG expression were observed in the *pal-1(zy117)* mutant background (Supplemental Figure 3.5B).

We next tested whether *sex-1* regulates *pal-1* expression. PAL-1::GFP is normally expressed and localized to the nuclei of a subset of DD, DA, and DB progenitors. In the *sex-1(zy130)* null background, PAL-1::GFP was absent from DD and DA progenitors but remained unaffected in DB progenitors at both the bean and 1.5-fold stages (Figure 3.5A). To confirm these observations, we quantified PAL-1::GFP expression based on whether it was co-expressed with *cnd-1* (DD and DA) or not co-expressed (DB and tail cells). To do this, we used Imaris

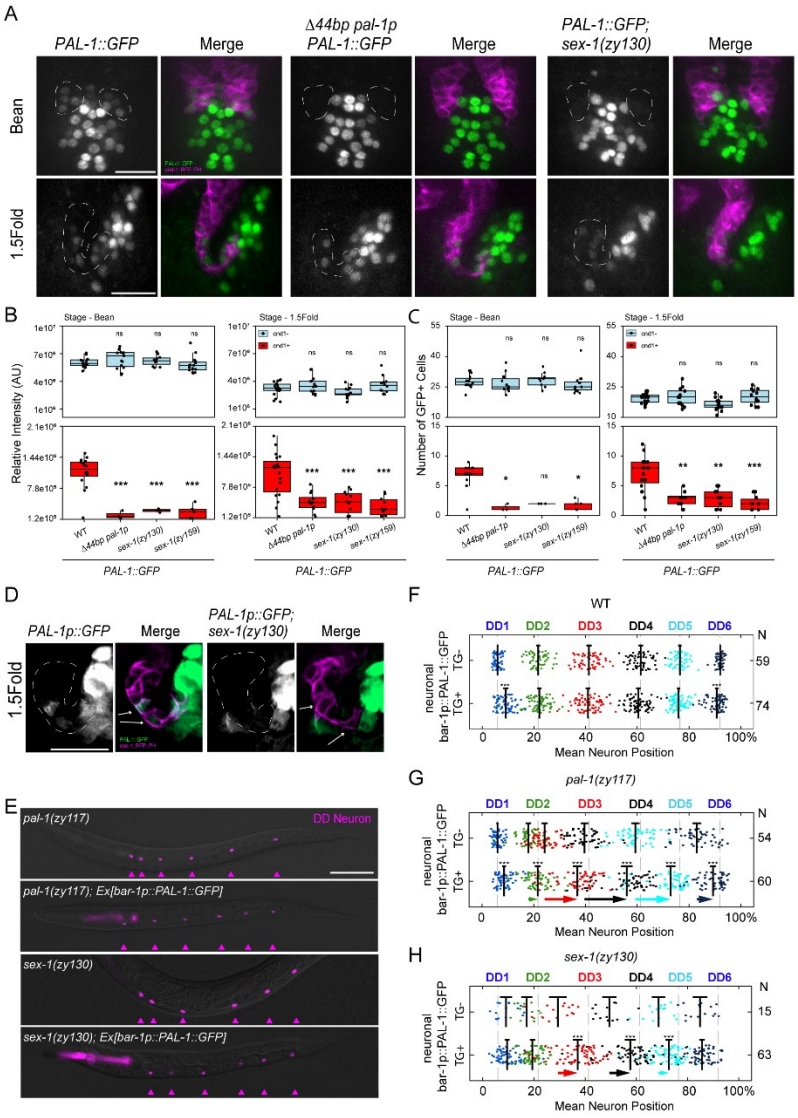

Figure 3.5: SEX-1 regulates PAL-1 expression. (A) Representative maximum projection images of *PAL-1::GFP* in WT, *pal-1(zy117) and sex-1* mutant embryos at bean and 1.5-fold stage. Hashed circles indicate regions with altered expression in mutant embryos. (B-C) Quantification of the (B) mean intensity and (C) number of nuclei expressing *PAL-1::GFP* in WT, *pal-1(zy117)* and *sex-1* mutant embryos. Nuclei were grouped based on their co-expression with *cnd-1*$^{+}$ cells, labelling the VNC. Means and 95% confidence intervals are indicated for each population with individual measurements shown. At the bean stage, N = 16, 15, 11 and 15, for WT, *pal-1(zy117), sex-1(zy130)* and *sex-1(zy159*), respectively. At the 1.5-fold stage, N = 19, 13, 13 and 12, for WT, *pal-1(zy117), sex-1(zy130)* and *sex-1(zy159*), respectively. (D) Representative images showing *pal-1p::GFP* transcriptional reporter in WT or *sex-1(zy130)* background. Number of embryos examined: N = 9 for WT and N = 1 for *sex-1(zy130)*. Arrows indicate regions of interest. (E) Representative images of DD neuron positions in *pal-1(zy117)* and *sex-1(zy130)* mutants with or without a *bar-1p::PAL-1::GFP* transgene. Arrowheads mark the position of DD neurons. Scale bar = 20µm. (F and G) Quantification of DD neuron position relative to the SABVL neuron and

the rectum in L1 stage (F) WT, (G) *pal-1(zy117)*, and (H) *sex-1(zy130)* with or without the extrachromosomal transgene. Means and 95% confidence intervals are indicated for each neuron and animals scored (N) indicated on the right. Hashed lines indicate the position of WT DD neurons. Arrows indicate the size and direction of the mean neuron position shift in each transgene expressing neuron from the mean position of their non-transgene equivalent. Statistics: (B) one-way ANOVA with Dunnet's Post-hoc Comparison, (C) Kruskal-Wallis Test with Dunn's Post-hoc Comparisons, (F-G) Welch's T-Test. *p<0.05, **p<0.01, ***p<0.001.

tools to segment PAL-1::GFP nuclear expression. These nuclei were then grouped based on whether they expressed *cnd-1* or not, and the mean sum intensity per cell was compared across genotypes.

We found that the average intensity of PAL-1::GFP in *cnd-1*$^{+}$ nuclei was dramatically reduced in embryos carrying the 44 bp *pal-1* promoter deletion and in both *sex-1* mutants (Figure 3.5B). In contrast, *cnd-1*$^{-}$ nuclei showed no significant change. This difference in intensity reflects the number of PAL-1::GFP positive nuclei detected in each region (Figure 3.5C). We further showed that this regulation occurs at the level of *pal-1* transcription by showing reduced GFP expression in embryos carrying a transgene driven by the *pal-1* promoter (Figure 3.5D). These findings indicate that PAL-1 expression in DD and DA neuronal progenitors requires transcriptional regulation by SEX-1.

If PAL-1 functions downstream of SEX-1, then expressing *pal-1* from a heterologous promoter active in VNC progenitors should bypass the requirement for *sex-1* and rescue the defects observed in *sex-1* mutants. To test this, we constructed a transgene in which the *pal-1* coding sequence is driven by the *bar-1* promoter, which is also active in DD and DA progenitors (Chan et al., 2025). This construct successfully rescued *zy117* defects and caused only minimal position defects when overexpressed in WT animals (Figure 3.5E, F and G). When introduced into a *sex-1(zy130)* mutant background, the transgene was able to partially rescue neuronal positioning defects (Figure 3.5E, F and H). These results are consistent with *pal-1* acting downstream of *sex-1* and, in agreement with our double mutant analysis, suggest that it is likely one of multiple targets through which SEX-1 mediates its effects on neuronal positioning.

Discussion

The integration of multiple signaling pathways is key to proper nervous system development. *Caudal* homeobox (HOX) transcription factors, including the CDX family in mammals and PAL-1 in *C. elegans,* act as key mediators of signaling pathways and are widely required for morphogenesis and cell-fate decisions during embryogenesis (van den Akker et al., 2002; Wilson et al., 2003; Palmer et al., 2021; Zhao et al., 2022). This includes early neural development, which depends on gene expression that is activated by retinoic acid, WNT, and HOX transcription factors (Nordström et al., 2006; Skromne et al., 2007; Young et al., 2009; Sturgeon et al., 2011; Sanchez-Ferras et al., 2016). In this study, we identify PAL-1/Caudal as a key regulator of VNC morphogenesis and show that its function relies in part on SEX-1/NHR-mediated regulation of *pal-1* expression but also involves SEX-1–independent mechanisms.

Disruption of a DD/DA progenitor-specific *pal-1* promoter element causes neuron position defects.

By examining endogenous *pal-1::GFP* expression, we found that *pal-1* is expressed in a subset of DD, DA, and DB progenitors during the bean to 1.5-fold stages of VNC development. The *pal-1* mutants used in this study, particularly the 44 bp *zy117* deletion, disrupt a promoter element that specifically drives expression in DD and DA progenitors but does not affect *pal-1* expression in DB progenitors. Although defects were observed in all three motor neuron classes (DD, DA, and DB), loss of *pal-1* expression driven by this promoter element primarily resulted in anteriorly mispositioned DD cell bodies, without apparent effect on embryonic or larval viability. In contrast, complete loss of PAL-1 activity results in embryonic and larval lethality due to defects in cell patterning and cell movement during embryogenesis that lead to severe morphological abnormalities (Edgar et al., 2001). Normal expression of cell fate markers and normal numbers of DD, DA, and DB neurons indicated that these defects were not due to alterations in cell fate.

Cdx genes are expressed in a temporally and spatially dynamic manner during early stages of mouse development. Gene expression begins in the primitive streak and tail bud early after implantation, then expands to neuroectodermal and mesodermal tissues, and gradually declines by late gestation (Meyer and Gruss, 1993; Beck et al., 1995; Chawengsaksophak et al., 1997; Benahmed et al., 2008). *pal-1* is similarly regulated in a complex temporal and spatial manner across multiple cell lineages (Hunter and Kenyon, 1996; Mootz et al., 2004; Edgar et al., 2001; Mainpal et al., 2011; Gilbert et al., 2020). This tightly controlled expression is mediated by

multiple regulatory regions, including a fragment of exon 5 that drives *pal-1* transcription specifically in ventral hypodermal cells (Gilbert et al., 2020). Our work adds to this regulatory complexity by identifying a *pal-1* promoter element specific to DD/DA progenitors, suggesting that precise spatial control of *pal-1* expression in the developing VNC is critical for its role in neuronal cell body positioning.

***pal-1/Cdx*, *vang-1/Vangl*, and *sax-3/Robo* act independently to regulate neuron position.**

We previously proposed that similarities in the cellular and molecular mechanisms underlying VNC morphogenesis and vertebrate neural tube formation might reflect an evolutionarily conserved process (Shah et al., 2017). Both involve convergent extension movements that narrow tissue along one axis while elongating it along another. They also share the formation and resolution of multicellular rosettes, the polarized distribution of PCP components such as VANG at cell membranes, and neighbour exchanges driven by actomyosin-mediated junctional contractions (Doudney et al., 2005; Ciruna et al., 2006; Ybot-Gonzalez et al., 2007; Williams et al., 2014). The involvement of the Caudal/CDX family protein PAL-1 in VNC assembly provides another point of similarity, as vertebrate CDX family members have also been implicated in PCP signaling during neurulation (Savory et al., 2011; Zhao et al., 2014). Consistent with this, loss of both *Cdx1* and *Cdx2* in mice results in the severe neural tube defect craniorachischisis (Savory et al., 2011; Zhao et al., 2014).

The neuronal cell body position defects in *pal-1(zy117)* are similar to those observed in *vang-1/Vangl* and *prkl-1/Prickle* mutants, which disrupt components of a PCP-like pathway, or in *sax-3/Robo* pathway mutants (Shah et al., 2017). These defects result from disrupted collective cell movements and failed intercalation of progenitor neurons at the midline during convergent extension, a process that brings progenitors to the midline and contributes to their single-file alignment and anterior-posterior distribution within the VNC. The *vang-1*/PCP-like and *sax-3/Robo* pathways function in independent, partially redundant pathways to regulate this process. Simultaneous disruption of both pathways severely impairs convergent extension, causing DD, DA, and DB progenitors to fail to move posteriorly, resulting in a clustering of neurons in the anterior VNC at hatching (Shah et al., 2017). A role for PAL-1 in these morphogenetic events would be consistent with its previously characterized functions. In particular, tissue-specific loss of *pal-1* in a subset of ventral hypodermal cells disrupts cell migration and intercalation during

late embryogenesis (Gilbert et al., 2020), and *pal-1* is also required for the migration of several dorsal hypodermal cell populations (Edgar et al., 2001).

Both *pal-1(zy117)* and the null mutant *vang-1(tm1422)* exhibit anterior mispositioning of DD and DA cell bodies, although the displacement of DD neurons is significantly more severe in *zy117*. This occurs despite *zy117* not being a null allele, but rather disrupting *pal-1* expression in only a subset of DD and DA neurons. *vang-1; pal-1* double mutants exhibit a striking synergistic enhancement of neuronal position defects compared to either single mutant. This suggests that *pal-1* and *vang-1* act in parallel or independent pathways to regulate neuronal cell body position. This finding contrasts with the role of CDX proteins during neurulation, which involves PCP signaling through the protein tyrosine kinase PTK7 (Savory et al., 2011), a protein that lacks an identified homologue in *C. elegans*. However, since the developmental processes underlying VNC formation are not fully understood, and likely involve the interaction of several mechanisms, we cannot exclude the possibility that PAL-1 contributes to PCP regulation in some context, in addition to acting through independent pathways. A similar conclusion can be drawn from the observation that most DD and DA cell bodies are more severely displaced toward the anterior in *sax-3; pal-1* double mutants compared to either single mutant.

***pal-1/Cdx* expression is regulated by SEX-1/NHR in DD and DA progenitors.**

The nuclear hormone receptor (NHR) SEX-1, which functions as a transcription factor, is primarily known for its role in sex determination and dosage compensation, acting in part through inhibition of the male-inducing transcription factor *xol-1* (Skipper et al., 1999; Gladden and Meyer, 2007; Meyer et al., 2010; Farboud et al., 2013). We found that SEX-1 is required for *pal-1* expression in DD and DA progenitors, representing a novel function for SEX-1 unrelated to sex determination. *sex-1* and *pal-1* mutants both exhibit anteriorly mispositioned DD and DA neuron cell bodies, although *pal-1* primarily affects DD neurons, whereas *sex-1* disrupts the positioning of both DD and DA neurons. The shared DD defects suggest that *sex-1* is important for DD neuron positioning, at least in part through its regulation of *pal-1* expression. However, it remains unclear whether this regulation involves direct binding of SEX-1 to the DD/DA promoter element in *pal-1*. The severe enhancement of DD and DA position defects in *sex-1(zy130); pal-1(zy117)* double mutants suggest that *sex-1* and *pal-1* also act in parallel or independent pathways to regulate neuron cell body positioning in the VNC. Since these defects resemble those caused by a strong disruption

of convergent extension during early VNC formation, this suggests that both *sex-1* and *pal-1* contribute to convergent extension.

The relationship between SEX-1/NHR and PAL-1/Cdx in VNC formation parallels the roles of their homologues in morphogenetic processes involving tissue shape changes or convergent extension. CDX family members are regulated by both autonomous and non-autonomous signals, include the canonical WNT signaling pathway and NHRs (Houle et al., 2003; Sanchez-Ferras et al., 2012; reviewed in Bodofsky et al., 2017). Prominent NHR families like the retinoic acid receptors (RARs), retinoid X receptors (RXR) and the orphan NHR *Xenopus* germ cell nuclear factor (xGCNF) play key roles in the regulation of neurulation or cellular behaviors (Wendling et al., 1999; Mic et al., 2002; Barreto et al., 2003; Kam et al., 2013; Gur et al., 2022; Koch et al., 2025). This process may be partly achieved through the regulation of convergent extension, which is disrupted by genetic manipulation of retinoic acid signaling or manipulation of xGCNF (Barreto et al., 2003; Gur et al., 2022). Of these families, retinoic acid receptors, and their endogenous retinoic acid ligands, as well as thyroid receptors have also been shown to regulate *cdx* gene expression in several different contexts (Plateroti et al., 2001; Houle et al., 2003). For example, retinoic acid promotes and maintains *cdx* expression during the specification of multiple mesodermal cell populations, including in early cardiogenesis, zebrafish pronephron development, and axial extension during late gastrulation in mice (Houle et al., 2003; Wingert et al., 2007; Lengerke et al., 2012). Interestingly, SEX-1 shares some sequence similarity with the NHR1 superfamily, which includes retinoic acid receptors (RARs) (Carmi et al., 1998). Overall, the involvement of NHR and Cdx family members in VNC formation and neurulation points to a conserved set of cellular and molecular mechanisms underlying central nerve cord development.

Materials and Methods

Strains and maintenance

All strains were maintained and examined at 20ºC. The Bristol N2 strain was used as wild type (WT), along with the following alleles and transgenes: LGII: *unc-4(syb1658[unc-4::GFP]).* LGIII: *pal-1(zy43), pal-1(zy44), pal-1(zy117)*. LGX: *sex-1(zy45), sex-1(zy130), sex-1(zy159), sax-3(zy5), vang-1(tm1422), zyIs36[cnd-1p::PH::mCherry myo-2p::mCherry]*.

Table 3.1: Key Resources used in *pal-1* experiments

Reagent or resource	Source	Identifier
Chemicals, Peptides, and Recombinant Proteins		
Levamisol hydrochloride	Millipore Sigma	31742; CAS:16595-80-5
Bacterial and Virus Strains		
E. coli: OP50	Caenorhabditis Genetics Center (CGC)	RRID: WB-STRAIN:WBStrain00041969
Experimental Models: Organisms/Strains		
C. elegans: N2 (wild isolate)	CGC	
C. elegans: OU792 (unc-4(zy123[unc-4::mNG]) zySi2[unc-30p::mcherry::H2B::unc-30]; vab-7(zy142[vab7::mNG::T2A::mScarlet-I::H2B])	Saharkhiz et al., 2024	N/A
C. elegans: OU734 (unc-4(zy123[unc-4::mNG]) zySi2[unc-30p::mcherry::H2B::unc-30])	Saharkhiz et al., 2024	N/A
C. elegans: *pal-1(zy43)* III	This study	N/A
C. elegans: *pal-1(zy44)* III	This study	N/A
C. elegans: *pal-1(zy117)* III	This study	N/A
C. elegans: *sex-1(zy130) X*	A. Colavita, unpublished	N/A
C. elegans: *sex-1(zy159) X*	A. Colavita, unpublished	N/A
C. elegans: *pal-1(zy112[pal-1::GFP])* III	This study	N/A
C. elegans: *sex-1(zy133[zy133[sex-1::mNG::AID])* X	This study	N/A
C. elegans: *ynIs37[flp-13p::gfp]* III	CGC	WB Strain: NY2037; WormBase: WBStrain00029158
C. elegans: *sax-3(zy5) X*	Shah et al., 2017	N/A
C. elegans: *vang-1(ok1142) X*	CGC	WB Strain: RB1125; WormBase: WBStrain00031829
C. elegans: *zyIs36(cnd-1::PH::mCherry; myo-2p::mCherry) X*	Antonio Colavita, Shah et al., 2017	N/A
C. elegans: *zyIs40(unc-30p::gfp; cnd-1::PH::mCherry)* Unassigned linkage	This study	N/A
Oligonucleotides		
DNA Oligonucleotides	Eurofins	See Table S1 for sequences and use.
Software and Algorithms		
Zeiss Zen 3.2	Zeiss	https://www.zeiss.com/microscopy/en/products/software/zeiss-zen.html
R 4.4.2	R Core Team, 2019	N/A
ggplot2	Wilkinson, 2011	https://github.com/tidyverse/ggplot2
Imaris 10	Oxford Instruments	https://imaris.oxinst.com/

pal-1 and *sex-1* alleles

pal-1(zy43), pal-1(zy44) and *sex-1(zy45)* were identified in a genetic screen for DD neuron position defects (A. Colavita, unpublished). Whole-genome sequencing, as described in Noblett et al. (2019), was used to identify the genes and their associated DNA lesions. Mutants were subsequently outcrossed at least three times and reverified by Sanger sequencing (performed at OHRI StemCore) using primers N35-N37 for *pal-1* (all primers listed in Supplemental Table 1).

The *pal-1(zy117)* deletion was generated via DNA repair of CRISPR-Cas9-induced double strand breaks (Waaijers et al., 2013). Briefly, the target site (GAATGTCATAATGACCTTTT) was identified using the IDT guide RNA design tool at idtdna.com. The sequence was inserted into the Cas9-sgRNA plasmid pDD162 (Addgene #47549) using the NEB Q5 Site-Directed Mutagenesis Kit to generate plasmid pAC564. Young adult worms containing the DD reporter transgene *ynIs37* were injected with a mix of 50 ng/µl of pAC564, 2.5 ng/µl of myo-2p::mCherry (pCFJ90, Addgene #19327) and pBluescript plasmid (Stratagene) to a concentration of 100 ng/µl. Progeny were screened for DD position defects that resembled those in *zy43* and *zy44*. Sequencing (OHRI StemCore) with primers N35 and N36 was used to identify the deletion. Subsequent genotyping was performed using primers N35-N37.

CRISPR-Cas9-mediated knock-ins

A GFP::3xFLAG and an mNG::AID::3xFLAG were inserted at the C-terminus of the endogenous *pal-1* and *sex-1* loci, respectively, using the CRISPR-Cas9 self-excising drug selection cassette approach described in Dickinson et al. (2015). Target sequences for *pal-1* (GTCGTGACAAACAGAAGATT) and *sex-1* (CAAAGGTGGCTAGCAGTGAA) insertions were cloned into the Cas9–sgRNA plasmid pDD162 to generate plasmids pAC487 and pAC703, respectively. The homology directed repair plasmids for *pal-1* (pAC486) and *sex-1* (pAC722) were constructed using the GFP (pDD282, Addgene #66823) and mNG::AID (pJW1582, Addgene #154312) selection cassette plasmids, respectively. The resulting knock-in alleles are *pal-1(zy112[pal-1::GFP])* and *sex-1(zy133[sex-1::mNG::AID])*.

Reporter and rescue constructs

A *pal-1p::mNG* transcriptional reporter (pAC499) was constructed using Gibson Assembly (New England Biolabs). This reporter combines approximately 1.8 kb of distal and 2.4

kb of proximal promoter elements upstream of an mNG cassette, with the pPD95.77 vector (a gift from Andrew Fire, Stanford) serving as the backbone. Primers N48-N53 were used for the assembly (Table S1).

A promoterless *pal-1::GFP* minigene plasmid (pAC936) was constructed using Gibson Assembly. This construct contains the *pal-1* genomic coding region, with introns 3 and 5 removed, fused to the *GFP::3X Flag* cassette from the endogenous knock-in allele *pal-1*(zy112). Primers N54-N61 were used for the assembly (Table S1). The *bar-1p::pal-1::GFP* rescue construct (pAC937) was made by inserting a 4.9 kb *bar-1* promoter into pAC936 using Gibson Assembly with primers N62-N65 (Table S1).

pAC499 and pAC936 were each injected at a concentration of 5 ng/µl, along with 2.5 ng/µl of *myo-2p::mCherry* (pCFJ90) and 92.5 ng/µl of pBluescript plasmid.

Embryonic Imaging

For widefield imaging, embryos were prepared as in Bao and Murray (2011). Briefly, several embryos were transferred from plates using a capillary attached to a glass pipette and mounted in a 3 µL drop of M9 containing approximately fifty 25 µm diameter polystyrene beads (Polyscience Inc.). The preparation was then sealed under a No. 1.5 coverslip using Vaseline. All widefield imaging was conducted on a Zeiss Imager M2, equipped with a Zeiss SVB-1 microscope signal distribution box/*TTL* trigger cable-controlled camera shutter to reduce phototoxicity. Single time-point images were taken across 15-30 0.5 µm slices at 63x (1.4NA). Unless otherwise stated, all images were deconvolved prior to analysis using constrained iterative deconvolution on Zen 3.2 (Zeiss) with a Gaussian algorithm, corrections for background and saturated pixels.

Quantification of motor neuron position defects in newly hatched larvae

Quantification of neuron position defects in L1 larvae was performed as follows. First stage larvae (L1) were mounted on 2% agarose pads using 200 µM levamisole (#31742, Sigma). Images were acquired using a Zeiss Imager M2, Colibri7 LED source, AxiocamHR camera and taken at 40x (1.4NA) over 5-7 0.5um slices. Brightfield, RFP and GFP channels were acquired. Images were measured on FIJI/Image J software, version 2.14. Using the segmented line tool, the position of each DD, DA and DB neuron (or only DD and DA neurons in OU734) was measured along the worm. These positions were then converted into percentage locations using SABVR = 0% and the

anus = 100%. Each percentage location was plotted using base R, version 4.4.2 (R Core Team, 2019) and geom_jitter from the ggplot2 suite (Wilkinson, 2011).

Quantification of PAL-1 expression

Embryonic imaging of *pal-1(zy112[pal-1::GFP])* and *sex-1(zy133[sex-1::mNG::AID])* was conducted on a DM16000B Quorum Spinning Disk (Leica) with a EMCCD (Hamamatsu) camera. Single time-point images were taken at 63x (1.4NA) with a pinhole size of 50um. Images were acquired with a Brightfield exposure of 223ms, at FITC exposure of 500ms and a Cy3 exposure of 700ms, across 12 0.5um slices.

Intensity measurements of *pal-1(zy112[pal-1::GFP])* were conducted using Imaris 10 (Bitplane) after data was processed using Fiji/ImageJ. Briefly, Z-stacks were opened in their native format in Fiji/ImageJ. Both red and green channels were merged to form a composite color image, which was converted into RGB before exporting as a TIFF. Data was then imported into Imaris. Semi-automated spot detection was used to identify GFP nuclei with a XY diameter of at least 1.15 µm and a quality above 42. Spots were classified using the Imaris machine learning tool based upon the RFP channel and their proximity to the RFP labelled VNC cells. After spot creation was complete, the original GFP image was used to remove false positive spots which were outside the embryo boundary. Spots details including class and SUM Intensity were exported for statistical analysis and graphing.

Statistics

Tests and the number of samples for each dataset are indicated in individual figure legends. Parametric data was analyzed using Weltch's T-Test or an analysis of variance (ANOVA), as appropriate. Proportional data was compared using a Chi-squared test with Monte Carlo simulation for 10,000 replicates. When this returned a significant result, a pairwise analysis was conducted using Fisher's Exact Test with Monte Carlo simulation for 10,000 replicates, adjusted with Holm corrections for multiple comparisons. Statistics were conducted using base R, version 4.4.2 (R Core Team, 2019), and the "multicomp" package for Dunnett's Multiple Comparison Test (Bretz et al., 2011). Measurements related to embryonic phenotypes (expression pattern and order measurements) were scored blind to genotype using the Blind Analysis Tools plugin for Fiji/ImageJ (https://imagej.net/plugins/blind-analysis-tools).

Acknowledgements

We thank Dr. Shohei Mitani for providing *vang-1(tm1422)* and Dr. Chris Li for providing *ynIs37*. Some strains were provided by the *Caenorhabditis* Genetics Center, which is funded National Institutes of Health Office of Research Infrastructure Programs (P40 OD010440). Data for *C. elegans* allele sequences was accessed through WormBase (http://www.wormbase.org, release WS294). The authors acknowledge the Cell Biology and Image Acquisition Core (RRID: SCR_021845) funded by the University of Ottawa, Natural Sciences and Engineering Research Council of Canada, and the Canada Foundation for Innovation. We would also like to acknowledge the assistance of StemCore Laboratories Genomics Core Facility (OHRI), RRID:SCR_012601. Studies presented in this report were supported by a Project Grant from the Canadian Institutes of Health Research (CIHR 123513 and 156160) to A. Colavita.

Supplemental Figures

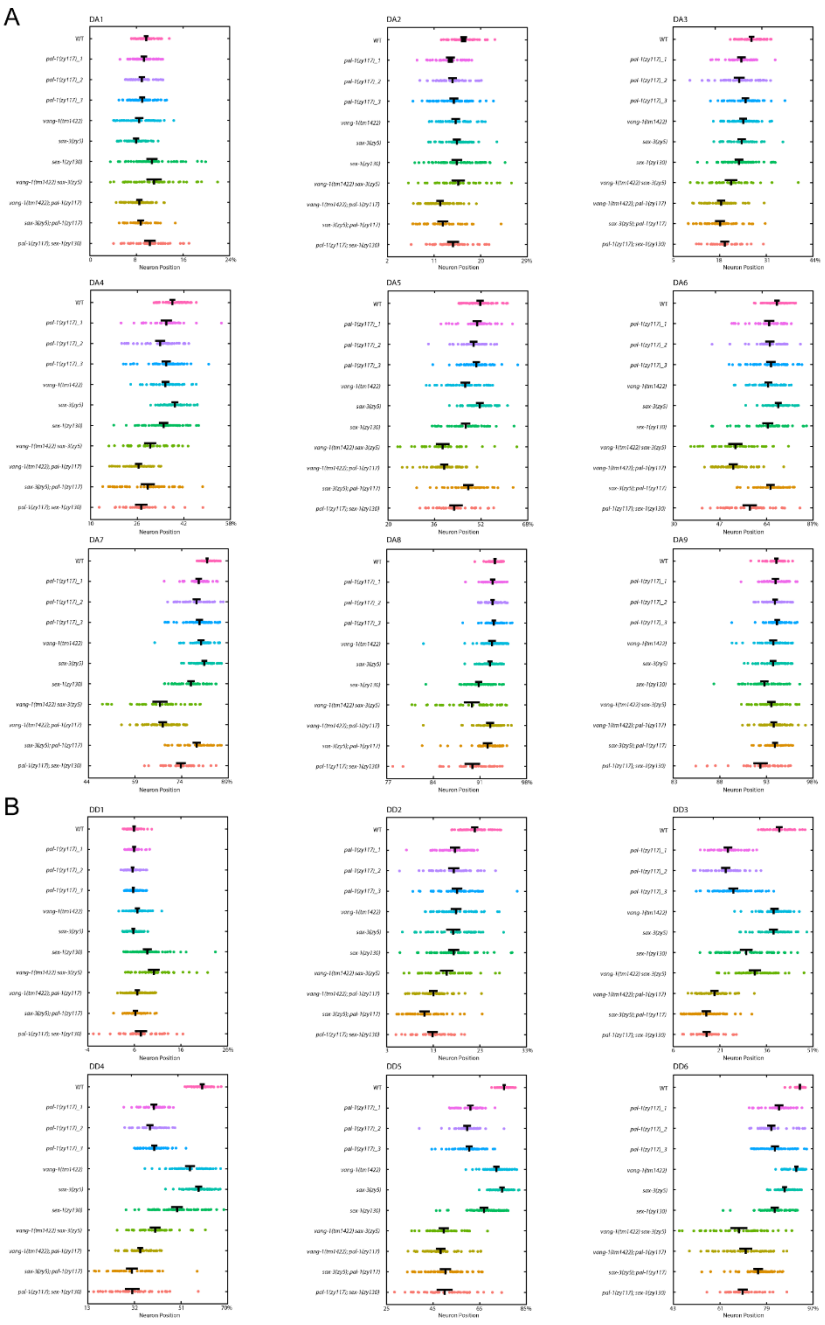

Supplemental Figure 3.1: Distribution of all DD, DA, and DB positions used to plot mean positions in Figure 2. (A-C) Quantification of (A) DA, (B) DB and (C) DD neuron position relative to the SABVL neuron and rectum in L1 stage worms. Data shows individual samples for the data presented in Figure 2. Neurons are plotted along the AP axis, where SABVL and the rectum mark the 0% and 100% positions respectively. Black bars represent the means and 95% confidence intervals.

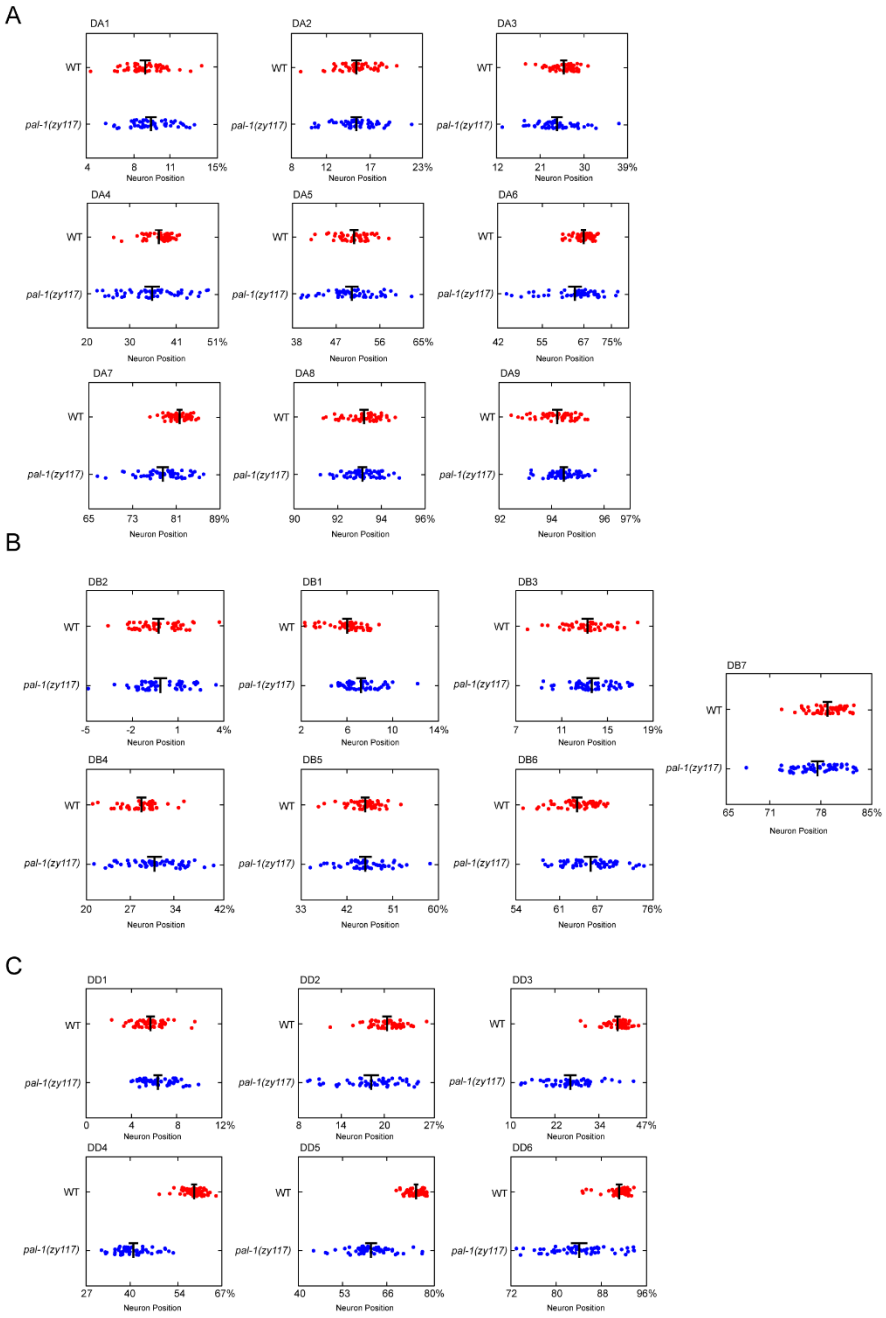

Supplemental Figure 3.2: Distribution of all DD and DA positions used to plot mean positions in Figure 3 and 4. (A-B) Quantification of (A) DA and (B) DD neuron position relative to the SABVL neuron and rectum in L1 stage worms. Each graph shows individual samples for the data presented in Figures 3 and 4. Neurons are plotted along the AP axis, where SABVL and the rectum mark the 0% and 100% positions respectively. Black bars represent the means and 95% confidence intervals.

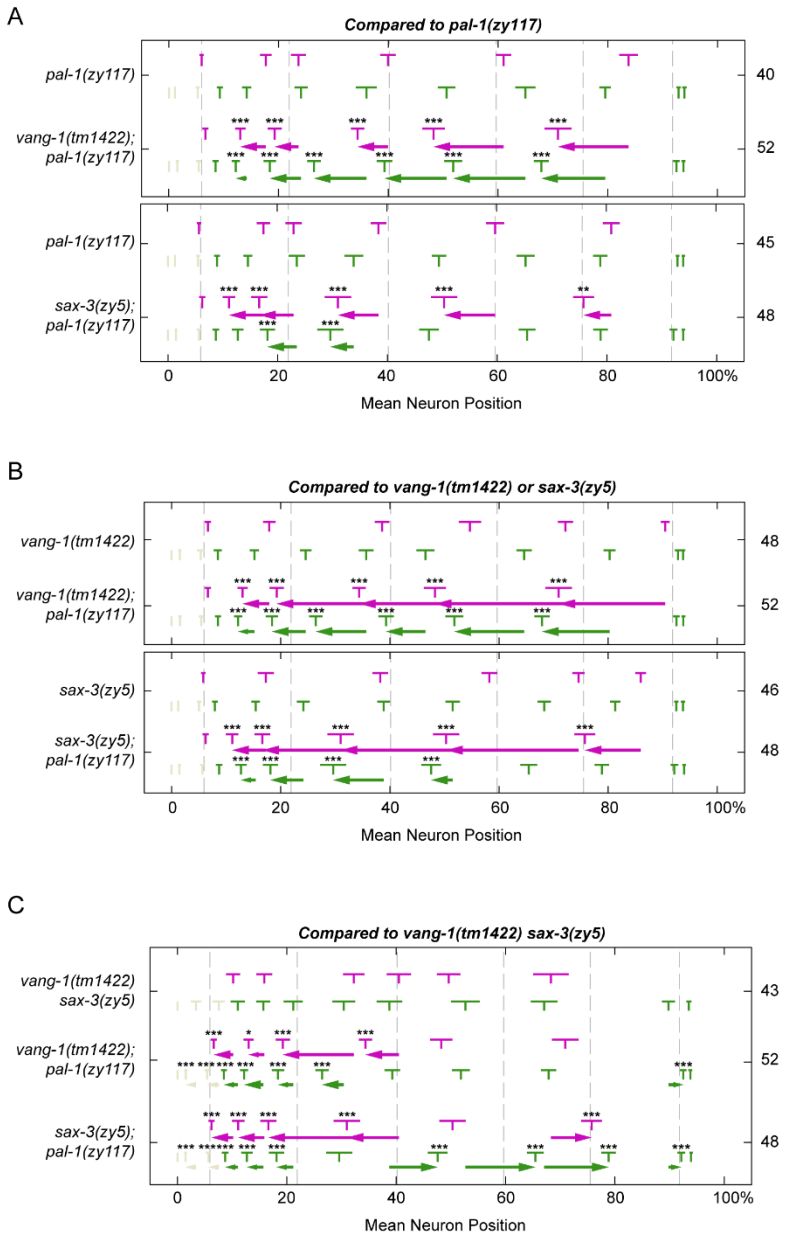

Supplemental Figure 3.3: Comparison of *pal-1(zy117)* double mutants with *vang-1(tm1422)* and *sax-3(zy5)*. (A-B) Each graph shows the mean position of DD and DA neurons in larvae as presented in Figure 3. Neurons are plotted along the AP axis, where SABVL and rectum mark the 0% and 100% positions respectively. Means and 95% confidence intervals are indicated for each neuron and animals scored (N) indicated on the right. Hashed lines indicate the mean position of WT DD neurons. Arrows indicate the size and direction of the mean neuron position shift in the double mutant from the mean neuron position in (A) *pal-1(zy117)*, (B) *vang-1(tm1422)* or *sax-3(zy5)* single mutants. Statistics: one-way ANOVA with Tukey's Post-hoc Comparisons. *p<0.05, **p<0.01, ***p<0.001.

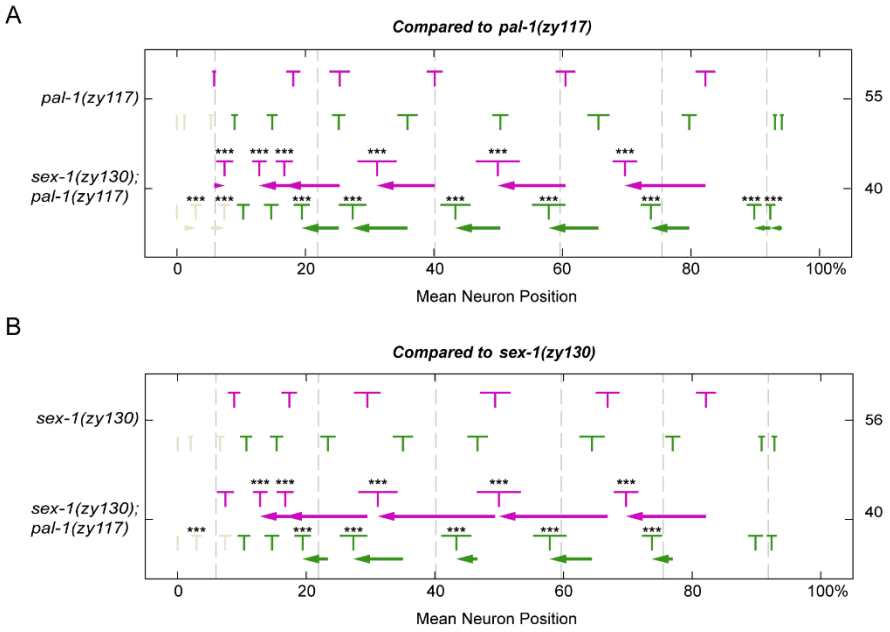

Supplemental Figure 3.4: Comparison of *sex-1(zy130); pal-1(zy117)* double mutants to single mutants. (A-B) Each graph shows the mean position of DD and DA neurons in larvae as presented in Figure 4. Neurons are plotted along the AP axis, where SABVL and the rectum mark the 0% and 100% positions respectively. Means and 95% confidence intervals are indicated for each neuron and animals scored (N) indicated on the right. Hashed lines indicate the mean position of WT DD neurons. Arrows indicate the size and direction of the mean neuron position shift in the double mutant from the mean neuron position in (A) *pal-1(zy117)* or (B) *sex-1(zy130)* single mutants. Statistics: one-way ANOVA with Tukey's Post-hoc Comparisons. *p<0.05, **p<0.01, ***p<0.001.

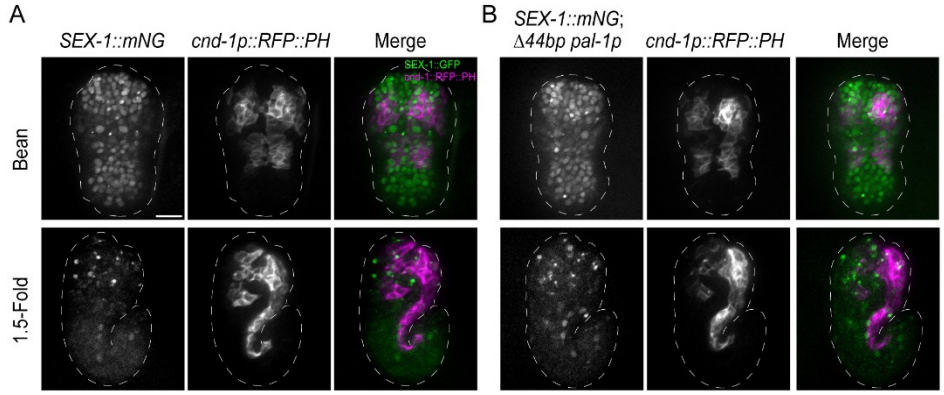

Supplementa1 Figure 3.5: Loss of PAL-1 does not affect the expression of endogenous SEX-1::GFP. Representative maximum projections of an endogenous *SEX-1::mNG* in WT (A) and *pal-1(zy117)* embryos (B). At the bean stage, N = 15 for both WT and *pal-1(zy117)*. At the 1.5-fold stage, N = 14 for WT and N = 15 for *pal-1(zy117)*. No visual changes are observed. Posterior *cnd-1p::RFP::PH* expression marks DD and DA neurons. The white hashed outline marks the embryo. Scale bar = 10µm.

Supplemental Table 3.1: Oligonucleotides used in *pal-1* experiments

Oligo #	DNA Oligos Sequence (5' – 3')	Source	Use
N34	GAATGTCATAATGACCTTTTGTTTAAGAGCTATGCTGGAA	Eurofins	SGRNA for the deletion found in *pal-1(zy117)*
N35	ACAACCTCAAGTACATACTGC	Eurofins	Sequence *pal-1(zy117)*
N36	ACTACAACGATGTTCACATCC	Eurofins	Sequence *pal-1(zy117)*
N37	CAATAATCTGACAGATGGTTGG	Eurofins	Sequence *pal-1(zy117)*
N38	GTCGTGACAAACAGAAGATTGTTTAAGAGCTATGCTGGAA	Eurofins	SGRNA for *PAL-1::GFP*
N39	ACGTTGTAAAACGACGGCCAGTCGCCGGCACACTCGCATGTTAAAGGGAG	Eurofins	Repair template for *PAL-1::GFP*
N40	CATCGATGCTCCTGAGGCTCCCGATGCTCCTAGACGAATCTTCTGTTTGTCACGA	Eurofins	Repair template for *PAL-1::GFP*
N41	CGTGATTACAAGGATGACGATGACAAGAGATAAGTACTCATCTACTTACAAAGAAAATGTAC	Eurofins	Repair template for *PAL-1::GFP*
N42	GGAAACAGCTATGACCATGTTATCGATTTCGCAACTACCAGCGACTTAC	Eurofins	Repair template for *PAL-1::GFP*
N43	CAAAGGTGGCTAGCAGTGAAGTTTAAGAGCTATGCTGGAA	Eurofins	SGRNA for the *SEX-1::mNG::AID*
N44	ACGTTGTAAAACGACGGCCAGTCGCCGGCATATGGATCATTGGCGGACGA	Eurofins	Repair template for *SEX-1::mNG::AID*
N45	CATCGATGCTCCTGAGGCTCCCGATGCTCCGCAGTGAACGGGAGTCTGTT	Eurofins	Repair template for *SEX-1::mNG::AID*
N46	CGTGATTACAAGGATGACGATGACAAGAGATAGCCACCTTTGTCAGATTCT	Eurofins	Repair template for *SEX-1::mNG::AID*
N47	GGAAACAGCTATGACCATGTTATCGATTTCTTCTGATAGAGGTCGACGG	Eurofins	Repair template for *SEX-1::mNG::AID*
N48	ACAACTTGGAAATGAAATACTGCTTGAGATGCAAAGCGA	Eurofins	*pal-1p::mNG* fragment 1
N49	CGATCAGAGCTATCGAGTAC	Eurofins	*pal-1p::mNG* fragment 1
N50	GTACTCGATAGCTCTGATCGGTCAAGTCTGCCGTTGTTC	Eurofins	*pal-1p::mNG* fragment 2
N51	TCTAGAGTCGACCTGCAGTGGTTGCAGCATCTTTTCTCTG	Eurofins	*pal-1p::mNG* fragment 2
N52	CTGCAGGTCGACTCTAGA	Eurofins	*pal-1p::mNG* fragment 3
N53	TATTTCATTTCCAAGTTGT	Eurofins	*pal-1p::mNG* fragment 3
N54	ACAACGATGGATACGCTAACATGTCGGTCGATGTCAAG	Eurofins	promoterless *pal-1::GFP* fragment 1
N55	ATCCCTGAAACTGTTGATAATCCATAAACGG	Eurofins	promoterless *pal-1::GFP* fragment 1
N56	TTATCAACAGTTTCAGGGATTCTCGTGG	Eurofins	promoterless *pal-1::GFP* fragment 2
N57	CTTTGCACGCCTATTTTGAAACCAAATCTTGATTTG	Eurofins	promoterless *pal-1::GFP* fragment 2
N58	TTCAAAATAGGCGTGCAAAGGATCGTCG	Eurofins	promoterless *pal-1::GFP* fragment 3
N59	CCGACTAGTGGGCAGATCTTACTGGATAGTTAATCTCATCAATTTCTGC	Eurofins	promoterless *pal-1::GFP* fragment 3
N60	AAGATCTGCCCACTAGTC	Eurofins	promoterless *pal-1::GFP* fragment 4
N61	GTTAGCGTATCCATCGTTG	Eurofins	promoterless *pal-1::GFP* fragment 4
N62	ATACGCTAACATCGAGTTGAATCCTCTGGC	Eurofins	*bar-1p::pal-1::GFP* fragment 1
N63	CATCGACCGAGATCCAGGCCATCCCAGTTTTC	Eurofins	*bar-1p::pal-1::GFP* fragment 1
N64	GGCCTGGATCTCGGTCGATGTCAAGTCG	Eurofins	*bar-1p::pal-1::GFP* fragment 2
N65	TCAACTCGATGTTAGCGTATCCATCGTTG	Eurofins	*bar-1p::pal-1::GFP* fragment 2

References

van den Akker, E., Forlani, S., Chawengsaksophak, K., de Graaff, W., Beck, F., Meyer, B. I., & Deschamps, J. (2002). Cdx1 and Cdx2 have overlapping functions in anteroposterior patterning and posterior axis elongation. *Development, 129(9), 2181–2193.*

Arnold, P. R., Wells, A. D., & Li, X. C. (2020). Diversity and emerging roles of enhancer RNA in regulation of gene expression and cell fate. *Frontiers in cell and developmental biology*, *7*, 377.Asahina, M., Ishihara, T., Jindra, M., Kohara, Y., Katsura, I., & Hirose, S. (2000). The conserved nuclear receptor Ftz-F1 is required for embryogenesis, moulting and reproduction in Caenorhabditis elegans. *Genes to Cells*, *5*(9), 711-723.

Bao, Z., & Murray, J. I. (2011). Mounting Caenorhabditis elegans embryos for live imaging of embryogenesis. *Cold Spring Harbor Protocols*, *2011*(9), pdb-prot065599.

Barreto, G., Reintsch, W., Kaufmann, C., & Dreyer, C. (2003). The function of Xenopus germ cell nuclear factor (xGCNF) in morphogenetic movements during neurulation. *Developmental Biology*, *257*(2), 329-342.

Baugh, L. R., Hill, A. A., Claggett, J. M., Hill-Harfe, K., Wen, J. C., Slonim, D. K., Eugene, L. B. & Hunter, C. P. (2005). The homeodomain protein PAL-1 specifies a lineage-specific regulatory network in the C. elegans embryo. *Development*, *132*(8), 1843–1854.

Beck, F., Erler, T., Russell, A., & James, R. (1995). Expression of Cdx-2 in the mouse embryo and placenta: possible role in patterning of the extra-embryonic membranes. *Developmental Dynamics*, *204*(3), 219-227.

Belakavadi, M., & Fondell, J. D. (2006). Role of the mediator complex in nuclear hormone receptor signaling. *Reviews of physiology, biochemistry and pharmacology*, 23-43.

Benahmed, F., Gross, I., Gaunt, S. J., Beck, F., Jehan, F., Domon–Dell, C., ... & Duluc, I. (2008). Multiple regulatory regions control the complex expression pattern of the mouse Cdx2 homeobox gene. *Gastroenterology*, *135*(4), 1238-1247.

Bodofsky, S., Koitz, F., & Wightman, B. (2017). Conserved and exapted functions of nuclear receptors in animal development. *Nuclear receptor research*, *4*, 101305.

Bonnelye, E., Vanacker, J. M., Desbiens, X., Begue, A., Stehelin, D., & Laudet, V. (1994). Rev-erbb, a new member of the nuclear receptor superfamily, is expressed in the nervous system during chicken development. *Cell Growth and Differentiation-Publication American Association for Cancer Research*, *5*(12), 1357-1366.

Bretz F, Hothorn T, Westfall PH. Multiple comparisons using R. Boca Raton, FL: CRC Press; 2011.

Brožová, E., Šimečková, K., Kostrouch, Z., Rall, J. E., & Kostrouchová, M. (2006). NHR-40, a Caenorhabditis elegans supplementary nuclear receptor, regulates embryonic and early larval development. *Mechanisms of Development*, *123*(9), 689-701.

Carmi, I., Kopczynski, J. B., & Meyer, B. J. (1998). The nuclear hormone receptor SEX-1 is an X-chromosome signal that determines nematode sex. *Nature*, *396*(6707), 168-173.

Chan, W., Evans, J., Roenspies, T., Rumley, J. D., Murray, J. I., & Colavita, A. (2025). Notch-mediated regulation of β-Catenin-TCF activity instructs anteroposterior neuron positioning in C. elegans. *bioRxiv*, https://doi.org/10.1101/2025.03.02.641079.

Chawengsaksophak, K. (2019). Cdx2 animal models reveal developmental origins of cancers. *Genes*, *10*(11), 928.

Ciruna, B., Jenny, A., Lee, D., Mlodzik, M., & Schier, A. F. (2006). Planar cell polarity signalling couples cell division and morphogenesis during neurulation. *Nature*, *439*(7073), 220-224.

Collinet, C., & Lecuit, T. (2021). Programmed and self-organized flow of information during morphogenesis. *Nature Reviews. Molecular Cell Biology*, *22*(4), 245–265. https://doi.org/10.1038/s41580-020-00318-6

Davis, M. B., Jash, E., Chawla, B., Haines, R. A., Tushman, L. E., Troll, R., & Csankovszki, G. (2022). Dual roles for nuclear RNAi Argonautes in Caenorhabditis elegans dosage compensation. *Genetics*, *221*(1), iyac033.

Devitt, C. C., Weng, S., Bejar-Padilla, V. D., Alvarado, J., & Wallingford, J. B. (2024). PCP and Septins govern the polarized organization of the actin cytoskeleton during convergent extension. *Current Biology*, *34*(3), 615-622.

Dickinson, D. J., Pani, A. M., Heppert, J. K., Higgins, C. D., & Goldstein, B. (2015). Streamlined genome engineering with a self-excising drug selection cassette. *Genetics*, *200*(4), 1035-1049.

Doudney, K., & Stanier, P. (2005, May). Epithelial cell polarity genes are required for neural tube closure. In *American Journal of Medical Genetics Part C: Seminars in Medical Genetics* (Vol. 135, No. 1, pp. 42-47). Hoboken: Wiley Subscription Services, Inc., A Wiley Company.

Dumas, K. J., Delaney, C. E., Flibotte, S., Moerman, D. G., Csankovszki, G., & Hu, P. J. (2013). Unexpected role for dosage compensation in the control of dauer arrest, insulin-like signaling, and FoxO transcription factor activity in Caenorhabditis elegans. *Genetics*, *194*(3), 619-629.

Edgar, L. G., Carr, S., Wang, H., & Wood, W. B. (2001). Zygotic expression of the caudal homolog pal-1 is required for posterior patterning in Caenorhabditis elegans embryogenesis. *Developmental Biology*, *229*(1), 71-88.

Farboud, B., Nix, P., Jow, M. M., Gladden, J. M., & Meyer, B. J. (2013). Molecular antagonism between X-chromosome and autosome signals determines nematode sex. *Genes & Development*, *27*(10), 1159-1178.

Frankel, N. (2012). Multiple layers of complexity in cis-regulatory regions of developmental genes. *Developmental Dynamics*, *241*(12), 1857-1866.

Gilbert, S. P., Mullan, T. W., Poole, R. J., & Woollard, A. (2020). Caudal-dependent cell positioning directs morphogenesis of the C. elegans ventral epidermis. *Developmental Biology*, *461*(1), 31-42.

Gladden, J. M., & Meyer, B. J. (2007). A ONECUT homeodomain protein communicates X chromosome dose to specify Caenorhabditis elegans sexual fate by repressing a sex switch gene. *Genetics*, *177*(3), 1621-1637.

Gold, D. A., Baek, S. H., Schork, N. J., Rose, D. W., Larsen, D. D., Sachs, B. D., ... & Hamilton, B. A. (2003). RORα coordinates reciprocal signaling in cerebellar development through sonic hedgehog and calcium-dependent pathways. *Neuron*, *40*(6), 1119-1131.

Gur, M., Edri, T., Moody, S. A., & Fainsod, A. (2022). Retinoic acid is required for normal morphogenetic movements during gastrulation. *Frontiers in cell and developmental biology*, *10*, 857230.

Hayes, M., Naito, M., Daulat, A., Angers, S., & Ciruna, B. (2013). Ptk7 promotes non-canonical Wnt/PCP-mediated morphogenesis and inhibits Wnt/β-catenin-dependent cell fate decisions during vertebrate development. *Development*, *140*(8), 1807-1818.

Houle, M., Sylvestre, J. R., & Lohnes, D. (2003). Retinoic acid regulates a subset of Cdx1 function in vivo. *Development*, *130*(26), 6555–6567.

Hunter, C. P., & Kenyon, C. (1996). Spatial and temporal controls target pal-1 blastomere-specification activity to a single blastomere lineage in C. elegans embryos. *Cell*, *87*(2), 217-226.

Ikeda, R., Tsuchiya, Y., Koike, N., Umemura, Y., Inokawa, H., Ono, R., ... & Yagita, K. (2019). REV-ERBα and REV-ERBβ function as key factors regulating Mammalian Circadian Output. *Scientific Reports*, *9*(1), 10171.

Jash, E., Tan, Z. M., Rakozy, A. I., Azhar, A. A., Mendoza, H., & Csankovszki, G. (2024). Multi-level transcriptional regulation of embryonic sex determination and dosage compensation by the X-signal element sex-1. *bioRxiv*.

Kam, R. K. T., Shi, W., Chan, S. O., Chen, Y., Xu, G., Bik-San Lau, C., ... & Zhao, H. (2013). Dhrs3 protein attenuates retinoic acid signaling and is required for early embryonic patterning. *Journal of Biological Chemistry*, *288*(44), 31477-31487.

Keller, M. S., Ezaki, T., Guo, R. J., & Lynch, J. P. (2004). Cdx1 or Cdx2 expression activates E-cadherin-mediated cell-cell adhesion and compaction in human COLO 205 cells. *American Journal of Physiology-Gastrointestinal and Liver Physiology*, *287*(1), G104-G114.

Khan, S. H., & Okafor, C. D. (2022). Interactions governing transcriptional activity of nuclear receptors. *Biochemical Society Transactions*, *50*(6), 1941-1952.

Koch, K., Schlüppmann, K., Hüsken, S., Stark, L. M., Förster, N., Masjosthusmann, S., Klose J, Dönmez A, & Fritsche, E. (2025). Nuclear hormone receptors control fundamental processes of human fetal neurodevelopment: Basis for endocrine disruption assessment. *Environment international*, *198*, 109400.

Kwon, J. Y., Park, J. M., Gim, B. S., Han, S. J., Lee, J., & Kim, Y. J. (1999). Caenorhabditis elegans mediator complexes are required for developmental-specific transcriptional activation. *Proceedings of the National Academy of Sciences*, *96*(26), 14990-14995.

Lees, J. A., Fawell, S. E., White, R., & G. Parker, M. (1990). A 22-amino-acid peptide restores DNA-binding activity to dimerization-defective mutants of the estrogen receptor. *Molecular and Cellular Biology*, *10*(10), 5529-5531.

Lengerke, C., Wingert, R., Beeretz, M., Grauer, M., Schmidt, A. G., Konantz, M., ... & Davidson, A. J. (2011). Interactions between Cdx genes and retinoic acid modulate early cardiogenesis. *Developmental biology*, *354*(1), 134-142.

Li, L., & Wunderlich, Z. (2017). An enhancer's length and composition are shaped by its regulatory task. *Frontiers in Genetics*, *8*, 63.

Lorentz, O., Duluc, I., Arcangelis, A. D., Simon-Assmann, P., Kedinger, M., & Freund, J. N. (1997). Key role of the Cdx2 homeobox gene in extracellular matrix–mediated intestinal cell differentiation. *Journal of Cell Biology*, *139*(6), 1553-1565.

Lu, Y., Ahamed, T., Mulcahy, B., Meng, J., Witvliet, D., Guan, S. A., Holmyard, D., Hung, W., Wen, Q., Chisholm, A. D., Samuel, A. D. T., & Zhen, M. (2022). Extrasynaptic signaling enables an asymmetric juvenile motor circuit to produce symmetric undulation. *Current Biology*, 32(21), 4631–4644.e5. doi:10.1016/j.cub.2022.09.002.

Ludewig, A. H., Kober-Eisermann, C., Weitzel, C., Bethke, A., Neubert, K., Gerisch, B., ... & Antebi, A. (2004). A novel nuclear receptor/coregulator complex controls C. elegans lipid metabolism, larval development, and aging. *Genes & Development*, *18*(17), 2120-2133.

Maduro, M. F., Kasmir, J. J., Zhu, J., & Rothman, J. H. (2005). The Wnt effector POP-1 and the PAL-1/Caudal homeoprotein collaborate with SKN-1 to activate C. elegans endoderm development. *Developmental Biology*, *285*(2), 510-523.

Mainpal, R., Priti, A., & Subramaniam, K. (2011). PUF-8 suppresses the somatic transcription factor PAL-1 expression in C. elegans germline stem cells. *Developmental Biology*, *360*(1), 195-207.

Martinez, S., Scerbo, P., Giordano, M., Daulat, A. M., Lhoumeau, A. C., Thomé, V., ... & Borg, J. P. (2015). The PTK7 and ROR2 protein receptors interact in the vertebrate WNT/planar cell polarity (PCP) pathway. *Journal of Biological Chemistry*, *290*(51), 30562-30572.

Meyer, B. I., & Gruss, P. (1993). Mouse Cdx-1 expression during gastrulation. *Development*, *117*(1), 191-203.

Meyer, B. J. (2010). Targeting X chromosomes for repression. *Current opinion in genetics & development*, *20*(2), 179-189.

Mic, F. A., Haselbeck, R. J., Cuenca, A. E., & Duester, G. (2002). Novel retinoic acid generating activities in the neural tube and heart identified by conditional rescue of Raldh2 null mutant mice. *Development*, *129*(9), 2271–2282.

Mitani, S., 2017. Comprehensive functional genomics using Caenorhabditis elegans as a model organism. Proc. Jpn. Acad. Ser. B, 93.

Mootz, D., Ho, D. M., & Hunter, C. P. (2004). The STAR/Maxi-KH domain protein GLD-1 mediates a developmental switch in the translational control of C. elegans PAL-1. *Development*, *131*(14), 3263–3272.

Mulcahy, B., Witvliet, D. K., Mitchell, J., Schalek, R., Berger, D. R., Wu, Y., Holmyard, D., Lu, Y., Ahamed, T., Samuel, A. D. T., Chisholm, A. D., Lichtman, J. W., & Zhen, M. (2022). Post-embryonic remodeling of the C. elegans motor circuit. *Current biology, 32*(21), 4645–4659.e3. https://doi.org/10.1016/j.cub.2022.09.065

Noblett, N., Wu, Z., Ding, Z. H., Park, S., Roenspies, T., Flibotte, S., ... & Colavita, A. (2019). DIP-2 suppresses ectopic neurite sprouting and axonal regeneration in mature neurons. *Journal of Cell Biology*, *218*(1), 125-133.

Noblett, N., Roenspies, T., Kirezi, C. B., Stubbert, C., Flibotte, S., Shah, P. K., & Colavita, A. (2025). IPPK-1 and IP6 contribute to ventral nerve cord assembly in C. elegans. *Developmental Biology*, *526*, 159–172.

Nordström, U., Maier, E., Jessell, T. M., & Edlund, T. (2006). An early role for WNT signaling in specifying neural patterns of Cdx and Hox gene expression and motor neuron subtype identity. *PLoS Biology*, *4*(8), e252.

Palmer, A. J., Savery, D., Massa, V., Copp, A. J., & Greene, N. D. (2021). Genetic interaction of Pax3 mutation and canonical Wnt signaling modulates neural tube defects and neural crest abnormalities. *Genesis*, *59*(11), e23445.

Plateroti, M., Gauthier, K., Domon-Dell, C., Freund, J. N., Samarut, J., & Chassande, O. (2001). Functional interference between thyroid hormone receptor α (TRα) and natural truncated TRΔα isoforms in the control of intestine development. *Molecular and cellular biology*, *21*(14), 4761-4772.

R Core Team (2019) R: a language and environment for statistical computing. R Foundation for Statistical Computing, Vienna, Austria. https://www.R-project.org.

Saharkhiz, S., Petite, M., Roenspies, T., Perkins, T., & Colavita, A. (2024). VNC-Dist: A machine learning-based pipeline for quantification of neuronal positioning in the ventral nerve cord of C. elegans. *bioRxiv*, https://doi.org/10.1101/2024.11.16.623955.

Sanchez-Ferras, O., Bernas, G., Farnos, O., Touré, A. M., Souchkova, O., & Pilon, N. (2016). A direct role for murine Cdx proteins in the trunk neural crest gene regulatory network. *Development*, *143*(8), 1363-1374.

Savory, J. G., Mansfield, M., Rijli, F. M., & Lohnes, D. (2011). Cdx mediates neural tube closure through transcriptional regulation of the planar cell polarity gene Ptk7. *Development*, *138*(7), 1361-1370.

Shah, P. K., Tanner, M. R., Kovacevic, I., Rankin, A., Marshall, T. E., Noblett, N., ... & Colavita, A. (2017). PCP and SAX-3/Robo pathways cooperate to regulate convergent extension-based nerve cord assembly in C. elegans. *Developmental Cell*, *41*(2), 195-203.

Shindo, A., Inoue, Y., Kinoshita, M., & Wallingford, J. B. (2019). PCP-dependent transcellular regulation of actomyosin oscillation facilitates convergent extension of vertebrate tissue. *Developmental Biology*, *446*(2), 159-167.

Skipper, M., Milne, C. A., & Hodgkin, J. (1999). Genetic and molecular analysis of fox-1, a numerator element involved in Caenorhabditis elegans primary sex determination. *Genetics*, *151*(2), 617-631.

Skromne, I., Thorsen, D., Hale, M., Prince, V. E., & Ho, R. K. (2007). Repression of the hindbrain developmental program by Cdx factors is required for the specification of the vertebrate spinal cord. *Development (Cambridge, England)*, *134*(11), 2147–2158.

Sturgeon, K., Kaneko, T., Biemann, M., Gauthier, A., Chawengsaksophak, K., & Cordes, S. P. (2011). Cdx1 refines positional identity of the vertebrate hindbrain by directly repressing Mafb expression. *Development*, *138*(1), 65-74.

Taneja, R., Rochette-Egly, C., Plassat, J. L., Penna, L., Gaub, M. P., & Chambon, P. (1997). Phosphorylation of activation functions AF-1 and AF-2 of RARα and RARγ is indispensable for differentiation of F9 cells upon retinoic acid and cAMP treatment. *The EMBO journal, 16(21), 6452–6465.*

Waaijers, S., & Boxem, M. (2014). Engineering the Caenorhabditis elegans genome with CRISPR/Cas9. *Methods*, *68*(3), 381-388.

Waring, D. A., & Kenyon, C. (1991). Regulation of cellular responsiveness to inductive signals in the developing C. elegans nervous system. *Nature*, *350*(6320), 712-715.

Webster, C. M., Wu, L., Douglas, D., & Soukas, A. A. (2013). A non-canonical role for the C. elegans dosage compensation complex in growth and metabolic regulation downstream of TOR complex 2. *Development*, *140*(17), 3601-3612.

Wehner, P., Shnitsar, I., Urlaub, H., & Borchers, A. (2011). RACK1 is a novel interaction partner of PTK7 that is required for neural tube closure. *Development*, *138*(7), 1321-1327.

Wen, Q., Gao, S., & Zhen, M. (2018). Caenorhabditis elegans excitatory ventral cord motor neurons derive rhythm for body undulation. *Philosophical Transactions of the Royal Society B: Biological Sciences*, *373*(1758), 20170370.

Wendling, O., Chambon, P., & Mark, M. (1999). Retinoid X receptors are essential for early mouse development and placentogenesis. *Proceedings of the National Academy of Sciences*, *96*(2), 547-551.

Wilkinson, L. (2011). ggplot2: elegant graphics for data analysis by WICKHAM, H.

Williams, M., Yen,W., Lu, X., & Sutherland A. (2014). Distinct Apical and Basolateral Mechanisms Drive Planar Cell Polarity-Dependent Convergent Extension of the Mouse Neural Plate. *Developmental Cell*, 29, 34–46.

Wilson, L., Gale, E., & Maden, M. (2003). The role of retinoic acid in the morphogenesis of the neural tube. *Journal of anatomy*, *203*(4), 357-368.

Wingert, R. A., Selleck, R., Yu, J., Song, H. D., Chen, Z., Song, A., ... & Davidson, A. J. (2007). The cdx genes and retinoic acid control the positioning and segmentation of the zebrafish pronephros. *PLoS genetics*, *3*(10), e189.

Ybot-Gonzalez, P., Savery, D., Gerrelli, D., Signore, M., Mitchell, C. E., Faux, C. H., ... & Copp, A. J. (2007). Convergent extension, planar-cell-polarity signalling and initiation of mouse neural tube closure. *Development*, *134*(4), 789–799.

Young, T., Rowland, J. E., van de Ven, C., Bialecka, M., Novoa, A., Carapuco, M., ... & Deschamps, J. (2009). Cdx and Hox genes differentially regulate posterior axial growth in mammalian embryos. *Developmental Cell*, *17*(4), 516-526.

Zamir, I., Harding, H. P., Atkins, G. B., Hörlein, A., Glass, C. K., Rosenfeld, M. G., & Lazar, M. A. (1996). A nuclear hormone receptor corepressor mediates transcriptional silencing by receptors with distinct repression domains. *Molecular and Cellular Biology*, *16*(10), 5458-5465.

Zhao, T., Gan, Q., Stokes, A., Lassiter, R. N., Wang, Y., Chan, J., ... & Zhou, C. J. (2014). β-catenin regulates Pax3 and Cdx2 for caudal neural tube closure and elongation. *Development*, *141*(1), 148-157.

Zhao, T., McMahon, M., Reynolds, K., Saha, S. K., Stokes, A., & Zhou, C. J. (2022). The role of Lrp6-mediated Wnt/β-catenin signaling in the development and intervention of spinal neural tube defects in mice. *Disease models & mechanisms*, *15*(6), dmm049517.

Zhu, Y., & Lohnes, D. (2022). Regulation of axial elongation by Cdx. *Developmental Biology*, *483*, 118-127.

Chapter 4. Conclusions and Discussion

The development and genetics of the ventral nerve cord (VNC) has been an area of interest for nematode researchers since Brenner, White, and Sulston first characterized their stereotyped lineage (Sulston et al., 1983; White et al., 1986). This includes all three subtypes of embryonically born motor neurons (DA, DB and DD), motor neuron subtypes which are born post hatching and interneurons which interconnect the motor neuron circuit required for sinusoidal movement. Over the past 50 years, research has expanded knowledge of the complexity within this relatively simple population of cells. Recent studies have identified a complex combinatorial code of HOX transcription factors required for motor neuron diversification, a continuing role for terminal factors in maintaining neuron identity, and extensive remodeling of synapses post-hatching (Kerk et al., 2017; Feng et al., 2022; Mulcahy et al., 2022). Similarly, embryonic development of the VNC has been shown to depend on collective cell behaviors including, convergent extension and multicellular rosette dynamics, which contribute to VNC specific anteroposterior positioning and spacing of motor neuron cell bodies (Shah et al., 2017).

As opposed to earlier events which are critical to embryonic development, such as polarization of the embryo or cell fate decisions, the regulatory mechanisms that influence collective cell movements during morphogenesis in *C. elegans* are poorly understood. This includes the question of how broader regulatory mechanisms, which coordinate the timing and directionality of intercalations, function across multiple tissues. Similarly, how these movements differ between tissue types, and which regulatory pathways facilitate these differences requires further study.

Research on defects in morphogenesis can be technically challenging due to the number of essential proteins involved in early embryonic development and the complex morphology of certain tissues. Thus, it is not surprising that the extent to which mechanisms during convergent extension and central nerve cord formation are conserved between nematodes and other models remains limited. While previous work from several groups has suggested that cellular mechanisms and role of the PCP pathway during cell intercalations are conserved (Shah et al., 2017; Williams et al., 2014; Sullivan-Brown et al., 2016; Xu et al., 2023), the specifics of these models remain underexplored. Here, we expand on our understanding of VNC morphogenesis to examine genetic regulation of collective cell movements. This dissertation specifically examines the inositol phosphate pathway, through its essential kinase IPPK-1 (Chapter 2), and the *Caudal* homolog

PAL-1 (Chapter 3). This chapter will discuss the overall findings in this study, the concepts that they raise and how they fit into current literature. It will also address several limitations of the study and raise some additional questions that may be examined in future research.

Spatial and Temporal Contributions of IPPK-1 and PAL-1 to VNC Assembly

Chapter 2 presents an investigation of inositol phosphate metabolism during VNC assembly, highlighting evidence for multiple stages of cell movements, complex interactions among studied regulators, and potential conservation between nematodes and chordates. We demonstrated using the *zy65* allele of the inositol pentakisphosphate kinase *ippk-1*, a strong temperature-sensitive hypomorph, that the gene is required for rosette-mediated convergent extension. As a result of the mutation in *ippk-1(zy65)*, the equilaterally distributed cell bodies of DD neurons are displaced towards the anterior of the worm. The DD and DA neuron subtypes are descended from neuroblasts born on opposite left and right lineages during embryogenesis. As the embryo develops, the lateral migration of these neuronal progenitors brings neurons from each side into contact at the midline. A series of rosette-mediated intercalations then aligns DA and DD neuronal progenitors into a single file with an alternating pattern. Within this pattern, neurons of left and right origin also alternate. The displacement caused by the loss of IPPK-1 results in an abnormal distribution of DD neurons, with alternating pairs of cell bodies positioned closer together. This could suggest that correct medial-lateral intercalation during convergent extension may be required to arrange the positioning of left and right originating neuronal progenitors.

Previous work has shown that embryonic development of the VNC relies on rosette-mediated convergent extension (Shah et al., 2017). The research presented in this dissertation suggests that IPPK-1 is also involved in rosette dynamics. Mutation of *ippk-1(zy65)* delayed the resolution of a central rosette. Our data also suggests that IPPK-1 may interact with the PCP component VANG-1 during rosette timing. Rosette timing is not enhanced in *vang-1(ok1142); ippk-1(zy65)* double mutants, in contrast to previous research which showed that rosettes in *vang-1(ok1142); sax-3(zy5)* double mutants persist longer than in either single mutant. While this observation is interesting, the *zy65* allele of *ippk-1* is not a null mutation and so further research will be needed to confirm the interaction.

The findings also introduce the importance of inositol phosphate metabolism to early development of the VNC, prior to the intercalation of DD and DA neurons at the midline. *ippk-*

1(zy65) mutants show disorganization among *cnd-1/NeuroD*-labelled neuronal progenitors during their movement toward the midline. This disorganisation appears to begin around the period when DA and DD progenitors undergo their terminal divisions. It is characterised by the disrupted arrangement of neuron progenitors on either side of the embryo, incorrect cell-cell junctions and ectopic rosettes. This resembles the disordered germline membrane architecture in adult *ippk-1(zy65)* mutants and may also resemble ectopic contacts that form between embryonic epithelial cells with disrupted IP3 signalling (Vazquez-Manrique et al., 2008; Lowry et al., 2015). These defects differ from those found when PCP signaling is disrupted in *vang-1(ok1142)/Vangl* and *prkl-1(ok3182)/Prickle* mutants. This may indicate that IPPK-1 functions independently of the PCP pathway during early development to ensure proper organisation of the cells. Several mechanisms could explain this disorganisation. IPPK-1 and its product IP6, for example, could function to prevent ectopic rosettes or the incorrect contraction of certain junctions. Likewise, it could be influencing the timing of junctional contractions needed to quickly resolve rosettes. The study can not rule out that disrupted timing or orientation of terminal cell divisions may also contribute to the phenotype. The orientation of cell divisions has been found to contribute to convergent extension during elongation of the *Drosophila* germband (da Silva and Vincent, 2007).

Collective cell movements like convergent extension require positional, temporal and metabolic information. In many models, including neurulation, this information is integrated through complex transcription factor cascades (Montell et al., 2012, van der Spuy et al., 2023). Chapter 3 investigated transcriptional regulation during VNC assembly, highlighting an interaction between the caudal homolog PAL-1 and the nuclear hormone receptor SEX-1. We found that the *zy117* allele of *pal*-1, which disrupts an enhancer region approximately 6.5kb upstream from the ATG start, results in a loss of *PAL-1* expression in DD and DA neurons. These mutants display anterior displacement of DD and DA cell bodies, suggesting that the transcription factor is required to regulate the placement of neuronal progenitors during development of the VNC. This role reflects previously described functions of *PAL-1* within several populations of cells that rely on migration during morphogenesis (Edgar et al., 2001; Gilbert et al., 2020). This includes ventral epithelial cells, which migrate to enclose the embryo at the end of gastrulation, and the posterior migration of muscle or dorsal epidermal cells during embryonic elongation. Likewise, PAL-1 is required in other ventral epithelial cells during mid to late embryogenesis to facilitate their migration and correct alignment, suggesting a broader role in morphogenesis

(Gilbert et al., 2020). Our work, however, also demonstrates that PAL-1 and IPPK-1 may act through independent mechanisms, reinforcing that collective cell movements can be differentially regulated. For example, *pal-1(zy117)* mutants display greater shifts in posterior neurons (DD3-DD6), whereas *ippk-1(zy65)* mutants show consistent displacement across both anterior and posterior cell body position.

The restricted expression of PAL-1 in mid to posterior DA and DD neuronal progenitors, which is lost in the *pal-1(zy117)*, suggests that specific control over the spatial distribution of PAL-1 is important. Consistent with this, PAL-1 expression in the posterior DB neurons is largely unaffected in pal-1(*zy117)*, suggesting that multiple regulatory elements are needed for its full activity in the VNC. This data aligns with the complex regulation of *pal-1* promoter activity within embryonic populations of epithelial, muscle, and neuronal cells which require multiple transcription cofactors to regulate cell fate decisions (Hunter and Kenyon, 1996; Mootz et al., 2004; Edgar et al., 2001; Mainpal et al., 2011; Gilbert et al., 2020). It is currently unclear why and how the expression of PAL-1 is specified in this tissue-specific manner. Future work may require utilizing a method to deplete PAL-1 in DB neurons, such as auxin-mediated protein degradation (Divekar et al., 2021).

A significant finding of this study was that PAL-1 expression within DA and DD neurons is dependent on the activity of the nuclear hormone receptor SEX-1. The nuclear hormone receptor (NHR) family are regulatory factors with widespread roles in development, including cell differentiation and morphogenic processes which require collective cell movements (Bhattacharya and Starz-Gaiano, 2024; reviewed in Bodofsky et al., 2017). NHRs represent a large family in the *C. elegans* genome with 289 genes compared to 48 in mammals (Miyabayashi et al., 1999; reviewed in Kostrouchova and Kostrouch, 2015; Bodofsky et al., 2017; Tao et al., 2020). Only a small number, however, display clear conservation between species. In *C. elegans*, NHRs are critical during embryogenesis through regulation of processes such as epidermal development, embryo elongation, and muscle cell fate specification (Asahina et al., 2000; Ludewig et al., 2004; Brožová et al., 2006; Simeckova et al., 2007). SEX-1 is considered an orphan NHR1 receptor as no endogenous ligand for it has been identified (Carmi et al., 1998). It has a well described canonical role in nematode sex determination and dosage compensation activity, where it directly inhibits expression of the male fate promoting transcription factor XOL-1 (Skipper et al., 1999;

Gladden et al., 2007; Farboud et al., 2013). SEX-1 is structurally related to the NHR1 family in mammals, with a well conserved DNA binding domain, ligand binding domain, and activated function-2 (AF-2) motif, which typically bind to transcriptional coactivators (Lee et al., 2001). SEX-1 shares approximately 50-70% of its sequence with the NHR1B subfamily, consisting of retinoic acid receptors (RARs), as well as other orphan NHR1 subfamilies (Carmi et al., 1998; Bonnelye et al., 1994; Gold et al., 2003; Ikeda et al., 2019). These include REV-ERBβ (NHR1D), RORα (NHR1F) and E78A in *Drosophila*. E78A, which shows the highest similarity to SEX-1, is a nuclear hormone receptor with sensitivity to the insect steroid ecdysone (Stone and Thummel, 1993; Carmi et al., 1998). The receptor regulates several developmental functions, including gastrulation, the timing of metamorphosis and establishing germline stem cell populations during female reproduction (Fisk and Thummel, 1995; Ables et al., 2015). The inhibitory role of SEX-1 is consistent with its similarity to NHR1 members like REV-ERB (Carmi et al., 1998). Unlike REV-ERB however, SEX-1 contains a conserved AF-2 motif. These are more often associated with NHRs, such as RARs, which display ligand-dependant activation (Lee et al., 2001; Kostrouchova and Kostrouch, 2015; Weikum et al., 2018). These differences could reflect additional roles for SEX-1, including its role in VNC development (Davis et al., 2022).

Spatial restriction of NHRs is a common feature of the family, observed in both mammals and nematodes, including glucocorticoid and retinoic acid receptors in mouse and NHR-2 or NHR-40 in nematodes (Strähle et al., 1992; Taneja et al., 1997; Sluder et al., 1997; Brožová et al., 2006). NHR expression is controlled by a variety of mechanisms, dependant upon cellular and metabolic contexts, including ligand binding, alternative splicing, post-translational modification and cofactor activity (Leroy et al., 1991; Folkers et al., 1998; Lefebvre et al., 2002; Mahony et al., 2011; Xie et al., 2023). Coactivator and corepressor activity is critical to the function of nuclear hormone receptors (reviewed in Bulynko and O'Malley, 2013; Talukdar and Chatterji, 2023). SEX-1 is broadly expressed during early embryogenesis, consistent with its role in sex determination (Carmi et al., 1998). However, it activates *PAL-1* expression only in DA and DD progenitors, not in DB progenitors, despite being expressed in those cells (Packer et al., 2019). Given the importance of transcriptional coactivators, investigation of proteins that bind to its upstream regulatory region using a purification method like reverse-ChIP could provide additional details on the activity of SEX-1 (MacKenzie et al., 2023).

Separate or Shared Mechanisms for DD, DA, DB Neuron Positioning

While loss of PAL-1, SEX-1, PCP components such as VANG-1, or IP pathway members lead to displacement in motor neuron cell body positioning in the VNC, these defects are not always shared uniformly between classes of motor neurons. *ippk-1(zy65)* mutants display noticeable displacement in DD neurons but show only minimal defects in DB neuron placement. Similarly, *pal-1(zy117)* mutants show strong displacement of DD neurons compared to their DA or DB counterparts. Differential effects are also observed in *pal-1(zy117)* double mutants with either *vang-1(tm1422)* or *sax-3(zy5)*. *vang-1(tm1422); pal-1(zy117)* double mutants display strong shifts in DD and DA cell body positions, whereas DA neurons are relatively unaffected in *sax-3(zy5); pal-1(zy117)* double mutants. These observations raise the possibility that movements in DA, DB or DD neurons may be independently regulated.

Several explanations may account for these class-specific differences. DB progenitors intercalate into the developing VNC later then their DA or DD counterparts and therefore may be spatially restricted by the placement of existing cell bodies or subjected to sorting mechanisms that direct their intercalation. It is also notable that intercalation of DB neurons occurs around the same time as the onset of muscle activity and embryo twitching, which could subject the developing VNC to additional mechanical force. Differences in the susceptibility of motor neuron classes to positional shifts may also reflect broader differences in adhesive complex components. Adhesion is required to promote proper intercalation and may facilitate convergent extension driven intercalation in the developing VNC (Weng et al., 2022; Lien and Wang, 2023). Adhesive components, such as cadherins or the LCAM homolog SAX-7, may be required to coordinate cell positions during the extension of the VNC between the 2-fold stage of embryogenesis and hatching (Bénard et al., 2012; Barnes et al., 2020; Majeed et al., 2025). Recent work has shown that while the expression of cadherins supports their broad roles within the nervous system, they still exhibit some variability in temporal and spatial patterning (Majeed et al., 2025). It is possible therefore, that some variation across cell adhesion molecules could account for some of these class specific differences.

Conservation of Mechanisms during *C. elegans* VNC assembly and Neurulation

Neurulation and notochord development are essential steps in embryogenesis that establish the basis of the vertebrate central nervous system. Despite lacking a notochord or neural tube, the

collective cell movements that comprise nerve cord assembly in nematodes and vertebrates involve conserved cellular and molecular mechanisms. Both processes require the regulation of cell intercalation during convergent extension (Ybot-Gonzalez et al., 2007; Shah et al., 2017). Similarly, they both rely on tissue-shape changes that are driven by actomyosin-dependant junctional contractions, which involve the formation of multicellular rosettes, and are influenced with non-canonical Wnt/PCP components such as *Vangl/vang-1* (Williams et al., 2014; Shah et al., 2017; Butler and Wallingford, 2018).

Inositol metabolism, which produces IP molecules, helps to establish the intercellular environment during developmental processes including neurulation (Watson and Walhout, 2015; Greene et al., 2017; Tu-Sekine and Kim, 2022). Our study demonstrates that the function of IPPK-1 during VNC development aligns with mammalian IP function during neurulation. The activity of IPPK-1 suggests a broader role for inositol phosphate metabolism, consistent with analysis of the upstream kinase IPMK-1 or rescue by exogenous IP6. *ipmk-1(tm2687)* mutants display milder defects compared to *ippk-1(zy65)*, which may reflect the presence of other kinases that are involved in phosphorylating IP3 to IP4 and IP5. Few studies have implicated highly phosphorylated forms of inositol with intercalation, despite strong evidence of neural tube development defects in mice with disrupted production of IP5 and IP6 (Frederick et al., 2005; Verbsky et al., 2005). We demonstrated that IPPK-1 and its product IP6 regulate the resolution dynamics of multicellular rosettes, which are important for the proper intercalation of DD and DA progenitors and convergent extension during VNC formation.

The CDX family of *Caudal* transcription factors have partially overlapping roles in cell fate determination, regionalization and axial extension (Chawengsaksophak et al., 2004; Skromne et al., 2007; Savory et al., 2011; Zhu and Lohnes, 2022). This includes the regulation of PCP signaling during neurulation, through transcription of the co-receptor PTK7 (Savory et al., 2011). PAL-1 plays similar roles during embryonic development, including regulating cell fate decisions and spacing of cells within the VNC (Baugh et al., 2005). Its posterior expression pattern also reflects that of CDX family members (Meyer and Gruss, 1993; Baugh et al., 2005). However, our study was limited in assessing the role of PAL-1 in individual cellular movements. Further work directly analyzing development of the embryonic VNC will be needed to confirm the role in convergent extension. Analysis of both Van Gogh/*vang-1* and β-catenin/*bar-1*, also suggest that

some interactions with the CDX family during neurulation are absent in *C. elegans*. The neuron displacement phenotype in *vang-1(tm1422); pal-1(zy65)* double mutants was stronger then either mutant, suggesting that PAL-1 functions in parallel with PCP signaling. This is not entirely unexpected, as nematodes lack the direct target of CDX transcription during neurulation, PTK7 (Savory et al., 2011). Additionally, while the *zy117* allele results in the loss of PAL-1 expression within DA and DD neurons, the protein is still expressed within DB neurons and cells posterior to the VNC. The allele therefore may not faithfully recapitulate a null phenotype for the purposes of genetic analysis.

Future Directions

While this work has described how neural cells contribute to VNC assembly, several broader questions remain about the specifics of cellular movements and the regulation of different aspects of this process. This includes how VNC assembly interacts with or involves additional tissues. Tissues which undergo dynamics movements surrounding the VNC may be of particular interest for future research. This includes ventral epithelial cells, which flank the VNC on the left and right and undergo ventral enclosure, as well as rectal cells to the posterior of the VNC. These posterior cells may be of particular interest as their posterior migration is disrupted in *pal-1* mutants (Edgar et al., 2001), potentially contributing to a broader role for the gene. For example, embryo elongation during *Drosophila* germband extension requires force generated by posterior migration (Collinet et al., 2015).

While our study has identified several regulatory mechanisms of VNC assembly, the specific sub-cellular mechanism targeted by these individual pathways will require further investigation. Inositol phosphates are versatile metabolites with broad effects on a range of cellular mechanisms, including chromatin modification, intracellular signalling and vesicle trafficking (Høy et al., 2002; Watson et al., 2016; Kapral et al., 2017; Marcum and Radhakrishnan, 2019; Li et al., 2022; Rameh et al., 2025; reviewed in Kim et al., 2024). As a result, defining a clear direction for future work is challenging. One exception is a subset of targets that regulate cytoskeletal dynamics (Rao et al., 2015; Cheng and Andrew, 2015; Fu et al., 2017; Schröterová et al., 2018; Rojas et al., 2019; Bhat et al., 2024). In particular, the septins, a group of hetero-oligomers which associate with actin have been found to physically interact with IP6 *in-vitro* (Shindo and Wallingford, 2014; Yin et al., 2016; Devitt et al., 2024). Another potential group of interest are

targets that bind with phosphatidyl inositol biphosphate (PIP2) and triphosphate (PIP3). Phosphorylation of PIP2 to PIP3 is an important step in insulin-like signalling, which recruits and activates targets that are involved with the cytoskeleton (Hopkins et al., 2020). Activation of the kinase AKT and the GTPase RAC are involved in remodeling of actin filaments, apical constriction and cell intercalation (Khayat et al., 2000; Miao et al., 2022). The activity of these membrane lipids is influenced by both *Ipmk*, which can phosphorylate PIP2 to PIP3, and inositol phosphate metabolites, which can competitively bind with PIP3 (Takeuchi et al., 1997; Blind et al., 2012; Chen et al., 2017). Given that the cytoskeleton underlies the activity of PCP components and intercalation behavior more generally, investigating the effects of *IPPK-1* loss on these targets may prove useful.

Another challenge will be to identify PAL-1 targets that are involved in VNC development. *Caudal* homologs have diverse targets which span different cell lineages and roles (Baugh et al., 2005; Foley et al., 2019). This includes genes that are regulated through epigenetic mechanisms (Foley and Lohnes, 2022). Given that much of the literature surrounding CDX and PAL-1 involves non-neuronal cell lineages, it is possible that investigating the nematode neuronal transcriptome using ChIP or ATAC-seq methods could provide novel results (Buenrostro et al., 2013; Araya et al., 2014). Additionally, several results from previous research on regulation by PAL-1 are of particular interest due to their importance in embryo morphogenesis. These include the T-box transcription factors *tbx-8* and *tbx-9*, homeobox transcription factors *ceh-16*, *mab-21* and *vab-7*, and NHRs *nhr-25* and *nhr-60* (Chow et al., 1995; Chen et al., 2004; Pocock et al., 2004; Cassata et al., 2005; Baugh et al., 2005; Šimečková et al., 2007; Sawyer et al., 2011; Gilbert et al. 2020).

Conclusions

This study has expanded on our knowledge of VNC formation, showing that convergent extension related cell-cell intercalation integrates inositol biosynthesis, a SEX-1/NHR and PAL-1/Caudal transcription cascade, and PCP signalling. I found that production of IP6 is required for the convergent extension movements of neuronal progenitors during VNC formation. Inositol phosphate signalling acts independently from PCP signaling during multicellular rosette mediated intercalations. I found that tissue specific expression of the caudal homolog *pal-1* is controlled by the nuclear hormone receptor SEX-1. Features of embryonic VNC morphogenesis are shared

among several mammalian models of convergent extension, suggesting that this model may help facilitate future work in delineating critical pathways.

Chapter 5: Bibliography

Ables, E. T., Bois, K. E., Garcia, C. A., & Drummond-Barbosa, D. (2015). Ecdysone response gene *E78* controls ovarian germline stem cell niche formation and follicle survival in *Drosophila*. *Developmental Biology*, *400*(1), 33–42. https://doi.org/10.1016/j.ydbio.2015.01.013

Ahrens, M. J., Li, Y., Jiang, H., & Dudley, A. T. (2009). Convergent extension movements in growth plate chondrocytes require gpi-anchored cell surface proteins. *Development (Cambridge, England)*, *136*(20), 3463–3474. https://doi.org/10.1242/dev.040592

Alan, J. K., Robinson, S. K., Magsig, K. L., Demarco, R. S., & Lundquist, E. A. (2018). The Atypical Rho GTPase CHW-1 Works with SAX-3/Robo To Mediate Axon Guidance in Caenorhabditis elegans. *G3: Genes|Genomes|Genetics*, *8*(6), 1885–1895. https://doi.org/10.1534/g3.118.200148

Andreeva, A., Lee, J., Lohia, M., Wu, X., Macara, I. G., & Lu, X. (2014). PTK7-Src signaling at epithelial cell contacts mediates spatial organization of actomyosin and planar cell polarity. *Developmental Cell*, *29*(1), 20–33. https://doi.org/10.1016/j.devcel.2014.02.008

Aquino-Nunez, W., Mielko, Z. E., Dunn, T., Santorella, E. M., Hosea, C., Leitner, L., McCalla, D., Simms, C., Verola, W. M., Vijaykumar, S., & Hudson, M. L. (2020). Cnd-1/NeuroD1 Functions with the Homeobox Gene ceh-5/Vax2 and Hox Gene ceh-13/labial To Specify Aspects of RME and DD Neuron Fate in Caenorhabditis elegans. *G3 Genes|Genomes|Genetics*, *10*(9), 3071–3085. https://doi.org/10.1534/g3.120.401515

Araya, C. L., Kawli, T., Kundaje, A., Jiang, L., Wu, B., Vafeados, D., Terrell, R., Weissdepp, P., Gevirtzman, L., Mace, D., Niu, W., Boyle, A. P., Xie, D., Ma, L., Murray, J. I., Reinke, V., Waterston, R. H., & Snyder, M. (2014). Regulatory analysis of the C. elegans genome with spatiotemporal resolution. *Nature*, *512*(7515), 400–405. https://doi.org/10.1038/nature13497

Araya, C., Ward, L. C., Girdler, G. C., & Miranda, M. (2016). Coordinating cell and tissue behavior during zebrafish neural tube morphogenesis. *Developmental Dynamics*, *245*(3), 197–208. https://doi.org/10.1002/dvdy.24304

Asahina, M., Ishihara, T., Jindra, M., Kohara, Y., Katsura, I., & Hirose, S. (2000). The conserved nuclear receptor Ftz-F1 is required for embryogenesis, moulting and reproduction in Caenorhabditis elegans. *Genes to Cells*, *5*(9), 711–723. https://doi.org/10.1046/j.1365-2443.2000.00361.x

Ashley, G. E., Duong, T., Levenson, M. T., Martinez, M. A. Q., Johnson, L. C., Hibshman, J. D., Saeger, H. N., Palmisano, N. J., Doonan, R., Martinez-Mendez, R., Davidson, B. R., Zhang, W., Ragle, J. M., Medwig-Kinney, T. N., Sirota, S. S., Goldstein, B., Matus, D. Q., Dickinson, D. J., Reiner, D. J., & Ward, J. D. (2021). An expanded auxin-inducible degron toolkit for Caenorhabditis elegans. *Genetics*, *217*(3), iyab006. https://doi.org/10.1093/genetics/iyab006

Au, V., Li-Leger, E., Raymant, G., Flibotte, S., Chen, G., Martin, K., Fernando, L., Doell, C., Rosell, F. I., Wang, S., Edgley, M. L., Rougvie, A. E., Hutter, H., & Moerman, D. G. (2019). CRISPR/Cas9 Methodology for the Generation of Knockout Deletions in Caenorhabditis elegans. *G3 (Bethesda, Md.)*, *9*(1), 135–144. https://doi.org/10.1534/g3.118.200778

Aydin, Z., Murray, J. I., Waterston, R. H., & Noble, W. S. (2010). Using machine learning to speed up manual image annotation: Application to a 3D imaging protocol for measuring single cell gene expression in the developing C. elegans embryo. *BMC Bioinformatics*, *11*, 84. https://doi.org/10.1186/1471-2105-11-84

Barnes, K. M., Fan, L., Moyle, M. W., Brittin, C. A., Xu, Y., Colón-Ramos, D. A., Santella, A., & Bao, Z. (2020). Cadherin preserves cohesion across involuting tissues during C. elegans neurulation. *eLife*, *9*, e58626. https://doi.org/10.7554/eLife.58626

Barreto, G., Reintsch, W., Kaufmann, C., & Dreyer, C. (2003). The function of Xenopus germ cell nuclear factor (xGCNF) in morphogenetic movements during neurulation. *Developmental Biology*, *257*(2), 329–342. https://doi.org/10.1016/S0012-1606(03)00109-X

Baugh, L. R., Hill, A. A., Claggett, J. M., Hill-Harfe, K., Wen, J. C., Slonim, D. K., Brown, E. L., & Hunter, C. P. (2005). The homeodomain protein PAL-1 specifies a lineage-specific regulatory network in the C. elegans embryo. *Development*, *132*(8), 1843–1854. https://doi.org/10.1242/dev.01782

Behrens, J., von Kries, J. P., Kühl, M., Bruhn, L., Wedlich, D., Grosschedl, R., & Birchmeier, W. (1996). Functional interaction of beta-catenin with the transcription factor LEF-1. *Nature*, *382*(6592), 638–642. https://doi.org/10.1038/382638a0

Bénard, C. Y., Blanchette, C., Recio, J., & Hobert, O. (2012). The Secreted Immunoglobulin Domain Proteins ZIG-5 and ZIG-8 Cooperate with L1CAM/SAX-7 to Maintain Nervous System Integrity. *PLOS Genetics*, *8*(7), e1002819. https://doi.org/10.1371/journal.pgen.1002819

Bénazéraf, B. (2019). Dynamics and mechanisms of posterior axis elongation in the vertebrate embryo. *Cellular and Molecular Life Sciences*, *76*(1), 89–98. https://doi.org/10.1007/s00018-018-2927-4

Bensch, R., Song, S., Ronneberger, O., & Driever, W. (2013). Non-directional radial intercalation dominates deep cell behavior during zebrafish epiboly. *Biology Open*, *2*(8), 845–854. https://doi.org/10.1242/bio.20134614

Berridge, M. J. (1993). Inositol trisphosphate and calcium signalling. *Nature*, *361*(6410), 315–325. https://doi.org/10.1038/361315a0

Bertet, C., Sulak, L., & Lecuit, T. (2004). Myosin-dependent junction remodelling controls planar cell intercalation and axis elongation. *Nature*, *429*(6992), 667–671. https://doi.org/10.1038/nature02590

Bhat, S. A., Malla, A. B., Oddi, V., Sen, J., & Bhandari, R. (2024). Inositol hexakisphosphate kinase 1 is essential for cell junction integrity in the mouse seminiferous epithelium. *Biochimica et Biophysica Acta (BBA) - Molecular Cell Research*, *1871*(1), 119596. https://doi.org/10.1016/j.bbamcr.2023.119596

Bhattacharya, M., & Starz-Gaiano, M. (2024). Steroid hormone signaling synchronizes cell migration machinery, adhesion and polarity to direct collective movement. *Journal of Cell Science*, *137*(5), jcs261164. https://doi.org/10.1242/jcs.261164

Blankenship, J. T., Backovic, S. T., Sanny, J. S. P., Weitz, O., & Zallen, J. A. (2006). Multicellular rosette formation links planar cell polarity to tissue morphogenesis. *Developmental Cell*, *11*(4), 459–470. https://doi.org/10.1016/j.devcel.2006.09.007

Blind, R. D., Suzawa, M., & Ingraham, H. A. (2012a). Direct modification and activation of a nuclear receptor-PIP_2 complex by the inositol lipid kinase IPMK. *Science Signaling*, *5*(229), ra44. https://doi.org/10.1126/scisignal.2003111

Blind, R. D., Suzawa, M., & Ingraham, H. A. (2012b). Direct modification and regulation of a nuclear receptor-PIP2 complex by the nuclear inositol-lipid kinase IPMK. *Science Signaling*, *5*(229), ra44. https://doi.org/10.1126/scisignal.2003111

Bodofsky, S., Koitz, F., & Wightman, B. (2017). CONSERVED AND EXAPTED FUNCTIONS OF NUCLEAR RECEPTORS IN ANIMAL DEVELOPMENT. *Nuclear Receptor Research*, *4*, 101305. https://doi.org/10.11131/2017/101305

Bolinger, C., Zasadil, L., Rizaldy, R., & Hildebrand, J. D. (2010). Specific isoforms of drosophila shroom define spatial requirements for the induction of apical constriction. *Developmental Dynamics: An Official Publication of the American Association of Anatomists*, *239*(7), 2078–2093. https://doi.org/10.1002/dvdy.22326

Bonnelye, E., Vanacker, J. M., Desbiens, X., Begue, A., Stehelin, D., & Laudet, V. (1994). Rev-erb beta, a new member of the nuclear receptor superfamily, is expressed in the nervous system during chicken development. *Cell Growth & Differentiation: The Molecular Biology Journal of the American Association for Cancer Research*, *5*(12), 1357–1365.

Borgne, R. L., Remaud, S., Hamel, S., & Schweisguth, F. (2005). Two Distinct E3 Ubiquitin Ligases Have Complementary Functions in the Regulation of Delta and Serrate Signaling in Drosophila. *PLOS Biology*, *3*(4), e96. https://doi.org/10.1371/journal.pbio.0030096

Böttcher, A., Büttner, M., Tritschler, S., Sterr, M., Aliluev, A., Oppenländer, L., Burtscher, I., Sass, S., Irmler, M., Beckers, J., Ziegenhain, C., Enard, W., Schamberger, A. C., Verhamme, F. M., Eickelberg, O., Theis, F. J., & Lickert, H. (2021). Non-canonical Wnt/PCP signalling regulates intestinal stem cell lineage priming towards enteroendocrine and Paneth cell fates. *Nature Cell Biology*, *23*(1), 23–31. https://doi.org/10.1038/s41556-020-00617-2

Brehm, M. A., Wundenberg, T., Williams, J., Mayr, G. W., & Shears, S. B. (2013). A non-catalytic role for inositol 1,3,4,5,6-pentakisphosphate 2-kinase in the synthesis of ribosomal RNA. *Journal of Cell Science*, *126*(2), 437–444. https://doi.org/10.1242/jcs.110031

Brenner, S. (1974). The genetics of Caenorhabditis elegans. *Genetics*, *77*(1), 71–94. https://doi.org/10.1093/genetics/77.1.71

Brown, S.-A., Morgan, F., Watras, J., & Loew, L. M. (2008). Analysis of Phosphatidylinositol-4,5-Bisphosphate Signaling in Cerebellar Purkinje Spines. *Biophysical Journal*, *95*(4), 1795–1812. https://doi.org/10.1529/biophysj.108.130195

Brožová, E., Šimečková, K., Kostrouch, Z., Rall, J. E., & Kostrouchová, M. (2006). NHR-40, a *Caenorhabditis elegans* supplementary nuclear receptor, regulates embryonic and early larval development. *Mechanisms of Development*, *123*(9), 689–701. https://doi.org/10.1016/j.mod.2006.06.006

Bryja, V., Andersson, E. R., Schambony, A., Esner, M., Bryjová, L., Biris, K. K., Hall, A. C., Kraft, B., Cajanek, L., Yamaguchi, T. P., Buckingham, M., & Arenas, E. (2009). The Extracellular Domain of Lrp5/6 Inhibits Noncanonical Wnt Signaling In Vivo. *Molecular Biology of the Cell*, *20*(3), 924–936. https://doi.org/10.1091/mbc.e08-07-0711

Buenrostro, J. D., Wu, B., Chang, H. Y., & Greenleaf, W. J. (2015). ATAC-seq: A Method for Assaying Chromatin Accessibility Genome-Wide. *Current Protocols in Molecular Biology*, *109*(1), 21.29.1-21.29.9. https://doi.org/10.1002/0471142727.mb2129s109

Bulynko, Y. A., & O'Malley, B. W. (2011). Nuclear Receptor Coactivators: Structural and Functional Biochemistry. *Biochemistry*, *50*(3), 313–328. https://doi.org/10.1021/bi101762x

Burren, K. A., Scott, J. M., Copp, A. J., & Greene, N. D. E. (2010). The genetic background of the curly tail strain confers susceptibility to folate-deficiency-induced exencephaly. *Birth Defects Research Part A: Clinical and Molecular Teratology*, *88*(2), 76–83. https://doi.org/10.1002/bdra.20632

Butler, M. T., & Wallingford, J. B. (2018). Spatial and temporal analysis of PCP protein dynamics during neural tube closure. *eLife*, *7*, e36456. https://doi.org/10.7554/eLife.36456

C. elegans Sequencing Consortium. (1998). Genome sequence of the nematode C. elegans: A platform for investigating biology. *Science (New York, N.Y.)*, *282*(5396), 2012–2018. https://doi.org/10.1126/science.282.5396.2012

Cadigan, K. M., & Waterman, M. L. (2012). TCF/LEFs and Wnt Signaling in the Nucleus. *Cold Spring Harbor Perspectives in Biology*, *4*(11), a007906. https://doi.org/10.1101/cshperspect.a007906

Cao, R., Gozlan, O., Airich, A., Tveriakhina, L., Zhou, H., Jiang, H., Cole, P. A., Aster, J. C., Klein, T., Sprinzak, D., & Blacklow, S. C. (2024). Structural requirements for activity of Mind bomb1 in Notch signaling. *Structure*, *32*(10), 1667-1676.e5. https://doi.org/10.1016/j.str.2024.07.011

Carmi, I., Kopczynski, J. B., & Meyer, B. J. (1998). The nuclear hormone receptor SEX-1 is an X-chromosome signal that determines nematode sex. *Nature*, *396*(6707), 168–173. https://doi.org/10.1038/24164

Carroll, S. H., Schafer, S., Kawasaki, K., Tsimbal, C., Jule, A. M., Hallett, S. A., Li, E., & Liao, E. C. (n.d.). Genetic requirement of dact1/2 to regulate noncanonical Wnt signaling and calpain 8 during embryonic convergent extension and craniofacial morphogenesis. *eLife*, *13*, RP91648. https://doi.org/10.7554/eLife.91648

Cassata, G., Shemer, G., Morandi, P., Donhauser, R., Podbilewicz, B., & Baumeister, R. (2005). Ceh-16/engrailed patterns the embryonic epidermis of Caenorhabditis elegans. *Development*, *132*(4), 739–749. https://doi.org/10.1242/dev.01638

Cast, A. E., Gao, C., Amack, J. D., & Ware, S. M. (2012). An essential and highly conserved role for Zic3 in left-right patterning, gastrulation and convergent extension morphogenesis. *Developmental Biology*, *364*(1), 22–31. https://doi.org/10.1016/j.ydbio.2012.01.011

Cavalli, P., & Ronda, E. (2017). Myoinositol: The Bridge (PONTI) to Reach a Healthy Pregnancy. *International Journal of Endocrinology*, *2017*, 5846286. https://doi.org/10.1155/2017/5846286

Cavanaugh, K. E., Staddon, M. F., Munro, E., Banerjee, S., & Gardel, M. L. (2020). RhoA Mediates Epithelial Cell Shape Changes via Mechanosensitive Endocytosis. *Developmental Cell*, *52*(2), 152-166.e5. https://doi.org/10.1016/j.devcel.2019.12.002

Chacon-Heszele, M. F., Ren, D., Reynolds, A. B., Chi, F., & Chen, P. (2012). Regulation of cochlear convergent extension by the vertebrate planar cell polarity pathway is dependent on p120-catenin. *Development*, *139*(5), 968–978. https://doi.org/10.1242/dev.065326

Chakraborty, A., Koldobskiy, M. A., Bello, N. T., Maxwell, M., Potter, J. J., Juluri, K. R., Maag, D., Kim, S., Huang, A. S., Dailey, M. J., Saleh, M., Snowman, A. M., Moran, T. H., Mezey, E., & Snyder, S. H. (2010). Inositol Pyrophosphates Inhibit Akt Signaling, Thereby Regulating Insulin Sensitivity and Weight Gain. *Cell*, *143*(6), 897–910. https://doi.org/10.1016/j.cell.2010.11.032

Challa, A. K., McWhorter, M. L., Wang, C., Seeger, M. A., & Beattie, C. E. (2005). Robo3 isoforms have distinct roles during zebrafish development. *Mechanisms of Development*, *122*(10), 1073–1086. https://doi.org/10.1016/j.mod.2005.06.006

Chan, W., Evans, J., Roenspies, T., Rumley, J. D., Murray, J. I., & Colavita, A. (2025a). *Notch-mediated regulation of β-Catenin-TCF activity instructs anteroposterior neuron positioning in C. elegans* (p. 2025.03.02.641079). bioRxiv. https://doi.org/10.1101/2025.03.02.641079

Chawengsaksophak, K., de Graaff, W., Rossant, J., Deschamps, J., & Beck, F. (2004). Cdx2 is essential for axial elongation in mouse development. *Proceedings of the National Academy of Sciences*, *101*(20), 7641–7645. https://doi.org/10.1073/pnas.0401654101

Chen, C., Yang, F., Liu, C., Cui, L., Fu, M., & Song, Y. (2017). Inositol hexaphosphate hydrolysate competitively binds to AKT to inhibit the proliferation of colon carcinoma. *Oncology Reports*, *38*(5), 2901–2910. https://doi.org/10.3892/or.2017.5943

Chen, L.-C., Tarone, R., Huynh, M., & De Luca, L. M. (1995). High dietary retinoic acid inhibits tumor promotion and malignant conversion in a two-stage skin carcinogenesis protocol using 7,12-dimethylbenz[*a*]anthracene as the initiator and mezerein as the tumor promoter in female SENCAR mice. *Cancer Letters*, *95*(1), 113–118. https://doi.org/10.1016/0304-3835(95)03868-W

Chen, W. H., Morriss-Kay, G. M., & Copp, A. J. (1995). Genesis and prevention of spinal neural tube defects in the curly tail mutant mouse: Involvement of retinoic acid and its nuclear receptors RAR-beta and RAR-gamma. *Development (Cambridge, England)*, *121*(3), 681–691. https://doi.org/10.1242/dev.121.3.681

Chen, Z., Eastburn ,Dennis J., & and Han, M. (2004). The Caenorhabditis elegans Nuclear Receptor Gene nhr-25 Regulates Epidermal Cell Development. *Molecular and Cellular Biology*, *24*(17), 7345–7358. https://doi.org/10.1128/MCB.24.17.7345-7358.2004

Chen, Z., Kuang, L., Finnell, R. H., & Wang, H. (2018). Genetic and functional analysis of SHROOM1-4 in a Chinese neural tube defect cohort. *Human Genetics*, *137*(3), 195–202. https://doi.org/10.1007/s00439-017-1864-x

Cheng, Y. L., & Andrew, D. J. (2015). Extracellular Mipp1 activity confers migratory advantage to epithelial cells during collective migration. *Cell Reports*, *13*(10), 2174–2188. https://doi.org/10.1016/j.celrep.2015.10.071

Choi, S.-C., & Han, J.-K. (2002). Xenopus Cdc42 regulates convergent extension movements during gastrulation through Wnt/Ca2+ signaling pathway. *Developmental Biology*, *244*(2), 342–357. https://doi.org/10.1006/dbio.2002.0602

Chomez, P., Neveu, I., Mansén, A., Kiesler, E., Larsson, L., Vennström, B., & Arenas, E. (2000). Increased cell death and delayed development in the cerebellum of mice lacking the rev-erbA(alpha) orphan receptor. *Development (Cambridge, England)*, *127*(7), 1489–1498. https://doi.org/10.1242/dev.127.7.1489

Chow, K. L., Hall, D. H., & Emmons, S. W. (1995). The mab-21 gene of Caenorhabditis elegans encodes a novel protein required for choice of alternate cell fates. *Development*, *121*(11), 3615–3626. https://doi.org/10.1242/dev.121.11.3615

Christodoulou, N., & Skourides, P. A. (2025). Calcium transients regulate the apical emergence of basally located progenitors during Xenopus skin development. *Nature Communications*, *16*(1), 6650. https://doi.org/10.1038/s41467-025-61610-7

Chung, H. A., Hyodo-Miura, J., Nagamune, T., & Ueno, N. (2005). FGF signal regulates gastrulation cell movements and morphology through its target NRH. *Developmental Biology*, *282*(1), 95–110. https://doi.org/10.1016/j.ydbio.2005.02.030

Ciruna, B., Jenny, A., Lee, D., Mlodzik, M., & Schier, A. F. (2006). Planar cell polarity signalling couples cell division and morphogenesis during neurulation. *Nature*, *439*(7073), 220–224. https://doi.org/10.1038/nature04375

Clarke, D. N., & Martin, A. C. (2021). Actin-based force generation and cell adhesion in tissue morphogenesis. *Current Biology*, *31*(10), R667–R680. https://doi.org/10.1016/j.cub.2021.03.031

Cockroft, D. L., Brook, F. A., & Copp, A. J. (1992). Inositol deficiency increases the susceptibility to neural tube defects of genetically predisposed (curly tail) mouse embryos in vitro. *Teratology*, *45*(2), 223–232. https://doi.org/10.1002/tera.1420450216

Cogram, P., Hynes, A., Dunlevy, L. P. E., Greene, N. D. E., & Copp, A. J. (2004). Specific isoforms of protein kinase C are essential for prevention of folate-resistant neural tube defects by inositol. *Human Molecular Genetics*, *13*(1), 7–14. https://doi.org/10.1093/hmg/ddh003

Collinet, C., Rauzi, M., Lenne, P.-F., & Lecuit, T. (2015). Local and tissue-scale forces drive oriented junction growth during tissue extension. *Nature Cell Biology*, *17*(10), 1247–1258. https://doi.org/10.1038/ncb3226

Condic, M. L., Fristrom, D., & Fristrom, J. W. (1991). Apical cell shape changes during Drosophila imaginal leg disc elongation: A novel morphogenetic mechanism. *Development*, *111*(1), 23–33. https://doi.org/10.1242/dev.111.1.23

Cook, S. J., Jarrell, T. A., Brittin, C. A., Wang, Y., Bloniarz, A. E., Yakovlev, M. A., Nguyen, K. C. Q., Tang, L. T.-H., Bayer, E. A., Duerr, J. S., Bülow, H. E., Hobert, O., Hall, D. H., & Emmons, S. W. (2019). Whole-animal connectomes of both Caenorhabditis elegans sexes. *Nature*, *571*(7763), 63–71. https://doi.org/10.1038/s41586-019-1352-7

Copp, A. J., Brook, F. A., & Roberts, H. J. (1988). A cell-type-specific abnormality of cell proliferation in mutant (curly tail) mouse embryos developing spinal neural tube defects. *Development*, *104*(2), 285–295. https://doi.org/10.1242/dev.104.2.285

Cui, C., Chatterjee, B., Lozito, T. P., Zhang, Z., Francis, R. J., Yagi, H., Swanhart, L. M., Sanker, S., Francis, D., Yu, Q., Agustin, J. T. S., Puligilla, C., Chatterjee, T., Tansey, T., Liu, X., Kelley, M. W., Spiliotis, E. T., Kwiatkowski, A. V., Tuan, R., … Lo, C. W. (2013). Wdpcp, a PCP Protein Required for Ciliogenesis, Regulates Directional Cell Migration and Cell Polarity by Direct Modulation of the Actin Cytoskeleton. *PLOS Biology*, *11*(11), e1001720. https://doi.org/10.1371/journal.pbio.1001720

Cunningham, T. J., & Duester, G. (2015). Mechanisms of retinoic acid signalling and its roles in organ and limb development. *Nature Reviews. Molecular Cell Biology*, *16*(2), 110–123. https://doi.org/10.1038/nrm3932

Curtin, J. A., Quint, E., Tsipouri, V., Arkell, R. M., Cattanach, B., Copp, A. J., Henderson, D. J., Spurr, N., Stanier, P., Fisher, E. M., Nolan, P. M., Steel, K. P., Brown, S. D. M., Gray, I. C., & Murdoch, J. N. (2003). Mutation of Celsr1 disrupts planar polarity of inner ear

hair cells and causes severe neural tube defects in the mouse. *Current Biology: CB*, *13*(13), 1129–1133. https://doi.org/10.1016/s0960-9822(03)00374-9

da Silva, S. M., & Vincent, J.-P. (2007). Oriented cell divisions in the extending germband of Drosophila. *Development*, *134*(17), 3049–3054. https://doi.org/10.1242/dev.004911

Davey, C. F., Mathewson, A. W., & Moens, C. B. (2016). PCP Signaling between Migrating Neurons and their Planar-Polarized Neuroepithelial Environment Controls Filopodial Dynamics and Directional Migration. *PLOS Genetics*, *12*(3), e1005934. https://doi.org/10.1371/journal.pgen.1005934

Davidson, L. A., & Keller, R. E. (1999). Neural tube closure in Xenopus laevis involves medial migration, directed protrusive activity, cell intercalation and convergent extension. *Development*, *126*(20), 4547–4556. https://doi.org/10.1242/dev.126.20.4547

Davis, M. B., Jash, E., Chawla, B., Haines, R. A., Tushman, L. E., Troll, R., & Csankovszki, G. (2022). Dual roles for nuclear RNAi Argonautes in Caenorhabditis elegans dosage compensation. *Genetics*, *221*(1), iyac033. https://doi.org/10.1093/genetics/iyac033

De Wals, P., Tairou, F., Van Allen, M. I., Uh, S.-H., Lowry, R. B., Sibbald, B., Evans, J. A., Van den Hof, M. C., Zimmer, P., Crowley, M., Fernandez, B., Lee, N. S., & Niyonsenga, T. (2007). Reduction in neural-tube defects after folic acid fortification in Canada. *The New England Journal of Medicine*, *357*(2), 135–142. https://doi.org/10.1056/NEJMoa067103

Desfougères, Y., Wilson, M. S. C., Laha, D., Miller, G. J., & Saiardi, A. (2019). ITPK1 mediates the lipid-independent synthesis of inositol phosphates controlled by metabolism. *Proceedings of the National Academy of Sciences of the United States of America*, *116*(49), 24551–24561. https://doi.org/10.1073/pnas.1911431116

Devitt, C. C., Weng, S., Bejar-Padilla, V. D., Alvarado, J., & Wallingford, J. B. (2024). PCP and Septins govern the polarized organization of the actin cytoskeleton during convergent extension. *Current Biology : CB*, *34*(3), 615-622.e4. https://doi.org/10.1016/j.cub.2023.12.025

Di Tommaso, P., Moretti, S., Xenarios, I., Orobitg, M., Montanyola, A., Chang, J.-M., Taly, J.-F., & Notredame, C. (2011). T-Coffee: A web server for the multiple sequence alignment of protein and RNA sequences using structural information and homology extension. *Nucleic Acids Research*, *39*(Web Server issue), W13–W17. https://doi.org/10.1093/nar/gkr245

Dickinson, D. J., & Goldstein, B. (2016). CRISPR-Based Methods for Caenorhabditis elegans Genome Engineering. *Genetics*, *202*(3), 885–901. https://doi.org/10.1534/genetics.115.182162

Divekar, N. S., Horton, H. E., & Wignall, S. M. (2021). Methods for rapid protein depletion in C. elegans using auxin-inducible degradation. *Current Protocols*, *1*(2), e16. https://doi.org/10.1002/cpz1.16

Doumpas, N., Lampart, F., Robinson, M. D., Lentini, A., Nestor, C. E., Cantù, C., & Basler, K. (2019). TCF/LEF dependent and independent transcriptional regulation of Wnt/β-catenin target genes. *The EMBO Journal*, *38*(2), e98873. https://doi.org/10.15252/embj.201798873

Driver, E. C., Northrop, A., & Kelley, M. W. (2017). Cell migration, intercalation and growth regulate mammalian cochlear extension. *Development*, *144*(20), 3766–3776. https://doi.org/10.1242/dev.151761

D'Souza, S. W., Copp, A. J., Greene, N. D. E., & Glazier, J. D. (2020). Maternal Inositol Status and Neural Tube Defects: A Role for the Human Yolk Sac in Embryonic Inositol Delivery? *Advances in Nutrition*, *12*(1), 212–222. https://doi.org/10.1093/advances/nmaa100

Duncan, S. A., Nagy, A., & Chan, W. (1997). Murine gastrulation requires HNF-4 regulated gene expression in the visceral endoderm: Tetraploid rescue of Hnf-4−/− embryos. *Development*, *124*(2), 279–287. https://doi.org/10.1242/dev.124.2.279

Dworkin, S., Jane, S. M., & Darido, C. (2011). Planar cell polarity pathway in vertebrate epidermal development, homeostasis and repair. *Organogenesis*, *7*(3), 202–208. https://doi.org/10.4161/org.7.3.18431

Edgar, L. G., Carr, S., Wang, H., & Wood, W. B. (2001). Zygotic Expression of the *caudal* Homolog *pal-1* Is Required for Posterior Patterning in *Caenorhabditis elegans* Embryogenesis. *Developmental Biology*, *229*(1), 71–88. https://doi.org/10.1006/dbio.2000.9977

Emmons, S. W. (2024). Comprehensive analysis of the C. elegans connectome reveals novel circuits and functions of previously unstudied neurons. *PLoS Biology*, *22*(12), e3002939. https://doi.org/10.1371/journal.pbio.3002939

Evans, J. (2018). *A role for Wnt-β-catenin signaling in positioning motor neurons along the ventral nerve cord in C. elegans* (Doctoral dissertation, Université d'Ottawa/University of Ottawa).

Farboud, B., Nix, P., Jow, M. M., Gladden, J. M., & Meyer, B. J. (2013). Molecular antagonism between X-chromosome and autosome signals determines nematode sex. *Genes & Development*, *27*(10), 1159–1178. https://doi.org/10.1101/gad.217026.113

Feng, W., Destain, H., Smith, J. J., & Kratsios, P. (2022). Maintenance of neurotransmitter identity by Hox proteins through a homeostatic mechanism. *Nature Communications*, *13*(1), 6097. https://doi.org/10.1038/s41467-022-33781-0

Fernandez-Gonzalez, R., Simoes, S. de M., Röper, J.-C., Eaton, S., & Zallen, J. A. (2009). Myosin II Dynamics Are Regulated by Tension in Intercalating Cells. *Developmental Cell*, *17*(5), 736–743. https://doi.org/10.1016/j.devcel.2009.09.003

Fischer, E., Legue, E., Doyen, A., Nato, F., Nicolas, J.-F., Torres, V., Yaniv, M., & Pontoglio, M. (2006). Defective planar cell polarity in polycystic kidney disease. *Nature Genetics*, *38*(1), 21–23. https://doi.org/10.1038/ng1701

Fisk, G. J., & Thummel, C. S. (1995). Isolation, regulation, and DNA-binding properties of three Drosophila nuclear hormone receptor superfamily members. *Proceedings of the National Academy of Sciences*, *92*(23), 10604–10608. https://doi.org/10.1073/pnas.92.23.10604

Foley, T. E., Hess, B., Savory, J. G. A., Ringuette, R., & Lohnes, D. (2019). Role of Cdx factors in early mesodermal fate decisions. *Development*, *146*(7), dev170498. https://doi.org/10.1242/dev.170498

Foley, T., & Lohnes, D. (2022). Cdx regulates gene expression through PRC2-mediated epigenetic mechanisms. *Developmental Biology*, *483*, 22–33. https://doi.org/10.1016/j.ydbio.2021.12.014

Folkers, G. E., van der Burg, B., & van der Saag, P. T. (1998). Promoter Architecture, Cofactors, and Orphan Receptors Contribute to Cell-specific Activation of the Retinoic Acid Receptor β2 Promoter*. *Journal of Biological Chemistry*, *273*(48), 32200–32212. https://doi.org/10.1074/jbc.273.48.32200

Fox, R. M., Von Stetina, S. E., Barlow, S. J., Shaffer, C., Olszewski, K. L., Moore, J. H., Dupuy, D., Vidal, M., & Miller, D. M. (2005). A gene expression fingerprint of C. elegans embryonic motor neurons. *BMC Genomics*, *6*, 42. https://doi.org/10.1186/1471-2164-6-42

Frederick, J. P., Mattiske, D., Wofford, J. A., Megosh, L. C., Drake, L. Y., Chiou, S.-T., Hogan, B. L. M., & York, J. D. (2005a). An essential role for an inositol polyphosphate multikinase, Ipk2, in mouse embryogenesis and second messenger production. *Proceedings of the National Academy of Sciences*, *102*(24), 8454–8459. https://doi.org/10.1073/pnas.0503706102

Frederick, J. P., Mattiske, D., Wofford, J. A., Megosh, L. C., Drake, L. Y., Chiou, S.-T., Hogan, B. L. M., & York, J. D. (2005b). An essential role for an inositol polyphosphate multikinase, Ipk2, in mouse embryogenesis and second messenger production. *Proceedings of the National Academy of Sciences*, *102*(24), 8454–8459. https://doi.org/10.1073/pnas.0503706102

Fridy, P. C., Otto, J. C., Dollins, D. E., & York, J. D. (2007). Cloning and Characterization of Two Human *VIP1*-like Inositol Hexakisphosphate and Diphosphoinositol Pentakisphosphate Kinases*. *Journal of Biological Chemistry*, *282*(42), 30754–30762. https://doi.org/10.1074/jbc.M704656200

Fu, C., Xu, J., Cheng, W., Rojas, T., Chin, A. C., Snowman, A. M., Harraz, M. M., & Snyder, S. H. (2017). Neuronal migration is mediated by inositol hexakisphosphate kinase 1 via α-actinin and focal adhesion kinase. *Proceedings of the National Academy of Sciences*, *114*(8), 2036–2041. https://doi.org/10.1073/pnas.1700165114

Gao, Y., & Wang, H. (2007). Inositol pentakisphosphate mediates Wnt/beta-catenin signaling. *The Journal of Biological Chemistry*, *282*(36), 26490–26502. https://doi.org/10.1074/jbc.M702106200

Garcia-Bermejo, M. L., Leskow, F. C., Fujii, T., Wang, Q., Blumberg, P. M., Ohba, M., Kuroki, T., Han, K.-C., Lee, J., Marquez, V. E., & Kazanietz, M. G. (2002). Diacylglycerol (DAG)-lactones, a New Class of Protein Kinase C (PKC) Agonists, Induce Apoptosis in LNCaP Prostate Cancer Cells by Selective Activation of PKCα*. *Journal of Biological Chemistry*, *277*(1), 645–655. https://doi.org/10.1074/jbc.M107639200

George, S. E., Simokat, K., Hardin, J., & Chisholm, A. D. (1998). The VAB-1 Eph receptor tyrosine kinase functions in neural and epithelial morphogenesis in C. elegans. *Cell*, *92*(5), 633–643. https://doi.org/10.1016/s0092-8674(00)81131-9

Gilbert, S. P. R., Mullan, T. W., Poole, R. J., & Woollard, A. (2020). Caudal-dependent cell positioning directs morphogenesis of the *C. elegans* ventral epidermis. *Developmental Biology*, *461*(1), 31–42. https://doi.org/10.1016/j.ydbio.2020.01.001

Giovannone, D., Reyes, M., Reyes, R., Correa, L., Martinez, D., Ra, H., Gomez, G., Kaiser, J., Ma, L., Stein, M.-P., & de Bellard, M. E. (2012). Slits Affect the Timely Migration of Neural Crest Cells via Robo Receptor. *Developmental Dynamics : An Official Publication of the American Association of Anatomists*, *241*(8), 1274–1288. https://doi.org/10.1002/dvdy.23817

Gladden, J. M., Farboud, B., & Meyer, B. J. (2007). Revisiting the X:A Signal That Specifies Caenorhabditis elegans Sexual Fate. *Genetics*, *177*(3), 1639–1654. https://doi.org/10.1534/genetics.107.078071

Gold, D. A., Baek, S. H., Schork, N. J., Rose, D. W., Larsen, D. D., Sachs, B. D., Rosenfeld, M. G., & Hamilton, B. A. (2003). RORα Coordinates Reciprocal Signaling in Cerebellar Development through Sonic hedgehog and Calcium-Dependent Pathways. *Neuron*, *40*(6), 1119–1131. https://doi.org/10.1016/S0896-6273(03)00769-4

González, B., Baños-Sanz, J. I., Villate, M., Brearley, C. A., & Sanz-Aparicio, J. (2010). Inositol 1,3,4,5,6-pentakisphosphate 2-kinase is a distant IPK member with a singular inositide binding site for axial 2-OH recognition. *Proceedings of the National Academy of Sciences*, *107*(21), 9608–9613. https://doi.org/10.1073/pnas.0912979107

Goto, T., & Keller, R. (2002). The Planar Cell Polarity Gene *Strabismus* Regulates Convergence and Extension and Neural Fold Closure in *Xenopus*. *Developmental Biology*, *247*(1), 165–181. https://doi.org/10.1006/dbio.2002.0673

Gredler, M. L., & Zallen, J. A. (2023). Multicellular rosettes link mesenchymal-epithelial transition to radial intercalation in the mouse axial mesoderm. *Developmental Cell*, *58*(11), 933-950.e5. https://doi.org/10.1016/j.devcel.2023.03.018

Green, J., Nusse, R., & van Amerongen, R. (2014). The Role of Ryk and Ror Receptor Tyrosine Kinases in Wnt Signal Transduction. *Cold Spring Harbor Perspectives in Biology*, *6*(2), a009175. https://doi.org/10.1101/cshperspect.a009175

Greene, N. D., & Copp, A. J. (1997). Inositol prevents folate-resistant neural tube defects in the mouse. *Nature Medicine*, *3*(1), 60–66. https://doi.org/10.1038/nm0197-60

Greene, N. D. E., & Copp, A. J. (2014). Neural Tube Defects. *Annual Review of Neuroscience*, *37*, 221–242. https://doi.org/10.1146/annurev-neuro-062012-170354

Greene, N. D. E., Gerrelli, D., Van Straaten, H. W. M., & Copp, A. J. (1998). Abnormalities of floor plate, notochord and somite differentiation in the *loop-tail* (*Lp*) mouse: A model of severe neural tube defects. *Mechanisms of Development*, *73*(1), 59–72. https://doi.org/10.1016/S0925-4773(98)00029-X

Greene, N. D. E., Leung, K., & Copp, A. J. (2017). Inositol, neural tube closure and the prevention of neural tube defects. *Birth Defects Research*, *109*(2), 68–80. https://doi.org/10.1002/bdra.23533

Greene, N. D. E., Stanier, P., & Copp, A. J. (2009). Genetics of human neural tube defects. *Human Molecular Genetics*, *18*(R2), R113–R129. https://doi.org/10.1093/hmg/ddp347

Gu, Y., Mohammad, I. S., & Liu, Z. (2020). Overview of the STAT-3 signaling pathway in cancer and the development of specific inhibitors. *Oncology Letters*, *19*(4), 2585–2594. https://doi.org/10.3892/ol.2020.11394

Guan, Z., Liang, Y., Zhu, Z., Yang, A., Li, S., Wang, X., & Wang, J. (2023). Genetic Effects of ITPK1 Polymorphisms on the Risk of Neural Tube Defects: A Population-Based Study. *Reproductive Sciences (Thousand Oaks, Calif.)*, *30*(5), 1585–1593. https://doi.org/10.1007/s43032-022-01116-5

Guan, Z., Wang, J., Guo, J., Wang, F., Wang, X., Li, G., Xie, Q., Han, X., Niu, B., & Zhang, T. (2014). The Maternal ITPK1 Gene Polymorphism Is Associated with Neural Tube Defects in a High-Risk Chinese Population. *PLoS ONE*, *9*(1), e86145. https://doi.org/10.1371/journal.pone.0086145

Gubb, D., & García-Bellido, A. (1982). A genetic analysis of the determination of cuticular polarity during development in Drosophila melanogaster. *Development*, *68*(1), 37–57. https://doi.org/10.1242/dev.68.1.37

Gur, M., Edri, T., Moody, S. A., & Fainsod, A. (2022). Retinoic Acid is Required for Normal Morphogenetic Movements During Gastrulation. *Frontiers in Cell and Developmental Biology*, *10*. https://doi.org/10.3389/fcell.2022.857230

Gustavsson, P., Greene, N. D. E., Lad, D., Pauws, E., de Castro, S. C. P., Stanier, P., & Copp, A. J. (2007). Increased expression of Grainyhead-like-3 rescues spina bifida in a folate-resistant mouse model. *Human Molecular Genetics*, *16*(21), 2640–2646. https://doi.org/10.1093/hmg/ddm221

Habas, R., Kato, Y., & He, X. (2001). Wnt/Frizzled activation of Rho regulates vertebrate gastrulation and requires a novel Formin homology protein Daam1. *Cell*, *107*(7), 843–854. https://doi.org/10.1016/s0092-8674(01)00614-6

Haigo, S. L., Hildebrand, J. D., Harland, R. M., & Wallingford, J. B. (2003a). Shroom Induces Apical Constriction and Is Required for Hingepoint Formation during Neural Tube Closure. *Current Biology*, *13*(24), 2125–2137. https://doi.org/10.1016/j.cub.2003.11.054

Haigo, S. L., Hildebrand, J. D., Harland, R. M., & Wallingford, J. B. (2003b). Shroom induces apical constriction and is required for hingepoint formation during neural tube closure. *Current Biology: CB*, *13*(24), 2125–2137. https://doi.org/10.1016/j.cub.2003.11.054

Hamblet, N. S., Lijam, N., Ruiz-Lozano, P., Wang, J., Yang, Y., Luo, Z., Mei, L., Chien, K. R., Sussman, D. J., & Wynshaw-Boris, A. (2002). Dishevelled 2 is essential for cardiac outflow tract development, somite segmentation and neural tube closure. *Development (Cambridge, England)*, *129*(24), 5827–5838. https://doi.org/10.1242/dev.00164

Hammond, G. R., & Burke, J. E. (2020). Novel roles of phosphoinositides in signaling, lipid transport, and disease. *Current Opinion in Cell Biology*, *63*, 57–67. https://doi.org/10.1016/j.ceb.2019.12.007

Hanakahi, L. A., Bartlet-Jones, M., Chappell, C., Pappin, D., & West, S. C. (2000). Binding of inositol phosphate to DNA-PK and stimulation of double-strand break repair. *Cell*, *102*(6), 721–729. https://doi.org/10.1016/s0092-8674(00)00061-1

Harding, M. J., McGraw, H. F., & Nechiporuk, A. (2014). The roles and regulation of multicellular rosette structures during morphogenesis. *Development (Cambridge, England)*, *141*(13), 2549–2558. https://doi.org/10.1242/dev.101444

Hayat, R., Manzoor, M., & Hussain, A. (2022). Wnt signaling pathway: A comprehensive review. *Cell Biology International*, *46*(6), 863–877. https://doi.org/10.1002/cbin.11797

Hayes, M., Naito, M., Daulat, A., Angers, S., & Ciruna, B. (2013). Ptk7 promotes non-canonical Wnt/PCP-mediated morphogenesis and inhibits Wnt/β-catenin-dependent cell fate decisions during vertebrate development. *Development*, *140*(8), 1807–1818. https://doi.org/10.1242/dev.090183

Heit, J. J., Apelqvist, A. A., Gu, X., Winslow, M. M., Neilson, J. R., Crabtree, G. R., & Kim, S. K. (2006). Calcineurin/NFAT signalling regulates pancreatic beta-cell growth and function. *Nature*, *443*(7109), 345–349. https://doi.org/10.1038/nature05097

Helsen, C., Kerkhofs, S., Clinckemalie, L., Spans, L., Laurent, M., Boonen, S., Vanderschueren, D., & Claessens, F. (2012). Structural basis for nuclear hormone receptor DNA binding. *Molecular and Cellular Endocrinology*, *348*(2), 411–417. https://doi.org/10.1016/j.mce.2011.07.025

Heydeck, W., & Liu, A. (2011). PCP effector proteins inturned and fuzzy play nonredundant roles in the patterning but not convergent extension of mammalian neural tube. *Developmental Dynamics*, *240*(8), 1938–1948. https://doi.org/10.1002/dvdy.22696

Hierholzer, A., & Kemler, R. (2010). Beta-catenin-mediated signaling and cell adhesion in postgastrulation mouse embryos. *Developmental Dynamics: An Official Publication of the American Association of Anatomists*, *239*(1), 191–199. https://doi.org/10.1002/dvdy.22075

Hildebrand, J. D. (2005). Shroom regulates epithelial cell shape via the apical positioning of an actomyosin network. *Journal of Cell Science*, *118*(22), 5191–5203. https://doi.org/10.1242/jcs.02626

Hildebrand, J. D., & Soriano, P. (1999). Shroom, a PDZ domain-containing actin-binding protein, is required for neural tube morphogenesis in mice. *Cell*, *99*(5), 485–497. https://doi.org/10.1016/s0092-8674(00)81537-8

Hillier, L. W., Coulson, A., Murray, J. I., Bao, Z., Sulston, J. E., & Waterston, R. H. (2005). Genomics in C. elegans: So many genes, such a little worm. *Genome Research*, *15*(12), 1651–1660. https://doi.org/10.1101/gr.3729105

Hopkins, B. D., Goncalves, M. D., & Cantley, L. C. (2020). Insulin–PI3K signalling: An evolutionarily insulated metabolic driver of cancer. *Nature Reviews. Endocrinology*, *16*(5), 276–283. https://doi.org/10.1038/s41574-020-0329-9

Hou, X., Chen, Y., Carrillo, N. D., Cryns, V. L., Anderson, R. A., Sun, J., Wang, S., & Chen, M. (2025). Phosphoinositide signaling at the cytoskeleton in the regulation of cell dynamics. *Cell Death & Disease*, *16*(1), 296. https://doi.org/10.1038/s41419-025-07616-x

Houle, M., Sylvestre, J.-R., & Lohnes, D. (2003). Retinoic acid regulates a subset of Cdx1 function in vivo. *Development*, *130*(26), 6555–6567. https://doi.org/10.1242/dev.00889

Høy, M., Efanov, A. M., Bertorello, A. M., Zaitsev, S. V., Olsen, H. L., Bokvist, K., Leibiger, B., Leibiger, I. B., Zwiller, J., Berggren, P.-O., & Gromada, J. (2002). Inositol hexakisphosphate promotes dynamin I- mediated endocytosis. *Proceedings of the National Academy of Sciences*, *99*(10), 6773–6777. https://doi.org/10.1073/pnas.102157499

Huebner, R. J., & Wallingford, J. B. (2018). Coming to Consensus: A Unifying Model Emerges for Convergent Extension. *Developmental Cell*, *46*(4), 389–396. https://doi.org/10.1016/j.devcel.2018.08.003

Huebner, R. J., Weng, S., Lee, C., Sarıkaya, S., Papoulas, O., Cox, R. M., Marcotte, E. M., & Wallingford, J. B. (2022). ARVCF catenin controls force production during vertebrate convergent extension. *Developmental Cell*, *57*(9), 1119-1131.e5. https://doi.org/10.1016/j.devcel.2022.04.001

Hunter, C. P., & Kenyon, C. (1996). Spatial and Temporal Controls Target pal-1 Blastomere-Specification Activity to a Single Blastomere Lineage in C. elegans Embryos. *Cell*, *87*(2), 217–226. https://doi.org/10.1016/S0092-8674(00)81340-9

Hunter, M. V., & Fernandez-Gonzalez, R. (2017). Coordinating cell movements *in vivo*: Junctional and cytoskeletal dynamics lead the way. *Current Opinion in Cell Biology*, *48*, 54–62. https://doi.org/10.1016/j.ceb.2017.05.005

Ikeda, R., Tsuchiya, Y., Koike, N., Umemura, Y., Inokawa, H., Ono, R., Inoue, M., Sasawaki, Y., Grieten, T., Okubo, N., Ikoma, K., Fujiwara, H., Kubo, T., & Yagita, K. (2019). REV-ERBα and REV-ERBβ function as key factors regulating Mammalian Circadian Output. *Scientific Reports*, *9*(1), 10171. https://doi.org/10.1038/s41598-019-46656-0

Irvine, K. D., & Wieschaus, E. (1994). Cell intercalation during Drosophila germband extension and its regulation by pair-rule segmentation genes. *Development*, *120*(4), 827–841. https://doi.org/10.1242/dev.120.4.827

Jacoby, M., Cox, J. J., Gayral, S., Hampshire, D. J., Ayub, M., Blockmans, M., Pernot, E., Kisseleva, M. V., Compère, P., Schiffmann, S. N., Gergely, F., Riley, J. H., Pérez-Morga, D., Woods, C. G., & Schurmans, S. (2009). INPP5E mutations cause primary cilium signaling defects, ciliary instability and ciliopathies in human and mouse. *Nature Genetics*, *41*(9), 1027–1031. https://doi.org/10.1038/ng.427

Jenny, A., Reynolds-Kenneally, J., Das, G., Burnett, M., & Mlodzik, M. (2005). Diego and Prickle regulate Frizzled planar cell polarity signalling by competing for Dishevelled binding. *Nature Cell Biology*, *7*(7), 691–697. https://doi.org/10.1038/ncb1271

Jorgensen, E. M., & Mango, S. E. (2002). The art and design of genetic screens: Caenorhabditis elegans. *Nature Reviews. Genetics*, *3*(5), 356–369. https://doi.org/10.1038/nrg794

Kam, R. K. T., Shi, W., Chan, S. O., Chen, Y., Xu, G., Lau, C. B.-S., Fung, K. P., Chan, W. Y., & Zhao, H. (2013). Dhrs3 Protein Attenuates Retinoic Acid Signaling and Is Required for Early Embryonic Patterning *. *Journal of Biological Chemistry*, *288*(44), 31477–31487. https://doi.org/10.1074/jbc.M113.514984

Kapral, M., Wawszczyk, J., Jesse, K., Paul-Samojedny, M., Kuśmierz, D., & Węglarz, L. (2017). Inositol Hexaphosphate Inhibits Proliferation and Induces Apoptosis of Colon Cancer Cells by Suppressing the AKT/mTOR Signaling Pathway. *Molecules*, *22*(10), Article 10. https://doi.org/10.3390/molecules22101657

Keller, R. (2002). Shaping the vertebrate body plan by polarized embryonic cell movements. *Science (New York, N.Y.)*, *298*(5600), 1950–1954. https://doi.org/10.1126/science.1079478

Keller, R., Davidson, L. A., & Shook, D. R. (2003). How we are shaped: The biomechanics of gastrulation. *Differentiation*, *71*(3), 171–205. https://doi.org/10.1046/j.1432-0436.2003.710301.x

Keller, R. E., Danilchik, M., Gimlich, R., & Shih, J. (1985). The function and mechanism of convergent extension during gastrulation of Xenopus laevis. *Development*, *89*(Supplement), 185–209. https://doi.org/10.1242/dev.89.supplement.185

Keller, R., & Tibbetts, P. (1989). Mediolateral cell intercalation in the dorsal, axial mesoderm of *Xenopus laevis*. *Developmental Biology*, *131*(2), 539–549. https://doi.org/10.1016/S0012-1606(89)80024-7

Kerk, S. Y., Kratsios, P., Hart, M., Mourao, R., & Hobert, O. (2017). Diversification of C. elegans motor neuron identity via selective effector gene repression. *Neuron*, *93*(1), 80–98. https://doi.org/10.1016/j.neuron.2016.11.036

Khayat, Z. A., Tong, P., Yaworsky, K., Bloch, R. J., & Klip, A. (2000). Insulin-induced actin filament remodeling colocalizes actin with phosphatidylinositol 3-kinase and GLUT4 in L6 myotubes. *Journal of Cell Science*, *113*(2), 279–290. https://doi.org/10.1242/jcs.113.2.279

Kida, Y. S., Sato, T., Miyasaka, K. Y., Suto, A., & Ogura, T. (2007). Daam1 regulates the endocytosis of EphB during the convergent extension of the zebrafish notochord. *Proceedings of the National Academy of Sciences of the United States of America*, *104*(16), 6708–6713. https://doi.org/10.1073/pnas.0608946104

Kim, H. Y., & Davidson, L. A. (2011). Punctuated actin contractions during convergent extension and their permissive regulation by the non-canonical Wnt-signaling pathway. *Journal of Cell Science*, *124*(4), 635–646. https://doi.org/10.1242/jcs.067579

Kim, S., Bhandari, R., Brearley, C. A., & Saiardi, A. (2024). The inositol phosphate signalling network in physiology and disease. *Trends in Biochemical Sciences*, *49*(11), 969–985. https://doi.org/10.1016/j.tibs.2024.08.005

Kinoshita, T., & Fujita, M. (2016). Biosynthesis of GPI-anchored proteins: Special emphasis on GPI lipid remodeling. *Journal of Lipid Research*, *57*(1), 6–24. https://doi.org/10.1194/jlr.R063313

Koch, K., Schlüppmann, K., Hüsken, S., Stark, L. M., Förster, N., Masjosthusmann, S., Klose, J., Dönmez, A., & Fritsche, E. (2025). Nuclear hormone receptors control fundamental processes of human fetal neurodevelopment: Basis for endocrine disruption assessment. *Environment International*, *198*, 109400. https://doi.org/10.1016/j.envint.2025.109400

Kong, D., Wolf, F., & Großhans, J. (2017). Forces directing germ-band extension in *Drosophila* embryos. *Mechanisms of Development*, *144*, 11–22. https://doi.org/10.1016/j.mod.2016.12.001

Kostrouchova, M., & Kostrouch, Z. (2015). Nuclear receptors in nematode development: Natural experiments made by a phylum. *Biochimica et Biophysica Acta (BBA) - Gene Regulatory Mechanisms*, *1849*(2), 224–237. https://doi.org/10.1016/j.bbagrm.2014.06.016

Kraft, B., Berger, C. D., Wallkamm, V., Steinbeisser, H., & Wedlich, D. (2012). Wnt-11 and Fz7 reduce cell adhesion in convergent extension by sequestration of PAPC and C-cadherin. *The Journal of Cell Biology*, *198*(4), 695–709. https://doi.org/10.1083/jcb.201110076

Kühl, M., Geis, K., Sheldahl, L. C., Pukrop, T., Moon, R. T., & Wedlich, D. (2001). Antagonistic regulation of convergent extension movements in Xenopus by Wnt/beta-catenin and Wnt/Ca2+ signaling. *Mechanisms of Development*, *106*(1–2), 61–76. https://doi.org/10.1016/s0925-4773(01)00416-6

Kumar, V., Sinha, A. K., Makkar, H. P. S., & Becker, K. (2010). Dietary roles of phytate and phytase in human nutrition: A review. *Food Chemistry*, *120*(4), 945–959. https://doi.org/10.1016/j.foodchem.2009.11.052

Lee, C., Le, M.-P., & Wallingford, J. B. (2009). The Shroom family proteins play broad roles in the morphogenesis of thickened epithelial sheets. *Developmental Dynamics : An Official Publication of the American Association of Anatomists*, *238*(6), 1480–1491. https://doi.org/10.1002/dvdy.21942

Lee, H. C., Oliveira, N. M. M., & Stern, C. D. (2022). Exploring the roles of FGF/MAPK and cVG1/GDF signalling on mesendoderm induction and convergent extension during chick primitive streak formation. *Development Genes and Evolution*, *232*(5–6), 115–123. https://doi.org/10.1007/s00427-022-00696-1

Lee*, J. W., Lee, Y. C., Na**, S.-Y., Jung, D.-J., & Lee***, S.-K. (2001). Transcriptional coregulators of the nuclear receptor superfamily: Coactivators and corepressors. *Cellular and Molecular Life Sciences CMLS*, *58*(2), 289–297. https://doi.org/10.1007/PL00000856

Lee, S., & Gleeson, J. G. (2020). Closing In on Mechanisms of Open Neural Tube Defects. *Trends in Neurosciences*, *43*(7), 519–532. https://doi.org/10.1016/j.tins.2020.04.009

Lefebvre, B., Ozato, K., & Lefebvre, P. (2002). Phosphorylation of histone H3 is functionally linked to retinoic acid receptor β promoter activation. *EMBO Reports*, *3*(4), 335–340. https://doi.org/10.1093/embo-reports/kvf066

Lehrbach, N. J., Ji, F., & Sadreyev, R. (2017). Next-generation sequencing for identification of EMS-induced mutations in Caenorhabditis elegans. *Current Protocols in Molecular Biology*, *117*, 7.29.1-7.29.12. https://doi.org/10.1002/cpmb.27

Lei, Y., Kim, S., Chen, Z., Cao, X., Zhu, H., Yang, W., Shaw, G. M., Zheng, Y., Zhang, T., Wang, H., & Finnell, R. H. (2019). Variants identified in PTK7 associated with neural tube defects. *Molecular Genetics & Genomic Medicine*, *7*(4), e00584. https://doi.org/10.1002/mgg3.584

Leroy, P., Krust, A., Zelent, A., Mendelsohn, C., Garnier, J. M., Kastner, P., Dierich, A., & Chambon, P. (1991). Multiple isoforms of the mouse retinoic acid receptor alpha are generated by alternative splicing and differential induction by retinoic acid. *The EMBO Journal*, *10*(1), 59–69. https://doi.org/10.1002/j.1460-2075.1991.tb07921.x

Lesko, A. C., Keller, R., Chen, P., & Sutherland, A. (2021). Scribble mutation disrupts convergent extension and apical constriction during mammalian neural tube closure. *Developmental Biology*, *478*, 59–75. https://doi.org/10.1016/j.ydbio.2021.05.013

Letcher, A. J., Schell, M. J., & Irvine, R. F. (2008). Do mammals make all their own inositol hexakisphosphate? *Biochemical Journal*, *416*(2), 263–270. https://doi.org/10.1042/BJ20081417

Leung, K.-Y., Weston, E., De Castro, S. C. P., Nikolopoulou, E., Sudiwala, S., Savery, D., Eaton, S., Copp, A. J., & Greene, N. D. E. (2024). Association of embryonic inositol status with susceptibility to neural tube defects, metabolite profile, and maternal inositol intake. *FASEB Journal: Official Publication of the Federation of American Societies for Experimental Biology*, *38*(11), e23738. https://doi.org/10.1096/fj.202400206R

Li, H., Datunashvili, M., Reyes, R. C., & Voglmaier, S. M. (2022). Inositol hexakisphosphate kinases differentially regulate trafficking of vesicular glutamate transporters 1 and 2. *Frontiers in Cellular Neuroscience*, *16*. https://doi.org/10.3389/fncel.2022.926794

Li, V. S. W., Ng, S. S., Boersema, P. J., Low, T. Y., Karthaus, W. R., Gerlach, J. P., Mohammed, S., Heck, A. J. R., Maurice, M. M., Mahmoudi, T., & Clevers, H. (2012). Wnt signaling through inhibition of β-catenin degradation in an intact Axin1 complex. *Cell*, *149*(6), 1245–1256. https://doi.org/10.1016/j.cell.2012.05.002

Lien, J.-C., & Wang, Y. (2023). Cyclic stretching combined with cell-cell adhesion is sufficient for inducing cell intercalation. *Biophysical Journal*, *122*(15), 3146–3158. https://doi.org/10.1016/j.bpj.2023.06.019

Lienkamp, S. S., Liu, K., Karner, C. M., Carroll, T. J., Ronneberger, O., Wallingford, J. B., & Walz, G. (2012). Vertebrate kidney tubules elongate using a planar cell polarity-dependent, rosette-based mechanism of convergent extension. *Nature Genetics*, *44*(12), 1382–1387. https://doi.org/10.1038/ng.2452

Lindqvist, M., Horn, Z., Bryja, V., Schulte, G., Papachristou, P., Ajima, R., Dyberg, C., Arenas, E., Yamaguchi, T. P., Lagercrantz, H., & Ringstedt, T. (2010). Vang-like protein 2 and Rac1 interact to regulate adherens junctions. *Journal of Cell Science*, *123*(3), 472–483. https://doi.org/10.1242/jcs.048074

Liu, J., Xiao, Q., Xiao, J., Niu, C., Li, Y., Zhang, X., Zhou, Z., Shu, G., & Yin, G. (2022). Wnt/β-catenin signalling: Function, biological mechanisms, and therapeutic opportunities. *Signal Transduction and Targeted Therapy*, *7*(1), 3. https://doi.org/10.1038/s41392-021-00762-6

Liu, W., Xiu, L., Zhou, M., Li, T., Jiang, N., Wan, Y., Qiu, C., Li, J., Hu, W., Zhang, W., & Wu, J. (2024). The Critical Role of the Shroom Family Proteins in Morphogenesis, Organogenesis and Disease. *Phenomics*, *4*(2), 187–202. https://doi.org/10.1007/s43657-023-00119-9

Liu, Y., Sepich, D. S., & Solnica-Krezel, L. (2017). Stat3/Cdc25a-dependent cell proliferation promotes embryonic axis extension during zebrafish gastrulation. *PLoS Genetics*, *13*(2), e1006564. https://doi.org/10.1371/journal.pgen.1006564

Loss, O., Wu, C. T., Riccio, A., & Saiardi, A. (2013). Modulation of inositol polyphosphate levels regulates neuronal differentiation. *Molecular Biology of the Cell*, *24*(18), 2981–2989. https://doi.org/10.1091/mbc.E13-04-0198

Lowry, J., Yochem, J., Chuang, C.-H., Sugioka, K., Connolly, A. A., & Bowerman, B. (2015). High-Throughput Cloning of Temperature-Sensitive Caenorhabditis elegans Mutants

with Adult Syncytial Germline Membrane Architecture Defects. *G3: Genes|Genomes|Genetics*, *5*(11), 2241–2255. https://doi.org/10.1534/g3.115.021451

Ludewig, A. H., Gimond, C., Judkins, J. C., Thornton, S., Pulido, D. C., Micikas, R. J., Döring, F., Antebi, A., Braendle, C., & Schroeder, F. C. (2017). Larval crowding accelerates C. elegans development and reduces lifespan. *PLOS Genetics*, *13*(4), e1006717. https://doi.org/10.1371/journal.pgen.1006717

Lukacs, M., Roberts, T., Chatuverdi, P., & Stottmann, R. W. (n.d.). Glycosylphosphatidylinositol biosynthesis and remodeling are required for neural tube closure, heart development, and cranial neural crest cell survival. *eLife*, *8*, e45248. https://doi.org/10.7554/eLife.45248

Lye, C. M., Blanchard, G. B., Naylor, H. W., Muresan, L., Huisken, J., Adams, R. J., & Sanson, B. (2015). Mechanical Coupling between Endoderm Invagination and Axis Extension in Drosophila. *PLOS Biology*, *13*(11), e1002292. https://doi.org/10.1371/journal.pbio.1002292

Maag, D., Maxwell, M. J., Hardesty, D. A., Boucher, K. L., Choudhari, N., Hanno, A. G., Ma, J. F., Snowman, A. S., Pietropaoli, J. W., Xu, R., Storm, P. B., Saiardi, A., Snyder, S. H., & Resnick, A. C. (2011). Inositol polyphosphate multikinase is a physiologic PI3-kinase that activates Akt/PKB. *Proceedings of the National Academy of Sciences of the United States of America*, *108*(4), 1391–1396. https://doi.org/10.1073/pnas.1017831108

MacKenzie, T. M. G., Cisneros, R., Maynard, R. D., & Snyder, M. P. (2023). Reverse-ChIP Techniques for Identifying Locus-Specific Proteomes: A Key Tool in Unlocking the Cancer Regulome. *Cells*, *12*(14), Article 14. https://doi.org/10.3390/cells12141860

Maduro, M. F. (2010). Cell fate specification in the C. elegans embryo. *Developmental Dynamics*, *239*(5), 1315–1329. https://doi.org/10.1002/dvdy.22233

Maduro, M. F., Kasmir, J. J., Zhu, J., & Rothman, J. H. (2005). The Wnt effector POP-1 and the PAL-1/Caudal homeoprotein collaborate with SKN-1 to activate C. elegans endoderm development. *Developmental Biology*, *285*(2), 510–523. https://doi.org/10.1016/j.ydbio.2005.06.022

Mahony, S., Mazzoni, E. O., McCuine, S., Young, R. A., Wichterle, H., & Gifford, D. K. (2011). Ligand-dependent dynamics of retinoic acid receptor binding during early neurogenesis. *Genome Biology*, *12*(1), R2. https://doi.org/10.1186/gb-2011-12-1-r2

Mainpal, R., Priti, A., & Subramaniam, K. (2011). PUF-8 suppresses the somatic transcription factor PAL-1 expression in *C. elegans* germline stem cells. *Developmental Biology*, *360*(1), 195–207. https://doi.org/10.1016/j.ydbio.2011.09.021

Majeed, M., Liao, C.-P., & Hobert, O. (2025). Nervous system–wide analysis of all C. elegans cadherins reveals neuron-specific functions across multiple anatomical scales. *Science Advances*, *11*(8), eads2852. https://doi.org/10.1126/sciadv.ads2852

Marcum, R. D., & Radhakrishnan, I. (2019). Inositol phosphates and core subunits of the Sin3L/Rpd3L histone deacetylase (HDAC) complex up-regulate deacetylase activity. *Journal of Biological Chemistry*, *294*(38), 13928–13938. https://doi.org/10.1074/jbc.RA119.009780

Marlow, F., Topczewski, J., Sepich, D., & Solnica-Krezel, L. (2002). Zebrafish Rho kinase 2 acts downstream of Wnt11 to mediate cell polarity and effective convergence and extension movements. *Current Biology: CB*, *12*(11), 876–884. https://doi.org/10.1016/s0960-9822(02)00864-3

Márquez-Moñino, M. Á., Ortega-García, R., Whitfield, H., Riley, A. M., Infantes, L., Garrett, S. W., Shipton, M. L., Brearley, C. A., Potter, B. V. L., & González, B. (2024). Substrate promiscuity of inositol 1,4,5-trisphosphate kinase driven by structurally-modified ligands and active site plasticity. *Nature Communications*, *15*(1), 1502. https://doi.org/10.1038/s41467-024-45917-5

Martin, A. C., Kaschube, M., & Wieschaus, E. F. (2009). Pulsed actin-myosin network contractions drive apical constriction. *Nature*, *457*(7228), 495. https://doi.org/10.1038/nature07522

McGreevy, E. M., Vijayraghavan, D., Davidson, L. A., & Hildebrand, J. D. (2015). Shroom3 functions downstream of planar cell polarity to regulate myosin II distribution and cellular organization during neural tube closure. *Biology Open*, *4*(2), 186–196. https://doi.org/10.1242/bio.20149589

McQuate, A., Latorre-Esteves, E., & Barria, A. (2017). A Wnt/Calcium Signaling Cascade Regulates Neuronal Excitability and Trafficking of NMDARs. *Cell Reports*, *21*(1), 60–69. https://doi.org/10.1016/j.celrep.2017.09.023

Menniti, F. S., Miller, R. N., Putney, J. W., & Shears, S. B. (1993). Turnover of inositol polyphosphate pyrophosphates in pancreatoma cells. *Journal of Biological Chemistry*, *268*(6), 3850–3856. https://doi.org/10.1016/S0021-9258(18)53551-1

Meyer, B. I., & Gruss, P. (1993). Mouse Cdx-1 expression during gastrulation. *Development*, *117*(1), 191–203. https://doi.org/10.1242/dev.117.1.191

Miao, H., Vanderleest, T. E., Budhathoki, R., Loerke, D., & Blankenship, J. T. (2021). A PtdIns(3,4,5)P3 dispersal switch engages cell ratcheting at specific cell surfaces. *Developmental Cell*, *56*(18), 2579-2591.e4. https://doi.org/10.1016/j.devcel.2021.08.016

Mic, F. A., Haselbeck, R. J., Cuenca, A. E., & Duester, G. (2002). Novel retinoic acid generating activities in the neural tube and heart identified by conditional rescue of Raldh2 null mutant mice. *Development*, *129*(9), 2271–2282. https://doi.org/10.1242/dev.129.9.2271

Mitchell, B., Stubbs, J. L., Huisman, F., Taborek, P., Yu, C., & Kintner, C. (2009). The PCP pathway instructs the planar orientation of ciliated cells in the Xenopus larval skin. *Current Biology: CB*, *19*(11), 924–929. https://doi.org/10.1016/j.cub.2009.04.018

Miyabayashi, T., Palfreyman, M. T., Sluder, A. E., Slack, F., & Sengupta, P. (1999). Expression and Function of Members of a Divergent Nuclear Receptor Family in Caenorhabditis elegans. *Developmental Biology*, *215*(2), 314–331. https://doi.org/10.1006/dbio.1999.9470

Miyagi, C., Yamashita, S., Ohba, Y., Yoshizaki, H., Matsuda, M., & Hirano, T. (2004). STAT3 noncell-autonomously controls planar cell polarity during zebrafish convergence and extension. *The Journal of Cell Biology*, *166*(7), 975–981. https://doi.org/10.1083/jcb.200403110

Miyakawa, T., Mizushima, A., Hirose, K., Yamazawa, T., Bezprozvanny, I., Kurosaki, T., & Iino, M. (2001). Ca2+-sensor region of IP3 receptor controls intracellular Ca2+ signaling. *The EMBO Journal*, *20*(7), 1674–1680. https://doi.org/10.1093/emboj/20.7.1674

Montcouquiol, M., Rachel, R. A., Lanford, P. J., Copeland, N. G., Jenkins, N. A., & Kelley, M. W. (2003). Identification of Vangl2 and Scrb1 as planar polarity genes in mammals. *Nature*, *423*(6936), 173–177. https://doi.org/10.1038/nature01618

Montell, D. J., Yoon, W. H., & Starz-Gaiano, M. (2012). Group choreography: Mechanisms orchestrating the collective movement of border cells. *Nature Reviews. Molecular Cell Biology*, *13*(10), 631–645. https://doi.org/10.1038/nrm3433

Montero, J.-A., Kilian, B., Chan, J., Bayliss, P. E., & Heisenberg, C.-P. (2003). Phosphoinositide 3-kinase is required for process outgrowth and cell polarization of gastrulating mesendodermal cells. *Current Biology: CB*, *13*(15), 1279–1289. https://doi.org/10.1016/s0960-9822(03)00505-0

Mootz, D., Ho, D. M., & Hunter, C. P. (2004). The STAR/Maxi-KH domain protein GLD-1 mediates a developmental switch in the translational control of C. elegans PAL-1. *Development*, *131*(14), 3263–3272. https://doi.org/10.1242/dev.01196

Mound, A., Vautrin-Glabik, A., Foulon, A., Botia, B., Hague, F., Parys, J. B., Ouadid-Ahidouch, H., & Rodat-Despoix, L. (2017). Downregulation of type 3 inositol (1,4,5)-trisphosphate receptor decreases breast cancer cell migration through an oscillatory Ca2+ signal. *Oncotarget*, *8*(42), 72324–72341. https://doi.org/10.18632/oncotarget.20327

Mukherjee, A., Dhar, N., Stathos, M., Schaffer, D. V., & Kane, R. S. (2018). Understanding how Wnt Influences Destruction Complex Activity and β-Catenin Dynamics. *iScience*, *6*, 13–21. https://doi.org/10.1016/j.isci.2018.07.007

Mukherjee, S., Luedeke, D. M., McCoy, L., Iwafuchi, M., & Zorn, A. M. (2022). SOX transcription factors direct TCF-independent WNT/β-catenin responsive transcription to govern cell fate in human pluripotent stem cells. *Cell Reports*, *40*(8). https://doi.org/10.1016/j.celrep.2022.111247

Mulcahy, B., Witvliet, D. K., Mitchell, J., Schalek, R., Berger, D. R., Wu, Y., Holmyard, D., Lu, Y., Ahamed, T., Samuel, A. D. T., Chisholm, A. D., Lichtman, J. W., & Zhen, M. (2022). Post-embryonic remodeling of the C. elegans motor circuit. *Current Biology*, *32*(21), 4645-4659.e3. https://doi.org/10.1016/j.cub.2022.09.065

Munjal, A., Philippe, J.-M., Munro, E., & Lecuit, T. (2015). A self-organized biomechanical network drives shape changes during tissue morphogenesis. *Nature*, *524*(7565), 351–355. https://doi.org/10.1038/nature14603

Murdoch, J. N., Damrau, C., Paudyal, A., Bogani, D., Wells, S., Greene, N. D. E., Stanier, P., & Copp, A. J. (2014). Genetic interactions between planar cell polarity genes cause diverse neural tube defects in mice. *Disease Models & Mechanisms*, *7*(10), 1153–1163. https://doi.org/10.1242/dmm.016758

Murdoch, J. N., Henderson, D. J., Doudney, K., Gaston-Massuet, C., Phillips, H. M., Paternotte, C., Arkell, R., Stanier, P., & Copp, A. J. (2003). Disruption of scribble (Scrb1) causes severe neural tube defects in the circletail mouse. *Human Molecular Genetics*, *12*(2), 87–98. https://doi.org/10.1093/hmg/ddg014

Myers, D. C., Sepich, D. S., & Solnica-Krezel, L. (2002). Bmp activity gradient regulates convergent extension during zebrafish gastrulation. *Developmental Biology*, *243*(1), 81–98. https://doi.org/10.1006/dbio.2001.0523

Neumann, N. M., Perrone, M. C., Veldhuis, J. H., Huebner, R. J., Zhan, H., Devreotes, P. N., Brodland, G. W., & Ewald, A. J. (2018). Coordination of receptor tyrosine kinase signaling and interfacial tension dynamics drive radial intercalation and tube elongation. *Developmental Cell*, *45*(1), 67-82.e6. https://doi.org/10.1016/j.devcel.2018.03.011

Nguyen Trung, M., Kieninger, S., Fandi, Z., Qiu, D., Liu, G., Mehendale, N. K., Saiardi, A., Jessen, H., Keller, B., & Fiedler, D. (2022). Stable Isotopomers of myo-Inositol Uncover a Complex MINPP1-Dependent Inositol Phosphate Network. *ACS Central Science*, *8*(12), 1683–1694. https://doi.org/10.1021/acscentsci.2c01032

Nikolopoulou, E., Galea, G. L., Rolo, A., Greene, N. D. E., & Copp, A. J. (2017). Neural tube closure: Cellular, molecular and biomechanical mechanisms. *Development (Cambridge, England)*, *144*(4), 552–566. https://doi.org/10.1242/dev.145904

Nishimura, T., Honda, H., & Takeichi, M. (2012). Planar Cell Polarity Links Axes of Spatial Dynamics in Neural-Tube Closure. *Cell*, *149*(5), 1084–1097. https://doi.org/10.1016/j.cell.2012.04.021

Nishimura, T., & Takeichi, M. (2008). Shroom3-mediated recruitment of Rho kinases to the apical cell junctions regulates epithelial and neuroepithelial planar remodeling. *Development (Cambridge, England)*, *135*(8), 1493–1502. https://doi.org/10.1242/dev.019646

Norris, F. A., Ungewickell, E., & Majerus, P. W. (1995). Inositol Hexakisphosphate Binds to Clathrin Assembly Protein 3 (AP-3/AP180) and Inhibits Clathrin Cage Assembly in Vitro(∗). *Journal of Biological Chemistry*, *270*(1), 214–217. https://doi.org/10.1074/jbc.270.1.214

Notredame, C., Higgins, D. G., & Heringa, J. (2000). T-coffee: A novel method for fast and accurate multiple sequence alignment1. *Journal of Molecular Biology*, *302*(1), 205–217. https://doi.org/10.1006/jmbi.2000.4042

Nutt, S. L., Dingwell, K. S., Holt, C. E., & Amaya, E. (2001). Xenopus Sprouty2 inhibits FGF-mediated gastrulation movements but does not affect mesoderm induction and patterning. *Genes & Development*, *15*(9), 1152–1166. https://doi.org/10.1101/gad.191301

Nychyk, O., Galea, G. L., Molè, M., Savery, D., Greene, N. D. E., Stanier, P., & Copp, A. J. (2022). Vangl2-environment interaction causes severe neural tube defects, without abnormal neuroepithelial convergent extension. *Disease Models & Mechanisms*, *15*(1), dmm049194. https://doi.org/10.1242/dmm.049194

Ohkawara, B., Yamamoto, T. S., Tada, M., & Ueno, N. (2003). Role of glypican 4 in the regulation of convergent extension movements during gastrulation in Xenopus laevis. *Development (Cambridge, England)*, *130*(10), 2129–2138. https://doi.org/10.1242/dev.00435

Olivares, E., Izquierdo, E. J., & Beer, R. D. (2021). A Neuromechanical Model of Multiple Network Rhythmic Pattern Generators for Forward Locomotion in C. elegans. *Frontiers in Computational Neuroscience*, *15*, 572339. https://doi.org/10.3389/fncom.2021.572339

Onai, T., Lin, H.-C., Schubert, M., Koop, D., Osborne, P. W., Alvarez, S., Alvarez, R., Holland, N. D., & Holland, L. Z. (2009). Retinoic acid and Wnt/β-catenin have complementary roles in anterior/posterior patterning embryos of the basal chordate amphioxus. *Developmental Biology*, *332*(2), 223–233. https://doi.org/10.1016/j.ydbio.2009.05.571

Ossipova, O., Chu, C.-W., Fillatre, J., Brott, B. K., Itoh, K., & Sokol, S. Y. (2015). The involvement of PCP proteins in radial cell intercalations during Xenopus embryonic development. *Developmental Biology*, *408*(2), 316–327. https://doi.org/10.1016/j.ydbio.2015.06.013

Otto, J. C., Kelly, P., Chiou, S.-T., & York, J. D. (2007). Alterations in an inositol phosphate code through synergistic activation of a G protein and inositol phosphate kinases. *Proceedings of the National Academy of Sciences of the United States of America*, *104*(40), 15653–15658. https://doi.org/10.1073/pnas.0705729104

Packer, J. S., Zhu, Q., Huynh, C., Sivaramakrishnan, P., Preston, E., Dueck, H., Stefanik, D., Tan, K., Trapnell, C., Kim, J., Waterston, R. H., & Murray, J. I. (2019). A lineage-resolved molecular atlas of C. elegans embryogenesis at single-cell resolution. *Science*, *365*(6459), eaax1971. https://doi.org/10.1126/science.aax1971

Paré, A. C., Vichas, A., Fincher, C. T., Mirman, Z., Farrell, D. L., Mainieri, A., & Zallen, J. A. (2014). A positional Toll receptor code directs convergent extension in Drosophila. *Nature*, *515*(7528), 523–527. https://doi.org/10.1038/nature13953

Paulson, A. F., Mooney, E., Fang, X., Ji, H., & McCrea, P. D. (2000). Xarvcf, *Xenopus* Member of the p120 Catenin Subfamily Associating with Cadherin Juxtamembrane Region*. *Journal of Biological Chemistry*, *275*(39), 30124–30131. https://doi.org/10.1074/jbc.M003048200

Piedrahita, J. A., Oetama, B., Bennett, G. D., van Waes, J., Kamen, B. A., Richardson, J., Lacey, S. W., Anderson, R. G., & Finnell, R. H. (1999). Mice lacking the folic acid-binding protein Folbp1 are defective in early embryonic development. *Nature Genetics*, *23*(2), 228–232. https://doi.org/10.1038/13861

Pocock, R., Ahringer, J., Mitsch, M., Maxwell, S., & Woollard, A. (2004). A regulatory network of T-box genes and the even-skippedhomologue vab-7 controls patterning and morphogenesis in C. elegans. *Development*, *131*(10), 2373–2385. https://doi.org/10.1242/dev.01110

Politi, A., Gaspers, L. D., Thomas, A. P., & Höfer, T. (2006). Models of IP3 and Ca2+ Oscillations: Frequency Encoding and Identification of Underlying Feedbacks. *Biophysical Journal*, *90*(9), 3120–3133. https://doi.org/10.1529/biophysj.105.072249

Poole, R. J., Flames, N., & Cochella, L. (2024). Neurogenesis in Caenorhabditis elegans. *Genetics*, *228*(2), iyae116. https://doi.org/10.1093/genetics/iyae116

Pukrop, T., Gradl, D., Henningfeld, K. A., Knöchel, W., Wedlich, D., & Kühl, M. (2001). Identification of Two Regulatory Elements within the High Mobility Group Box Transcription Factor XTCF-4 *. *Journal of Biological Chemistry*, *276*(12), 8968–8978. https://doi.org/10.1074/jbc.M007533200

Pyrgaki, C., Liu, A., & Niswander, L. (2011). *Grainyhead-like 2* regulates neural tube closure and adhesion molecule expression during neural fold fusion. *Developmental Biology*, *353*(1), 38–49. https://doi.org/10.1016/j.ydbio.2011.02.027

Qin, K., Yu, M., Fan, J., Wang, H., Zhao, P., Zhao, G., Zeng, W., Chen, C., Wang, Y., Wang, A., Schwartz, Z., Hong, J., Song, L., Wagstaff, W., Haydon, R. C., Luu, H. H., Ho, S. H., Strelzow, J., Reid, R. R., … Shi, L. L. (2023). Canonical and noncanonical Wnt signaling: Multilayered mediators, signaling mechanisms and major signaling crosstalk. *Genes & Diseases*, *11*(1), 103–134. https://doi.org/10.1016/j.gendis.2023.01.030

Qiu, D., Wilson, M. S., Eisenbeis, V. B., Harmel, R. K., Riemer, E., Haas, T. M., Wittwer, C., Jork, N., Gu, C., Shears, S. B., Schaaf, G., Kammerer, B., Fiedler, D., Saiardi, A., & Jessen, H. J. (2020). Analysis of inositol phosphate metabolism by capillary electrophoresis electrospray ionization mass spectrometry. *Nature Communications*, *11*(1), 6035. https://doi.org/10.1038/s41467-020-19928-x

Rameh, L. E., York, J. D., & Blind, R. D. (2025). Inositol phosphates dynamically enhance stability, solubility, and catalytic activity of mTOR. *Journal of Biological Chemistry*, *301*(2). https://doi.org/10.1016/j.jbc.2024.108095

Range, R. C., Angerer, R. C., & Angerer, L. M. (2013). Integration of Canonical and Noncanonical Wnt Signaling Pathways Patterns the Neuroectoderm Along the Anterior–Posterior Axis of Sea Urchin Embryos. *PLOS Biology*, *11*(1), e1001467. https://doi.org/10.1371/journal.pbio.1001467

Rao, F., Xu, J., Fu, C., Cha, J. Y., Gadalla, M. M., Xu, R., Barrow, J. C., & Snyder, S. H. (2015). Inositol pyrophosphates promote tumor growth and metastasis by antagonizing liver kinase B1. *Proceedings of the National Academy of Sciences of the United States of America*, *112*(6), 1773–1778. https://doi.org/10.1073/pnas.1424642112

Rastinejad, F., Huang, P., Chandra, V., & Khorasanizadeh, S. (2013). Understanding Nuclear Receptor Form and Function Using Structural Biology. *Journal of Molecular Endocrinology*, *51*(3), T1–T21. https://doi.org/10.1530/JME-13-0173

Ren, Q., Chen, J., & Liu, Y. (2021). LRP5 and LRP6 in Wnt Signaling: Similarity and Divergence. *Frontiers in Cell and Developmental Biology*, *9*, 670960. https://doi.org/10.3389/fcell.2021.670960

Rochard, L., Monica, S. D., Ling, I. T. C., Kong, Y., Roberson, S., Harland, R., Halpern, M., & Liao, E. C. (2016). Roles of Wnt pathway genes wls, wnt9a, wnt5b, frzb and gpc4 in regulating convergent-extension during zebrafish palate morphogenesis. *Development*, *143*(14), 2541–2547. https://doi.org/10.1242/dev.137000

Rojas, T., Cheng, W., Gao, Z., Liu, X., Wang, Y., Malla, A. P., Chin, A. C., Romer, L. H., Snyder, S. H., & Fu, C. (2019). Inositol hexakisphosphate kinase 3 promotes focal adhesion turnover via interactions with dynein intermediate chain 2. *Proceedings of the National Academy of Sciences of the United States of America*, *116*(8), 3278–3287. https://doi.org/10.1073/pnas.1817001116

Saharkhiz S, Chan W, Kirezi CB, Petite M, Roenspies T, Perkins TJ, et al. (2025) VNC-Dist: A machine learning-based semi-automated pipeline for quantification of neuronal position in the *C. elegans* ventral nerve cord. PLoS One 20(8): e0331188. https://doi.org/10.1371/journal.pone.0331188

Saraswathy, V. M., Kurup, A. J., Sharma, P., Polès, S., Poulain, M., & Fürthauer, M. (2022). The E3 ubiquitin ligase mindbomb1 controls planar cell polarity-dependent convergent extension movements during zebrafish gastrulation. *eLife*, *11*, e71928. https://doi.org/10.7554/eLife.71928

Sarmah, B., Winfrey, V. P., Olson, G. E., Appel, B., & Wente, S. R. (2007). A role for the inositol kinase Ipk1 in ciliary beating and length maintenance. *Proceedings of the National Academy of Sciences*, *104*(50), 19843–19848. https://doi.org/10.1073/pnas.0706934104

Sato, A., Yamamoto, H., Sakane, H., Koyama, H., & Kikuchi, A. (2010). Wnt5a regulates distinct signalling pathways by binding to Frizzled2. *The EMBO Journal*, *29*(1), 41–54. https://doi.org/10.1038/emboj.2009.322

Savory, J. G. A., Mansfield, M., Rijli, F. M., & Lohnes, D. (2011). Cdx mediates neural tube closure through transcriptional regulation of the planar cell polarity gene Ptk7. *Development (Cambridge, England)*, *138*(7), 1361–1370. https://doi.org/10.1242/dev.056622

Sawyer, J. M., Glass, S., Li, T., Shemer, G., White, N. D., Starostina, N. G., Kipreos, E. T., Jones, C. D., & Goldstein, B. (2011). Overcoming redundancy: An RNAi enhancer screen for

morphogenesis genes in Caenorhabditis elegans. *Genetics*, *188*(3), 549–564. https://doi.org/10.1534/genetics.111.129486

Schaefer, K. N., Bonello, T. T., Zhang, S., Williams, C. E., Roberts, D. M., McKay, D. J., & Peifer, M. (2018). Supramolecular assembly of the beta-catenin destruction complex and the effect of Wnt signaling on its localization, molecular size, and activity in vivo. *PLOS Genetics*, *14*(4), e1007339. https://doi.org/10.1371/journal.pgen.1007339

Schlessinger, K., McManus, E. J., & Hall, A. (2007). Cdc42 and noncanonical Wnt signal transduction pathways cooperate to promote cell polarity. *The Journal of Cell Biology*, *178*(3), 355–361. https://doi.org/10.1083/jcb.200701083

Schröterová, L., Ježková, A., Rudolf, E., Caltová, K., Králová, V., & Hanušová, V. (2018). Inositol hexaphosphate limits the migration and the invasiveness of colorectal carcinoma cells in vitro. *International Journal of Oncology*, *53*(4), 1625–1632. https://doi.org/10.3892/ijo.2018.4488

Shade sequence alignments with Boxshade. Retrieved August 22, 2025, from https://junli.netlify.app/apps/boxshade/

Shah, P. K., Tanner, M., Kovacevic, I., Rankin, A., Marshall, T. E., Noblett, N., Tran, N. N., Roenspies, T., Hung, J., Chen, Z., Slatculescu, C., Perkins, T. J., Bao, Z., & Colavita, A. (2017). PCP and SAX-3/Robo pathways cooperate to regulate convergent-extension-based nerve cord assembly in C. elegans. *Developmental Cell*, *41*(2), 195-203.e3. https://doi.org/10.1016/j.devcel.2017.03.024

Shewan, A., Eastburn, D. J., & Mostov, K. (2011). Phosphoinositides in Cell Architecture. *Cold Spring Harbor Perspectives in Biology*, *3*(8), a004796. https://doi.org/10.1101/cshperspect.a004796

Shi, D.-L. (2024). Canonical and Non-Canonical Wnt Signaling Generates Molecular and Cellular Asymmetries to Establish Embryonic Axes. *Journal of Developmental Biology*, *12*(3), Article 3. https://doi.org/10.3390/jdb12030020

Shi, W., Peyrot, S. M., Munro, E., & Levine, M. (2009). FGF3 in the floor plate directs notochord convergent extension in the Ciona tadpole. *Development (Cambridge, England)*, *136*(1), 23–28. https://doi.org/10.1242/dev.029157

Shih, J., & Keller, R. (1992). Patterns of cell motility in the organizer and dorsal mesoderm of Xenopus laevis. *Development*, *116*(4), 915–930. https://doi.org/10.1242/dev.116.4.915

Shindo, A. (2018). Models of convergent extension during morphogenesis. *WIREs Developmental Biology*, *7*(1), e293. https://doi.org/10.1002/wdev.293

Shindo, A., Inoue, Y., Kinoshita, M., & Wallingford, J. B. (2019). PCP-dependent transcellular regulation of actomyosin oscillation facilitates convergent extension of vertebrate tissue. *Developmental Biology*, *446*(2), 159–167. https://doi.org/10.1016/j.ydbio.2018.12.017

Shindo, A., & Wallingford, J. B. (2014). PCP and septins compartmentalize cortical actomyosin to direct collective cell movement. *Science (New York, N.Y.)*, *343*(6171), 649–652. https://doi.org/10.1126/science.1243126

Shook, D. R., Wen, J. W., Rolo, A., O'Hanlon, M., Francica, B., Dobbins, D., Skoglund, P., DeSimone, D. W., Winklbauer, R., & Keller, R. E. (2022). Characterization of convergent thickening, a major convergence force producing morphogenic movement in amphibians. *eLife*, *11*, e57642. https://doi.org/10.7554/eLife.57642

Šimečková, K., Brožová, E., Vohánka, J., Pohludka, M., Kostrouch, Z., Krause, M. W., Rall, J. E., & Kostrouchová, M. (2007). Supplementary Nuclear Receptor NHR-60 is Required for Normal Embryonic and Early Larval Development of Caenorhabditis elegans. *Folia Biologica*, *53*(3), 85–96. https://doi.org/10.14712/fb2007053030085

Simões, S. D. M., Mainieri, A., & Zallen, J. A. (2014). Rho GTPase and Shroom direct planar polarized actomyosin contractility during convergent extension. *Journal of Cell Biology*, *204*(4), 575–589. https://doi.org/10.1083/jcb.201307070

Skipper, M., Milne, C. A., & Hodgkin, J. (1999). Genetic and Molecular Analysis of fox-1, a Numerator Element Involved in Caenorhabditis elegans Primary Sex Determination. *Genetics*, *151*(2), 617–631. https://doi.org/10.1093/genetics/151.2.617

Sknepnek, R., Djafer-Cherif, I., Chuai, M., Weijer, C., & Henkes, S. (2023). Generating active T1 transitions through mechanochemical feedback. *eLife*, *12*. https://doi.org/10.7554/elife.79862

Skoglund, P., Rolo, A., Chen, X., Gumbiner, B. M., & Keller, R. (2008). Convergence and extension at gastrulation require a myosin IIB dependent cortical actin network. *Development (Cambridge, England)*, *135*(14), 2435–2444. https://doi.org/10.1242/dev.014704

Skromne, I., Thorsen, D., Hale, M., Prince, V. E., & Ho, R. K. (2007). Repression of the hindbrain developmental program by Cdx factors is required for the specification of the vertebrate spinal cord. *Development (Cambridge, England)*, *134*(11), 2147–2158. https://doi.org/10.1242/dev.002980

Sluder, A. E., Mathews, S. W., Hough, D., Yin, V. P., & Maina, C. V. (1999). The Nuclear Receptor Superfamily Has Undergone Extensive Proliferation and Diversification in Nematodes. *Genome Research*, *9*(2), 103–120. https://doi.org/10.1101/gr.9.2.103

Slusarski, D. C., Corces, V. G., & Moon, R. T. (1997). Interaction of Wnt and a Frizzled homologue triggers G-protein-linked phosphatidylinositol signalling. *Nature*, *390*(6658), 410–413. https://doi.org/10.1038/37138

Smith, J. J., & Kratsios, P. (2024). Hox gene functions in the C. elegans nervous system: From early patterning to maintenance of neuronal identity. *Seminars in Cell & Developmental Biology*, *152–153*, 58–69. https://doi.org/10.1016/j.semcdb.2022.11.012

Smith, J. J., Taylor, S. R., Blum, J. A., Feng, W., Collings, R., Gitler, A. D., Miller, D. M., & Kratsios, P. (2024). A molecular atlas of adult C. elegans motor neurons reveals ancient diversity delineated by conserved transcription factor codes. *Cell Reports*, *43*(3), 113857. https://doi.org/10.1016/j.celrep.2024.113857

Spencer, A. K., Siddiqui, B. A., & Thomas, J. H. (2015). Cell shape change and invagination of the cephalic furrow involves reorganization of F-actin. *Developmental Biology*, *402*(2), 192–207. https://doi.org/10.1016/j.ydbio.2015.03.022

Stamos, J. L., & Weis, W. I. (2013). The β-catenin destruction complex. *Cold Spring Harbor Perspectives in Biology*, *5*(1), a007898. https://doi.org/10.1101/cshperspect.a007898

Stephens, L., Radenberg, T., Thiel, U., Vogel, G., Khoo, K. H., Dell, A., Jackson, T. R., Hawkins, P. T., & Mayr, G. W. (1993). The detection, purification, structural characterization, and metabolism of diphosphoinositol pentakisphosphate(s) and bisdiphosphoinositol tetrakisphosphate(s). *The Journal of Biological Chemistry*, *268*(6), 4009–4015.

Strähle, U., Schmidt, A., Kelsey, G., Stewart, A. F., Cole, T. J., Schmid, W., & Schütz, G. (1992). At least three promoters direct expression of the mouse glucocorticoid receptor gene. *Proceedings of the National Academy of Sciences*, *89*(15), 6731–6735. https://doi.org/10.1073/pnas.89.15.6731

Sullivan-Brown, J. L., Tandon, P., Bird, K. E., Dickinson, D. J., Tintori, S. C., Heppert, J. K., Meserve, J. H., Trogden, K. P., Orlowski, S. K., Conlon, F. L., & Goldstein, B. (2016). Identifying Regulators of Morphogenesis Common to Vertebrate Neural Tube Closure and Caenorhabditis elegans Gastrulation. *Genetics*, *202*(1), 123–139. https://doi.org/10.1534/genetics.115.183137

Sulston, J. E. (1976). Post-embryonic development in the ventral cord of Caenorhabditis elegans. *Philosophical Transactions of the Royal Society of London. Series B, Biological Sciences*, *275*(938), 287–297. https://doi.org/10.1098/rstb.1976.0084

Sulston, J. E., Schierenberg, E., White, J. G., & Thomson, J. N. (1983). The embryonic cell lineage of the nematode Caenorhabditis elegans. *Developmental Biology*, *100*(1), 64–119. https://doi.org/10.1016/0012-1606(83)90201-4

Sun, Z., Amourda, C., Shagirov, M., Hara, Y., Saunders, T. E., & Toyama, Y. (2017). Basolateral protrusion and apical contraction cooperatively drive Drosophila germ-band extension. *Nature Cell Biology*, *19*(4), 375–383. https://doi.org/10.1038/ncb3497

Sutherland, A., Keller, R., & Lesko, A. (2020). Convergent extension in mammalian morphogenesis. *Seminars in Cell & Developmental Biology*, *100*, 199–211. https://doi.org/10.1016/j.semcdb.2019.11.002

Szabó, A., Cobo, I., Omara, S., McLachlan, S., Keller, R., & Mayor, R. (2016). The Molecular Basis of Radial Intercalation during Tissue Spreading in Early Development. *Developmental Cell*, *37*(3), 213–225. https://doi.org/10.1016/j.devcel.2016.04.008

Tada, M., & Heisenberg, C.-P. (2012). Convergent extension: Using collective cell migration and cell intercalation to shape embryos. *Development*, *139*(21), 3897–3904. https://doi.org/10.1242/dev.073007

Tahinci, E., Thorne, C. A., Franklin, J. L., Salic, A., Christian, K. M., Lee, L. A., Coffey, R. J., & Lee, E. (2007). Lrp6 is required for convergent extension during Xenopus gastrulation. *Development (Cambridge, England)*, *134*(22), 4095–4106. https://doi.org/10.1242/dev.010272

Takeuchi, H., Kanematsu, T., Misumi, Y., Sakane, F., Konishi, H., Kikkawa, U., Watanabe, Y., Katan, M., & Hirata, M. (1997). Distinct specificity in the binding of inositol phosphates by pleckstrin homology domains of pleckstrin, RAC-protein kinase, diacylglycerol kinase and a new 130 kDa protein. *Biochimica et Biophysica Acta (BBA) - Molecular Cell Research*, *1359*(3), 275–285. https://doi.org/10.1016/S0167-4889(97)00109-2

Talukdar, P. D., & Chatterji, U. (2023). Transcriptional co-activators: Emerging roles in signaling pathways and potential therapeutic targets for diseases. *Signal Transduction and Targeted Therapy*, *8*(1), 1–41. https://doi.org/10.1038/s41392-023-01651-w

Tan, N. S., Icre, G., Montagner, A., Heggeler, B. B., Wahli, W., & Michalik, L. (2007). The Nuclear Hormone Receptor Peroxisome Proliferator-Activated Receptor β/δ Potentiates Cell Chemotactism, Polarization, and Migration. *Molecular and Cellular Biology*, *27*(20), 7161–7175. https://doi.org/10.1128/MCB.00436-07

Tanegashima, K., Zhao, H., & Dawid, I. B. (2008). WGEF activates Rho in the Wnt–PCP pathway and controls convergent extension in Xenopus gastrulation. *The EMBO Journal*, *27*(4), 606–617. https://doi.org/10.1038/emboj.2008.9

Taneja, R., Rochette-Egly, C., Plassat, J., Penna, L., Gaub, M., & Chambon, P. (1997). Phosphorylation of activation functions AF-1 and AF-2 of RARα and RARγ is indispensable for differentiation of F9 cells upon retinoic acid and cAMP treatment. *The EMBO Journal*, *16*(21), 6452–6465. https://doi.org/10.1093/emboj/16.21.6452

Tao, L. J., Seo, D. E., Jackson, B., Ivanova, N. B., & Santori, F. R. (2020). Nuclear Hormone Receptors and Their Ligands: Metabolites in Control of Transcription. *Cells*, *9*(12), 2606. https://doi.org/10.3390/cells9122606

Taylor, S. R., Santpere, G., Weinreb, A., Barrett, A., Reilly, M. B., Xu, C., Varol, E., Oikonomou, P., Glenwinkel, L., McWhirter, R., Poff, A., Basavaraju, M., Rafi, I., Yemini, E., Cook, S. J., Abrams, A., Vidal, B., Cros, C., Tavazoie, S., … Miller, D. M. (2021). Molecular topography of an entire nervous system. *Cell*, *184*(16), 4329-4347.e23. https://doi.org/10.1016/j.cell.2021.06.023

Teotico, D. G., Frazier, M. L., Ding, F., Dokholyan, N. V., Temple, B. R. S., & Redinbo, M. R. (2008). Active Nuclear Receptors Exhibit Highly Correlated AF-2 Domain Motions. *PLoS Computational Biology*, *4*(7), e1000111. https://doi.org/10.1371/journal.pcbi.1000111

Tissir, F., & Goffinet, A. M. (2010). Planar cell polarity signaling in neural development. *Current Opinion in Neurobiology*, *20*(5), 572–577. https://doi.org/10.1016/j.conb.2010.05.006

Trichas, G., Smith, A. M., White, N., Wilkins, V., Watanabe, T., Moore, A., Joyce, B., Sugnaseelan, J., Rodriguez, T. A., Kay, D., Baker, R. E., Maini, P. K., & Srinivas, S. (2012). Multi-Cellular Rosettes in the Mouse Visceral Endoderm Facilitate the Ordered Migration of Anterior Visceral Endoderm Cells. *PLoS Biology*, *10*(2), e1001256. https://doi.org/10.1371/journal.pbio.1001256

Tsui, M. M., & York, J. D. (2010). ROLES OF INOSITOL PHOSPHATES AND INOSITOL PYROPHOSPHATES IN DEVELOPMENT, CELL SIGNALING AND NUCLEAR PROCESSES. *Advances in Enzyme Regulation*, *50*(1), 324–337. https://doi.org/10.1016/j.advenzreg.2009.12.002

Tucker, J. A., Mintzer, K. A., & Mullins, M. C. (2008). The BMP signaling gradient patterns dorsoventral tissues in a temporally progressive manner along the anteroposterior axis. *Developmental Cell*, *14*(1), 108–119. https://doi.org/10.1016/j.devcel.2007.11.004

Tu-Sekine, B., & Kim, S. F. (2022). The Inositol Phosphate System—A Coordinator of Metabolic Adaptability. *International Journal of Molecular Sciences*, *23*(12), Article 12. https://doi.org/10.3390/ijms23126747

Ucuncu, E., Rajamani, K., Wilson, M. S. C., Medina-Cano, D., Altin, N., David, P., Barcia, G., Lefort, N., Banal, C., Vasilache-Dangles, M.-T., Pitelet, G., Lorino, E., Rabasse, N., Bieth, E., Zaki, M. S., Topcu, M., Sonmez, F. M., Musaev, D., Stanley, V., … Cantagrel, V. (2020). MINPP1 prevents intracellular accumulation of the chelator inositol hexakisphosphate and is mutated in Pontocerebellar Hypoplasia. *Nature Communications*, *11*(1), 6087. https://doi.org/10.1038/s41467-020-19919-y

Unterseher, F., Hefele, J. A., Giehl, K., De Robertis, E. M., Wedlich, D., & Schambony, A. (2004). Paraxial protocadherin coordinates cell polarity during convergent extension via Rho A and JNK. *The EMBO Journal*, *23*(16), 3259–3269. https://doi.org/10.1038/sj.emboj.7600332

Van Den Akker, E., Forlani, S., Chawengsaksophak, K., De Graaff, W., Beck, F., Meyer, B. I., & Deschamps, J. (2002). *Cdx1*and*Cdx2*have overlapping functions in anteroposterior patterning and posterior axis elongation. *Development*, *129*(9), 2181–2193. https://doi.org/10.1242/dev.129.9.2181

Van Der Spuy, M., Wang, J. X., Kociszewska, D., & White, M. D. (2023). The cellular dynamics of neural tube formation. *Biochemical Society Transactions*, *51*(1), 343–352. https://doi.org/10.1042/BST20220871

Vázquez-Manrique, R. P., Nagy, A. I., Legg, J. C., Bales, O. A. M., Ly, S., & Baylis, H. A. (2008). Phospholipase C-ε Regulates Epidermal Morphogenesis in Caenorhabditis elegans. *PLoS Genetics*, *4*(3), e1000043. https://doi.org/10.1371/journal.pgen.1000043

Verbsky, J., Lavine, K., & Majerus, P. W. (2005). Disruption of the mouse inositol 1,3,4,5,6-pentakisphosphate 2-kinase gene, associated lethality, and tissue distribution of 2-kinase expression. *Proceedings of the National Academy of Sciences*, *102*(24), 8448–8453. https://doi.org/10.1073/pnas.0503656102

Vincent, A., Blankenship, J. T., & Wieschaus, E. (1997). Integration of the head and trunk segmentation systems controls cephalic furrow formation in Drosophila. *Development (Cambridge, England)*, *124*(19), 3747–3754. https://doi.org/10.1242/dev.124.19.3747

Vogel, T. W., Carter, C. S., Abode-Iyamah, K., Zhang, Q., & Robinson, S. (2012). The role of primary cilia in the pathophysiology of neural tube defects. *Neurosurgical Focus*, *33*(4), E2. https://doi.org/10.3171/2012.6.FOCUS12222

Voigt, B., Frazier, K., Yazdi, D., Klein, J., Gontarz, P., Zhang, B., Sepich, D. S., Mo, J., Smeeton, J., Solnica-Krezel, L., & Gray, R. S. (2025). Cell expansion for notochord mechanics and endochondral bone lengthening in zebrafish depends on the 5′-inositol phosphatase Inppl1a. *Current Biology*, *35*(9), 1949-1962.e6. https://doi.org/10.1016/j.cub.2025.03.022

Vroomans, R. M. A., Hogeweg, P., & Tusscher, K. H. W. J. ten. (2015). Segment-Specific Adhesion as a Driver of Convergent Extension. *PLOS Computational Biology*, *11*(2), e1004092. https://doi.org/10.1371/journal.pcbi.1004092

Walck-Shannon, E., & Hardin, J. (2014). Cell intercalation from top to bottom. *Nature Reviews Molecular Cell Biology*, *15*(1), 34–48. https://doi.org/10.1038/nrm3723

Walck-Shannon, E., Lucas, B., Chin-Sang, I., Reiner, D., Kumfer, K., Cochran, H., Bothfeld, W., & Hardin, J. (2016). CDC-42 Orients Cell Migration during Epithelial Intercalation in the Caenorhabditis elegans Epidermis. *PLoS Genetics*, *12*(11), e1006415. https://doi.org/10.1371/journal.pgen.1006415

Walck-Shannon, E., Reiner, D., & Hardin, J. (2015). Polarized Rac-dependent protrusions drive epithelial intercalation in the embryonic epidermis of C. elegans. *Development (Cambridge, England)*, *142*(20), 3549–3560. https://doi.org/10.1242/dev.127597

Wallingford, J. B., Ewald, A. J., Harland, R. M., & Fraser, S. E. (2001). Calcium signaling during convergent extension in Xenopus. *Current Biology: CB*, *11*(9), 652–661. https://doi.org/10.1016/s0960-9822(01)00201-9

Wallingford, J. B., Fraser, S. E., & Harland, R. M. (2002). Convergent Extension: The Molecular Control of Polarized Cell Movement during Embryonic Development. *Developmental Cell*, *2*(6), 695–706. https://doi.org/10.1016/S1534-5807(02)00197-1

Wallingford, J. B., & Harland, R. M. (2002). Neural tube closure requires Dishevelled-dependent convergent extension of the midline. *Development*, *129*(24), 5815–5825. https://doi.org/10.1242/dev.00123

Wang, J., Chitsaz, F., Derbyshire, M. K., Gonzales, N. R., Gwadz, M., Lu, S., Marchler, G. H., Song, J. S., Thanki, N., Yamashita, R. A., Yang, M., Zhang, D., Zheng, C., Lanczycki, C.

J., & Marchler-Bauer, A. (2023). The conserved domain database in 2023. *Nucleic Acids Research*, *51*(D1), D384–D388. https://doi.org/10.1093/nar/gkac1096

Wang, J., Hamblet, N. S., Mark, S., Dickinson, M. E., Brinkman, B. C., Segil, N., Fraser, S. E., Chen, P., Wallingford, J. B., & Wynshaw-Boris, A. (2006). Dishevelled genes mediate a conserved mammalian PCP pathway to regulate convergent extension during neurulation. *Development*, *133*(9), 1767–1778. https://doi.org/10.1242/dev.02347

Wang, M., de Marco, P., Capra, V., & Kibar, Z. (2019). Update on the Role of the Non-Canonical Wnt/Planar Cell Polarity Pathway in Neural Tube Defects. *Cells*, *8*(10), 1198. https://doi.org/10.3390/cells8101198

Wang, X., Merkel, M., Sutter, L. B., Erdemci-Tandogan, G., Manning, M. L., & Kasza, K. E. (2020). Anisotropy links cell shapes to tissue flow during convergent extension. *Proceedings of the National Academy of Sciences*, *117*(24), 13541–13551. https://doi.org/10.1073/pnas.1916418117

Warrington, S. J., Strutt, H., & Strutt, D. (2013). The Frizzled-dependent planar polarity pathway locally promotes E-cadherin turnover via recruitment of RhoGEF2. *Development*, *140*(5), 1045–1054. https://doi.org/10.1242/dev.088724

Watson, E., Yilmaz, L. S., & Walhout, A. J. M. (2015). Understanding Metabolic Regulation at a Systems Level: Metabolite Sensing, Mathematical Predictions, and Model Organisms. *Annual Review of Genetics*, *49*(Volume 49, 2015), 553–575. https://doi.org/10.1146/annurev-genet-112414-055257

Watson, P. J., Millard, C. J., Riley, A. M., Robertson, N. S., Wright, L. C., Godage, H. Y., Cowley, S. M., Jamieson, A. G., Potter, B. V. L., & Schwabe, J. W. R. (2016). Insights into the activation mechanism of class I HDAC complexes by inositol phosphates. *Nature Communications*, *7*(1), 11262. https://doi.org/10.1038/ncomms11262

Weikum, E. R., Liu, X., & Ortlund, E. A. (2018). The nuclear receptor superfamily: A structural perspective. *Protein Science : A Publication of the Protein Society*, *27*(11), 1876–1892. https://doi.org/10.1002/pro.3496

Wendling, O., Chambon, P., & Mark, M. (1999). Retinoid X receptors are essential for early mouse development and placentogenesis. *Proceedings of the National Academy of Sciences*, *96*(2), 547–551. https://doi.org/10.1073/pnas.96.2.547

Weng, S., Devitt, C. C., Nyaoga, B. M., Alvarado, J., & Wallingford, J. B. (2025). PCP-dependent polarized mechanics in the cortex of individual cells during convergent extension. *Developmental Biology*, *523*, 59–67. https://doi.org/10.1016/j.ydbio.2025.04.007

Weng, S., Huebner, R. J., & Wallingford, J. B. (2022). Convergent extension requires adhesion-dependent biomechanical integration of cell crawling and junction contraction. *Cell Reports*, *39*(4), 110666. https://doi.org/10.1016/j.celrep.2022.110666

Werner, J. M., Negesse, M. Y., Brooks, D. L., Caldwell, A. R., Johnson, J. M., & Brewster, R. M. (2021). Hallmarks of primary neurulation are conserved in the zebrafish forebrain. *Communications Biology*, *4*, 147. https://doi.org/10.1038/s42003-021-01655-8

Wernike, D., Chen, Y., Mastronardi, K., Makil, N., & Piekny, A. (2016). Mechanical forces drive neuroblast morphogenesis and are required for epidermal closure. *Developmental Biology*, *412*(2), 261–277. https://doi.org/10.1016/j.ydbio.2016.02.023

Westfall, T. A., Brimeyer, R., Twedt, J., Gladon, J., Olberding, A., Furutani-Seiki, M., & Slusarski, D. C. (2003). Wnt-5/pipetail functions in vertebrate axis formation as a negative regulator of Wnt/beta-catenin activity. *The Journal of Cell Biology*, *162*(5), 889–898. https://doi.org/10.1083/jcb.200303107

White, J. G., Southgate, E., Thomson, J. N., & Brenner, S. (1976). The structure of the ventral nerve cord of Caenorhabditis elegans. *Philosophical Transactions of the Royal Society of London. Series B, Biological Sciences*, *275*(938), 327–348. https://doi.org/10.1098/rstb.1976.0086

White, J. G., Southgate, E., Thomson, J. N., & Brenner, S. (1986). The structure of the nervous system of the nematode Caenorhabditis elegans. *Philosophical Transactions of the Royal Society of London. Series B, Biological Sciences*, *314*(1165), 1–340. https://doi.org/10.1098/rstb.1986.0056

White, J. G., Southgate, E., Thomson, J. N., & Brenner, S. (1997). The structure of the nervous system of the nematode Caenorhabditis elegans. *Philosophical Transactions of the Royal Society of London. B, Biological Sciences*, *314*(1165), 1–340. https://doi.org/10.1098/rstb.1986.0056

Williams, M. L., & Solnica-Krezel, L. (2020). Nodal and planar cell polarity signaling cooperate to regulate zebrafish convergence and extension gastrulation movements. *eLife*, *9*, e54445. https://doi.org/10.7554/eLife.54445

Williams, M., Yen, W., Lu, X., & Sutherland, A. (2014). Distinct apical and basolateral mechanisms drive PCP-dependent convergent extension of the mouse neural plate. *Developmental Cell*, *29*(1), 34–46. https://doi.org/10.1016/j.devcel.2014.02.007

Wilson, L., Gale, E., & Maden, M. (2003). The role of retinoic acid in the morphogenesis of the neural tube. *Journal of Anatomy*, *203*(4), 357–368. https://doi.org/10.1046/j.1469-7580.2003.00230.x

Wilson, M. P., Hugge, C., Bielinska, M., Nicholas, P., Majerus, P. W., & Wilson, D. B. (2009). Neural tube defects in mice with reduced levels of inositol 1,3,4-trisphosphate 5/6-kinase. *Proceedings of the National Academy of Sciences of the United States of America*, *106*(24), 9831–9835. https://doi.org/10.1073/pnas.0904172106

Wolpert, L., Smith, J. C., Keller, R., Davidson, L., Edlund, A., Elul, T., Ezin, M., Shook, D., & Skoglund, P. (2000). Mechanisms of convergence and extension by cell

intercalation. *Philosophical Transactions of the Royal Society of London. Series B: Biological Sciences*, *355*(1399), 897–922. https://doi.org/10.1098/rstb.2000.0626

Xie, X., Li, C., Yu, J., Chang, S., Cheng, X., Wang, F., Bao, Y., Zhang, T., & Wang, S. (2023). MTHFD1 is critical for the negative regulation of retinoic acid receptor signalling in anencephaly. *Brain*, *146*(8), 3455–3469. https://doi.org/10.1093/brain/awad084

Xie, Z., & Bankaitis, V. A. (2022). Phosphatidylinositol transfer protein/planar cell polarity axis regulates neocortical morphogenesis by supporting interkinetic nuclear migration. *Cell Reports*, *39*(9), 110869. https://doi.org/10.1016/j.celrep.2022.110869

Xu, Y., Cheng, Y., Chen, A. T., & Bao, Z. (2023). A compound PCP scheme underlies sequential rosettes-based cell intercalation. *Development*, *150*(8), dev201493. https://doi.org/10.1242/dev.201493

Yamada, T. (1994). Caudalization by the amphibian organizer: Brachyury, convergent extension and retinoic acid. *Development (Cambridge, England)*, *120*(11), 3051–3062. https://doi.org/10.1242/dev.120.11.3051

Yamashita, S., Miyagi, C., Carmany-Rampey, A., Shimizu, T., Fujii, R., Schier, A. F., & Hirano, T. (2002). Stat3 Controls Cell Movements during Zebrafish Gastrulation. *Developmental Cell*, *2*(3), 363–375. https://doi.org/10.1016/s1534-5807(02)00126-0

Yang, S. N., Yu, J., Mayr, G. W., Hofmann, F., Larsson, O., & Berggren, P. O. (2001). Inositol hexakisphosphate increases L-type Ca2+ channel activity by stimulation of adenylyl cyclase. *FASEB Journal: Official Publication of the Federation of American Societies for Experimental Biology*, *15*(10), 1753–1763. https://doi.org/10.1096/fj.00-0799com

Yang, Z.-L., Chen, J.-N., Lu, Y.-Y., Lu, M., Wan, Q.-L., Wu, G.-S., & Luo, H.-R. (2021). Inositol polyphosphate multikinase IPMK-1 regulates development through IP3/calcium signaling in *Caenorhabditis elegans*. *Cell Calcium*, *93*, 102327. https://doi.org/10.1016/j.ceca.2020.102327

Ybot-Gonzalez, P., Savery, D., Gerrelli, D., Signore, M., Mitchell, C. E., Faux, C. H., Greene, N. D. E., & Copp, A. J. (2007). Convergent extension, planar-cell-polarity signalling and initiation of mouse neural tube closure. *Development*, *134*(4), 789–799. https://doi.org/10.1242/dev.000380

Yemini, E., Lin, A., Nejatbakhsh, A., Varol, E., Sun, R., Mena, G. E., Samuel, A. D. T., Paninski, L., Venkatachalam, V., & Hobert, O. (2021). NeuroPAL: A Multicolor Atlas for Whole-Brain Neuronal Identification in C. elegans. *Cell*, *184*(1), 272-288.e11. https://doi.org/10.1016/j.cell.2020.12.012

Yeo, S. Y., Little, M. H., Yamada, T., Miyashita, T., Halloran, M. C., Kuwada, J. Y., Huh, T. L., & Okamoto, H. (2001). Overexpression of a slit homologue impairs convergent extension of the mesoderm and causes cyclopia in embryonic zebrafish. *Developmental Biology*, *230*(1), 1–17. https://doi.org/10.1006/dbio.2000.0105

Yin, M., Catimel, B., Gregory, M., Condron, M., Kapp, E., Holmes, A. B., & Burgess, A. W. (2016). Synthesis of an inositol hexakisphosphate (IP6) affinity probe to study the interactome from a colon cancer cell line. *Integrative Biology*, *8*(3), 309–318. https://doi.org/10.1039/c5ib00264h

Yokota, C., Kofron, M., Zuck, M., Houston, D. W., Isaacs, H., Asashima, M., Wylie, C. C., & Heasman, J. (2003). A novel role for a nodal-related protein; Xnr3 regulates convergent extension movements via the FGF receptor. *Development (Cambridge, England)*, *130*(10), 2199–2212. https://doi.org/10.1242/dev.00434

Yoon, J., Kumar, V., Goutam, R. S., Kim, S.-C., Park, S., Lee, U., & Kim, J. (2021). Bmp Signal Gradient Modulates Convergent Cell Movement via Xarhgef3.2 during Gastrulation of Xenopus Embryos. *Cells*, *11*(1), 44. https://doi.org/10.3390/cells11010044

York, J. D. (2006). Regulation of nuclear processes by inositol polyphosphates. *Biochimica et Biophysica Acta (BBA) - Molecular and Cell Biology of Lipids*, *1761*(5), 552–559. https://doi.org/10.1016/j.bbalip.2006.04.014

Zallen, J. A., & Wieschaus, E. (2004). Patterned gene expression directs bipolar planar polarity in Drosophila. *Developmental Cell*, *6*(3), 343–355. https://doi.org/10.1016/s1534-5807(04)00060-7

Zallen, J. A., Yi, B. A., & Bargmann, C. I. (1998). The conserved immunoglobulin superfamily member SAX-3/Robo directs multiple aspects of axon guidance in C. elegans. *Cell*, *92*(2), 217–227. https://doi.org/10.1016/s0092-8674(00)80916-2

Zanardelli, S., Christodoulou, N., & Skourides, P. A. (2013). Calpain2 protease: A new member of the Wnt/Ca2+ pathway modulating convergent extension movements in *Xenopus*. *Developmental Biology*, *384*(1), 83–100. https://doi.org/10.1016/j.ydbio.2013.09.017

Zhao, T., McMahon, M., Reynolds, K., Saha, S. K., Stokes, A., & Zhou, C. J. (2022). The role of Lrp6-mediated Wnt/β-catenin signaling in the development and intervention of spinal neural tube defects in mice. *Disease Models & Mechanisms*, *15*(6), dmm049517. https://doi.org/10.1242/dmm.049517

Zhen, M., & Samuel, A. D. T. (2015). C. elegans locomotion: Small circuits, complex functions. *Current Opinion in Neurobiology*, *33*, 117–126. https://doi.org/10.1016/j.conb.2015.03.009

Zhou, J., Pal, S., Maiti, S., & Davidson, L. A. (2015). Force production and mechanical accommodation during convergent extension. *Development*, *142*(4), 692–701. https://doi.org/10.1242/dev.116533

Zhu, Y., & Lohnes, D. (2022). Regulation of axial elongation by Cdx. *Developmental Biology*, *483*, 118–127. https://doi.org/10.1016/j.ydbio.2021.12.011

Zilber, Y., Babayeva, S., Seo, J. H., Liu, J. J., Mootin, S., & Torban, E. (2013). The PCP effector Fuzzy controls cilial assembly and signaling by recruiting Rab8 and Dishevelled to the primary cilium. *Molecular Biology of the Cell*, *24*(5), 555–565. https://doi.org/10.1091/mbc.E12-06-0437